LABORATORY ASSESSMENT OF PAVEMENT FOUNDATION MATERIALS

by

Lam Wah Cheung, B.Eng.(Hons)

Thesis submitted to the University of Nottingham

for the degree of Doctor of Philosophy

March 1994

ACKNOWLEDGEMENTS

CONTENTS

****

CHAPTER 1 INTRODUCTION

****

PART A   REVIEW

****

PART B   ASSESSMENT TESTS FOR UNBOUND GRANULAR MATERIALS

****

PART C   ASSESSMENT TESTS FOR SOILS

****

**PART D   CONCLUSIONS, PRACTICAL IMPLICATIONS
            AND RECOMMENDATIONS FOR FUTURE WORK**

****

APPENDICES

ABSTRACT

The main aim of this research was to improve laboratory test methods for describing pavement foundation materials so that analytical design based on appropriate mechanical parameters of materials could be performed in practice. The study started by assessing the relevance of currently available methods to describe materials in pavement foundations and reviewing factors influencing the responses of these materials to repeated loading.

Two simplified repeated load triaxial apparatuses of different sizes have been developed and their capabilities in characterizing materials in sub-base and subgrade layers have been examined. The large one is for specimens of size 280 mm diameter and 560 mm high and is suitable for full scale Department of Transport Type 1 sub-base granular materials. The small one is for cohesive soil specimens, either recompacted or undisturbed, with a diameter of 103 mm and height of 206 mm. Both apparatuses are equipped with simple loading mechanisms, user-friendly computer data acquisition systems and high precision on-sample, but easy to fix, instrumentation to monitor axial and radial displacements.

A complete testing method necessitated the provision of the associated testing techniques. The whole test, including aggregate and soil preparation and testing, was designed to be conducted by one person. Development of the test procedures is detailed.

Evaluation of the simplified repeated load apparatuses and the testing techniques involved testing 13 aggregate specimens and more than 26 soil specimens. Furthermore, comprehensive preliminary tests have been performed on the tested materials to provide background information which enabled results from the simplified repeated load triaxial apparatuses to be assessed in detail. For unbound granular materials, the tests included a series of particle examinations and shear box testing. For soils, besides classification tests, the soil suctions and the permanent deformation development under wheel loading were examined. To check the reliability of the two simplified facilities, tests were also carried out on pre-existing sophisticated repeated load triaxial apparatuses.

Comparison of aggregate test results has enabled further understanding of the effects on resilient strain, permanent deformation and compressive strength of grading, density, shape, surface profile, surface friction and material type to be gained. Effects from waveform and frequency of load pulses were also discussed. For soils, sufficient test results not only allowed different materials to be compared but also permitted models to describe resilient strain behaviour and permanent deformation development to be developed.

LIST OF ABBREVIATIONS

100TA   Simplified repeated load triaxial apparatus for a soil specimen of diameter 103 mm

280TA   Simplified repeated load triaxial apparatus for an aggregate specimen of diameter 280 mm

75TA   Existing repeated load triaxial apparatus for a soil specimen of diameter 75 mm

AAV   Aggregate Abrasion Value

AIV   Aggregate Impact Value

AN   Angularity Number

BS   British Standard

CBR   California Bearing Ratio

DD10   Permanent deformation obtained after dropping a weight on a plate resting on the top of a CBR specimen

DoT   Department of Transport

LL   Liquid Limit

LVDT   Linear Variable Differential Transformer

MCA   Manually-Controlled Actuator

MCV   Moisture Condition Value

PI   Plasticity Index

PL   Plastic Limit

R   Roundness

RD1000   Rut depth developed after 1000 passes of the wheel in the wheel tracking test

RF   Roughness Factor

TRL   Transport Research Laboratory

LIST OF SYMBOLS

C_u	Unconfined undrained shear strength
G_s	Specific density of a soil
e	Elongation ratio
f	Flatness ratio
F	Shape factor
K_o	Coefficient of earth pressure at rest
M_r	Resilient modulus
M_{ra}	Axial resilient modulus obtained from the large shear box
N	Number of load repetitions
p	Mean normal stress ($\frac{\sigma_1 + 2\sigma_3}{3}$)
p'	Effective mean normal stress
Δp	Change in mean normal stress
q	Deviator stress ($\sigma_1 - \sigma_3$)
Δq	Change in deviator stress
q_r	Repeated deviator stress
q_t	Deviator stress at the accumulated axial plastic strain of 1% in the multi-stress path test
S	Soil suction
S_r	Degree of Saturation
U	Uniformity coefficient
y'	The degree of working sphericity
α	Soil compressibility factor
δx	Displacement in x direction
δy	Displacement in y direction
ε_a	Resilient axial strain
ε_p	Permanent strain
ε_r	Resilient radial strain
ε_s	Resilient shear strain $\frac{2}{3}(\varepsilon_1 - \varepsilon_3)$
ε_v	Resilient volumetric strain $\varepsilon_1 + 2\varepsilon_3$
ε_x	Strain in x direction
ε_y	Strain in y direction
ϕ	Apparent friction angle
ϕ'	Effective apparent friction angle
ϕ_s	Angle of surface frictional resistance

σ_1	Major principal stress
σ_3	Minor principal stress
σ_{xx}	Normal stress in x direction
σ_{yy}	Normal stress in y direction
σ_v	Vertical normal stress
σ_h	Horizontal normal stress
τ	Shear stress
τ_{xy}, τ_{yx}	Shear stress in x-y direction
ν	Poisson's ratio
υ	Dilatancy angle
ω	Moisture content
χ	Angle of principal stresses
γ_{xy}	Direct shear strain in x direction on x-y plane

These symbols are used in this thesis or otherwise stated.

LIST OF FIGURES

Figures in appendices

LIST OF PLATES

LIST OF TABLES

CHAPTER 1

INTRODUCTION

The importance of an adequate foundation was emphasized by Mr L J Cox, the former president of the Institution of Highways and Transportation. After having been actively involved in pavement design and construction for 50 years, he said, "do not skimp the foundation at the expense of what goes on top" (Cox 1987). In the U.K. a road foundation is primarily made up of two distinguishable layers known as sub-base and subgrade. The sub-base usually consists of granular materials comprising crushed rock. The subgrade is the upper part of the natural soil or fill material. If the subgrade is weak, an intermediate layer (often granular), known as 'capping', may be laid on top of the soil. Figure 1.1 shows cross-sections of two typical pavement foundations in the U.K. Even before the completion of a road, the foundation has already performed its most demanding role by providing a structural platform to bear direct loading from heavy construction plant. Then it supports loads from road traffic (transmitted through the upper bound layers) throughout its design life. It must provide this support without deforming excessively. Otherwise, excessive rutting, causing discomfort and danger to drivers, will be reflected on the surface of roads and finally makes the road untraffickable. Even if the deformation is recoverable, excessive resilience can shatter the upper bound layers by allowing the entire pavement structure to flex too much. To provide a reliable pavement foundation, it is important for the designer to make a good prediction of the response of such foundation layers to traffic loading.

A description of materials in terms of both :-

a)   resilient response, and
b)   resistance to permanent deformation

is necessary because the resilient response governs the load spreading ability and enables a structural analysis to be performed. The resistance to permanent deformation relates directly to the way in which foundations fail by rutting.

The materials of concern in a foundation are essentially geotechnical ones. As such their properties may be expected to vary in accordance with:

1
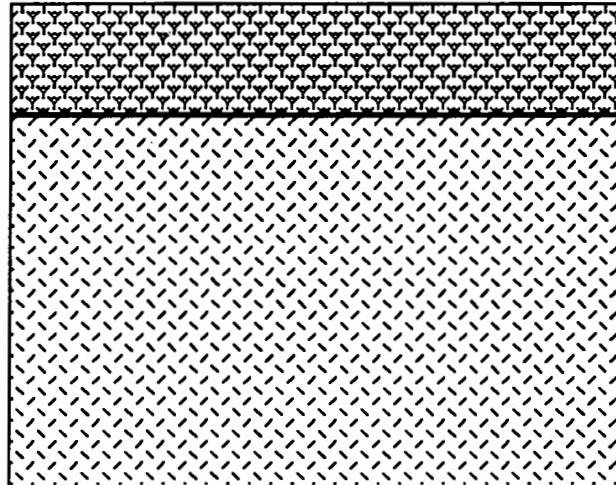
sub-base layer
(unbound granular
materials)

subgrade
(soils)

Figure 1.1a A typical pavement foundation
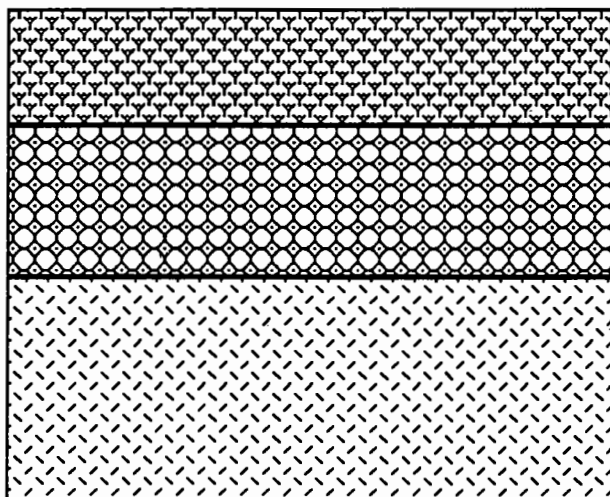
sub-base
(unbound granular
materials)

capping
(unbound granular
material)

subgrade
(soils)

Figure 1.1b A pavement foundation for weak subgrade

a)   location (geographical variability),

b)   environmental effects - particularly moisture, and

c)   stress regíme - geotechnical materials are normally highly stress dependent as far as their mechanical properties are concerned.

Due to these complexities and the lack of understanding of material behaviour, it is not difficult to see why current foundation design and material property characterization are largely empirical. However, the best that an empirical test value can give is a comparison of different materials. No satisfactory analytical design method based on understanding of material behaviour can possibly be evolved from it.

Current situation

The main pavement design documents in use in the U.K. are produced by the Department of Transport, DoT, (1987 and 1993). They are supplemented by TRL Laboratory Report 1132 by Powell et al (1984) and Research Report 87 by Mayhew and Harding (1987). Indirect methods for the control of pavement foundation materials dominate the DoT's specification (1992). The TRL report emphasizes the need for the use of a rational design method but the tests it relies on are basically empirical in nature. Perhaps the most relevant test is the California Bearing Ratio, CBR (described in Chapter 2) but it is (at best) a strength test and thus can only be empirically related to the fundamental properties of resilient response and permanent deformation resistance mentioned above. Other common measures to describe foundation materials are particle size distribution analysis, plasticity tests, compaction tests, moisture content tests etc. Meeting these requirements of the specification cannot guarantee adequate performance, although progressive tightening of the permissible limits over the years now prevents excessive problems. Nevertheless, in so doing, many perfectly adequate sub-base granular materials are excluded simply because it has not been possible to formulate an empirical rule which will confidently discriminate between good and bad. It does not allow a thinner than typical layer of sub-base for materials of excellent load spreading abilities. Furthermore, in order to allow for the inadequacy in predicting the actual material response under trafficking, under-estimation of the ability of the subgrade to support traffic is often made as an inevitable consequence.

Clearly the deficiencies in the current procedure - which is unable to provide the resilient strain and the permanent deformation characteristics of foundation materials - may lead to inefficiency by :-

(a)   unnecessarily excluding some materials,

(b)   not fully capitalizing on the materials which are used, and

(c)   making over-conservative assumptions about the subgrade.

From the economic viewpoint any appraisal of pavement failure should appreciate the tremendous effect of a defective foundation; it is not cheap to strengthen the surface, dearer to replace the road base but most expensive to dig the foundation up. A high cost to society will also be incurred when premature failure does occur, causing traffic congestion due to substantial road maintenance. On the other hand, pressure from limited resources and available budgets discourages any form of overdesign of the pavement and its foundation. It is for these reasons that a reliable design procedure based, in turn, on accurate material characterization, is required. In the light of such a need, Transport Research Laboratory, TRL, initiated a research programme in order to look into ways to improve the current pavement foundation design. The work presented in this thesis was part of this programme and was sponsored by TRL.

Possible solutions

For a reliable pavement design procedure, it would be necessary to examine the behaviour of the foundation materials as they exist in-situ during the life of the pavement. A partial means of meeting this goal would be by means of full-scale testing. However, the time involved and money required to carry out full-scale tests are enormous. Furthermore such testing can only describe the soil and aggregate under the stress and ground water conditions current at the time of testing. Due to these restrictions it is impractical to use this type of test as a routine design procedure. A better way of meeting the aims is by means of relevant laboratory testing. Carefully designed laboratory tests allow materials of different types, grading, density, moisture content, plasticity and other parameters to be assessed under stresses representative of in-situ conditions at any chosen time. Materials proposed to be used in the sub-base layer can thus be tested before being selected. The ability of the existing subgrade soils to support the upper layers can also be examined.

In the last few decades, substantial research effort has been directed to the study of the behaviour of pavement foundation materials. As a result, the non-linear stress-dependent behaviour of both unbound granular materials (Hicks 1970, Pappin 1979, Thom 1988) and soils (Brown and Pappin 1982, Loach 1987) has been modelled. Furthermore, rapid growth of computer technology has led to success in developing

computer programs to calculate the response of the pavement based on these non-linear models (Brown and Pappin 1982, Almeida 1993). To determine these stress-strain relationships, various types of apparatus designed to simulate the effect generated by a moving wheel have been developed at the University of Nottingham :

(a)   repeated load triaxial apparatus (Lashine 1971),
(b)   cyclic simple shear box (Ansell 1977), and
(c)   repeated load hollow cylinder apparatus (O'Reilly 1985).

Of these, the repeated load triaxial apparatus, although not without its limitations (which are discussed in Chapter 2), has found most favour. There are two major reasons. A triaxial specimen is not difficult to set up when compared with other repeated loading tools and the repeated load triaxial apparatus is able to simulate most stress conditions under the wheel such as repeated loading, shape of load pulse and loading frequency. Hence, this apparatus is a promising device to be used in material testing for routine purposes. However, its relative complexity in the current form means that such a device has never been used for the routine assessment of the U.K. pavement foundation materials.

Aims, approach and scope

In response to the foregoing, the main objective of the research constituting the basis of this thesis has been to develop laboratory test methods for the determination of the fundamental parameters, for analytical pavement design and analysis purposes, of foundation materials. In so doing, the aims have been to provide tests and procedures which

(a)   can provide appropriate test conditions,
(b)   have the capacity to describe pavement foundation material behaviour, and
(c)   can be routinely used in practice.

This approach should then enable a rational pavement design based on the mechanical behaviour of the materials to be carried out and a maximization of the available resource to be made.

To achieve these aims, two simplified repeated load triaxial apparatuses, one for granular materials and one for soils, were developed. It was also necessary to develop

associated testing procedures for describing the behaviour of the materials in the sub-base and the subgrade. The apparatuses and testing techniques developed were critically examined to assess their applicabilities and to demonstrate their likely performance. To do this, materials were first examined by existing routine tests and available non-standard tests before the main investigation. Although the major effort has been the development work, in the process of the study attention was also given to develop a further understanding of materials under repeated loading.

While this research was going on, there were two other parallel studies concerning other aspects of pavement foundation design improvement, which were also sponsored by TRL. The first one was a pilot scale site trial (Fleming and Rogers 1993) to study the performance of unpaved road foundations. The work should contribute much information to check the ability of mechanistic design methods and to calibrate and validate the test methods described here. The other was to develop a device which would enable on-site evaluation of the performance of pavement foundations to be carried out routinely (Brown 1992). These two projects were carried out at Loughborough University of Technology. However, site trials and on-site evaluation work are not within the scope of this study.

Although foundations do, from time to time, include bound or cemented materials, it was not the intention of this research to extend the scope to cover these materials. Furthermore, the study of frost heave and permeability, which constitute other pavement foundation criteria, are also outside the scope of this research.

Thesis arrangement

This thesis is presented in eleven chapters which, apart from the introductory chapter, are grouped into four parts.

Part A, containing the second chapter, is a literature review including coverage of the dynamic responses of pavement foundation materials and of the capabilities of the repeated load triaxial apparatus and other possible laboratory devices.

Part B, is devoted to the work on unbound granular materials. The development and details of a simplified repeated load triaxial apparatus fully instrumented to provide accurate test results and suitable for testing granular materials at full grading, are presented in Chapter 3. The selected materials and the related preliminary testing are

dealt with in Chapter 4. This is part of the investigation into the potential of the testing method to describe materials of different nature, grading, density and particle shape etc. The tests for characterizing granular materials by the newly developed repeated load triaxial apparatus are described in Chapter 5. Details of the test results are also presented and discussed.

Part C presents the work on subgrade soils and it similarly consists of three chapters. The design and development of a smaller repeated load triaxial apparatus for soil specimens is described in Chapter 6. In Chapter 7 preliminary tests on the selected soils are described. The permanent deformation behaviour of soils under direct wheel loads is also studied. Details of the tests on soils using the new repeated load triaxial apparatus, including their results and discussion, are presented in Chapter 8.

Part D comprises the last three chapters of the thesis. Chapter 9 summarizes the main features of the two simplified repeated load triaxial apparatuses developed in this study. Presentation of the main conclusions on the test results is given. In Chapter 10 the practical implications, which result from the provision of the new test methods, are discussed. Finally, recommendations for future work are made in Chapter 11.

PART A

REVIEW

CHAPTER 2

REVIEW OF LITERATURE

This literature review starts by looking at current U.K. practice (DoT 1992 and Powell et al 1984), focusing on the degree of relevance of the tests for pavement layers engineered to provide an adequate support for construction and normal traffic loads. Realizing the shortcomings of the current practice, the review moves firstly to identify the general characteristics of stresses in the pavement foundation layers induced by wheel loads. Then the mechanical behaviour of the component materials of the foundations under such loading is reviewed. Other factors contributing to the mechanical behaviour of the materials are highlighted. Analytical design also requires that material or layer testing generates the correct parameters for incorporation into design procedures. For the past few decades, the University of Nottingham has played a leading role in developing test methods for pavement design. An appraisal of the laboratory testing methods mainly developed in Nottingham is made.

2.1   CURRENT DESIGN TESTS

At the present time the chief tests for pavement foundation materials, common to the sub-base aggregates and the subgrade soils in the U.K. are; the California Bearing Ratio test, the grading test, the plasticity and the moisture content tests (DoT 1992 and Powell et al 1984). Other tests for soils are the Moisture Condition Value (MCV) and compaction determinations. For granular materials additional tests employed are the Ten Percent Fines (TPF) and aggregate soundness tests.

(a)   CBR test

Most of these methods provide little or no information which describes material response under trafficking. The most relevant test in the specification which gives an indication of material performance is the California Bearing Ratio (CBR) test. The test was a method developed for road aggregates in the USA in the late 1930s. As a matter of urgency during the second world war this test was adopted for subgrade strength determination; because of its simplicity the CBR test has been used in many countries and the U.K. continues to adopt it as a basis for road foundation design. It is a small

scale shear test. In practice this should limit the test to soils finer than gravel-size. Hight and Stevens (1982) highlighted the shortcomings inherent in the CBR test showing that the stresses on the specimen under the plunger were complex and indeterminate. Dawson et al (1990), after a comprehensive review, recommended that the first task for pavement foundation design was to consider the failure (or serviceability) modes. They are:

(a) excessive resilience (may cause large resilient strains and hence fatigue in higher layers),

(b) excessive permanent deformation under repeated loading (may result in surface rutting), and

(c) excessive deformation under single loading (leads to large localised shear distortion).

Each of them can be related to a conceptually simple material parameter - elastic stiffness, plastic behaviour (resistance to permanent deformation) and shear strength respectively. Dawson et al further suggested that the first two are normally the critical criteria. Based on low stress wave propagation techniques, Heukelom and Klomp (1962) proposed a relationship between the stiffness, E_r or M_r and the CBR values:-

$$M_r = 10 \, CBR \quad (MPa) \tag{2.1}$$

Another attempt to develop a single relationship between M_r and CBR value was made by Powell et al (1984). They modified the equation to:-

$$M_r = 17.6 \, CBR^{0.64} \quad (MPa) \tag{2.2}$$

Hight and Stevens (1982), however, pointed out that the test was unlikely to yield any purely elastic parameter but, rather, would give an indication of the combined effect from the stiffness and shear strength of the specimen. Based on results from a series of tests using both repeated load triaxial and CBR apparatuses, Brown et al (1987) concluded that direct correlation between elastic modulus and CBR value was unrealistic. The stiffness depended on the magnitude of repeated deviator stress, q_r, and was affected by soil types (Figure 2.1). Although the formula suggested by Powell et al (1984) had made an improvement to the earlier relationship (Equation 2.1) and put the curve into the correct shape, it was only true for one particular deviator stress and took no account of the effect of the soil types. Sweere (1990), working on

8
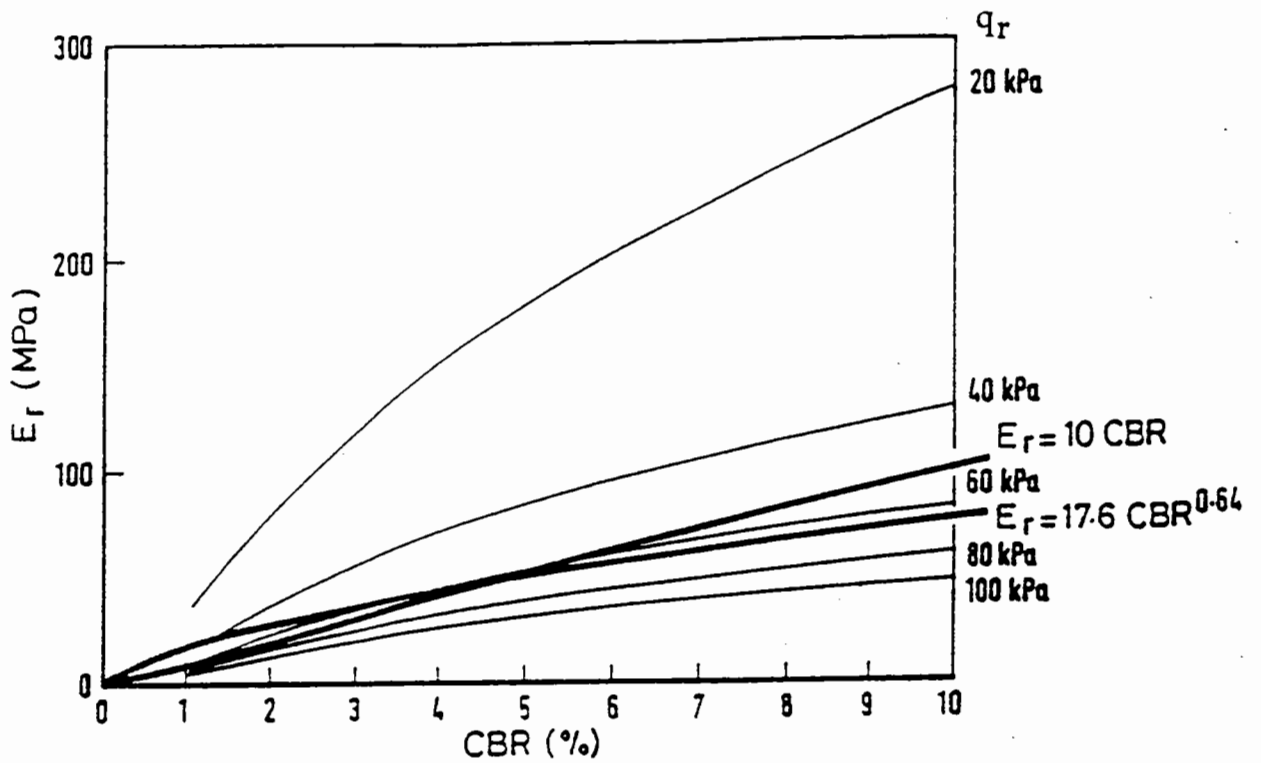
Figure 2.1a The relationship between stiffness and CBR for compacted samples of Keuper Marl for a range of stress pulse amplitudes (Brown et al 1987)
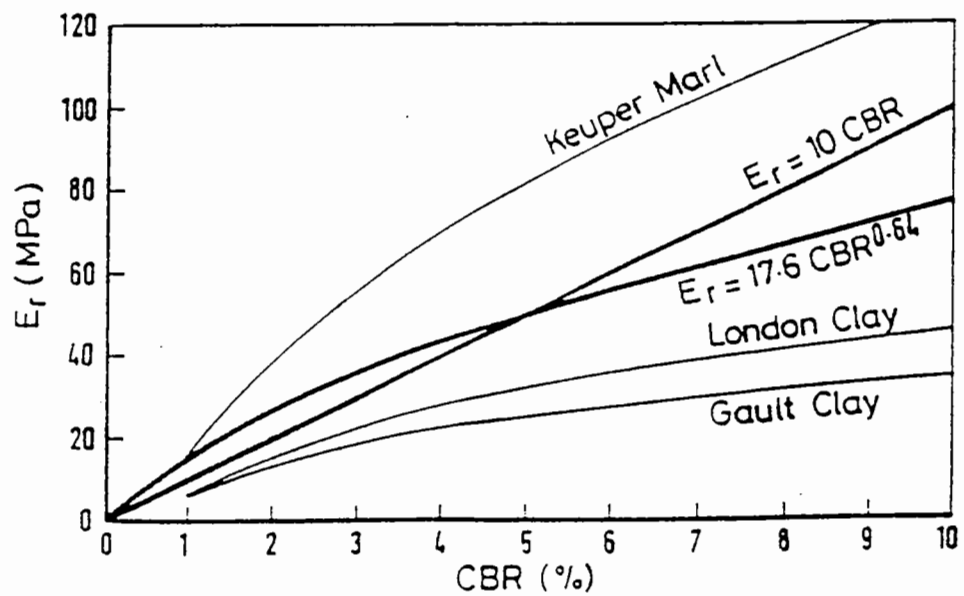
Figure 2.1b The relationship between stiffness and CBR for a stress pulse of 40 kPa for different compacted soils (Brown et al 1987)

unbound granular materials, concluded that there was no relationship between CBR values and material stiffnesses.

(b)   Other tests for aggregates

Most specifications include a grading requirement for sub-base materials. It is thought that the intention is to keep a high density and a concomitantly high shear strength. By trafficking trials on gravels and sands, Earland and Pike (1985) noticed that materials outside the grading envelope specified by the DoT provided the stability that a road foundation required and thereby demonstrated that an abundantly available resource could be excluded from pavements simply because of a failure to comply with the empirical grading envelope.

A limiting plasticity index value for aggregate fines is often specified. The purpose of the plasticity requirement for sub-base materials is to limit variation of shear strength due to water content fluctuation and also because aggregate including more plastic materials are generally weaker. However, achieving the plasticity requirement gives little or no guarantee of good material performance under trafficking. The ten percent fines value test and the soundness test are provided to describe the degree to which aggregate particle may degrade. Strength to resist aggregate breakdown from compaction force is therefore assured. The tests may also provide a measure of confidence against in-service compaction and irrecoverable deformation arising from particle degradation (Collis and Fox 1985). Nevertheless, by no means can the results obtained from these aggregate particle tests be used as a direct input for prediction of the ultimate performance of the sub-base materials.

(c)   Other tests for soils

On the other hand, the grading test for soils in subgrades is mainly used as a means of material classification with respect to their particle size distribution. The MCV test and the compaction test provide a guide for field compaction. Hence, proper compaction to a high density can be assured. The main reason for measuring the plasticity and the moisture content is chiefly to estimate the possibility of excessive swelling and shrinkage in remoulded soils after compaction. Again, the results of all these soil tests provide little information for the structural design of pavement foundations.

Realizing the shortfalls of the existing empirical design methods, appeals for representative tests to determine the stress-strain response of foundation materials have been made by Croney (1977), Wood and Boud (1987), Curtis and Loveday (1987) and Dawson, Brown and Barksdale (1989).

2.2 STRESSES UNDER A MOVING WHEEL

Extensive research has shown that both resilient and permanent deformation responses are sensitive to stress level (Barksdale 1972, Boyce 1976, Pappin 1979, Lentz 1979, Mayhew 1983, Loach 1987 and Jouve et al 1987). The complex stress pattern induced by a travelling wheel on an element in a pavement foundation is illustrated in Figure 2.2. Radial and vertical stresses produced are positive since unbound materials in a foundation do not carry significant tensile stresses. Both stresses are similar in shape to a haversine. The form of the shear stress pulse looks like a modified sinusoidal curve with zero shear stress at the maximum vertical pressure. Due to the form of the shear stress pulse, the axes of principal stresses rotate according to the location of wheel. The amplitude of the individual stress depends on the depth of the element considered, the wheel loading and the stress-strain relationship of the materials. Another characteristic of the wheel load is the time period of stress pulses (which determines the frequency of a pulse) generated. This was studied by Barksdale (1971). He reported that the time period was a function of vehicle speed and the depth of the elements beneath the pavement surface. For a typical flexible pavement with a 300 mm thick bound layer on top of a 250 mm thick unbound sub-base, the estimated pulse time is about 0.04 s at the top of sub-base layer and 0.07 s at the surface of the subgrade when a vehicle is travelling at 72 km/h. During the construction period and after completion of the foundation, assuming the normal speed of construction plant is 24 km/h, the pulse period will be 0.06 s at the surface and 0.11 s at the formation level.

To get a general picture of the magnitude of vertical stresses generated by wheel loads at various depths in the foundation structure, the computer program, BISTRO (Peutz et al 1968), which is based on linear elastic theory, was called upon (but noting that the behaviour of foundation materials is non-linear). Details of the pavement sections and the result are shown in Figure 2.3. Very high vertical stresses are found at the formation level and at the top of sub-base during the construction period. In this example, the stress levels in the unfinished pavement are about 10 times higher than that in the finished road at the top of the foundation and 8 times higher at the surface of the subgrade.

10

σ_V vertical normal stress
σ_h horizontal normal stress
τ shear stress
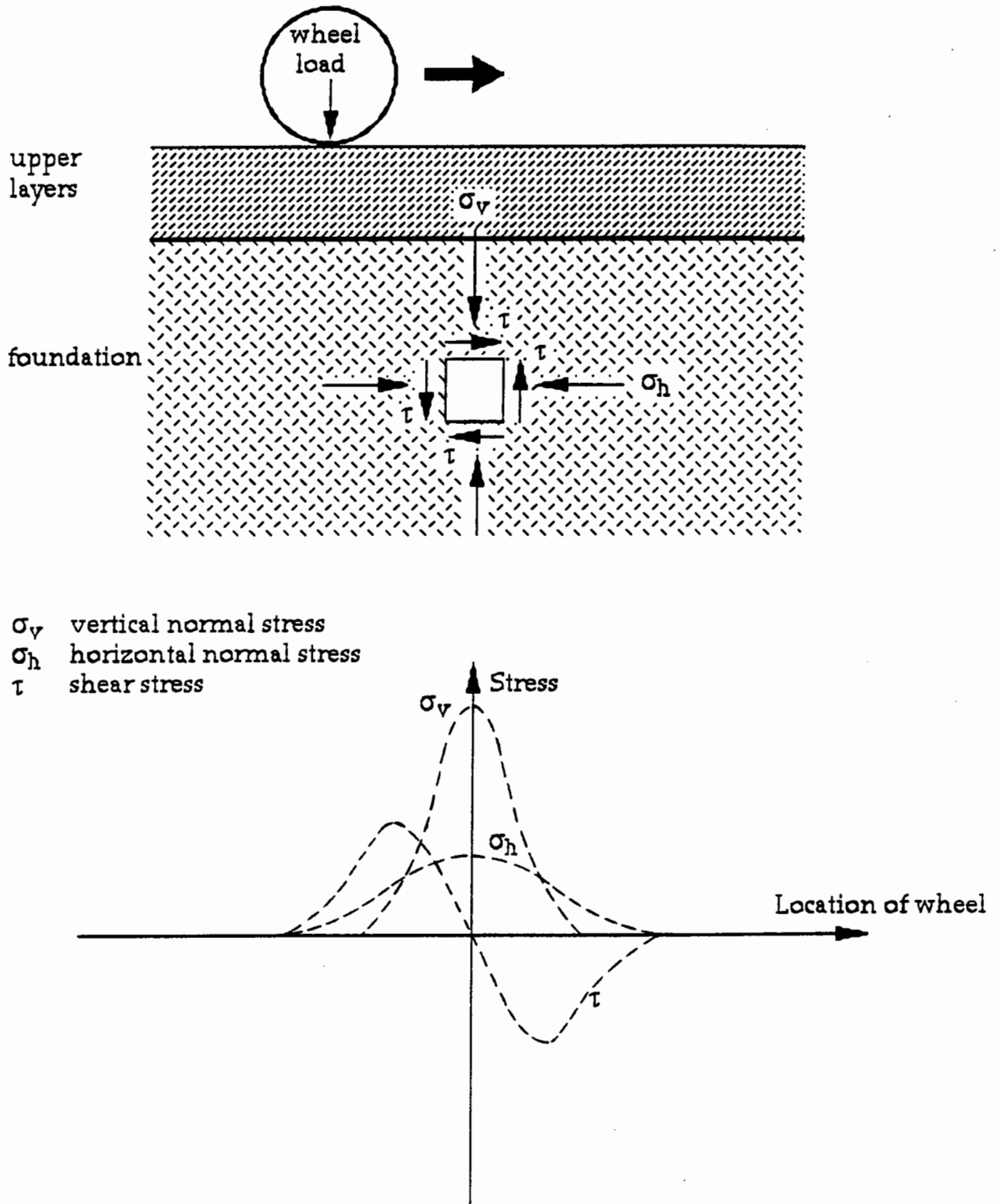
Figure 2.2   Stresses in road foundation under wheel load

contact stress = 700kPa
wheel diameter = 300mm

thickness = 300mm   bituminous
     E = 2100MPa   material
     v = 0.4 $\sigma_V = 50\,kPa$

thickness = 250mm   unbound
     E = 150MPa $\sigma_V = 18\,kPa$ granular
     v = 0.3   material

     E = 50MPa   soil
     v = 0.4
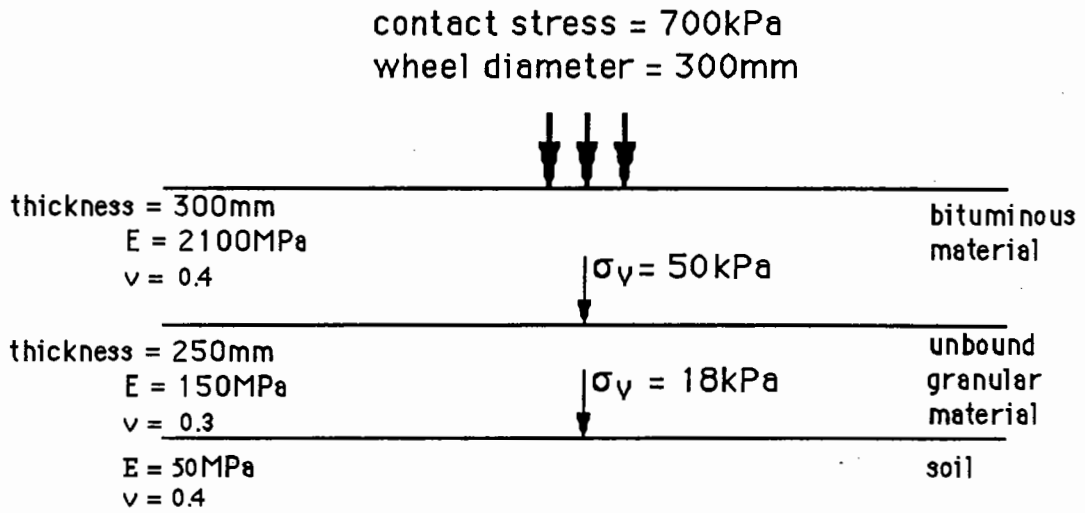
Figure 2.3a Vertical stresses of in-service road pavement

contact stress = 500kPa
wheel diameter = 400mm

thickness = 250mm   unbound
     E = 150MPa $\sigma_V = 140\,kPa$ granular
     v = 0.3   material

     E = 50MPa   soil
     v = 0.4
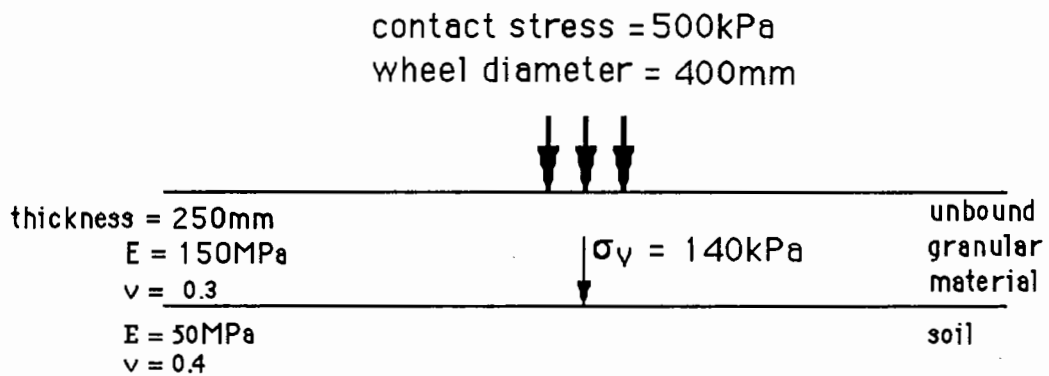
Figure 2.3b Vertical stresses of road pavement under construction

2.3 BEHAVIOUR OF UNBOUND GRANULAR MATERIALS

2.3.1 Effect of repeated loads

2.3.1.1 Resilient deformation

The load spreading ability of a material can be described by its resilient stiffness, which is determined from the recoverable strains during unloading. Materials of low stiffness do not spread loads well. Secant modulus has been widely adopted as the basic parameter to describe resilient strain behaviour. The secant modulus simplifies an unloading stress-strain curve by considering the end points of the curve only. In order to characterize materials more fully, it is increasingly common to present the resilient deformation behaviour in terms of volumetric and shear deformations.

The stress dependency of granular materials has been well documented. Brown (1967) carried out tests on model pavements and observed that the stiffness of granular materials increased non-linearly with applied stresses. Hicks and Monismith (1971) reported that the resilient stiffness of aggregates was heavily influenced by the summation of the three principal stresses. Materials became stiffer according to increasing confining stress. On the other hand, the stiffness decreased initially with increasing deviator stresses and then increased when higher deviator stresses were applied. Similar results were presented by Crockford and Chau (1988). Boyce (1976) reported that both volumetric strains and shear strains were functions of the applied stresses and could be expressed in terms of mean normal effective stress (p') and the stress ratio (q/p'). Pappin (1979) noticed that resilient shear strains were related to the length of stress path, the change in stress ratio, q/p', and the mean normal stress. Volumetric strains were independent of the stress path length but primarily related to the change in p' and affected by the change in q/p'. Chan (1990) investigated results from the repeated load triaxial test and the hollow cylinder test. He noticed that effects from torsional shear stresses on volumetric strains were apparent. On the other hand, the rotation of principal stress had little effect on the resilient shear strain.

2.3.1.2 Permanent deformation

Many previous researchers have reported that the accumulation rate of permanent strain under repeated loading decreases with the number of load applications. Barksdale (1972) noticed that the accumulation of permanent deformation of granular materials

11

was proportional to the logarithm of the number of load cycles. Chan (1990) applied repeated axial and shear loading to granular materials of maximum grain size of 5 mm by a hollow cylinder apparatus. He made a similar observation that most components of strain obeyed the logarithmic rule with regard to their development with the number of repetitions. Shenton (1974), testing single size granular materials, found that permanent deformation generated in the first cycle could be used to predict plastic strain development.

Lentz (1979) reported that permanent strains were not only related to the number of load cycles but also depended on the shape of the monotonic loading curve. Shaw (1980) proposed that loads with stress paths having peak values near to failure strength had significant effect on the permanent deformation response. Pappin (1979) suggested that the plastic strain development was a function of the number of repeated loads, the length of the stress path and the q/p' ratio. Thom (1988) made further observations on the non-recoverable strains of granular materials. He agreed with Lentz, Pappin and Shaw. A typical result from Thom showing the plastic strain development is reproduced in Figure 2.4. The stress dependent nature of aggregates is obvious. When the magnitude of the maximum deviator stress is the same, greater stress path length generates more strain. A lower maximum deviator stress of the same path length produces less strain. Furthermore, more strain will be obtained when the maximum deviator stress is closer to the monotonic loading curve. Thom also observed that the development of plastic strain of road aggregates under repeated loads depended on loading period. The plastic strain rate would be approximately doubled if the loading period rose by a factor of ten.

Wong and Arthur (1985), working with a directional shear cell on aggregates, found that plastic volumetric strain could be mobilized simply by rotation of principal stresses. Chan (1990) compared permanent deformation formed within samples when they were stressed with and without rotation of principal stresses in the hollow cylinder apparatus. He noted that the rate of plastic strain development was significantly increased when the stresses rotated. The effect of principal stress rotation was confirmed by his work on applying wheel loads on slabs of granular materials. Permanent deformation produced by a travelling wheel was found to be three times more than that when repeated wheel loads were statically applied in his test.
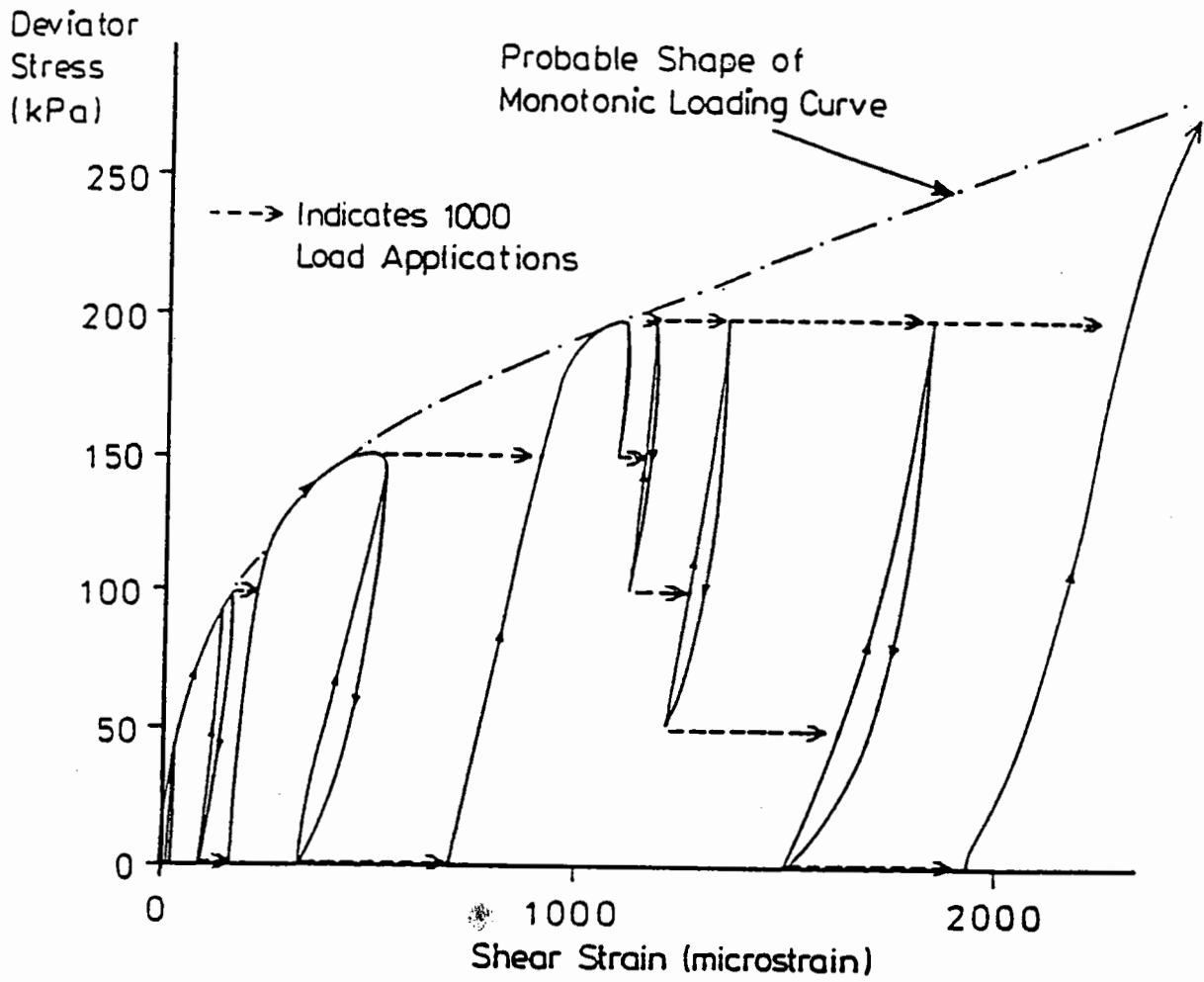
Figure 2.4 **Typical plastic strain development of unbound granular material** (Thom 1988)

2.3.2 Other factors affecting the material response

Most researchers have reported that the loading history does not have a significant effect on the resilient response of granular materials but does affect the plastic strain response (Brown and Hyde 1975). Barksdale and Itani (1989) and Thom (1988) published similar results indicating that greater compaction reduced the amount of plastic strains under repeated loading. Selig (1987) noticed that resilient response was unaffected by previous loading even when the load magnitude applied was near to the shear strength of the material. Brown (1974) applied a large number of conditioning load cycles before readings were taken in order to eliminate any sample imperfections caused during preparation. Allen and Thompson (1974) reported that after application of 50 to 100 numbers of repeated loads, a reasonably stable resilient response could be achieved. O'Reilly (1985) tested an idealized granular material made of single sized spherical to ellipsoidal particles. He observed that a resilient condition was attained after a few numbers of repeated loads. Sweere (1990) measured the resilient response of sub-base material at the 100th cycle. Measurements of resilient response were taken by Boyce (1976) during the first few cycles. Mayhew (1983) observed that, in general, materials became slightly stiffer after the first few hundred cycles.

Environmental effects were studied by Rada and Witczak (1981). They suggested that the resilient property was not only a function of stress but also depended on the degree of compaction. Nataatmadja (1989) noticed that provided sufficient drainage was allowed, the influence of moisture on both resilient and permanent deformation of uniformly graded materials was small. The influence of moisture was great on broadly graded materials. Thom (1988) suggested that the process of wetting and drying affected the resilient response. Little effect was found on materials which were wetting up. More severe effects were observed on materials which were drying - resilient stiffness could be double at drier states. When Nataatmadja examined the effect of the plasticity of the fines, he concluded that the effect of plasticity probably varied with the moisture content, amount of fines, grading and type of materials.

Barksdale and Itani (1989) illustrated that the surface characteristics of granular materials such as particle shape, angularity, surface texture and roundness affected the stiffness and permanent deformation characteristics of the sub-base aggregates. The significance of these physical properties was also noted by Thom (1990) when he studied the performance of aggregates from various sources under repeated loads. He pointed out that the surface characteristics of the large and small particles in the same

material could be different. He suggested that the stiffness was a function of the microtexture, and that the macrotexture of aggregates contributed to the resistance to permanent deformation and to the shear strength of the material. Nataatmadja reported that at the same compactive effort and with the same shape of particle grading curve, materials with larger maximum particle size produced smaller resilient strains. Aggregates following the Fuller's (1907) curve with a grading exponent, n, of 0.3 gave the highest resilient stiffness. Nataatmadja also presented results showing that there was an optimum grading for minimum plastic strain under repeated loading. For materials with a maximum particle size of 19 mm, a grading with an n value of 0.3 produced the least plastic strain. The optimum n value shifted to 0.5 when the maximum particle size was reduced.

2.4 BEHAVIOUR OF COHESIVE SOILS

2.4.1 Effect of repeated loads

2.4.1.1 Resilient deformation

Brown (1967) worked on a silty clay in model pavements. He concluded that the resilient stiffness of cohesive soils decreased non-linearly when the applied stress levels increased. Hyde (1974), testing an overconsolidated silty clay, demonstrated that soil stiffness increased with decreasing deviator stresses. Parr (1972) carried out repeated load testing on London clay and observed that the stiffness of soil specimens dropped when the pore water pressure increased. Lashine (1971) worked on a normally consolidated silty clay. He noticed that the soil stiffened with increasing mean normal effective stresses. Brown et al (1975) demonstrated that the resilient stiffness of cohesive soils varied with the deviator stress to effective normal stress ratio. When the stress ratio increased, the stiffness dropped. Results from Loach's (1987) work on both overconsolidated and normally consolidated soils showed good agreement with Brown's findings.

Linear relationships between soil suction and resilient stiffness were reported by Brown et al (1975). This finding was supported by Finn et al (1972). Fredlund et al (1975) tested clay soils. They noticed that the higher the soil suction, the higher the resilient modulus. The increase of stiffness they found was non-linear. A similar observation was made by Richards and Gordon (1972). They tested a clay soil and noticed that the

soil suction had a significant effect on the resilient stiffness. They used a logarithmic function to represent the relationship between them. Loach (1987) showed that the resilient axial strain of compacted soils could be represented as a set of contoured lines on a graph of deviator stress against suction. He concluded that the soil suction of a partially saturated cohesive soil had the equivalent effect to a mean normal effective stress of the same magnitude. He expressed the resilient strains in terms of the deviator stress to soil suction ratio.

In general, no conclusive effect on the resilient strain behaviour of cohesive soils due to the rate of loading has been reported (Seed et al 1955, Lashine 1971). Brown et al (1975) tested a silty clay at a loading frequency between 0.01 Hz and 10 Hz. They reported that resilient stiffness seemed not to be affected by the loading frequency. Wood (1980) suggested that the loading rate might affect the pore water pressure of samples. Materials of higher plasticity are more susceptible to the increase of pore water pressure. Loach (1987) applied large numbers of repeated loads at loading periods of 1 s and of 20 s on a saturated silty clay. He noticed that the mean normal effective stress remained unchanged and hence excess pore water had not been built up in his soil samples.

2.4.1.2 Permanent deformation

Parr (1972) studied the behaviour of London clay under repeated loads. He noted that generally the development of plastic axial strain increased linearly with the logarithm of cycle numbers. Jouve et al (1987) reported that both the plastic shear and volumetric strain characteristics of soils were quite similar to those of crushed rocks and related to the number of load cycles.

Kawakamo and Ogawa (1965) performed repeated loading tests on different types of soils under various confining pressures and compared the plastic strain rate at 10000 repetitions. For each soil type no obvious effect of confining pressure was found. Loach (1987) observed similar results on a silty clay at various confining pressures. He reported that the permanent deformation behaviour of his soil was not affected by variation of confining pressure. Seed and McNeill (1958) allowed the confining stress to cycle in phase with the axial stress. They noted that the permanent strain produced was slightly higher than that for static confinement.

Overy (1982) carried out tests on a silty clay. He reported that the soil could stand repeated loads of stresses higher than the failure strength obtained from compressive tests. Brown et al (1975) compared the resulting permanent deformations from static load testing with those obtained after 10^6 cycles in repeated load testing on a silty clay when the pore pressures and deviator stresses in the samples of both tests were the same. He noted that the latter test always produced less deformation. Hence the permanent deformation behaviour of soils under static and repeated loads are different. It is unlikely to predict plastic strains of repeated loads from the permanent deformation results of static tests.

Parr (1972) tested London clay at loading frequencies between 0.5 Hz and 30 Hz. No consistent difference in the permanent strain developed was recorded. A similar report was made by Seed et al (1955) when he applied load pulses at different time intervals.

2.4.2 Other factors affecting the material response

The influence of soil history has been studied by previous researchers. Generally, the history effect can be divided into two areas:

(a)   effect of overconsolidation (stress dependent) and
(b)   effect of thixotropy (time dependent).

Humphries and Wahls (1968) investigated the effect of overconsolidation in kaolinite and bentonite on soil resilient response. They reported that the effect from overconsolidation was negligible for the two materials. Results of Brown et al (1975) showed that resilient strains seemed to be independent of overconsolidation ratio. This was supported by Loach (1987) when he tested a silty clay at overconsolidation ratios between 6 and 18.

Material thixotropy was noted by Seed et al (1962) when they studied the change of soil stiffness under repeated loading. They found that soils stored for a period of time before testing were much stiffer than those tested immediately after compaction. They noted that the thixotropy effect was removed after about 4000 cycles of repeated loading. Loach (1987) studied the effect of thixotropy on different soil states. He observed that overconsolidated materials regained their original stiffness if time was allowed between two series of tests. For compacted samples the stiffness in the latter

16

series was found to be higher than before when sufficient rest time was allowed. He attributed the effect to reorganization of the internal soil structure during the rest period. Material thixotropy can be defined as the effect of stiffening solely attributed to time. Conversely, a softening effect, attributed to stress, was reported by Loach. He measured the resilient strains of three types of compacted clay soils at the 1st cycle and the 100th cycle of load. In his test program, samples were subjected to a series of repeated loads of increasing magnitude and then to a series of repeated loads of decreasing magnitude. The soils initially suffered from stress softening and the resilient strain generated in the 1st cycle was less than that in the 100th cycle. This was also reported by Lashine (1971). He reported that resilient modulus decreased with the number of load repetitions and became stable after 10^5 cycles. In Loach's unloading series, the resilient strains in the 1st and the 100th cycles were the same. But the resilient strain was greater than those in the earlier series at any given stress level. Results from a similar series but taken to a different maximum stress showed that the resilient strains of the unloading series were influenced by the previous maximum repeated load level.

Ahmed and Larew (1962) observed that when the soil moisture content increased, the resilient modulus decreased. Kirwan and Snaith (1976) applied repeated loading to a silty clay. They found that the resilient modulus could be related to the moisture content and the degree of compaction. Kirwan et al (1982) expressed the resilient modulus as a function of moisture content and dry density. Loach (1987) noticed that the resilient Poisson's ratio of all his compacted cohesive soils decreased with decreasing moisture content. He also noticed that the resilient modulus of compacted soils depended on soil suction which was in turn related to moisture content, but he reported that the resilient modulus was relatively unaffected by the change of dry density.

2.5 LABORATORY TESTING TECHNIQUE

In the laboratory, simulation of in-situ environmental and stress conditions can be attempted by tests of different degrees of sophistication. An appraisal of seven potential laboratory tests, each of which might have a useful place in an improved design method, is now made. Particular attention is given to:-

(1)   sophistication,
(2)   cost,

17

(3) ability of the test to produce stresses similar to those induced by traffic loading,

(4) ability of the test to yield parameters which measure resilient behaviour and/or permanent deformation susceptibility.

Table 2.1 gives a summary of the special features of the tests.

Table 2.1 Features of the laboratory tests

Facility	Large shear box	NAT	Repeated load triaxial	HCA	Pavement test facility	Slab test facility	SRTF	Traffic
Mode of loading	static	static & dynamic	static & dynamic	static & dynamic	single wheel	single wheel	single wheel	dual wheel
Peak vertical stress (kPa)	300	1400	1000	850	500	500	300	700
Static confining stress (kPa)	?	0	<400	<500	approx 0-35	approx 0-10	approx 0-2	approx 0-100
Loading time (ms)	0.12 mm/min	100-200	$10-10^6$	$10-10^6$	>150	>800	>1000	approx 30-100
Principal planes rotate	Yes	No	Instant 0-90	Yes	Yes	Yes	Yes	Yes
Diameter of contact area (mm)	300 square	150 or less	150 or less	O.D.280 I.D.224	<200	<150	approx 30	approx 300
Presentation of results	SS	SS Mr, PD	SS Mr, PD	SS Mr, PD	SD Mr, PD	SD Mr, PD	SD	
Multi-layer test	No	No	No	No	Yes	No	No	
Method of recording	manual	auto	auto	auto	auto	auto	manual	
Relative initial cost	medium	low	high	high	high	high	low	
Relative testing speed	fast	fast	fast	medium	slow	medium	fast	

where :- SS is shear strength, Mr is resilient modulus, SD is surface deformation and PD is plastic deformation. NAT, HCA and SRTF are Nottingham 'Asphalt' Tester, Hollow Cylinder Apparatus and Soil Rut Testing Facility respectively. O.D. is outside diameter and I.D. is inside diameter.

18

2.5.1 Large shear box

The idea of using a shear box (Figure 2.5) to correlate the performance of road sub-base materials has been developed by Pike (1973). A metal split box of size 300 mm square in plan by 180 mm deep is employed. This enables fairly representative aggregates, both in size and grading, to be tested. A static normal force is exerted on a steel cap at the top of the box, which is free to move vertically. Materials inside the box are then sheared along the gap between the top and bottom of the box by applying a static (i.e. slowly increasing) horizontal stress to the top half. Earland and Pike (1985), after conducting a series of full-scale trafficking trials and shear box tests, suggested that the ratio between the ultimate shear stress and the normal stress, the latter being set at 10 kPa, was able to distinguish the stability (resistance to permanent deformation) of unbound granular materials under wheel loads. A threshold ratio of 2.8 was proposed and the stability of granular materials were broadly classified into three zones:-

Low strength   = stress ratio < 1.9
Medium strength = 1.9 < stress ratio < 2.8
High strength   = stress ratio > 2.8

Thom (1988), from repeated load triaxial test results, also found the same general phenomenon that those materials of higher strength possessed better resistance to the development of permanent deformation under repeated loading.

Although the state of stresses in the shear box is somewhat indeterminate, and the test does not simulate the effect of moving wheels in terms of stress and time of loading, its simplicity makes it a very attractive test method. Furthermore, once the shear force is applied, the principal stress planes of the elements on the pre-defined shear surface rotate (Figure 2.5). This may be an additional advantage of the shear box test since principal stress rotation does effect the permanent deformation behaviour of granular materials (Chan 1990).

As indicated in Table 2.1, the large shear box may provide one of the cheaper solutions for dealing with large particle materials. However, it gives little indication of the resilient strain characteristic owing to the inherent difficulty of measuring or estimating stresses in the tested specimen and to the fact that it is unable to provide accurate displacement measurement required by resilient strain testing.

axial
load
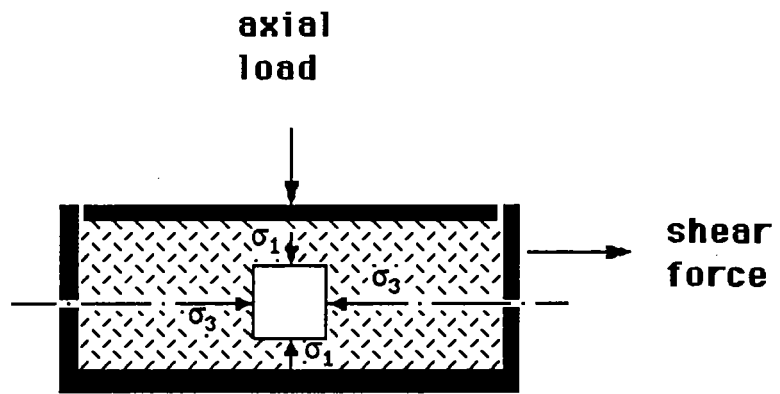
shear
force

Figure 2.5a Simplified diagram of shear box

axial
load
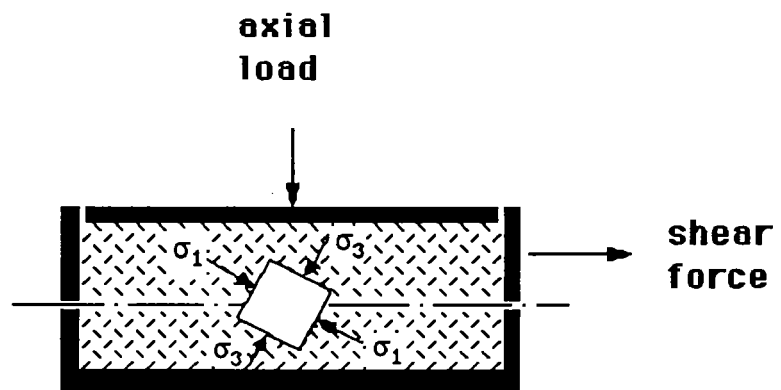
shear
force

Figure 2.5b Rotation of principal stress when shear force > 0

2.5.2 Repeated load triaxial apparatus

There are two repeated load triaxial facilities in Nottingham, one for testing unbound granular materials of specimen diameter 150 mm and the other one for soils of specimen diameter 75 mm. Both of them were constructed in the 1970's. Details of the latest development of the set-ups for granular materials and soils may be found in Karasahin (1993) and Raybould (1991) respectively. The principles of the construction of the two facilities are similar except that unbound granular materials necessitate an adequate specimen size (i.e. larger) to eliminate the particle to specimen size effect (refer to Section 3.2 for more details). The description of the apparatus given here is mainly based on the one for granular materials and only the main differences between the two are highlighted.

A cross-section of the apparatus for testing aggregates is included as Figure 2.6. This apparatus is able to generate independent cyclic or other repeated axial and confining stresses by a servo-hydraulic control system and a high pressure pump. Silicon fluid is used to transfer the confining stress to the specimen. Figure 2.7 shows the typical stress conditions produced by the facility. The vertical and horizontal stress pulses can be similar to those in pavements induced by traffic (Figure 2.2) but the applied shear stress is omitted. With the assistance of a signal generator, loading frequencies between 0.001 and 10 Hz can be provided to the confining stress and up to 100 Hz to the axial stress. Various wave forms including triangular, rectangular and sinusoidal are available. The magnitude of the applied stresses is controlled by a feedback system via load and pressure cells. The measurement of vertical deformation is made by a pair of Linear Variable Differential Transformers (LVDTs) mounted on the side of the specimen whilst radial strains are measured by two strain gauged hoops fixed across the specimen's diameter. They provide high precision displacement measurement. Signals transmitted from load cells, strain gauges and LVDTs are recorded digitally by a computer-based data acquisition system. In the repeated load apparatus for testing soil two pairs of LVDTs are used for monitoring vertical strains and two proximity transducers for radial strains.

It has been noted that the use of high precision displacement instrumentation is indispensable (Boyce 1976) especially when measuring the small movement involved in tests for determining resilient strain properties. Although only two independently controlled stress components are modelled by the repeated load triaxial apparatus and continuous rotation of principal stress cannot be reproduced by this equipment, when

- Hydraulic ram
- Pressure applied to cell
- Shear pin connection
- Loading ram
- Load cell
- Evacuated cavity
- O ring
- Top platen
- Brass stud
- Confining fluid
- Membrane
- Specimen
- LVDT
- Cell wall
- Strain hoop
- Bottom platen
- O ring
- Evacuated cavity
- Mounting block
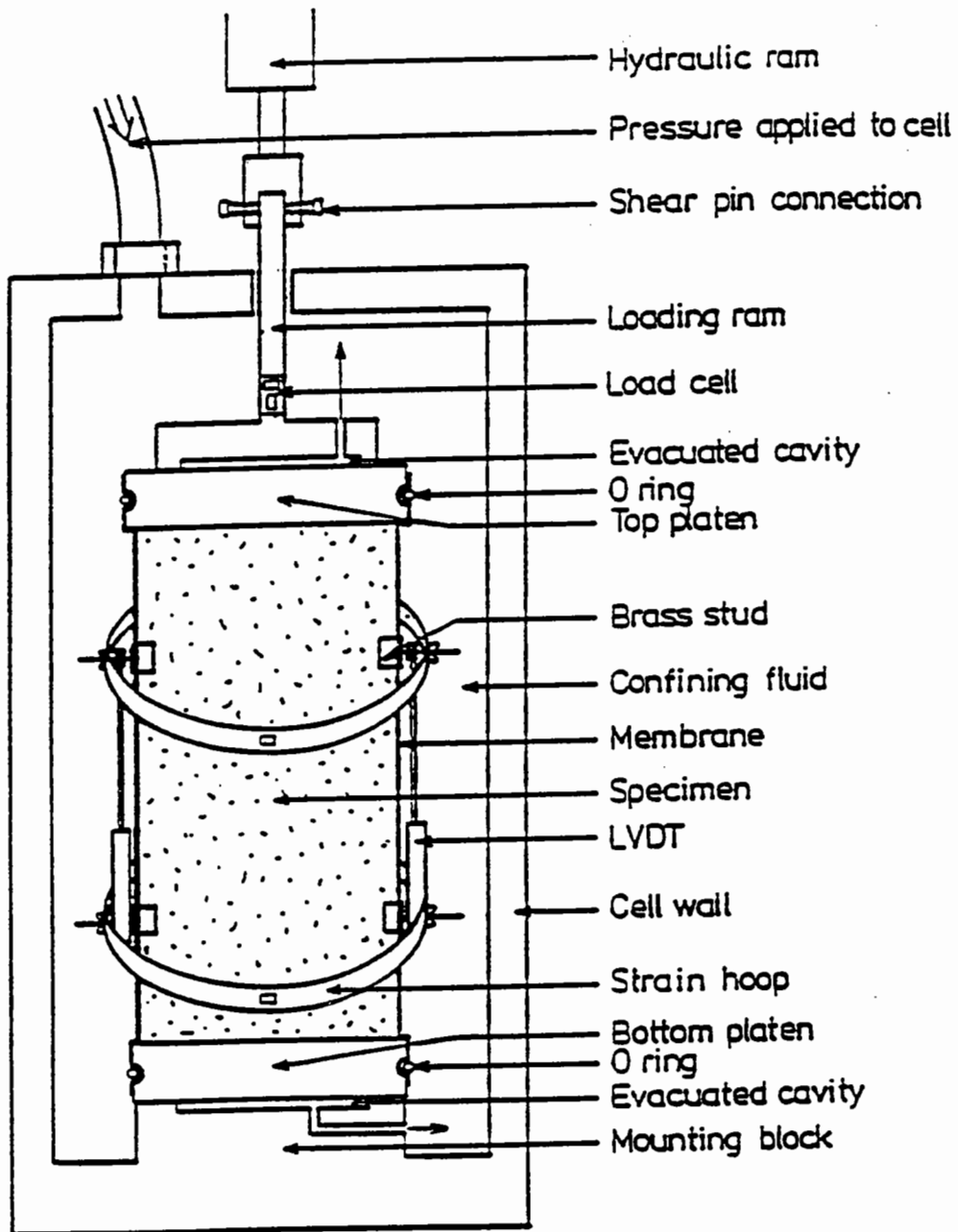
Figure 2.6 Repeated load triaxial apparatus (Thom 1988)

Total axial stress σ_1

Radial stress exerted
by fluid pressure σ_3

Cylindrical
soil sample

σ_3

σ_1

Stress

Haversine waveforms

σ_1

σ_3

Time
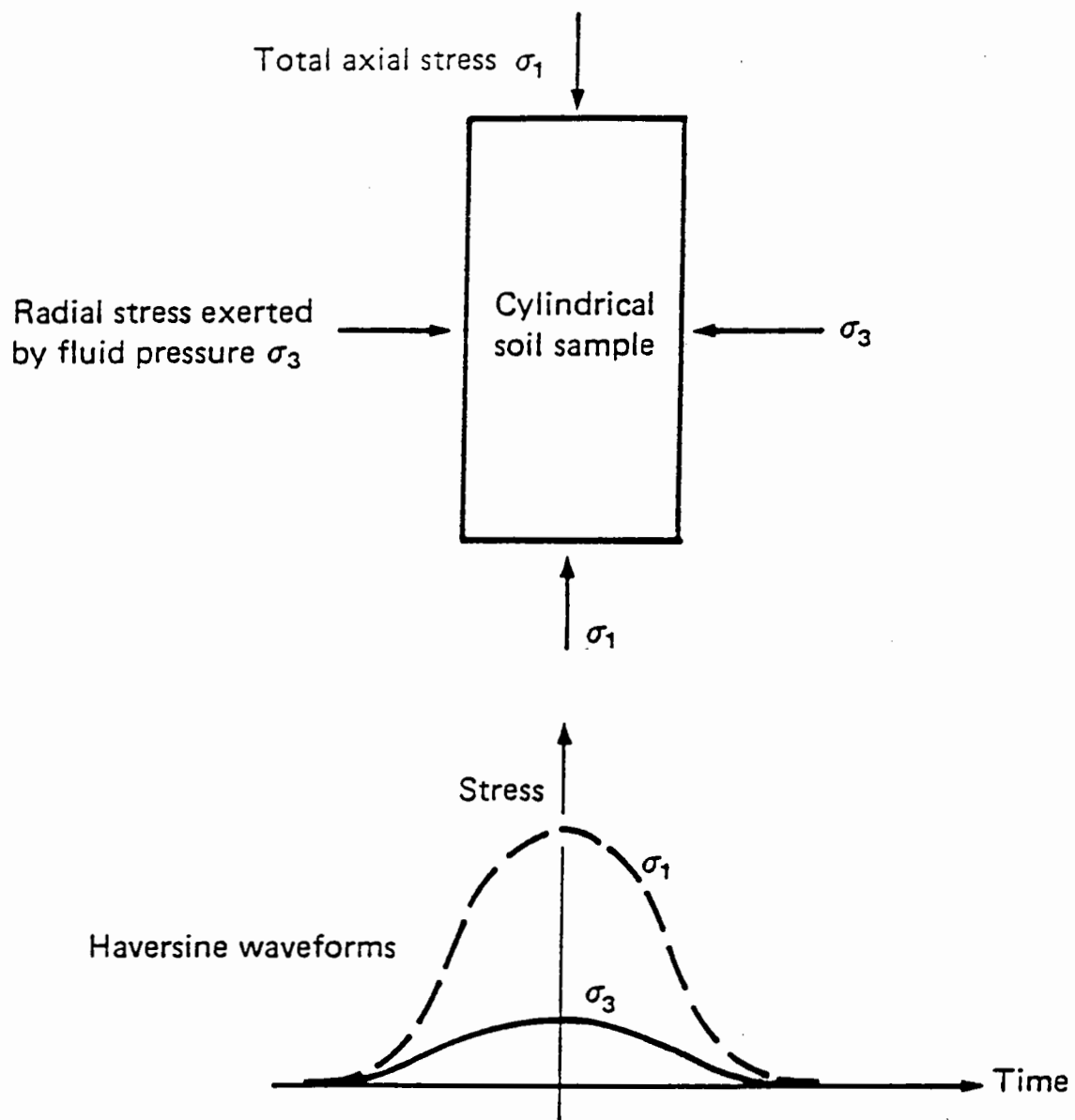
Figure 2.7 Principal stresses applied in the repeated load triaxial test
(Boyce 1976)

comparing with other devices such as the CBR apparatus or the shear box, it is one step closer to generate the real stress conditions in the pavement and to enable investigation of the fundamental behaviour of materials. The apparatus has been recognized as a research tool with which to understand the mechanical characteristics of soils and aggregates for use in road foundation design and with which to provide a sensible compromise between the complicated stresses produced by a wheel load and those reproducible in the laboratory . Indeed, the use of the repeated load triaxial apparatus has been recommended by the American Association of State Highway and Transportation Officials (AASHTO 1986) in the United States for resilient modulus determination of soils.

However, the current state of the device, including the complexity and the cost, would probably preclude its economic use for routine purposes in the U.K.

2.5.3 Nottingham asphalt tester

The Nottingham Asphalt Tester (NAT) is a flexible piece of equipment developed in Nottingham (Cooper and Brown 1989) to provide an easy-to-operate device for determining the fundamental mechanical behaviour of bituminous materials. In fact, since the development of the apparatus, it has begun to be accepted as one of the basic tools for investigating the resilient and permanent strain responses of bitumen bound materials (Elliott 1990). Because of its simplicity, it is considered that soil and, perhaps, unbound granular specimens might also be set up in the apparatus and their stress-strain relationships found.

The equipment is shown diagrammatically in Figure 2.8. The apparatus consists of a pneumatic loading system, supporting frame and a microcomputer. Axial stresses up to 100 kPa on a 150 mm diameter platen in a form approximating to a square wave can be applied by the loading system. The supporting frame is so simple that it can be changed to any reasonable size suitable for different kinds of materials. It also acknowledges the requirement of accurate strain measurement by incorporating high resolution displacement transducers consisting of LVDTs. With the assistance of a two way signal converter, a microcomputer can control the entire progress of the test and record signals sensed by the load cell and the LVDTs.

21
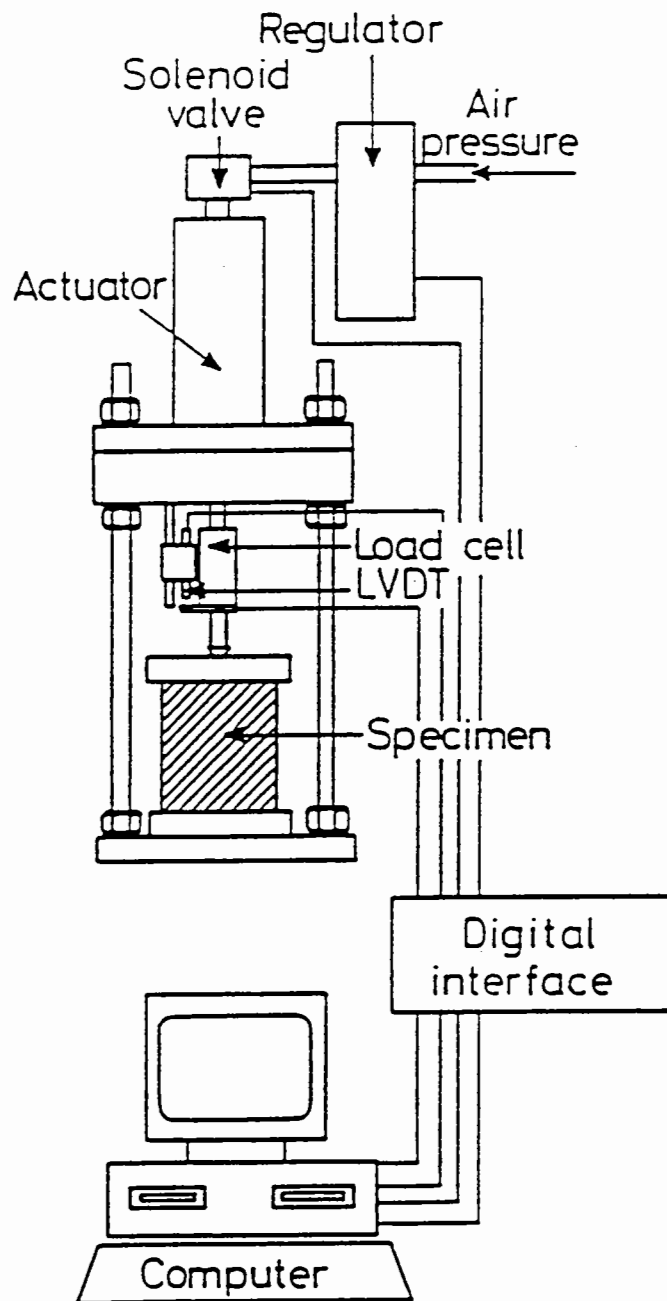
Figure 2.8 Diagrammatic layout of Nottingham Asphalt Tester
(Cooper and Brown 1989)

The present form of the equipment is, in effect, a simplified version of the repeated load triaxial apparatus without the external cell to provide confining pressures. Therefore, it can simulate the vertical stresses induced by a moving vehicle. A major difference from the Nottingham repeated load triaxial apparatus is that in the NAT the repeated axial load is applied by a pneumatic rather than a hydraulic system. Pressurized air is supplied from an air compressor or it can be conveniently provided by a compressed air cylinder.

The NAT is a simple device capable of applying uniaxial repeated loads. Not only the elastic behaviour, which is the necessary input data to a rational pavement design method, but also the resistance to permanent deformation can be measured. The reasons why the NAT have gained wide acceptance in the industry in a rather short period of time are, besides the ability to evaluate material performance in terms of resilient and permanent strain responses, that the initial and running costs are relatively low and the test procedure is relatively simple. However, any form of uniaxial repeated loading test may only simulate the vertical stress condition under road traffic.

2.5.4 Hollow cylinder apparatus

The Hollow Cylinder Apparatus (HCA) developed at Nottingham was designed by O'Reilly (1985) and modified by Thom (1988) and Chan (1990). It is a device which not only allows repeated loading but also permits the directions of the principal stresses to be rotated or, stated another way, for shear stresses to be applied to the tested specimen. This is the major advantage of the HCA over the repeated load triaxial apparatus which only allows one pattern of principal stress rotation (i.e. instantaneous 0-90 degrees).

The schematic diagram of the HCA is included as Figure 2.9. A cylindrical specimen of 280 mm outside diameter, height 500 mm and wall thickness 28 mm is used in the test. Two actuators are used to apply axial loads and torques. The figure also demonstrates the stress conditions on an element in the wall of the cylinder. When the specimen is only subjected to static axial and radial compression (from the cell pressure), it is similar to a pavement element at rest. When cyclic torque is directly applied, rotation of principal stress is induced. A maximum confining pressure of 500 kPa can be applied by compressed air both outside and inside the cylinder. Since the

22

HYDRAULIC PRESSURE SUPPLY

Servo-Controlled Hydraulic Actuator

Slip Coupling

Smoothing Bush

Top Cap

Load Cell

Load Platen

Top Plate

Outer Perspex Cell

Upper Specimen Ring

Hollow Cylinder Specimen

Sample Height 500mm

I.D. 224mm

O.D. 280mm

Lower Specimen Ring

Base

Steel Frame
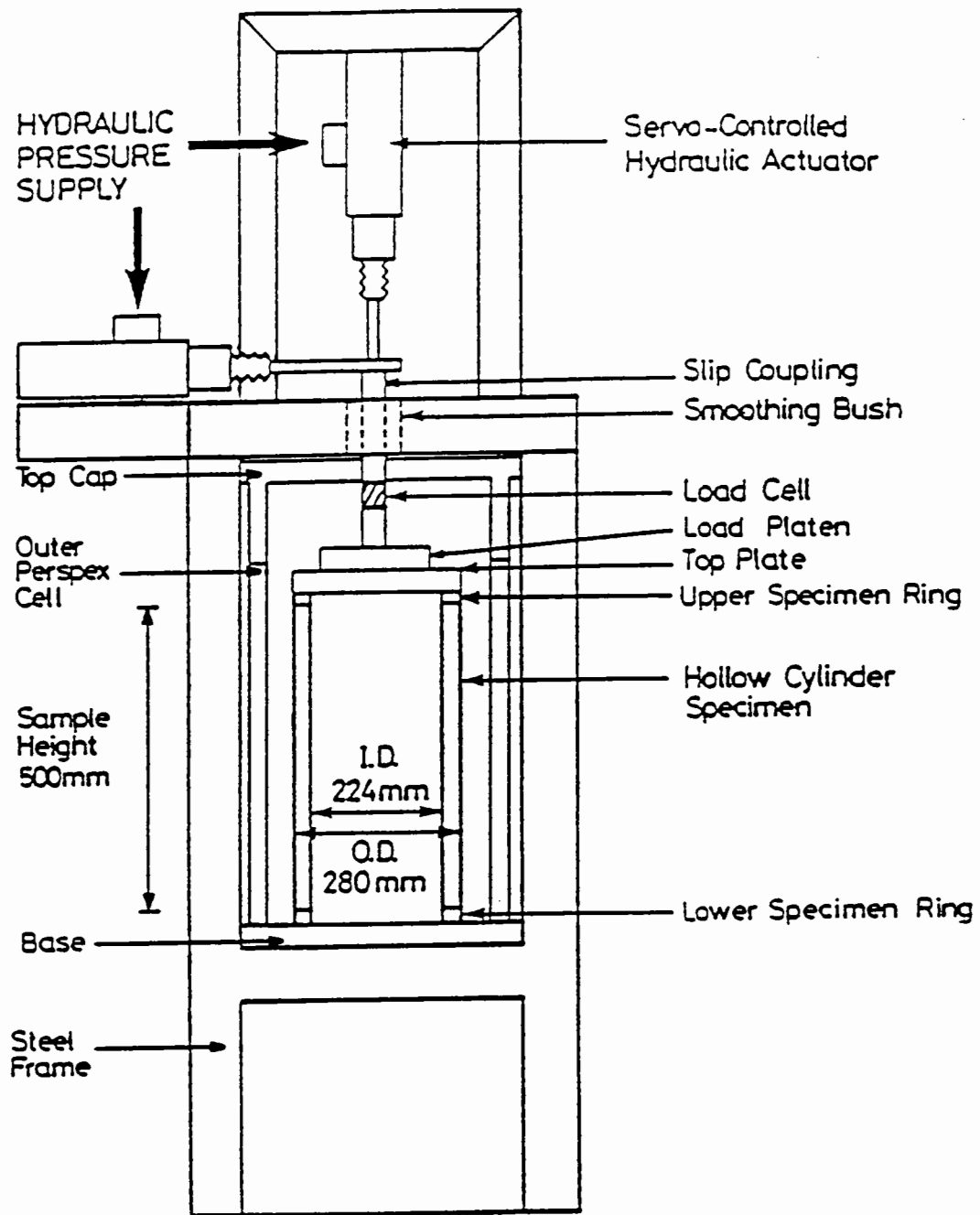
Figure 2.9a Diagrammatic layout of the repeated load hollow cylinder apparatus (Chan 1990)

σ_θ = circumferential stress
σ_z = vertical stress
$\tau_{\theta z}$ = shear stress in the θ–z plane
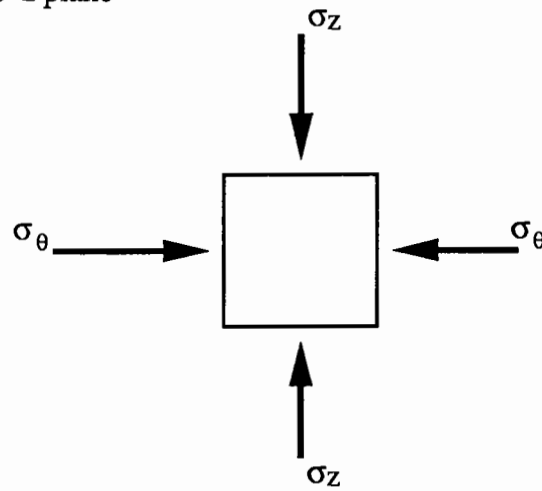
Figure 2.9b Condition with no shear in the hollow cylinder apparatus
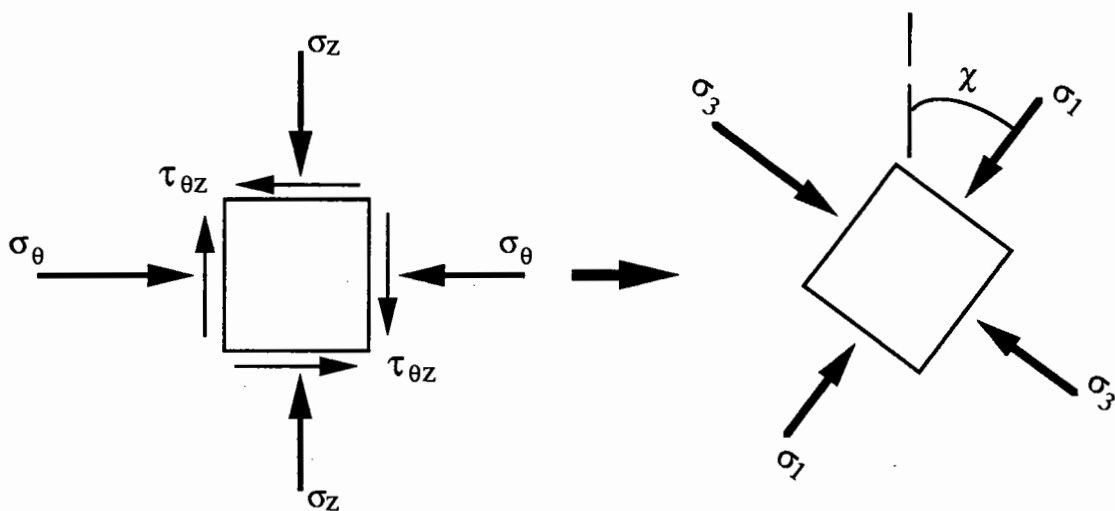
Figure 2.9c Condition with shear in the hollow cyclinder apparatu

two pressures can be controlled separately, it is possible to vary the radial stresses, as well as the circumferential stresses, on the specimen.

A similar control, instrumentation and data acquisition system are used as employed in the triaxial equipment (Section 2.5.2). The major differences are that two LVDT's orientated at 45° to the horizontal and two pairs of inductance coils are used to allow shear strains and changes of thickness in the wall to be assessed respectively. Hence accurate on-sample displacement measurement is provided.

Due to the sophisticated instrumentation and the ability to generate cyclic shear stresses and repeated loads in vertical and horizontal directions in the specimen, the HCA is one of the best laboratory devices to simulate traffic loads. The limitation of the HCA is that only small or scaled-down aggregates can be tested due to the thin wall (28 mm) of the cylinder. It is not able to test roadstones at their full grading: it is thus used primarily as a research tool in which to investigate the effects of repeated stress rotation so that this effect can be properly allowed for in design procedures which are based on more simple tests. Furthermore, because of the complexity of the setting up and testing procedures, it is not suitable for routine material testing even for fine grained materials.

2.5.5 Pavement test facility

The Pavement Test Facility (PTF) at Nottingham is a facility able to generate accurate performance data from a pavement of realistic size and under well controlled conditions. In effect it is a large model having most of the advantages of comparable full-scale test facilities but without the considerable labour and material consequences of full-scale testing.

The facility, which was described by Brown and Brodrick (1981), is illustrated in Figure 2.10. It consists of a pneumatic tyre of diameter 560 mm and width 150 mm fitted to a moving carriage which is in turn guided by two end beams. Realistic contact pressures up to 500 kPa with a wheel load of 15 kN can be applied by the hydraulic system. The maximum travelling speed of the wheel is 16 km/h and the wheel can travel loaded in one or both directions. The equipment is housed in a temperature controlled room. A pavement section up to 4.8 by 2.4 m with a depth of 1.5 m can be constructed. Stress and strain responses anywhere in the pavement can be closely

23
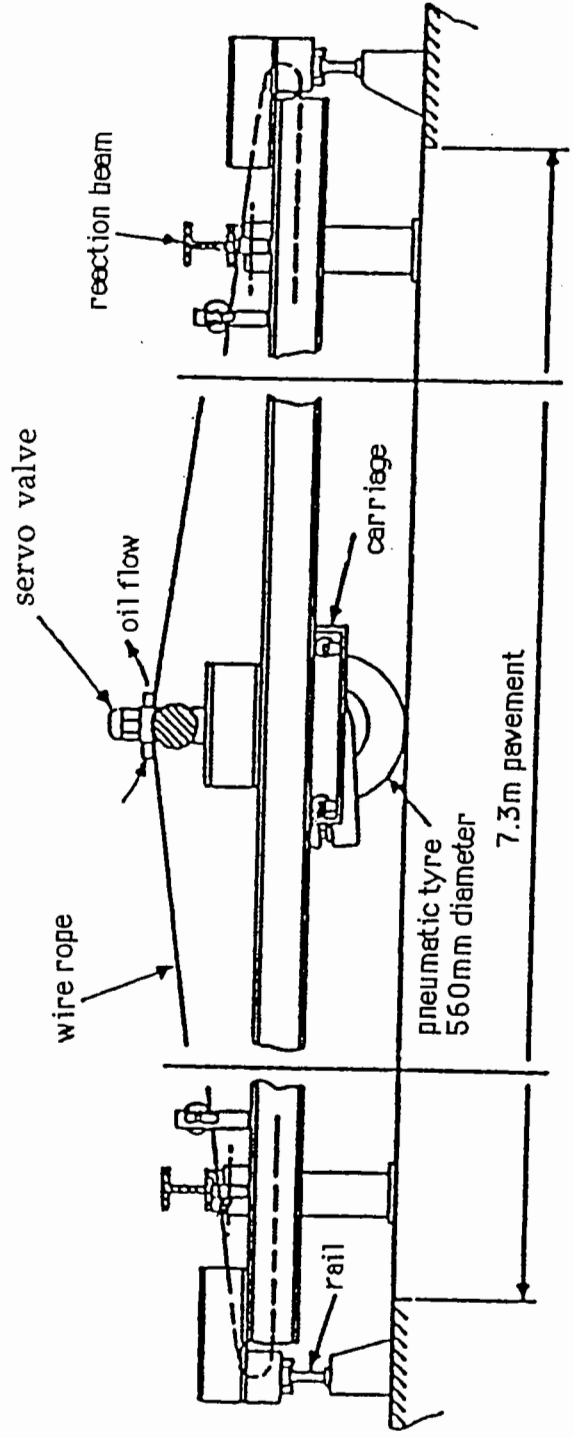
Figure 2.10 Elevation of the pavement test facility (Brown and Brodrick 1981)

monitored by pressure cells and inductance coils. Profiles of surface rutting are measured by an automated profilometer.

The PTF provides a medium to close the gap between road performance in real life and the design prediction based on simplified test techniques, and is a useful facility to validate any theoretical predictions of pavement behaviour. However, the cost of the facility and the amount to be paid in maintenance and running are high when compared with other laboratory tests. Furthermore, considerable amounts of materials and time are required to perform a trial, hence, the PTF cannot be used for routine purposes.

2.5.6 Slab test facility

The Slab Test Facility (STF) is a small scale PTF. However, it allows samples in the form of 250 mm thick slabs to be tested under wheel loads. The specimen preparation method can be by roller compaction that is similar to, although not exactly the same as, the compaction technique used on construction sites so that direct comparison of results can be made.

The slab test facility designed at Nottingham is illustrated in Figure 2.11. The main parts of the facility consist of two parallel steel beams supported at both ends which guide a carriage, on which a wheel 125 mm wide is mounted. A constant load up to 10 kN and a maximum contact pressure of 500 kPa can be applied through the servo-hydraulic system. Travel speed can be varied from zero to 6 km/hr. Accurate stress and strain measurements in the slab can be obtained by transducers installed in the specimen. Although the ability to assess the stress-strain responses of a full depth multi-layer pavement is limited by the depth of the slab, the time required to set up the test is small when compared with the full scale PTF. Therefore, it is used as a convenient device to represent the PTF when only the characteristics of a foundation material are to be assessed by a moving wheel. Testing one material at a time can be an advantage because it does not allow influence from other layers to be incorporated in the test results that complicates data analysis. Comparison of material performances is possible because standard support is provided. However, both the running cost and the amount of materials to be handled are still considered too much for routine testing. In practice the equipment is more likely to be of use in a research situation for design validation purposes.

24
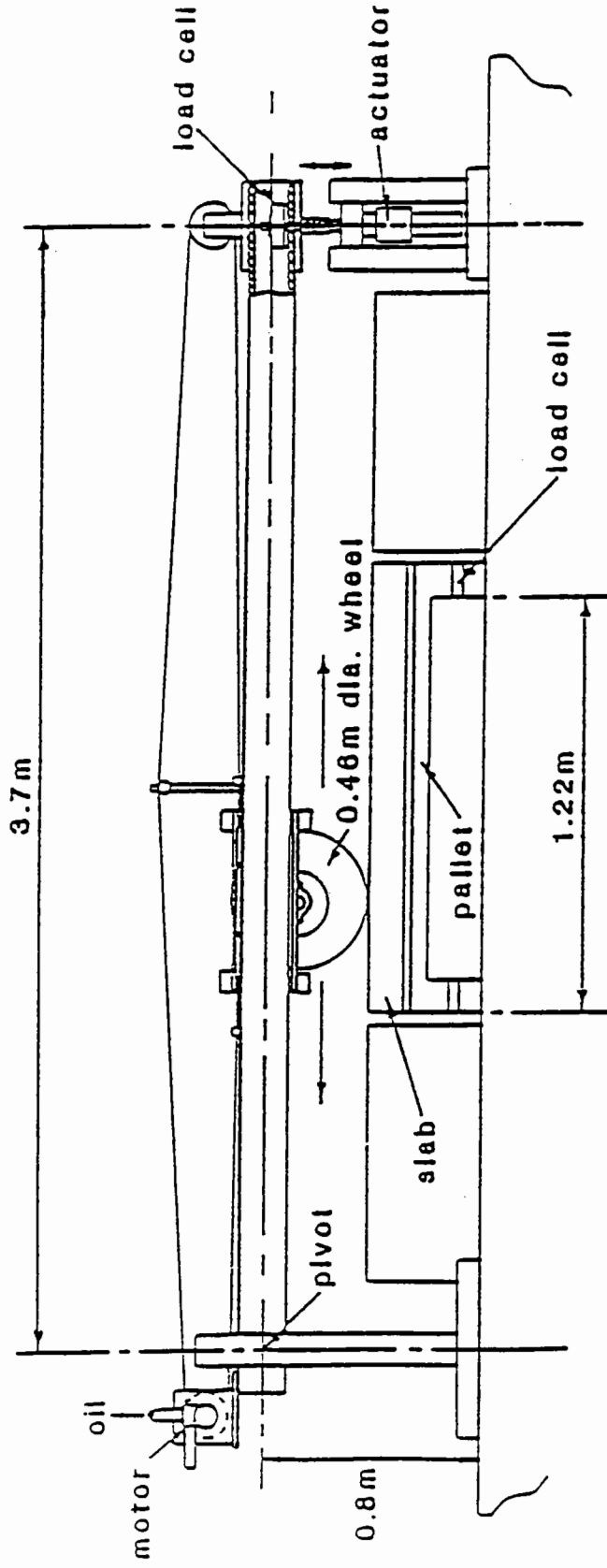
Figure 2.11 Elevation of the slab test facility (Chan 1990)

2.5.7 Soil rut testing facility

The Soil Rut Testing Facility (SRTF) was initially developed for the evaluation of plastic deformation of bituminous materials (Cooper and Brown 1986). In this project it is extended to investigate the rutting susceptibilities of fine grained soils under wheel loading.

Plate 2.1 shows the device. It comprises a pneumatic tyred wheel inflated to 300 kPa and a chain loop of six identical moulds of size 400 by 280 by 110 mm which is driven by a steel conveyer coupled to a motor. The moulds contain soil which is thus subjected to direct trafficking in a single direction. Wheel loads are applied through a simple mechanical system consisting of a lever arm and variable weights. Rut depth developed on the surface is measured at three prefixed points by a dial gauge capable of reading to 0.01 mm. Readings are taken when the conveyor is halted.

The main advantage of the SRTF is that by providing real wheel loads in the test, it may be expected to give a direct correlation to actual traffic (Nievelt 1989). The soil rut testing facility could be a quick and efficient tool to distinguish the resistance to permanent deformation of soils. Six specimens in varying states or environmental conditions such as different moisture contents and densities etc. can be tested simultaneously. However, it gives no information on the resilient strain properties of the materials tested. Furthermore the size of the wheel is too small for adequate testing of normal road sub-base materials.

2.6 SUMMARY

2.6.1 General

(1)   The above sections have indicated that the resilient elastic stiffness and permanent strain behaviour of both unbound granular materials and subgrade soils in the pavement foundation are heavily stress dependent.

(2)   Ideally test loading should replicate all characteristics of real pavement loading. Stress magnitude, rotation and period together with the correct combination of stresses should all be modelled. Failure to do so will limit a test's usefulness to a greater or lesser degree.

(3)   The behaviour of the materials which comprise the foundation is clearly significantly affected by their condition. In particular, moisture content, pore suction and density may all be expected to have an important influence on their properties. For a realistic test, the condition of a sample should be representative of the construction or in-service period.

(4)   The physical properties of the constituent particles of unbound granular material should be given greater attention than is often the case and only a sample of an appropriate grading can hope to have the correct mechanical properties as only then will the correct interplay of micro and macro texture come into force.

(5)   In general, the current standard laboratory tests fail to replicate the typical loading and material conditions of pavement foundation materials.

2.6.2 Requirements for unbound granular material characterization

Requirements for successful characterization of unbound granular materials for use in analytical pavement design are, ideally:

(1)   Repeated loads should be used to determine the resilient strain properties and the permanent deformation characteristics.

(2)   Testing conditions representative of those during construction and in-service should be provided.

(3)   High precision instrumentation to measure small resilient displacements should be employed.

(4)   Test apparatus and procedure should be simple and reliable so as to encourage routine implementation. Capital and running costs should be low.

(5)   Testing of granular materials should be at their full gradings, appropriate moisture and density conditions.

(6)   Sufficient specimen size should be provided to reduce the effect from large aggregate particles (see Chapter 3 for further detail).
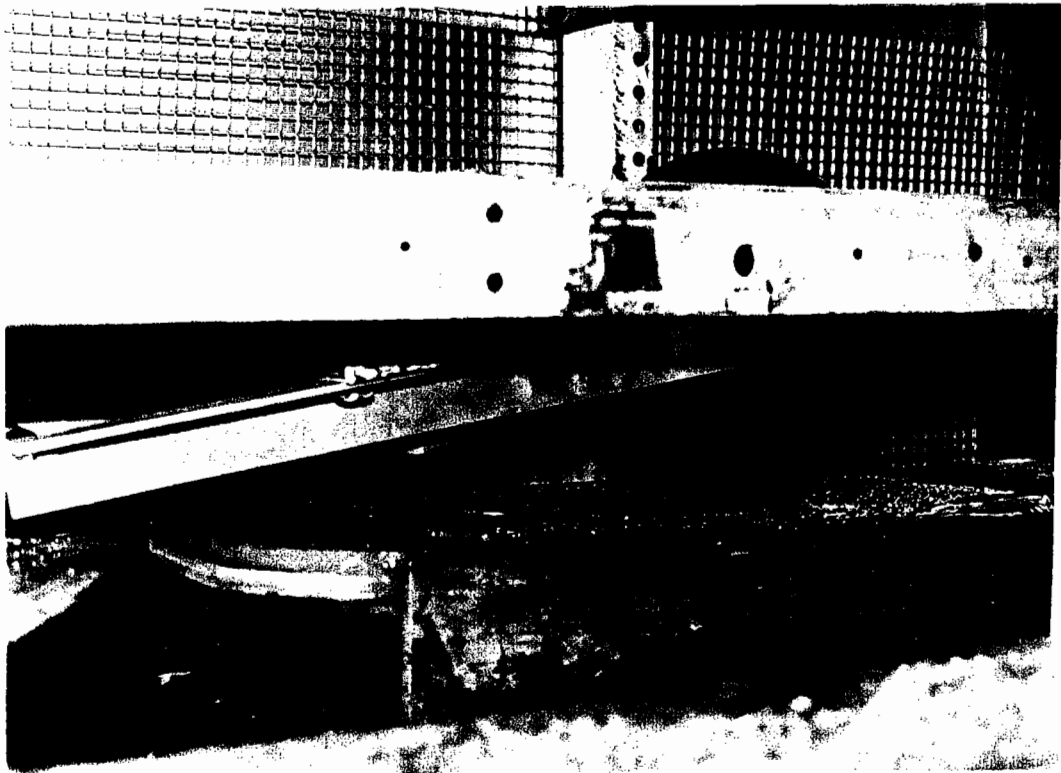
(a) A testing specimen
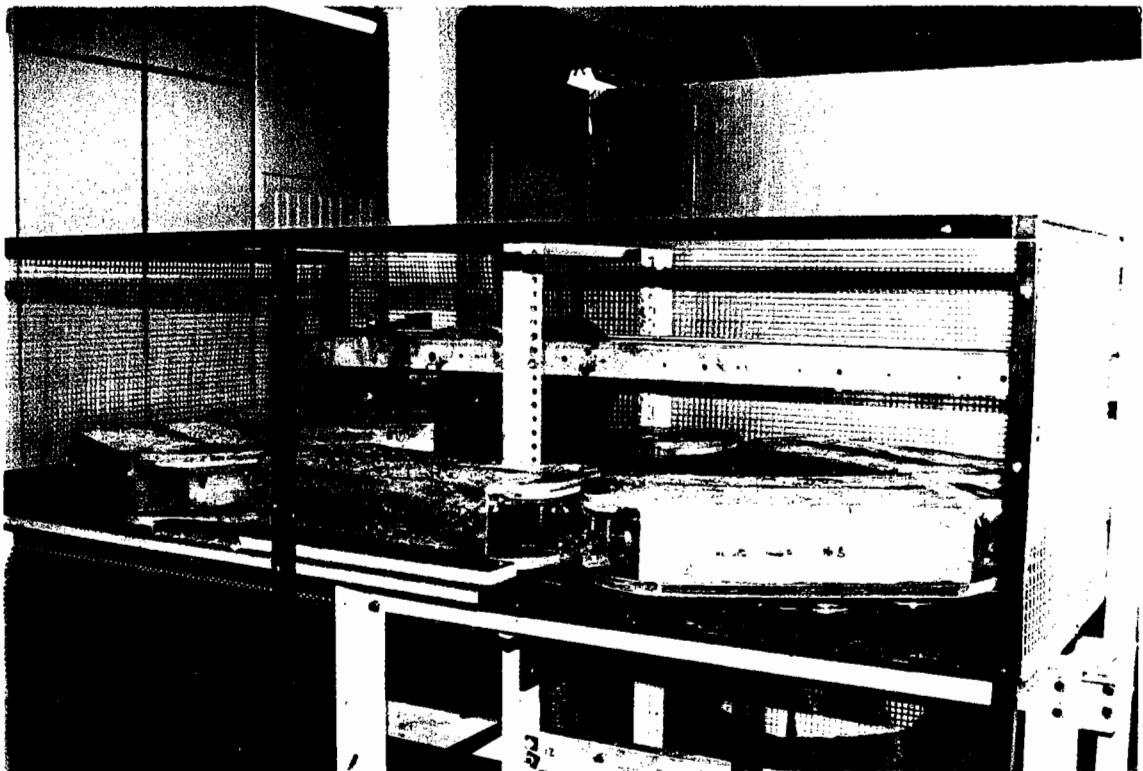
(b) General view

Plate 2.1 Soil rut testing facility

2.6.3 Requirements for soil characterization

For soils, the basic requirements, (1) to (4) recommended for unbound granular material characterization, are equally applicable. Nevertheless, attention is more on testing under representative environmental conditions than on effects from particle size. Therefore, in addition to the common requirements, the following should, ideally, be met as well:

(5)   Testing conditions at the appropriate moisture content and pore pressure or soil suction should be replicated.

(6)   Both undisturbed and compacted samples should be capable of being assessed so as to cover natural and fill soils (more discussion is included in Section 6.7.1).

2.6.4 Preferred test method

Meeting the requirements outlined above should ensure meaningful and useful design parameters, however, it is not possible to meet all of them. A fully simulative equipment would preclude a simple, practical and reliable implementation method. As previously presented in Table 2.1, laboratory tests which can provide stress condition close or relatively similar to those in the road foundation are the pavement test facility, slab test facility, hollow cylinder apparatus and repeated load triaxial apparatus. They are also able to measure materials in terms of resilient modulus and/or permanent deformation under repeated loading. Nevertheless, the complexities of these equipment have resulted in their high initial costs (Table 2.1) and have limited them to be used as research tools.

On the other hand, the simpler apparatuses including the large shear box and soil rut testing facility cannot provide sufficient information for an analytical design.

Balance must be sought between idealization and simplicity. The Nottingham Asphalt Tester (NAT), which is in fact a simplified version of the repeated load triaxial apparatus specially designed for testing bituminous material, has been proved to be a successful and practical tool in many engineering laboratories to obtain the essential

27

properties (resilient modulus and plastic strain behaviour) of the top layer of the flexible road pavement.

On this basis the methodology used in the repeated load triaxial test was selected as offering the most reasonable compromise. By using this method, most of the requirements for the aggregate and soil characterization stated in the Sections 2.6.2 and 2.6.3 can be met. Samples of granular materials and soils of in cylindrical form at conditions similar to those in road foundations may be obtained or reproduced. Table 2.1 shows that stress magnitude and load pulse shape are readily provided. The only inherent limitation of any types (simplified or sophisticated) of repeated triaxial apparatus is that no continuous stress rotation, as occurs in real pavements, can be produced.

To test granular material of full grading and to reduce effects from large aggregate particles, it is necessary to provide a large enough size sample for aggregate testing. Therefore, two apparatuses of different sizes, one for unbound granular materials and the other for soils, will be needed. Furthermore, due to the complexity of the current repeated load triaxial apparatus, simplified versions of the device are required.

PART B

ASSESSMENT TESTS FOR
UNBOUND GRANULAR MATERIALS

CHAPTER 3

DEVELOPMENT OF A LARGE DIAMETER REPEATED LOAD TRIAXIAL APPARATUS FOR FULL SIZE SUB-BASE MATERIALS (280TA)

3.1 INTRODUCTION

This chapter discusses the design, construction and method of use of a 280 mm diameter repeated load triaxial apparatus (280TA) for testing typical sub-base granular materials. There are four major components for the new apparatus. They are the loading system, sealing system, displacement measuring system and data acquisition units. Each of these is discussed in turn in this chapter. Figure 3.1 shows a schematic diagram of the laboratory set-up of this device. The chief modification from the traditional techniques is that confining pressure is supplied by applying suction to the specimen. Hence, the large and cumbersome external triaxial cell is eliminated. Vertical repeated load can either be applied by an advanced servo hydraulic system or by a very simple hand operated hydraulic jack. For routine use the latter is proposed. A cheap disposable PVC membrane is employed. Horizontal and vertical displacements are measured by an accurate but low cost on-sample instrumentation system which is glued to the membrane.

3.2 SIZE OF SPECIMEN

The size of the specimen must be a function of the maximum dimension of the road aggregates to be tested. Sweere (1990) and other previous researchers observed that an insufficient ratio of particle to specimen size significantly affected the behaviour of granular materials. Vallerga et al (1975) stated that the ratio of 1 to 3 or 1 to 4 should be observed. A similar recommendation of 4 to 5 times the maximum particle size was made in the Special Report 162 by the Transportation Research Board (1975). In the AASHTO T 274-82 specification (AASHTO 1986), a particle to specimen size ratio of 6 was recommended. To test materials with particles size up to 50 mm, Dupas et al (1988) made 300 mm diameter triaxial specimens. Observations made by Marachi et al in 1969 indicated that if the ratio between specimen diameter and the nominal size of well graded materials was less than 7, higher shear strength would be generated. They defined the nominal size of particles, d_{70}, as the sieve size at which 70% of tested

29
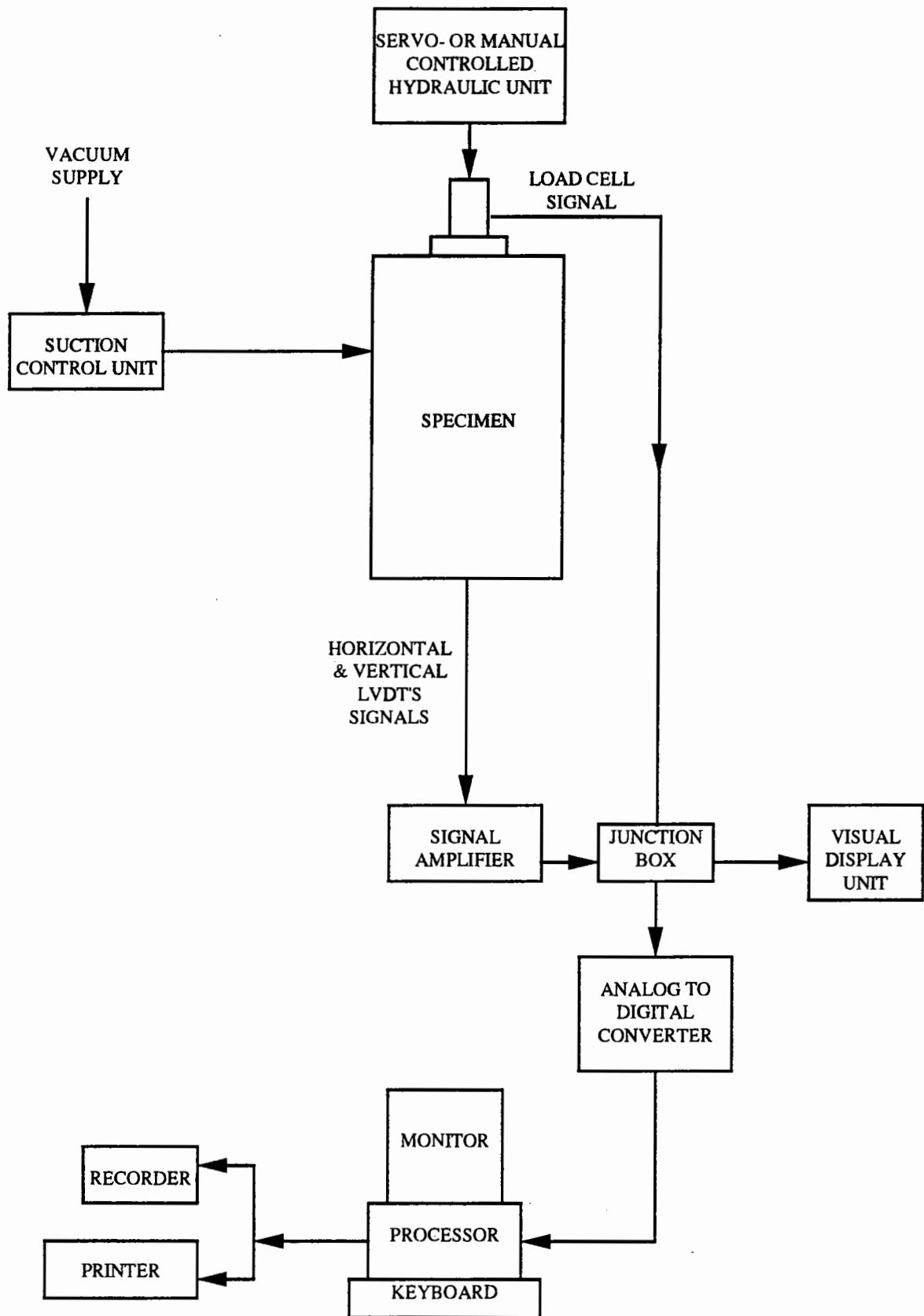
Figure 3.1 General arrangement of the repeated load triaxial apparatus (280TA) for aggregate testing

materials in weight passed through. Sweere (1990) performed four sets of repeated load triaxial testing on specimens of 150 mm and 400 mm diameters on 0-40 mm aggregates. Higher resilient stiffness was found in two of the smaller specimens. He suggested that the 150 mm triaxial apparatus might not be large enough for testing unbound granular materials in the pavement foundation. The reason was that when the specimen/particle size ratio was too small, the overall particle packing arrangement would be affected. However, the 400 mm diameter specimen of about 200 kg in weight proved laborious to handle although the 1 to 10 particle to specimen size ratio was believed to be sufficient.

Having considered the ratio of particle to specimen size effect, its potential influence on results and the practicality of testing a large specimen, a ratio of 1 to 7 was selected as a reasonable compromise. Since about 87.5% of the coarser end of the DoT Type 1 sub-base materials is smaller than 40 mm, this particle size was chosen as the nominal maximum. Hence, the diameter of the specimen of 280 mm was used. Using Marachi's definition of nominal size and assuming a (typical) d_{70} of 25 mm this gives a particle/sample ratio of 1 to 11.

Taylor (1941) carried out tests on triaxial specimens of different height to diameter ratios. He concluded that if the ratio of height to diameter was about 2, end effects on the strength measurement would be insignificant. Results from the theoretical study by Dehlen (1969) showed that the size effect was negligible when a minimum height to diameter ratio of 2 was reached. Therefore, a ratio of 2 was used and the height of the specimen was 560 mm. A reduction of 65% from the weight of Sweere's samples was thus achieved.

3.3   LOADING SYSTEM

3.3.1 Axial load

Loading systems of various degrees of complexity ranging from mechanical to sophisticated computer controlled servo-hydraulic equipment have been developed by different researchers. A pneumatic loading system was used by Seed and McNeill (1958). Grainger and Lister (1962) used a mechanical system to cycle the axial and the confining pressures to the triaxial specimen. A hydraulic-pneumatic system was employed by Vaid et at (1988) to test materials under cyclic loading. Brown et al

(1989) developed a closed-loop servo-hydraulic system to investigate the properties of granular materials. Barksdale and Itani (1989) applied slow repeated loading to test granular materials and suggested that the resilient behaviour of unbound aggregates could be evaluated by conventional triaxial testing. Sweere (1990) used his servo-hydraulic equipment to simulate hand operated on-off loading for which he obtained similar results to those obtained by more conventional sine or haversine loading.

Normally, a pneumatic system provides the cheapest solution for applying axial load, but the ability to create controlled load pulses degenerates rapidly when the magnitude, or the frequency, of repeated loading is high. Good control of the shape of load pulses can be obtained by using servo-hydraulic systems, but, the cost of the resulting device is relatively high. Manually controlled loading can provide a well-shaped pulse but at the cost of a greatly increased pulse length.

Plate 3.1 shows the simple 'Rugby Goal Post' load frame used for the testing of the 280 mm diameter triaxial specimen. The frame is made of standard structural steel members. It comprises two vertical columns and a cross beam. The columns are secured to the floor slab by bolts and the beam is fixed to the top ends of the columns. Two loading devices have been chosen for testing unbound granular materials. The first is a manually operated load ram, one of the cheapest and simplest forms of loading mechanism. Nevertheless, its ability is limited and only slow repeated loading to tested specimens can be applied. For the purpose of validating this simplified testing method, a servo-hydraulic actuator has also been used in this project. As shown in the plate, both automatic and manually controlled actuators can be mounted onto the frame with the ability for them to slide along the beam of the frame. The two loading devices are able to provide the same maximum load of 100 kN. Both of them have a stroke length of 150 mm and, hence, up to 27% axial strain can be accommodated.

Thom (1988), as well as many other previous researchers, observed that the generation of non-recoverable strains of aggregates depended upon stress history. To fully understand the permanent deformation behaviour of granular materials, a new specimen would be required for each stress application. Obviously, such a testing method is important when developing a material model but is inappropriate for routine testing. As stated in Section 2.3.1.2, Chan (1990) carried out testing by using a hollow cylinder apparatus, and demonstrated that the rotation of principal stresses due to traffic loading was a crucial factor in the development of plastic strains. However, the repeated load triaxial apparatus is unable to produce continuous stress rotation. The permanent
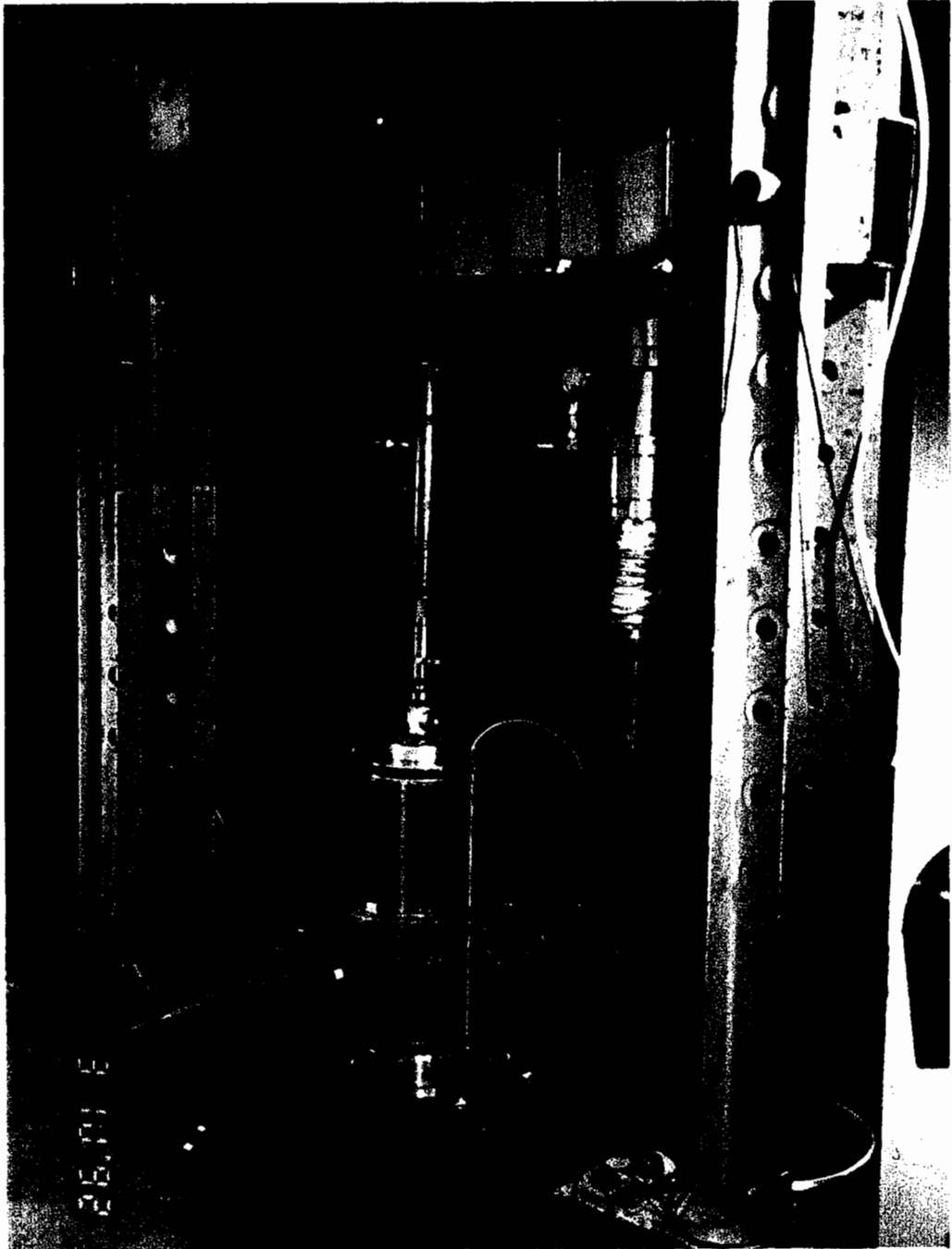
Plate 3.1 Load frame and actuators for the repeated load
triaxial apparatus (280TA) for aggregates

deformation results obtained by the triaxial testing should thus be treated as indicative information. Therefore, it is justifiable to find a simple testing technique which provides an indicator of the rut potential of the tested materials under repeated loads. A device consisted of a guide rod and drop hammer of weight 10 kg (Plate 3.2) to provide high repeated vertical loads has therefore been designed. Hence, the loading system of the 280TA is able to provide three different modes of loading: impact loading of known energy, cyclic loading of high accuracy and manually controlled static or repeated loading.

To transfer the axial load and to measure the magnitude of the force applied to the test specimen, a load cell with built-in strain gauges is seated on the top platen into which the actuator engages (Plate 3.3). The main feature of the connection is a ball joint to ensure direct transmission of vertical loading and to eliminate any shear load transfer.

Plate 3.4 shows the bottom platen and the base plate to support the specimen. The 30 mm thick steel base plate served two purposes:- it ensures that a horizontal flat platform is maintained during testing and it provides a rigid support for heavy compaction during specimen preparation. Removable wheels are provided at its corners to allow the sample to be compacted away from the load frame in a place where the noise can be accommodated. On the surface of the base plate, a guide rail and an end stop are incorporated. They help to locate the final position and to restrict movement of the bottom platen during testing.

The hydraulic actuator is operated through an electronic control system which is capable of comparing feedback signals from the load cell with command signals from the control panel. When these signals are different, an error message is received by the servo valve and automatic adjustment of loading is immediately made. Hence, accurate control of applied loads is achieved. The load cell employed is able to monitor axial loads up to 100 kN. Calibration results, as shown in Appendix A, indicate that it is a high precision load cell with the capacity to read 1 kPa for the current specimen size. Different frequencies and waveforms of load pulses are provided by a signal generator. The signal generator is able to produce square, triangular and sinusoidal electronic signals at frequencies up to 100 Hz. To reduce the static friction and "stiction" on the load ram of the hydraulic actuator, hence improve the performance of the loading system, a dither signal of high frequency and low magnitude is applied. Figure 3.2 illustrates the interrelationship between parts of the axial load control system.
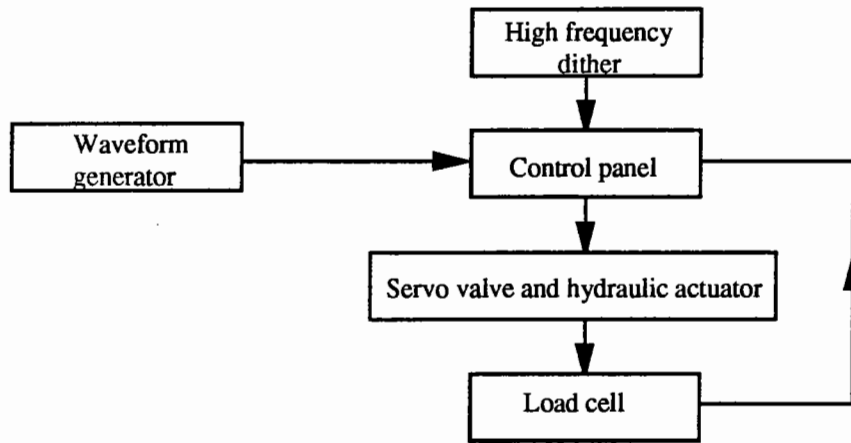
Figure 3.2 Interrelationship between parts of the axial load control system (280TA)

PVC MEMBRANE

SEALANT

STICKY TAPE
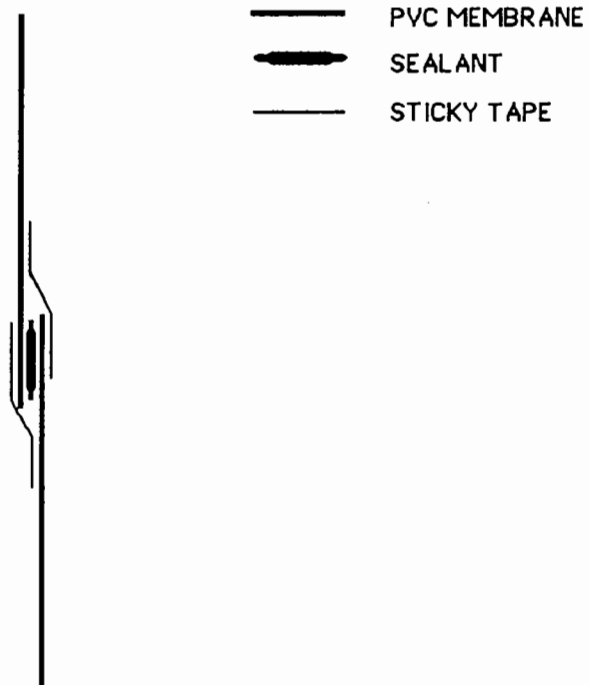
Figure 3.3 Joint details of the PVC membrane (280TA)
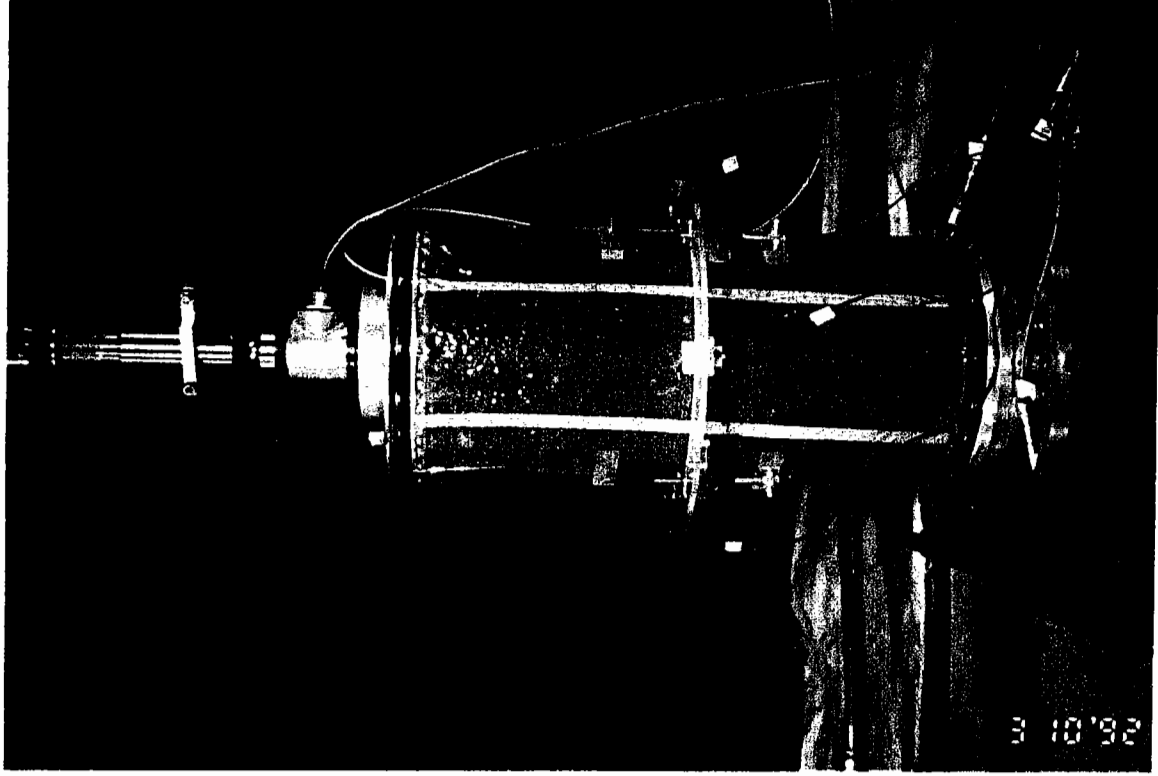
Plate 3.3 Load and displacement acquisition system for the 280TA
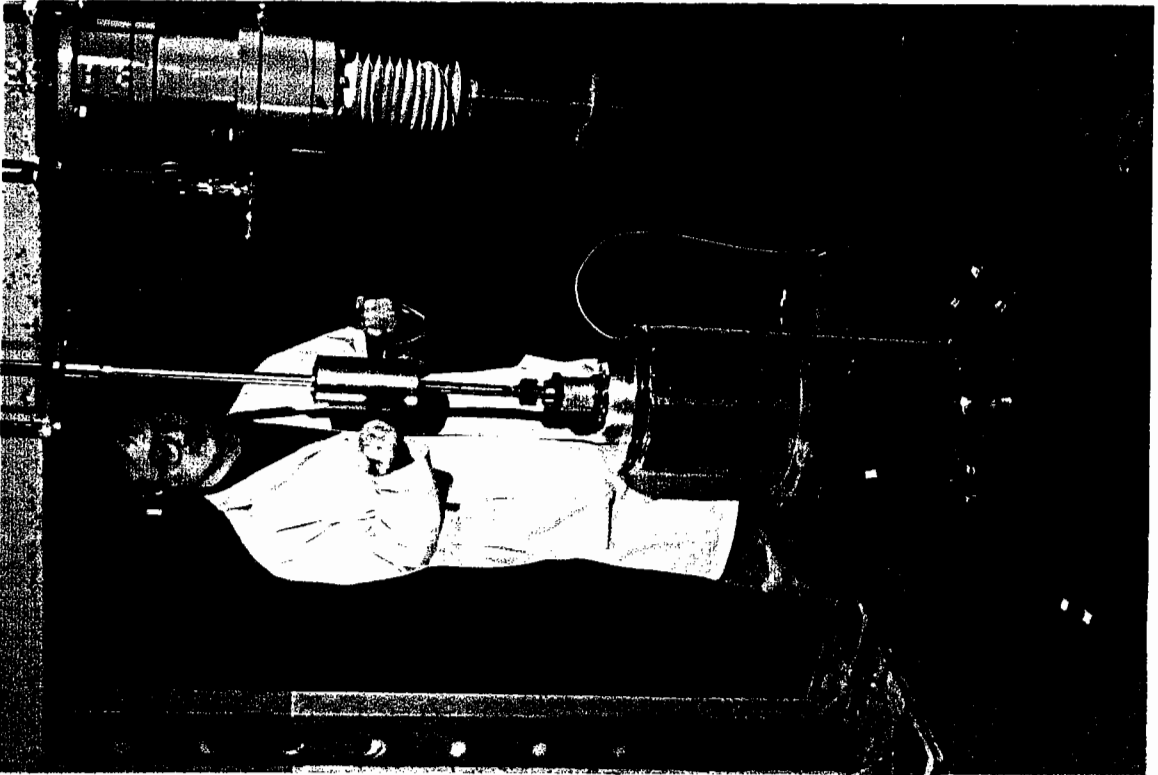
Plate 3.2 Drop hammer system for the repeated load triaxial apparatus (280TA)

Plate 3.5 Big LVDT for monitoring large vertical movement for strength test (280TA)

Plate 3.4 Bottom platen and base plate (280TA)

Controlling the applied loading with the manually operated load ram is relatively simple. An oil hand pump is used. Vertical loads are supplied by pumping pressurized oil into the load ram. Unloading is achieved by turning on the pressure relief valve. To monitor the loading, a digital voltage meter or an oscilloscope is connected to the load cell to provide instant visual display of the current axial load.

3.3.2 Confining pressure

The conventional triaxial apparatus (Bishop and Henkel 1962) is able to provide a range of confining pressure to test specimens. During axial loading, the cell pressure is kept constant. To understand the dynamic responses of pavement foundation materials, Williams (1963) was among the first to apply repeated vertical stresses onto the triaxial specimen. A better simulation of the in-situ conditions was made (Allen and Thompson 1974, Brown and Hyde 1975) by upgrading the apparatus to incorporate the ability to apply simultaneous repeated vertical and confining stresses. Allen and Thompson compared results from testing granular materials under repeated and constant confining conditions. They reported that the constant cell pressure test slightly overestimated the resilient modulus and yielded much higher resilient Poisson's ratio. Further investigations on the difference between constant and repeated confining stress tests were made by Brown and Hyde (1975). They demonstrated that both tests produced the same resilient modulus when the mean value of the repeated confining stress was used in the constant cell pressure test. They then concluded that if the stress applied to the specimen did not cause dilation, the same stress-strain relationship would be obtained in both cases.

On this basis for the large repeated load triaxial apparatus an adjustable, constant, confining pressure is used. This is provided by applying partial vacuum to the cylindrical test specimens. Such a method has proved successful at Aachen (Schultze 1975) and Delft (Sweere 1990). The main advantages of this method are that it eliminates the large and cumbersome external cell and permits direct access to all transducers at any moment during testing. However, the vacuum method does have limitations. For instance, the maximum confining stress is limited, in practice, to about 90 kPa. Testing of saturated sub-base materials is difficult because complicated device and control will be needed. Nevertheless, these limitations are not critical for the testing of sub-base materials because

(a)   The total confining pressure from the thin overburden and the wheel load in the sub-base of a servicing road are expected to be smaller than 90 kPa (discussed in detail in Section 5.5.1.1).

(b)   For a well designed road, the provision of an effective drainage system to lower the ground water table and of an impervious upper layer to exclude surface water from entering into the foundation (Bentsen 1990) prevents the saturation of the sub-base and keeps the moisture content low.

To control the vacuum supply a needle valve was tried. However, it was found that the suction pressure applied to the specimen fluctuated with the main supply in the laboratory. Steady vacuum control was difficult. In order to provide a stable and controllable confining pressure to specimens, an electronic vacuum controller was installed. The main part of the controller is an electronic vacuum regulator, Electro Pneumatic Vacuum Regulator IT209-302B, supplied by SMC Pneumatics (U.K.) Ltd. By means of an internal sensor, built into the regulator, it ensures that the suction applied to the specimen is stable and remains at the specified value in accordance with the input electronic signal. Thus it eliminates all the unnecessary errors caused by the fluctuation of suction from the laboratory main vacuum supply during testing. The regulator has been calibrated against a mercury manometer. The results and performance of the device is shown in Appendix A. A good match between the required and the obtained pressure is achievable. To check the suction, vacuum meters with precision of 0.7 kPa are connected to both ends of the specimen. Hence suction might be applied to one end and monitored at the other if desired.

The partial vacuum is supplied through the top and bottom platens. Porous filters made of sintered bronze with a diameter of 22 mm have been fixed to both platens. The filters make sure that no solid particles from the specimen are allowed to enter the vacuum lines.

3.4   SEALING SYSTEM

To make sure an effective vacuum to the specimen can be maintained, a good sealing system is essential. For the 280 mm diameter specimen, the sealing system comprises two main components: a cylindrical membrane and the end platens to which both ends of the membrane are affixed.

As recommended in B.S.1377 (1990), a rubber membrane of thickness of about 0.25 mm is generally found satisfactory for most triaxial testing. The material of the membrane is normally made of latex. However, when the tested samples are crushed stones, which consist of sharp edges and angles, the membrane is often found punctured during specimen preparation. Thus, for testing of sub-base materials, a second membrane is sometimes used (Brown et al 1989). For large samples latex membranes are very expensive. A membrane made of 0.4 mm thick PVC film (heat welded to form a cylinder) had been tried and found satisfactory by Sweere (1990) in his 400 mm diameter triaxial specimen. Sweere noticed that the PVC membrane would provide unwanted lateral support to the tested specimen, so he made the shape of the membrane into a barrel form to eliminate any possible extra confining stress developed as the specimen swelled diametrically. A similar arrangement is adopted for the present apparatus.

For the material of the cylindrical membrane a PVC film of 0.25 mm is selected. This membrane is prepared by cutting a piece of PVC sheet to rectangular shape and joining a pair of parallel edges with sealant and sticky tape as illustrated in Figure 3.3.

Henkel and Gilbert (1952) noticed that triaxial soil specimens with rubber membranes on were stronger than those without. Pierre et at (1988) suggested different membrane correction methods for materials failing in bulging and shear modes respectively.

To investigate the possible confining effects of the PVC membrane, studies of the stress-strain relationship of the confining material have been carried out. Theoretically, the effect from the membrane constraint can be calculated if the stress-strain relationship of the confining material is known. A simple test was therefore performed, as described in Appendix B, from which it was concluded that the use of the 0.25 mm thick PVC membrane should not cause undue specimen confinement.

To make sure that no excessive confinement is caused to the specimen by the membrane, the diameter of the membrane is made 5 mm larger than that of the specimen.

Two membranes are used to ensure that no leakage occurs. The second membrane is placed on the specimen after the aggregate has been compacted, for the first membrane can become damaged during compaction. The sealing system is completed by securing the membranes with two pairs of rubber "O" rings at both the top and bottom platens

where recesses for the rings are provided. Figure 3.4 shows the sealing method employed. In between the "O" rings, a stretchable 2 mm thick tape sealant supplied by Monaflex is used. Since the sealant is very sticky and deformable, it readily takes up a shape which can easily accommodate the slight oversize of the membrane as well as any folds or creases.

3.5 DISPLACEMENT MEASUREMENT UNITS

Friction developed between the end platens and the triaxial specimen creates semi-rigid zones at both ends of the specimen. To ensure homogeneous stress distribution, low friction ends were employed by Loach (1987). He placed layers of silicone grease and rubber sheeting between the platen and the specimen. However, this arrangement created uncertainty in vertical displacement measurement which was normally measured above the top platen. Boyce (1976) avoided the bedding error by measuring deformation at the middle third height of the specimen.

Instrumentation fixed to studs which are in turn installed within the aggregates through the membrane is commonly used to measure strain, (Jouve et al 1987 and Brown et al 1989). However such a method is not straightforward to carry out and complicates compaction. Sweere (1990) simplified the method by affixing instrumentation to plastic blocks which were glued to the specimen membrane and promising results were obtained. Another technique to avoid the complication of compaction is being developed as part of a project funded by the European Community (Gillett et al 1991). To measure radial strains of triaxial specimens, a train of 12 pairs of wheels with a displacement transducer attached to the ends wrapping around the cylindrical specimen is being developed. The train method has the advantage of providing more contact points. For the equipment described here, the 'glue-on' approach is adopted. Due to penetration of individual particles, the thickness of the membrane will change when the confining pressure varies, such an approach will not be desirable if cyclic confining pressures are to be used.

Two sets of "on-sample" displacement transducers, each consisting of three light-weight Linear Variable Differential Transformers (LVDTs), are employed to measure the vertical and horizontal deformation respectively. Displacements are then converted to electrical signals. To minimise instrument-induced effects, light-weight LVDTs with off-sample signal conditioning are selected as the on-sample instrumentation units.

Aluminium platen
"O" ring
Sealant
PYC membrane
Specimen
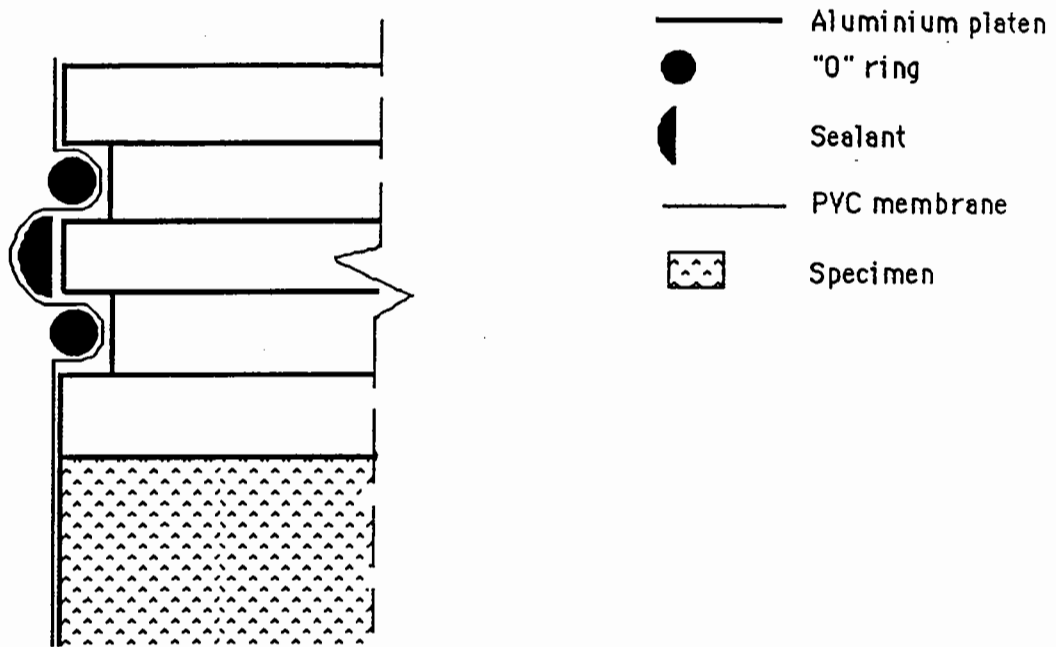
Figure 3.4 Membrane sealing arrangement of the specimen (280TA)

SUPPORTING STUD

'PERSPEX' RING

SPECIMEN

PVC BLOCK

GLUE CONNECTION
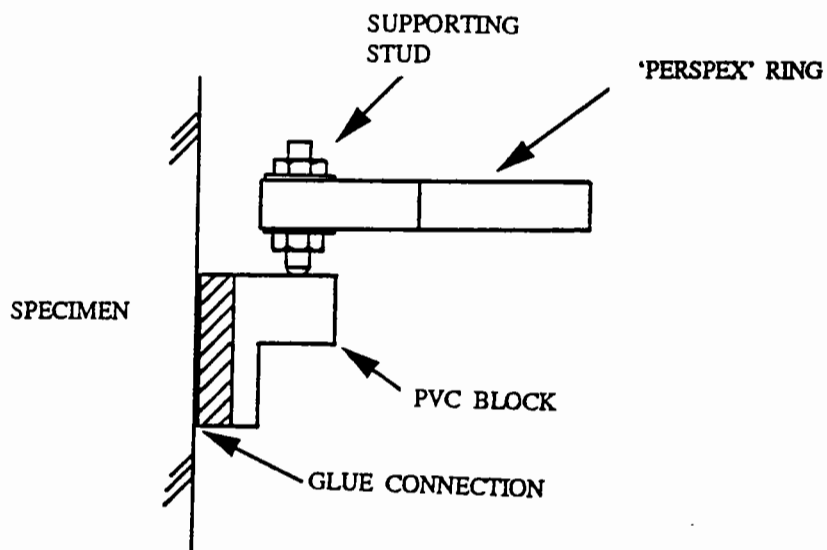
Figure 3.5 Details of instrument ring support (280TA)

Calibration of the LVDTs (Appendix A) shows that they give extremely high resolution and output signals are very stable. The precision of the vertical displacement transducers is 17 microstrain while the transducers measuring the horizontal movement of the specimen is 27 microstrain. The precision can be further increased by decreasing the measuring range when necessary.

In order to avoid the effect from end platens, the measurement of the transient movements is carried out over the middle portion of the specimen. The radial deformation is measured at mid-height of the specimen by three spring loaded LVDTs. These are clamped on a transparent 'Perspex' ring which sits loosely on three plastic blocks glued to the membrane. The plastic blocks (Figure 3.5) are machined from a piece of 22 mm thick PVC bar. The LVDT tips rest onto metal plates which are also glued onto the membrane. The arrangement and the details are shown in Figure 3.6. The ring moves up and down with the specimen when repeated loading is applied. Therefore, readings from the horizontal LVDTs are not significantly affected by vertical movements. The measuring range of these horizontal LVDTs is 6 mm. Vertical transient movements are measured over the central third of the specimen. LVDTs with free cores and with a measuring length of 12 mm are clamped into the plastic blocks. Details of the mounting device are illustrated in Figure 3.7.

Finally, to monitor large vertical movement of the specimen (for example during failure testing), the load actuator is equipped with a 100 mm stroke LVDT. This big LVDT is much heavier than those mounted on the specimen because the signal conditioning unit is a part of the body. However, since it is fixed off-sample (Plate 3.5), weight is not a design criterion. It is able to read to 86 microstrain, an accuracy which is more than sufficient for measuring large specimen movement.

As the quality of the displacement readings depends on a good adhesive contact, the selection of a suitable adhesive is important. The primary requirement of the adhesive is to provide a firm grip between materials so that no relative movement occurs. Secondly, the adhesive should not be harmful to the PVC membrane. Thirdly, the hardening time should not be too long or too short. 14 types of adhesives ranging from double sided tape to glue were tried. Most of them were rejected for the following reasons:-
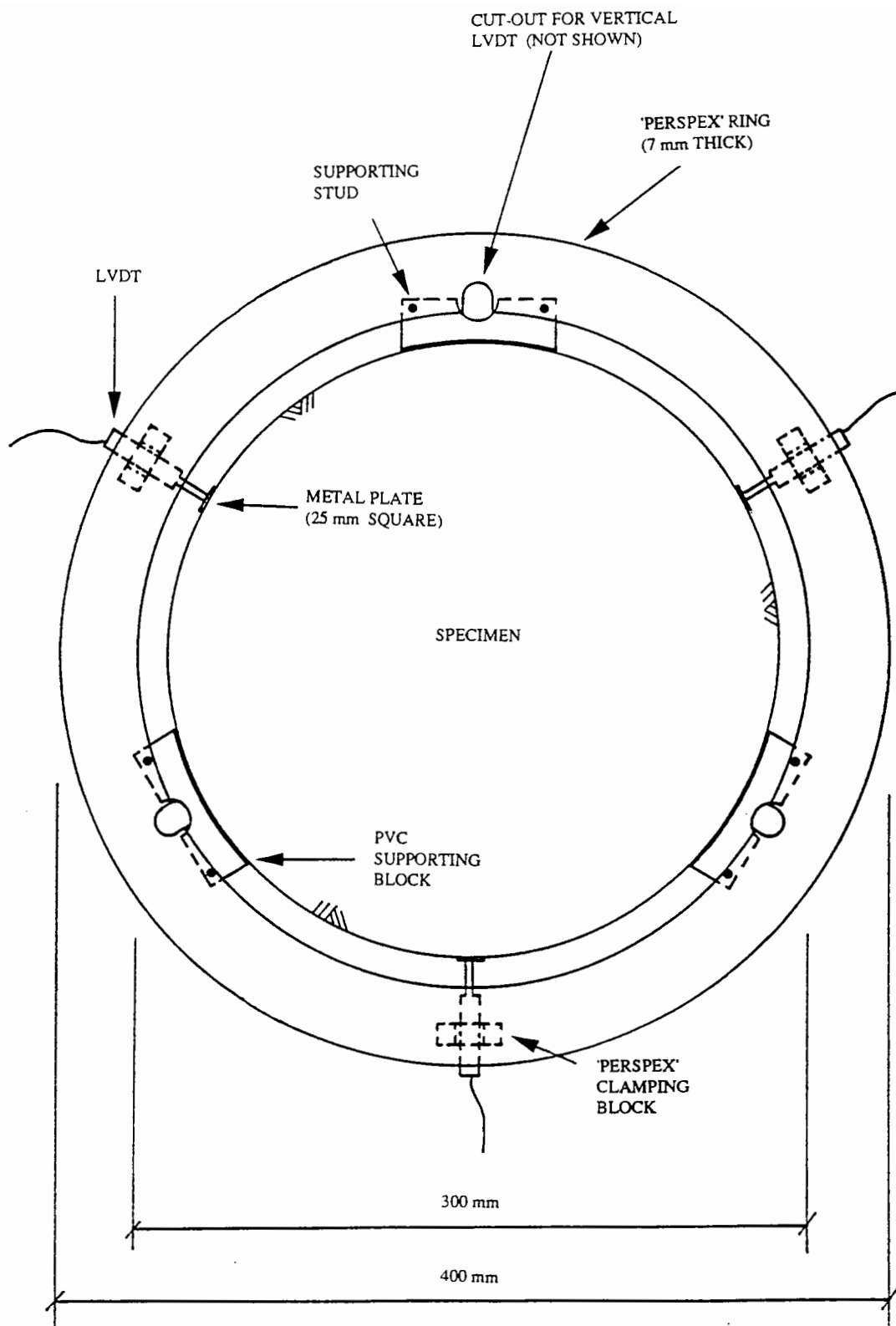
Figure 3.6 Instrument ring for horizontal displacement measurement (280TA)

Labels in figure:

CUT-OUT FOR VERTICAL LVDT (NOT SHOWN)

'PERSPEX' RING (7 mm THICK)

SUPPORTING STUD

LVDT

METAL PLATE (25 mm SQUARE)

SPECIMEN

PVC SUPPORTING BLOCK

'PERSPEX' CLAMPING BLOCK

300 mm

400 mm

GLUED SURFACE

SPECIMEN

PVC BLOCK

PLAN

BRASS FRAME

SPECIMEN

1 mm ROLLER

STAINLESS
STEEL ROD
1.5 mm DIA.

BRASS
EXTENSION
ROD TO
LVDT BODY

ELEVATION OF EXTENSION ROD

SECTION
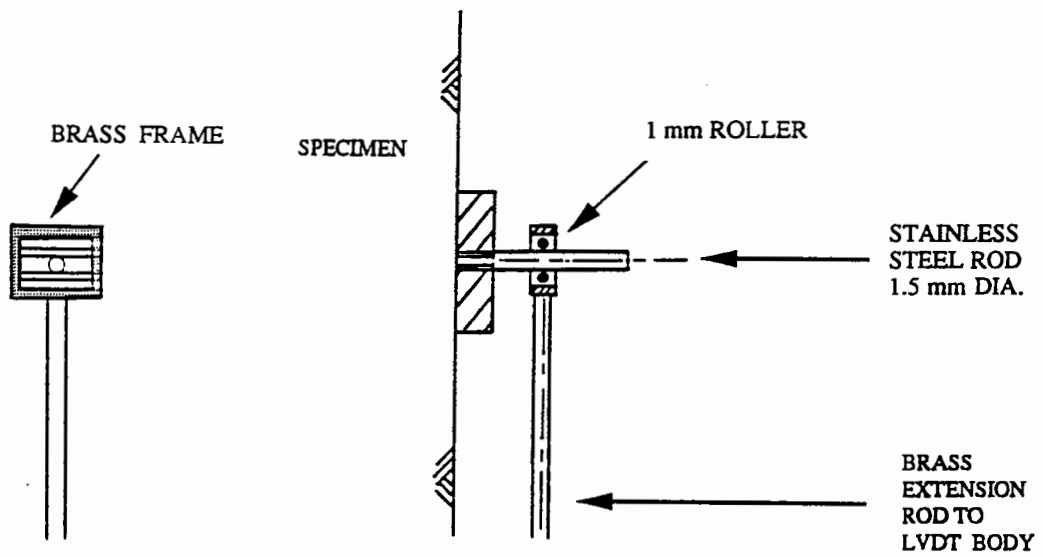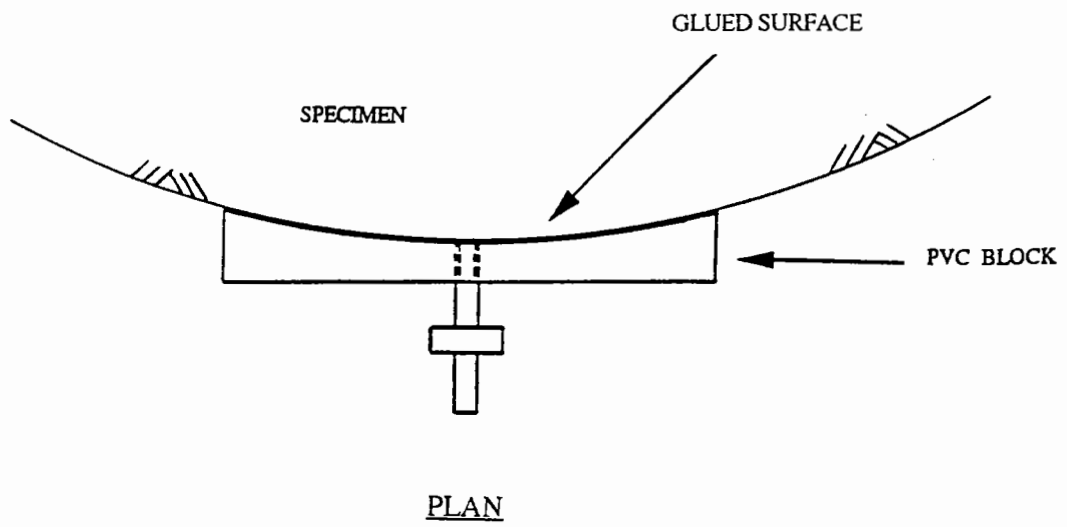
SCALE 1:1

Figure 3.7a   Fixing arrangement for vertical LVDT core (280TA)

GLUED SURFACE

SPECIMEN

PVC BLOCK

PERSPEX CLAMPING BLOCK

PLASTIC GRUB SCREW

PLAN

SPECIMEN

LVDT BODY

SCALE 1:1

SECTION
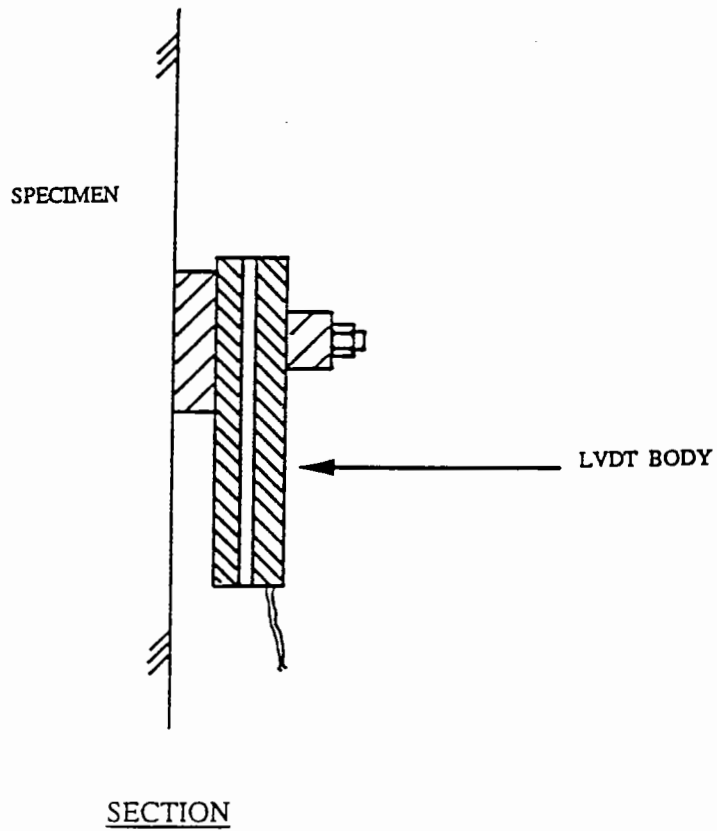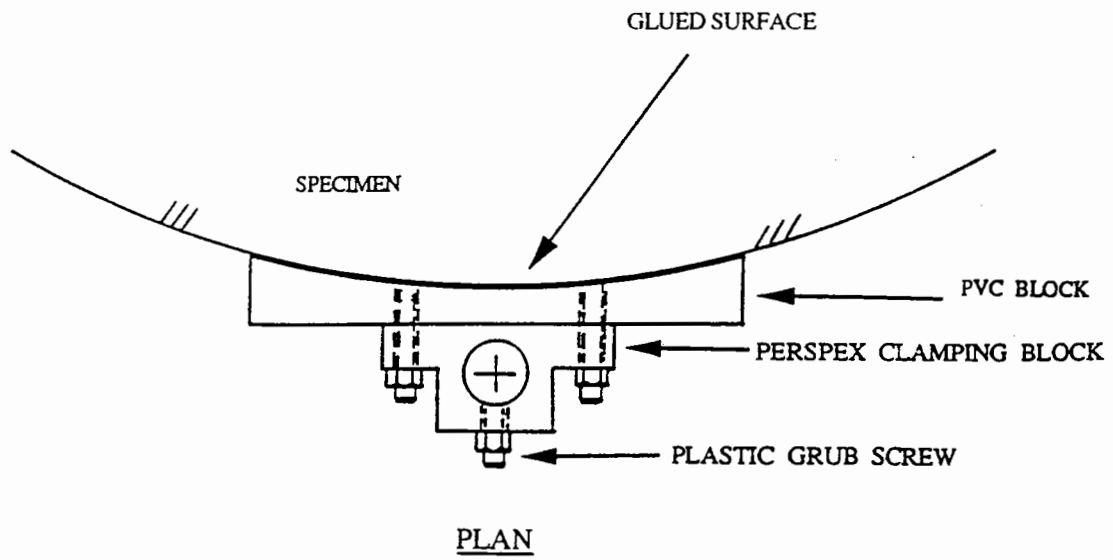
Figure 3.7b   Fixing arrangement for vertical LVDT body (280TA)

1)   The PVC membrane was attacked and weakened by the adhesive.

2)   The adhesive force was too weak.

3)   A hard surface was formed and peeled off easily when the adhesive was dry.

Eventually only two adhesives were found to be suitable as the bonding agent for the PVC membrane. They are "clear glue" from Loctite and "all purpose No 1 clear adhesive" from Bostik.

A jig (as shown in Plate 3.6) has been manufactured and is used to clamp the glue-on blocks and metal plates in their correct locations whilst the adhesive sets. As the membrane is accessible after the specimen has been prepared, instrumentation can be fixed immediately prior to testing.

3.6   DATA ACQUISITION SYSTEM

The inter-relationship between the different electronic units, which form the data acquisition system, can be found in Figure 3.1. A junction box has been made to simplify the electronic network. All conditioned signals, including those from the LVDTs and the load cell are firstly sent to the junction box. From there, connections are made to the computer interface unit and visual display devices. The interface unit, which comprises an eight channel, 12 bit, high speed analogue to digital signal convertor and an IEEE 488 interface card, provides the communication link between the computer and all transducers. A 386 SX AT personal computer equipped with two floppy disk drives, 1.44 mega byte and 1.2 mega byte, and a 40 mega byte hard disk is used to record and analyse the input signals.

An user-friendly software program (modelled on existing programs (Chan 1990)) has been developed to store and analyse data. The interactive nature of the software permits users to communicate with the computer. The software consists of five sections:- control, data acquisition, analysis, storing and printing. Figure 3.8 illustrates the structure of the program and details of the software can be found in a report written by Cheung (1991). The system allows data from all the transducers to be read in every 22 milliseconds. A maximum of 256 readings per channel can be obtained during a test. Signals from each instrument are recorded separately. The malfunction of any individual strain transducer can, thus, be detected.

Plate 3.7 Aggregate compaction mould

Plate 3.6 Fixing of the glue-on blocks and metal plates (280TA)
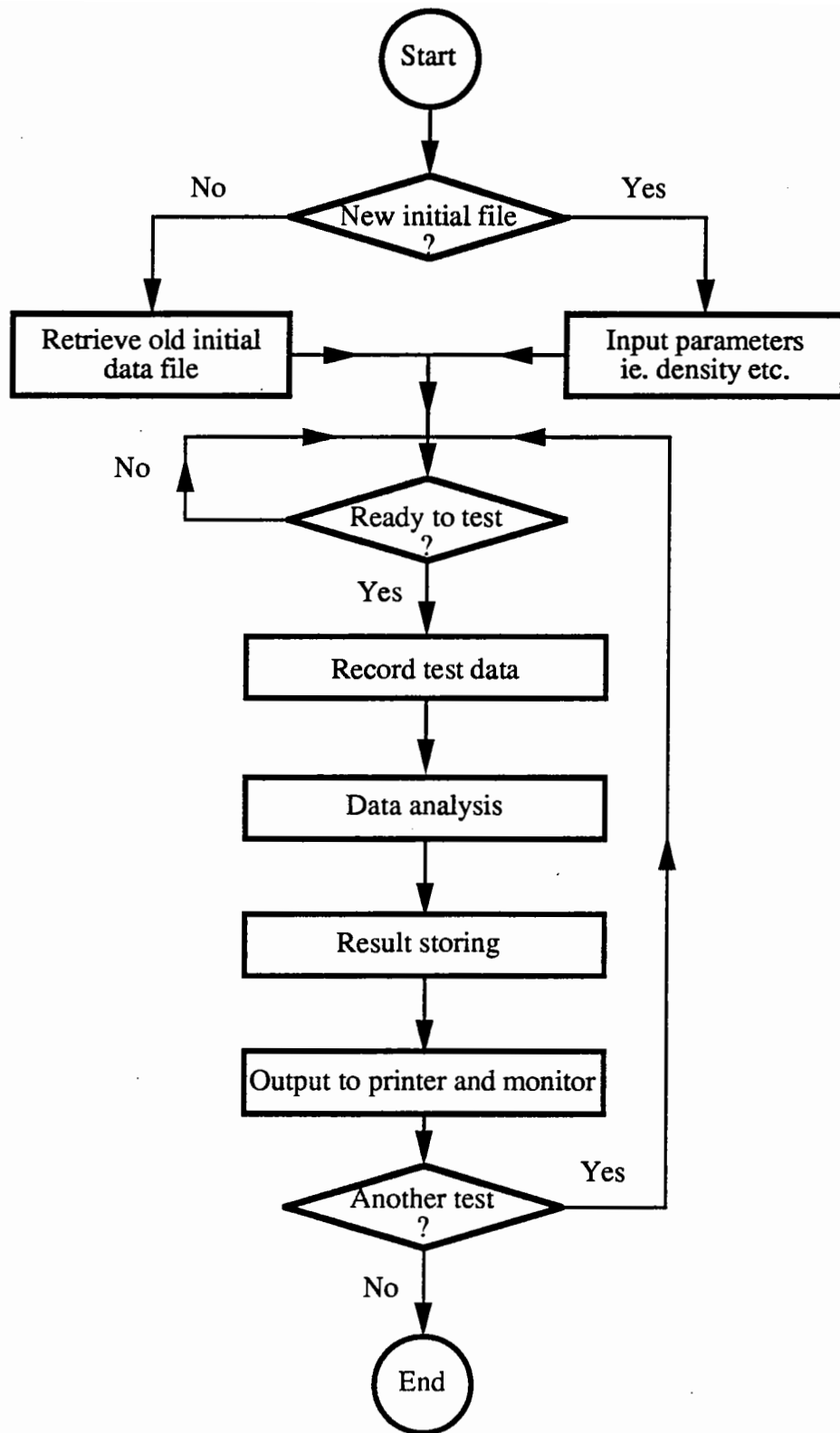
Figure 3.8 Data acquisition program structure (280TA)

Digital voltmeters and an oscilloscope are used to provide a visual display of the various measurements. They allow stresses on, and movement of, the specimen to be observed during the testing so that immediate action can be taken whenever it is necessary. Finally, a dot-matrix printer is used to produce hard copies of results in tabular and graphic forms. A tape is used to store back-up copies of testing data.

Details of the electronic components of the apparatus are summarised in Appendix C.

3.7 SPECIMEN PREPARATION

3.7.1 Development of compaction technique

A good specimen preparation method, able to repeatably produce samples of high density to represent in-situ conditions, is an essential pre-requisite of a successful test. Studies of compaction methods to produce high density samples for aggregates have taken place since the 1930's (Loos 1936). British Standard 1377 (1990) recommends three different forms of compaction for small diameter specimens. Static loading, dynamic compaction by a hand rammer and dynamic compaction by a vibrating hammer are suggested. Broms and Forssbland (1969) studied factors affecting the compactibility of granular materials and observed that vibratory compaction produced materials of high density. In the U.K., a compaction method based on the vibratory hammer technique is used for determining the compactibility of aggregates (B.S. 5835 1980) of particle sizes up to 50 mm. The compaction method initially chosen for the 280 mm diameter specimens in this study, therefore, uses a full-face vibration plate giving an effect similar to that prescribed by the B.S. 5835 test.

Figure 3.9 shows the sample preparation arrangement. The vibratory force is supplied by a vibration equipment: a Kango Hammer, Type 800X. During compaction, a constant static pressure of 25 kPa is applied through a lever system. Trial tests have been carried out to investigate the efficiency and the suitability of the compaction set-up. The material chosen for the trial was dolomitic limestone of a grading at the fine side of the DoT Type 1 sub-base grading envelope (Department of Transport 1986).

The specimen was prepared in eight equal layers and the surface of every layer, except the last one, was scarified to increase the homogeneity before the next layer was added. For each layer materials were compacted to refusal. Pettibone and Hardin (1964)

LEVER ARM

VIBRATION HAMMER

SUPPORT

COMPACTING HEAD

SPECIMEN

WEIGHT
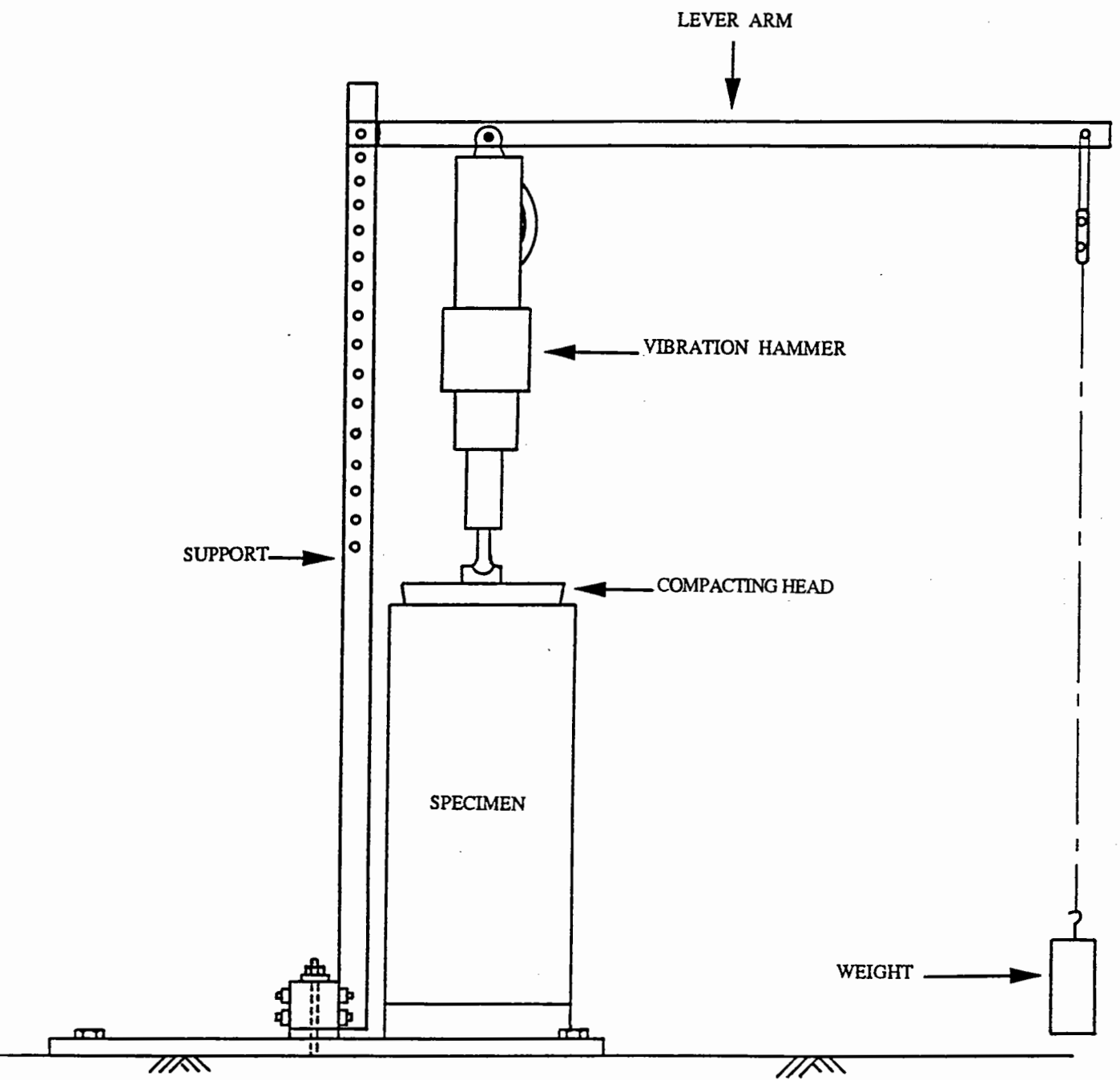
Figure 3.9   General arrangement of aggregate compaction equipment

compacted cohesionless soils by means of a vibration table. They noticed that the time required to reach refusal density was about six minutes. For the current compaction method, it was found that fifteen minutes were needed. At this point no further progress of the hammer in the mould was observed.

Test results indicated that the compaction method produced materials with an average density 4% below the maximum density (for details of the standard test results refer to Appendix H) as defined by the B.S. 5835 test so an improved technique has been developed. The same number of layers and surface treatment between layers are used. Each layer is compacted to refusal density to ensure that lower layers are not further densified as the specimen is built up. Two minutes of compaction using a vibrating hammer with a 100 mm diameter head are applied randomly by hand followed by the 15 minutes of full face compaction with the lever system. An average density of 2343 kg/m^3, which is equivalent to 99% of the maximum density obtained by the British Standard test, was achieved by the modified method. More details about the effect of compaction are presented in Chapter 5.

Although a compaction technique to produce high density for aggregates has been developed, the method is not yet suitable for routine purposes. More work is needed to reduce the labour intensive element of the present technique.

3.7.2 Routine set-up procedure

Materials obtained from quarries are first dried in an oven and separated into different sizes by sieving. These fractions are carefully recombined into the desired grading. For materials taken from site, the water content of the aggregates is determined. Water content is then adjusted to the desired level. To make sure every particle is fully wetted, samples are left overnight. Furthermore, in order to minimize segregation and uneven moisture distribution, the recombination and mixing process is carried out in small batches of 10 kg of aggregate.

The oversized membrane, described in Section 3.4, is then put inside the sample preparation mould which comprises a split aluminium cylindrical tube joined with four Jubilee clips and bolts. A photograph of the mould is presented in Plate 3.7. The specimen is then prepared in eight layers as described in Section 3.7.1. Compaction of the sample is carried out in a closed room to accommodate the noise generated (up to

110 dB). When the mould is removed, the specimen is found to be stable under its own internal suction and interlocking even though the membrane is usually punctured by the heavy compaction.

To reduce the time to achieve suction equilibrium in the specimen in later stages of the test (when the applied internal partial vacuum will be changed from one level to another), a thin filter cloth is laid on top of the specimen and six vertical filter strips are placed at equal spacing onto the first membrane. To ensure satisfactory connection between the filter strips and the specimen, small holes, at 50 mm spacing, are made through the membrane at the locations of the filter strips. This system provides air channels between the porous filter in the platens and the specimen.

Before the second membrane is put on, a small amount of glue is applied to the first membrane at locations where the plastic blocks for the on-sample instrument are to be fixed. This is a precaution to prevent slip between the two membranes. Once the second membrane has been loosely placed, the first membrane is cut so that it ends at the interface between the platens and the specimen. This allows the second membrane to be directly in contact with the stretchable sealant and, thereby, ensures a good seal at the platens. The second membrane is then secured to the platens as described in Section 3.4.

After the sealing work has been finished, vacuum lines are connected to the top and bottom platens. Once the suction has been applied, the specimen is ready for installation of the on-sample instrumentation.

The instrument installation process is relatively easy since a jig (Plate 3.6)has been made to fix the plastic blocks which hold the LVDTs at predetermined locations. Plastic blocks are fixed onto the PVC membrane with the glue as recommended in Section 3.5. Once the glue has hardened, the LVDTs are installed in a period of about half an hour.

3.8 SUMMARY

(1) A simple load frame capable of withstanding repeated loads of high magnitude provides the principal structure of the apparatus for unbound granular material testing.

(2) Provision of axial forces is mainly made by two simple hand devices:- a manually operated actuator and a drop hammer. The consequence of successfully applying load by hand would be a huge saving in both the initial and the running costs. In order to assess the effect of using simple load devices, a servo-controlled hydraulic actuator with the capacity of providing precise load control has been installed.

(3) Constant confining pressures are supplied by applying partial vacuum to the tested specimens. This simplifies the apparatus further by eliminating the need for a very large cell.

(4) Oversized membranes made of 0.25 mm thick PVC film are used to replace the conventional latex membrane. The PVC membrane provides a cheap solution. The possible extra confinement pressure due to the PVC membrane has been investigated. The conclusion is that it has negligible effect.

(5) To provide an air-tight seal to the tested specimens, a method using a stretchable sealant has been developed to accommodate the oversized PVC membrane.

(6) Measurements of vertical displacement are taken over the middle third height of specimen using three high precision LVDTs to avoid end effects from the load platens. Measurements of radial movement are made at the mid-height of specimen by three spring loaded LVDTs fixed to a horizontal ring.

(7) An automatic data acquisition system has been developed to record signals from the instrumentation.

(8) A compacting method, having the ability to produce specimens of high density, has been developed.

CHAPTER 4

PRELIMINARY STUDY OF THE TEST MATERIALS

4.1 INTRODUCTION

The main purpose of performing laboratory tests is to characterise pavement foundation materials in terms of resilient stiffness and resistance to permanent deformation, as highlighted in Chapter 1 and Section 2.6. These two properties of granular materials, however, cannot be determined by the current routine laboratory design tests, the limitations of which have also been discussed in Section 2.1.

The significance of the influence of various material conditions and characteristics (such as particle size, grading, angularity, roughness, moisture content and compaction etc.) on the elastic and plastic responses observed by previous researchers (Barksdale et al 1988 and Thom 1990) has been illustrated in Chapter 2. An important implication of this is that only samples at their full gradings can hope to have the correct mechanical properties as only then will the correct interplay of micro and macro texture come into force. Furthermore, understanding the different aspects of the constituent particles is an essential element in explaining the material behaviour *en-masse*. Therefore, it is worthwhile to make a study of the basic physical characteristics and mechanical properties of particles of the selected unbound aggregates.

For particle characterization, a series of classification tests mainly in accordance with B.S. 812 (1990) which included relative density testing, water absorption testing, particle angularity and roundness determination, sphericity analysis and shape analysis were carried out to assess the physical conditions of stone particles. To investigate the mechanical properties, 10% Fines Value, Aggregate Impact Value, Aggregate Abrasion Value and surface friction tests were performed.

As described in Section 2.5.1, Earland and Pike (1985) concluded that the ultimate shear stress values obtained by shearing materials at low vertical stresses in a large shear box were able to classify the stability performance of granular materials under construction traffic. They also suggested that the apparatus was able to accommodate most pavement foundation aggregates at their full gradings with maximum particle size up to 50 mm. On this basis, it was decided to include the large shear box testing as part

of the preliminary test programme to provide an indication of the performance due to particle interaction in aggregates at their full gradings. As the large shear box is relatively uncomplicated, an attempt was made to determine the resilient and the permanent deformation behaviour of unbound granular materials by applying repeated stresses to the specimen. This also provided an opportunity to assess the potential of the shear box for use as a simple tool for testing pavement foundation materials.

The results from the various tests provide a characterization of the granular materials against which the performance and output of the triaxial test apparatus described in Chapter 3 may be assessed.

4.2 MATERIALS

In view of the effects of material types on the engineering properties of pavement foundation materials, three types of aggregate were chosen for testing. They were dolomitic limestone from Whitwell Quarry (Derbyshire), granodiorite from Mountsorrel Quarry (Leicestershire) and a Trent Valley gravel from Attenborough (Nottinghamshire). These materials came from entirely different origins and, hence, significant variation in behaviour could be expected.

Limestones are widely used as sub-base materials for flexible pavements in the U.K. The dolomitic limestone from Whitwell was excavated at about 35 metres below ground level. It is a chemical sedimentary rock. Stones have a low abrasion resistance - a knife can easily scratch the surface. The main mineral constituents are dolomite and calcite with a higher proportion of the former mineral. Dolomitic limestones tend to have a low crushing strength.

The Mountsorrel granodiorite is an intrusive igneous rock, formed from plutonic masses, with an appearance similar to that of granite (coarsely crystalline), but with less quartz and higher mica, hornblende and augite contents. It is a transition rock between granite and diorite. Particles of the granodiorite have a moderate to high crushing strength, a medium to coarse surface texture and reddish grey colour because of a slight degree of weathering.

The gravels from the Trent valley were, like any other river gravels, deposited after being transported by water over a distance. The chief constituents of the gravel were,

as expected, harder than crushed rock from quarries, because attrition actions during transportation had removed (or broken up) the weaker particles.

4.3 PARTICLE CHARACTERISATION

4.3.1 Particle shape

Methods to express the particle shape of aggregates have been developed by Wadell (1932), Zingg (1935), Rösslein (1941), Krumbein (1941) and Lees (1964) over the last sixty years or so. Arbitrary limits of flatness ratio (f) and elongation ratio (e) were used to divide particles of different shapes into four general groups :- blade, disc, equidimensional or cubic and rod according to the limits last drawn by B.S. 812 (1975). For establishing relationships between shape and behaviour, this type of grouping method was criticized by Lees (1964) as being too imprecise.

In this project, the method, created by Aschenbrenner (1956), developed from the concept of the tetrakaidekahedron (Figure 4.1) and Wadell's definition of sphericity, were used to analyse particle shapes. The degree of working sphericity (y'), ranging between 0 and 1, and the shape factor (F) were used to define the shape. When y' is unity, a cubic shape is expected. The main advantage of the sphericity measure is that the surface area of a particle can be compared with that of a sphere of the same volume. The parameters, F and y', are defined as follows:

$$F = \frac{f}{e} \qquad (4.1)$$

$$y' = \frac{12.8^3\sqrt{f^2\,e}}{1 + f\,(1 + e) + 6\sqrt{1 + f^2\,(1 + e^2)}} \qquad (4.2)$$

where:-   f = flatness ratio (c/b)
            e = elongation ratio (b/a)
            a = half the greatest length
            b = half the intermediate length
            c = half the shortest length

Fifty particles, retained on a 20 mm sieve from each type of aggregate were examined. Measurement of the axial lengths was by means of a pair of digital callipers. The mean results are given in Table 4.1. Only a small variation in shape was found between the

a > b > c
where a, b and c are half-axes
which are parallel to X, Y and Z
respectively
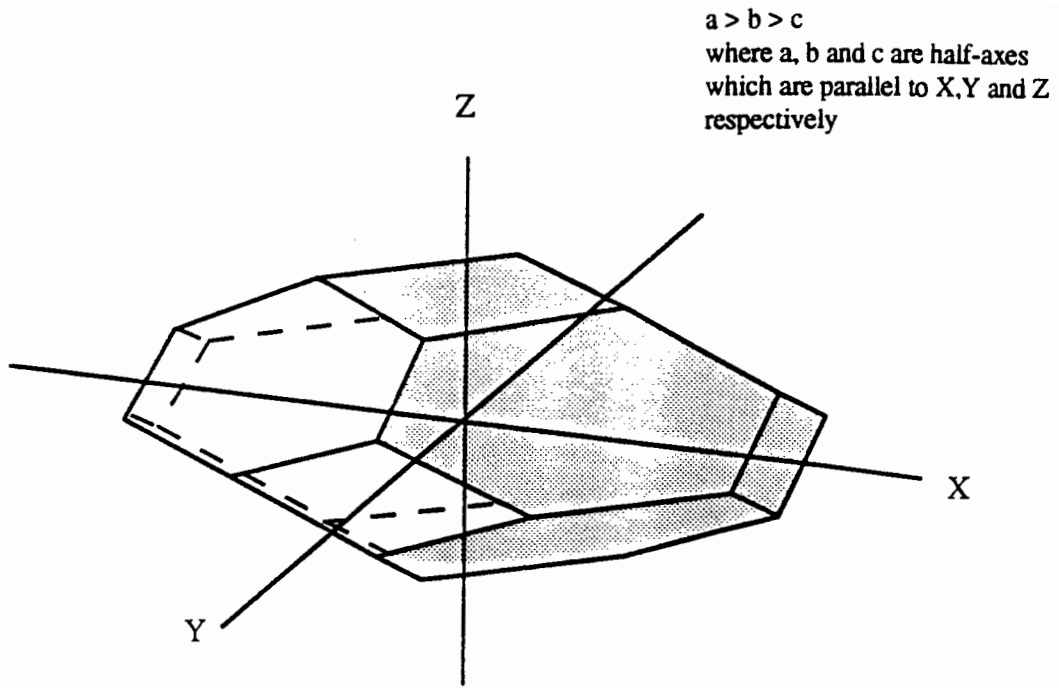
Figure 4.1 Tetrakaidekahedron in diametric projection (after Aschenbrenner 1956)

ROUNDNESS = .1 .2 .3 .4 .5
BROKEN PEBBLES
.6 .7 .8 .9
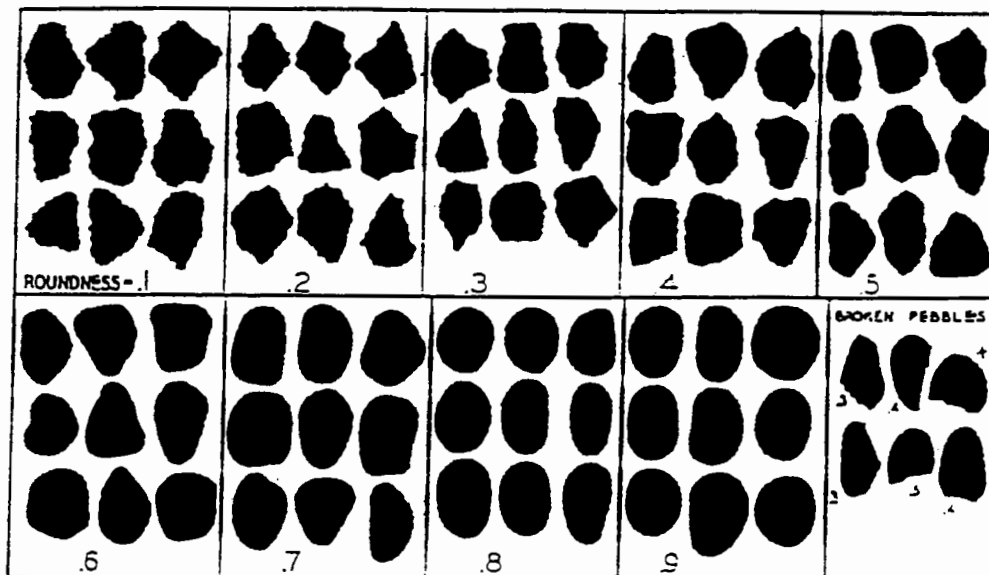
Figure 4.2 Chart for roundness examination (after Krumbein 1941)

different materials. The mean working sphericity was about 0.9 and the shape factor was about 0.83. Thus all the chosen aggregates were well within the cubic zone of the British Standard classification. Perhaps the results should have been expected since the materials from quarries were carefully crushed and the river gravels were normally of spherical or elliptical form.

Table 4.1 Results of sphericity testing

Mean Measures	Granodiorite	Dolomitic Limestone	Gravel
f	0.63	0.69	0.65
e	0.77	0.8	0.82
F	0.82	0.87	0.8
y'	0.88	0.9	0.9

4.3.2 Roughness

One of the physical properties which may affect inter-granular slip is the surface texture. Six broad qualitative classes, i.e. glassy, smooth, granular, rough crystalline, honeycombed and porous, are outlined in B.S. 812 (1975), but this descriptive method is insufficient for analytical measurement. The idea of a Roughness Factor, RF, developed by Wright (1955), was employed to express the surface topography of aggregates. To prepare a test specimen, a particle was firstly embedded in resin. It was then cut into two by a saw and the cut surfaces were polished. These surfaces were then magnified 100 times by a projection microscope and the interface between stone and resin was traced at the enlarged size. At this scale the RF ranging from 0 (smooth) to about 20 (extremely rough) was calculated by comparing the length of the traced uneven line covered by four lengths of an 8 cm chord with the total chord length (i.e. 32 cm).

$$RF = \frac{100\ Y}{32} \tag{4.3}$$

where:-   Y is the difference between the length of the roughness line covered by four 8 cm chord lengths and the total length of the chords in cm.

     RF > 10   rough texture

     RF = 7-10   medium texture

     RF < 7   smooth texture

Results are presented in Table 4.2. The dolomitic limestone could be classified as having medium texture since the RF was between 7 and 10. The other two materials were within the smooth texture category in which the gravel was the smoothest and the granodiorite was on the border line of smooth and medium roughness.

Table 4.2 Summary of physical property of particle

	Granodiorite	Dolomitic Limestone	Gravel
Specific Gravity			
saturated surface dry	2.65	2.69	2.61
oven-dried	2.64	2.62	2.59
apparent	2.67	2.82	2.65
Water absorption value	0.5%	2.7%	0.9%
Angularity	9	9	4
Roundness	0.3	0.3	0.6
Roughness Factor	5.3	8.8	1.6
Sphericity	0.88	0.9	0.9
Shape Factor	0.82	0.87	0.8

4.3.3 Angularity

The angularity of the materials was examined by using the B.S. 812 method (1975) and recorded in terms of Angularity Number (AN) which was a measure of the proportion of voids after compaction. The AN ranges normally between 0 and 12. Aggregates of well rounded particles have a lower number. The reasoning behind this is that, at the same compaction effort, the void ratio will gradually increase as a material contains an increasing proportion of angular particles. AN is defined as:

$$AN = 67 - \frac{100\,M}{c\,G_S} \qquad (4.4)$$

where:-   M is the mass of aggregate (g)

c is the mass of water required to fill the same volume of aggregate (g)

G_S is the oven-dried specific density of the material

The test results (Table 4.2) shows that the gravel had an AN of four while the crushed stones had values more than twice as high. The results were later supported by the visual roundness test.

4.3.4 Roundness

The visual roundness examination method proposed by Krumbein (1941) was used to provide more information about the particles of aggregate. Roundness (R) varying from 0.1 to 0.9 provided the measurement of the sharpness of corners. It is a function of wear and tear undergone by individual stones.

$$R > 0.6 \qquad \text{high roundness}$$
$$R = 0.4\text{-}0.6 \qquad \text{medium roundness}$$
$$R < 0.4 \qquad \text{low roundness}$$

In this study, the simplified roundness chart as shown in Figure 4.2 was used, although it has the drawback of introducing operator variability. For each type of material, fifty particles were observed and the average results are presented in Table 4.2. The gravel had a high roundness value of 0.6. This was double those of the two materials from quarries. An approximation was made using Equation 4.5 to translate the roundness values into AN values.

$$AN = (0.9 - R) \frac{12}{0.8} \qquad (4.5)$$

It was found that the translated AN's of the gravel and the crushed stones were 4.5 and 9 respectively which were comparable to the results from the angularity testing.

4.3.5 Specific gravity and water absorption

Measurement of the saturated surface dry, oven-dry and apparent specific gravity (G_s) was made in accordance with B.S. 812 (1975). All three types of aggregates were of similar G_S (oven-dried) of 2.61 ± 0.03 (Table 4.2). As indicated by the difference between the saturated surface dry and the oven-dried specific gravities, the dolomitic limestone showed the highest value of water absorption, 2.7%. Collis and Fox (1985) observed that particles with high absorption tended to be less resistant to mechanical

forces. The relationship was confirmed in the subsequent mechanical testing on particles. The dolomitic limestone gave the lowest resistance to compressive forces, impact loads and abrasion.

4.3.6 Aggregate Impact Value (AIV)

Several mechanical tests were performed on particles of each aggregate. The AIV test recommended by B.S. 812 (1975), measures the resistance to pulverization in an aggregate mass due to sudden shock. Materials for this test must pass a 14 mm B.S. test sieve and be retained on a 10 mm sieve. The samples suffer degradation after being loaded with a series of standard impact forces. The AIV of each type of granular material is expressed in terms of percentage by mass passing a 2.36 mm sieve relative to the original mass. Results from the aggregate impact test, summarized in Table 4.3, show that under the same impact effort, the granodiorite produced only 17.7% fines which was 2% lower than the AIV for the gravel and was only about half of that for the dolomitic limestone.

Table 4.3 Summary of mechanical property of particle

	Granodiorite	Dolomitic Limestone	Gravel
10% Fines Value	225 kN	130 kN	305 kN
Aggregate Impact Value (AIV)	17.7%	31.3%	19.6%
Aggregate Abrasion Value (AAV)	3	16	1.9
Surface Friction Angle (ϕ_s)	27°	31°	26°

4.3.7   10% Fines Value

To reflect the resistance of aggregate to a continuous load by an increasing compressive force, each material was tested to find its 10% Fines Value. The size of particles used is the same as for the AIV test. The 10% Fines Value was deduced from measurements of the maximum force required to produce 7.5% to 12.5% of fine particles which passed the 2.36 mm sieve.

$$10\% \text{ fines} = \frac{14 \, x}{y + 4} \qquad\qquad (4.6)$$

where:-   x is the maximum force   (kN)

y is the percentage of fines

Results, given in Table 4.3, indicate that the gravel, and not the granodiorite, showed the greatest resistance to crushing. Hence, the crushing resistance of stone particles from static testing does not necessarily give the same ranking as that from impact load testing. Nevertheless, the ranking of the dolomitic limestone either by the 10% Fines Value test or the AIV test was unchanged. The particles of the dolomitic limestone were the weakest of the three materials tested.

4.3.8 Aggregate Abrasion Value (AAV)

In order to determine the resistance to surface wear (which may be related to the effect of cleavage and the strength of internal bonds, and the brittleness and the hardness of the constituent minerals), the AAV test according to B.S. 812 (1975) was carried out. Samples were set on resin backing with aggregate particles protruding by about 6 mm. With the stone surface held against a rotating disc and Leighton Buzzard Sand used as the abrasive material, the AAV was found. The value varies from 1 for aggregates of high hardness to over 15 for very weak stones. It was found by referring to the mass lost after 500 revolutions.

$$AAV = \frac{3 \, (A - B)}{d} \qquad\qquad (4.7)$$

where:-   A is the mass of specimen before testing (g)

B is the mass of specimen after testing (g)

d is the relative density of surface dry sample

The gravel showed the greatest resistance to wearing. The ability to resist abrasion was eight times greater than for the dolomitic limestone and 1.5 times higher than for the granodiorite.

4.3.9 Surface friction

To study the surface friction of the particles, simple index testing was performed. Three 20 mm particles from one source were set in a cement mortar backing with the stones protruding by 5 mm. With the three aggregate asperities resting on a hard concrete surface, the specimen was then loaded so that the total weight, W, including the tested specimen, was 5 kg. The minimum force, F, to produce sliding movement was noted and the surface friction, expressed in terms of an angle of apparent surface frictional resistance, ϕ_s, was calculated.

$$\phi_s = \tan^{-1}(\frac{F}{W}) \qquad (4.8)$$

Figure 4.3 shows the arrangement. The results are given in Table 4.3 from which it is evident that the dolomitic limestone demonstrated the greatest surface friction characteristic. Comparing results with the corresponding roughness factors of each material, it was noticed that aggregates of higher surface roughness showed larger surface friction.

4.4   LARGE SHEAR BOX TESTS

4.4.1 Introduction

The particle interaction of the selected granular materials was examined using a large shear box (sample size 300 x 300 x 180 mm). This shear box testing was carried out at the Nottinghamshire County Council Materials Testing Laboratory. Plates 4.1 and 4.2 show the apparatus and the composition of the box respectively, which consisted of three main parts:- the loading system, the metal shear box and the recording system. Vertical and horizontal loads were supplied by hydraulic pressure units. The rate of shearing, controlled by a set of gears, was fixed at 0.12 mm/min. Load cells of capacity measuring up to 25 kN were used to monitor the applied shear and normal stresses resulting in a maximum stress discrimination of 280 kPa. Movements parallel and perpendicular to the notional shear surface were measured by dial gauges which were able to read to a discrimination of 0.002 mm.

The possibility of observing the resilient behaviour of unbound granular materials in the shear box by applying repeated stresses to the sample was investigated. Figure 4.4
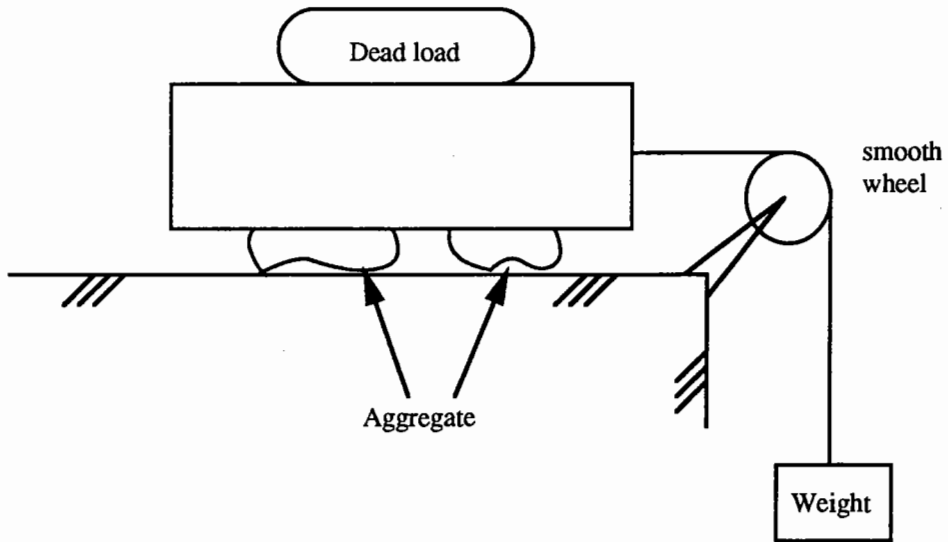
Figure 4.3 Determination of aggregate surface friction
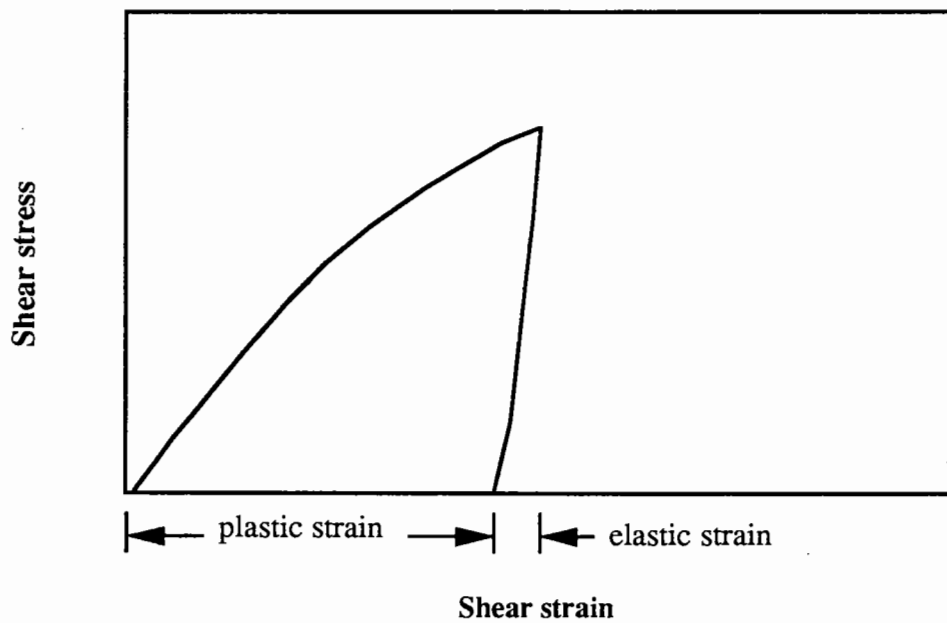
Figure 4.4 Elasto-plastic behaviour of crushed stone

illustrates a typical stress-strain curve for the first cycle of an elasto-plastic material such as a crushed rock. As the load increases, the total strain (including elastic and plastic strains) increases correspondingly. After unloading, there is a small amount of elastic recovery leaving a large permanent strain. Shenton (1987) performed repeated load triaxial test on ballast materials (composed of essentially single-sized 25 - 50 mm diameter particles) and found that the rate of plastic axial strain during repeated load applications was proportional to the plastic strain produced by the first load cycle. Earland and Pike (1985) recommended that shear strength was able to distinguish the performance of aggregates under wheel loading (refer to Section 2.5.1). For these reasons, the use of a shear box to determine the permanent deformation resistance of granular materials under repeated loading was looked into. The test consisted of three parts.

At the beginning of the test, a series of vertical repeated loads was applied to check the resilient behaviour of the materials. Then plastic deformation generated by repeating the horizontal shear force was examined. Finally, the ultimate shear strength of the aggregates was determined by shearing the materials until failure was reached.

4.4.2 Stress condition in the test specimen

Before horizontal loads are applied, the major and the minor principal stress directions of elements inside the shear box are essentially parallel to the walls and to the top of the metal box respectively. The major principal stress, σ_1, is equal to the axial load divided by the horizontal area of the box. For the minor principal stress, Equation 4.9 suggested by Jakey (1948) for the prediction of coefficient of earth pressure at rest, K_o, might be used.

$$K_0 = 1 - \sin \phi' \qquad\qquad (4.9)$$

where:- ϕ' is the effective angle of internal friction of materials.

However, the equation was developed for loosely compacted granular materials. The locked-in stresses created by heavy compaction were not taken into account. Furthermore, Pike (1973) reported that the ϕ' value of granular materials was stress dependent, varying especially at low confining stresses. Shaw (1980) measured lateral stresses of dense granular materials on the wall of his simple shear box when only
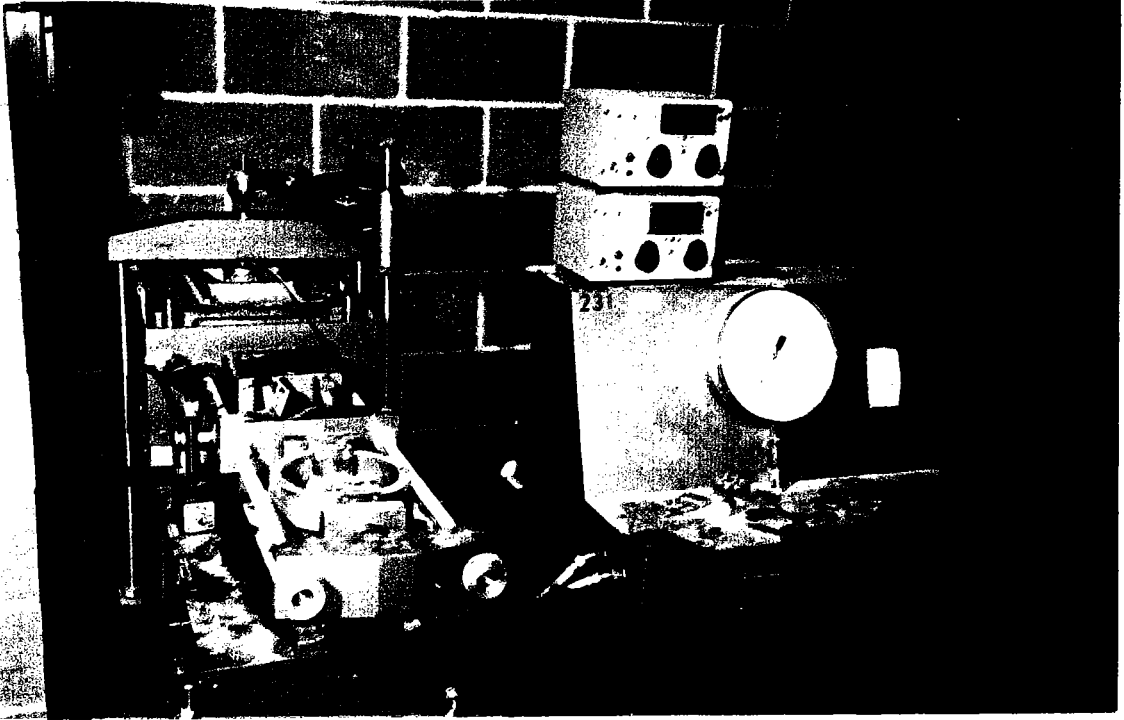
Plate 4.1   The large shear box
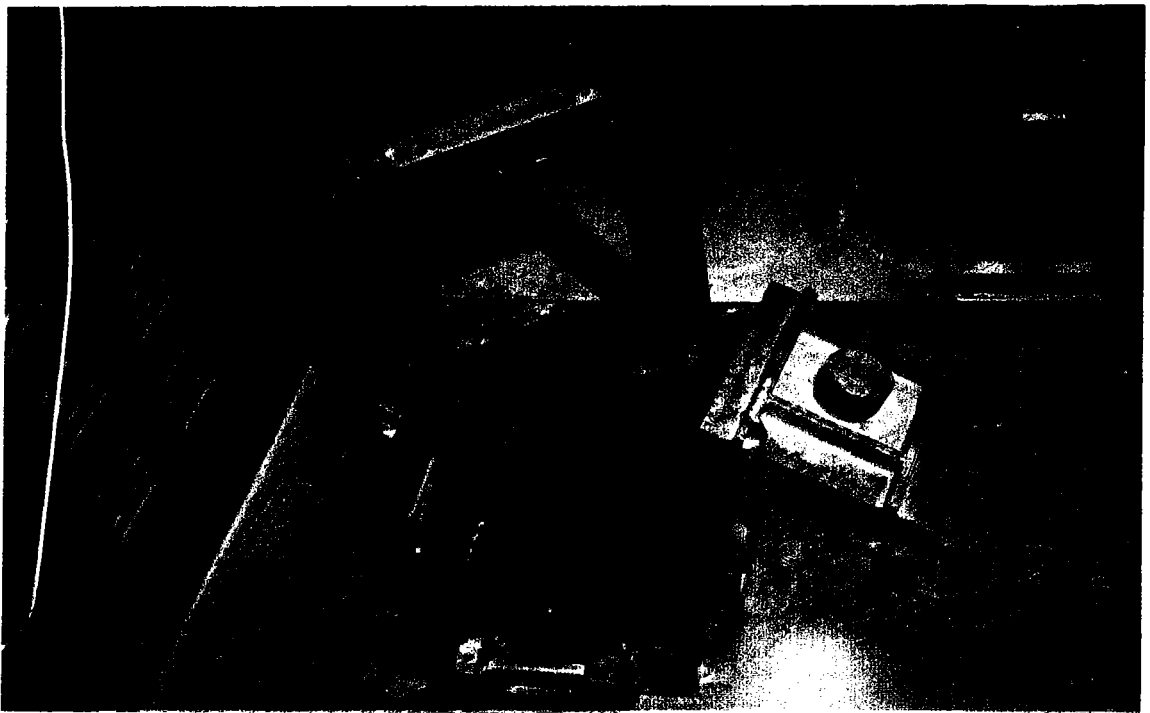
Plate 4.2   Components of the large shear box

vertical loading was applied. He found much lower K_0 values than those derived from Jakey's equation. He also observed that the value of K_0 was not constant. It decreased with increasing vertical stresses.

The stress conditions inside the shear box specimen when subjected to a horizontal shear couple are more difficult to determine since the measurements of loading and displacement are made outside the box and no measurement is made directly on the specimen. More details of the stress conditions in the box including estimation of principal stresses during shearing are presented in Appendix D.

4.4.3 Preparation and testing procedure

Six tests were performed in the large shear box. Table 4.4 summarizes the details of the tested specimens.

Table 4.4 Summary of tested materials for the large shear box

Sample No.	Materials	Grading	Time of Compaction (minutes)	Dry Density (kg/m^3)
DA2	Dolomitic Limestone	A	2	1798
DB2	Dolomitic Limestone	B	2	2194
DB0.5	Dolomitic Limestone	B	$\frac{1}{2}$	1965
DC2	Dolomitic Limestone	C	2	2145
GB2	Granodiorite	B	2	2207
SB2	Sand and Gravel	B	2	2205

Note :-

Grading A is a Fuller's curve with n=1.5 and maximum particle size of 40 mm.

Grading B is the fine end of Type 1 sub-base curve of the specification of the DoT.

Grading C is the fine end of capping 6F1 of the specification of the DoT.

Four samples of dolomitic limestone, one sample of sand and gravel and one sample of granodiorite were carefully constructed from single size fractions. Figure 4.5 shows the particle size distributions. Most of the specimens were tested at the medium grading, B, being the fine side of the Type 1 sub-base envelope of the DoT specification (1992). To represent extreme gradings, a sample to the Fuller's (1907)
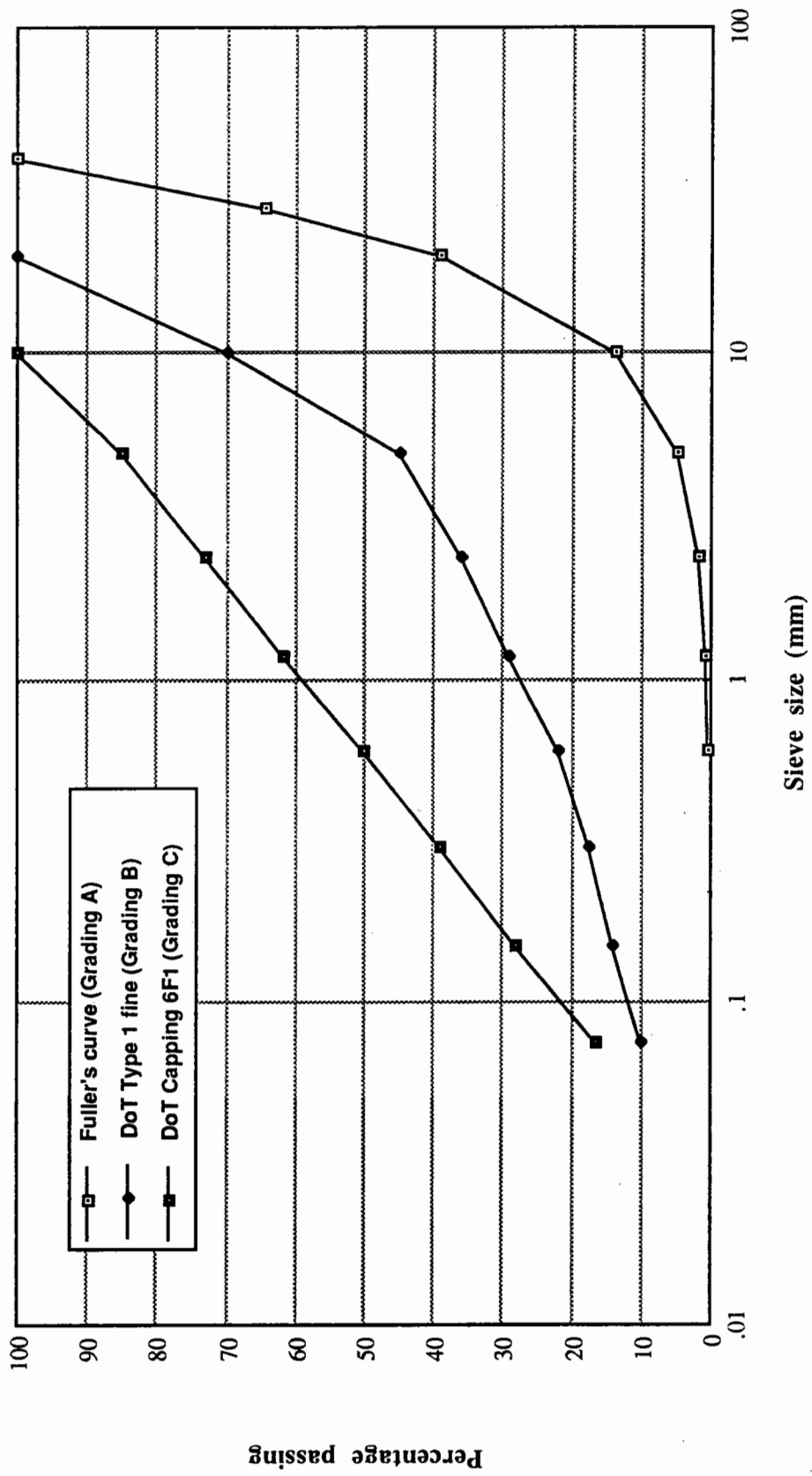
Figure 4.5 Aggregate gradings used in testing (refer to Table 4.4)

grading curve with n = 1.5 and maximum particle size of 40 mm and another with a grading at the fine end of the capping 6F1 envelope from the same DoT specification were chosen. Because of time limitations, only dolomitic limestone was tested at these gradings. Materials were compacted in three approximately equal layers and the compaction effort was standardized to two minutes of a hand-held vibrating hammer, except for one sample which was compacted for only thirty seconds per layer to investigate the effects of low compaction effort. The density from the thirty second compaction was only 90% of that from the two minute compaction (Table 4.4). Since the main purpose of the test was to study the performance of an aggregate mix due to particle interaction, it was justifiable to test materials in dry conditions.

To settle each specimen so that seating errors might be reduced, a pre-loading vertical stress of 70 kPa was applied for 1 minute. Then the specimens were subjected to a series of repeated vertical loads as shown in Table 4.5. The second series of tests involved repeated horizontal shear stresses at a fixed vertical load of 10 kPa. Table 4.6 shows the details of the horizontal stresses applied. It was noticed that the strain recorded under low shear stress cycles (2-4 kPa) fluctuated. This might have been due to inaccuracy of measurement at small displacements. More reliable results were obtained at the higher stress level. The final stage was the shear strength testing. With the normal stress at 10 kPa, the specimens were steadily sheared until the failure point was reached.

Table 4.5   Schedule of repeated vertical load testing

Vertical Stress (kPa)	No. of Cycles
10 - 20	2
20 - 30	2
30 - 40	2
40 - 50	2
50 - 60	2
60 - 70	2

54

Table 4.6 Schedule of repeated horizontal shear testing

Constant Vertical Stress (kPa)	Horizontal Shear Stress (kPa)	No. of Cycles
10	2 - 4	5
10	5 - 10	5
10	15 - 20	5

4.4.4   Results and discussion

4.4.4.1 Particle effect on material density

Table 4.4 has presented the dry densities of the tested materials after compaction. The samples (DB2, GB2 and SB2), which possessed the same particle grading curve and were compacted under the same compactive effort, were found to have very similar density although their constituent particles were of different angularity, roundness and surface roughness, especially sample SB2. Nevertheless, according to Table 4.2 all these three materials have particles of similar shape factor. Hence, to produce high density samples, the shape of aggregates plays an important role.

Furthermore, when the samples (DA2, DB2 and DC2) of the same material type and with the same compaction are compared, the sample with the medium grading was found to produce the highest density. Hence, there appears to be an optimum particle size distribution curve which generates maximum density. Materials comprising too many single size particles or too high a fines content are not able to produce high density.

4.4.4.2 Strength

Typical results showing the shape of the monotonic load-displacement curve, as well as of the deformation response under repeated shear force, are given in Figure 4.6. It is interesting to notice that the shape of the monotonic curve does not appear to be affected by the repeated shear load applied.

The horizontal displacements of the six samples during the strength testing stage are presented in Figures 4.7 and 4.8. Results from the three dolomitic limestone samples
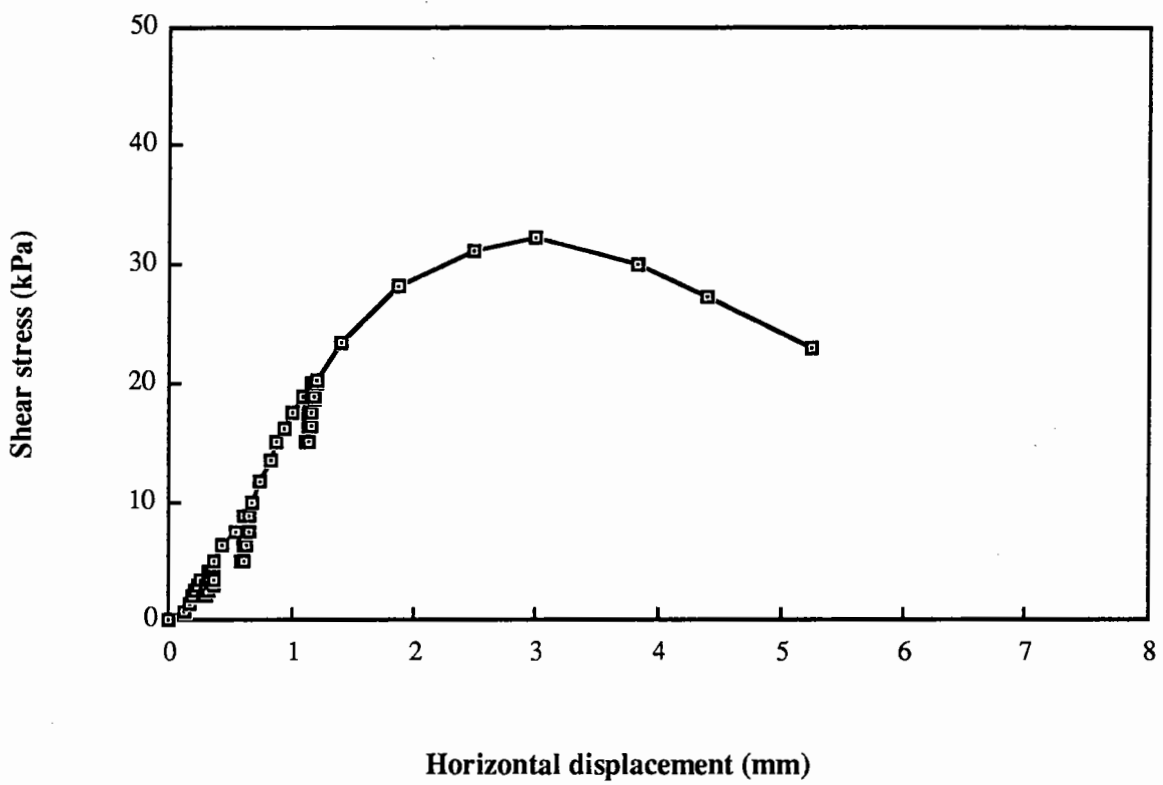
Figure 4.6 Typical load and displacement relationship of unbound granular materials in the large shear box (Sample SB2)
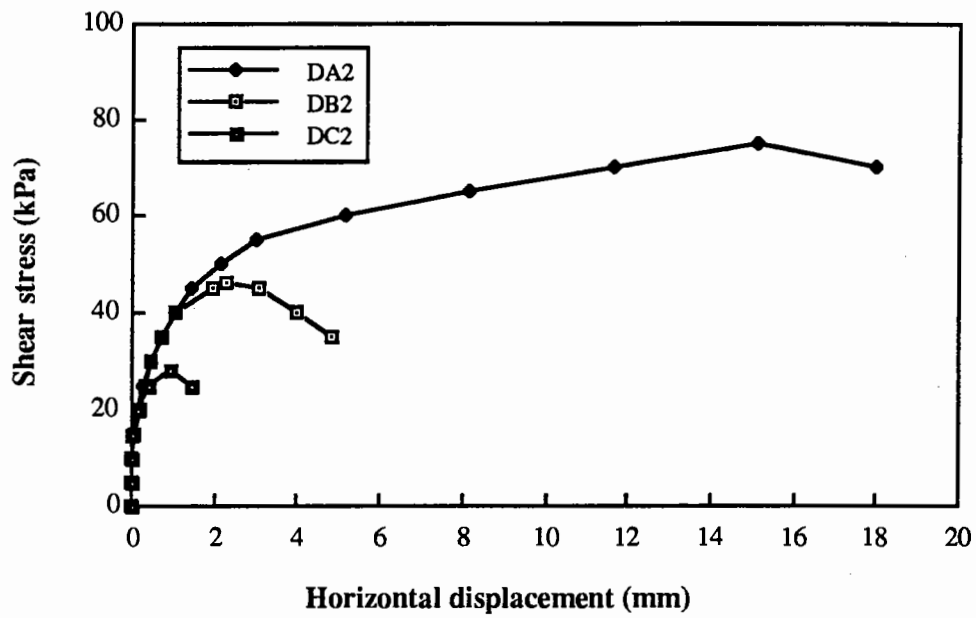
Figure 4.7 Horizontal displacements of dolomitic limestone of different gradings in the large shear box
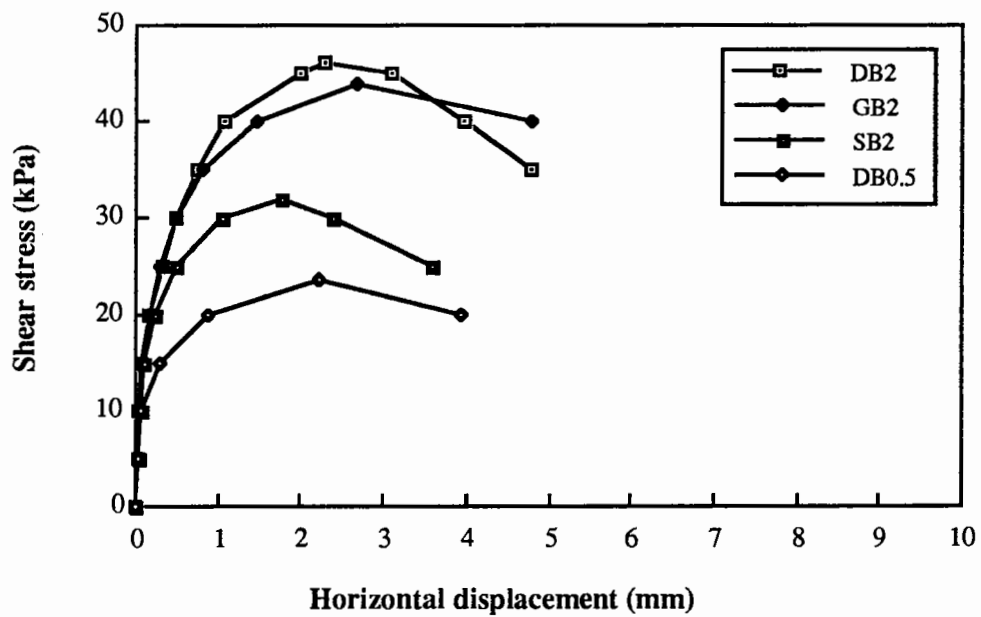
Figure 4.8 Horizontal displacements of granular material of different natures and of different compaction time in the large shear box

at normal compaction levels are grouped in Figure 4.7 while samples with the same grading are grouped together in Figures 4.8. For clarity, the strains and stresses of the repeated loads in the midst of the test are not included. In the early stages of each test, stresses increase with only a small amount of lateral movement of the box. Then, the rate of displacement increases until the peak stress is reached. After having reached the peak, the lateral stress decreases with further displacement.

Figure 4.7 shows results from the samples of dolomitic limestone with different gradings indicating that the material, DA2, with the coarsest grading had the highest shear strength whilst the material with the finest grading possessed the lowest ultimate strength. The horizontal displacement of DA2 was extraordinarily high as well. However, DA2 was the sample which possessed the lowest density. The density was about 80% of that for DB2 indicating that DA2 was less well compacted. A lower strength is thus to be expected.

The high strength phenomenon of the material containing large aggregates might be explained by the particle size effect coupled with the particular failure mode of the shear box testing. Let us consider the failure mechanism of materials tested by the shear box. The specimen is sheared at a pre-determined surface at the mid-height of the shear box. If large particles are allowed to occupy this surface, the formation of a shallow failure band at the mid-height will be prohibited. Other failure surfaces will be formed depending on the size of particles. The larger the particle, the deeper will be the new failure surface into the box. Since particles located deeper into the upper and the lower half of the shear box are more confined by the shallow box, more energy will be required to shear the material. Hence, boundary effects on samples with a high percentage of large particles would be much higher than those comprising fine materials. Jewell and Wroth (1987) recommended a minimum ratio of 50 between the length of the box and the particle size of D_{50} to make sure that the shear strength obtained from the shear box testing was from particle interaction and not from the size effect. This ratio was not even approached in the testing being described for which the ratio was about 12.

The importance of particle interlocking due to increasing density was demonstrated when results from the samples with two minute compaction and with thirty second compaction were compared (Figure 4.8). The latter sample, whose density was about 90% of the former's, exhibited very low strength. The result was foreseeable since loose materials were not expected to provide a high level of interlocking.

A summary of the direct measurements and the derived stresses at ultimate conditions during the shearing test at a normal stress of 10 kPa are detailed in Table 4.7. The angles of the principal stress axes, χ, at the maximum shear load were found to be in a range between 60 and 73 degrees using the approach outlined in Appendix D. The derived values of the minor principal stress were small and negative. Dry granular materials are not expected to be able to carry tensile stresses. The negative values may have arisen from inappropriate assumptions concerning homogeneity in the shear zone and the assumption that the boundary effect of the box could be ignored. Nevertheless, all the negative values were small in magnitude, probably indicating, in effect, unconfined conditions. The magnitudes of the derived major principal stresses seem reasonable; they may be used with some confidence especially as obvious errors with the minor principal stresses are small.

Table 4.7   Results of shear strength testing

Sample number	Shear stress at failure (kPa)	Horizontal displacement at failure (mm)	Vertical displacement at failure (mm)	σ_1 (kPa)	σ_3 (kPa)	χ (degree)
DA2	75	14.5	15.1	225	-13	73
DB2	46	2.3	2.3	121	-9	67
DB0.5	23	4.5	2.2	51	-3	60
DC2	29	3.1	0.9	79	-2	67
GB2	44	4.5	2.7	131	-6	70
SB2	32	3	1.8	79	-3	66

Note:- for calculation of σ_1, σ_3 and χ in a shear box, see Appendix D

The ranking of the tested materials according to the major principal stress at failure is presented in Figure 4.9 (excluding sample DA2, whose strength might have been governed by the particle size effects). Again the loose sample, DB0.5, was the weakest. A low shear strength value was observed for the material containing the highest fines content. When specimens of the same compactive effort are compared it can be seen that both the dolomitic limestone (DB2) and the granodiorite (GB2) possess high and similar resistance to shear stresses. The ultimate strength of the sand and gravel (SB2) was about 63% of the highest of these, indicating that materials containing round particles are weak in shear strength.
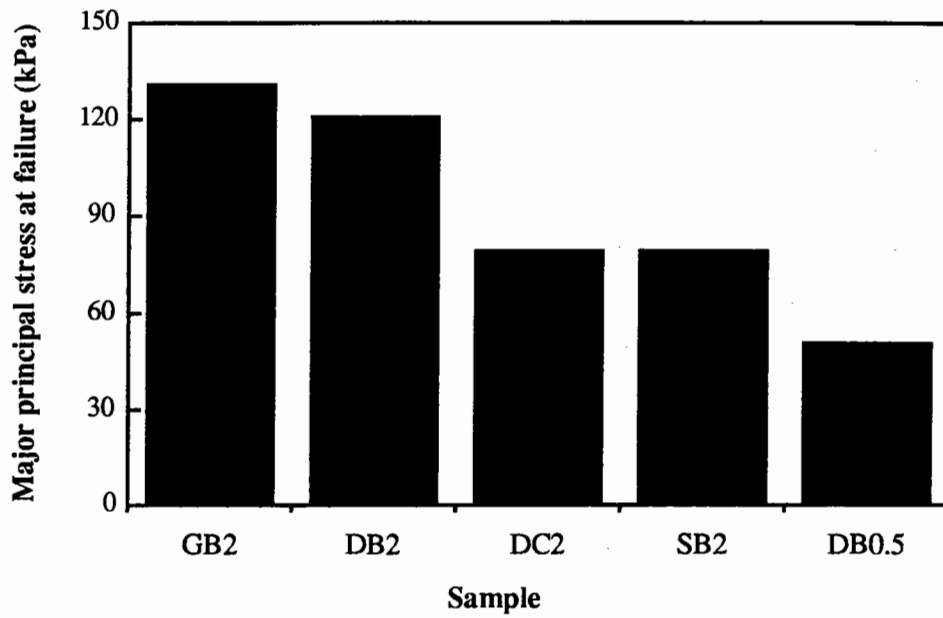
Figure 4.9 Ranking of materials according to the major principal stress at failure
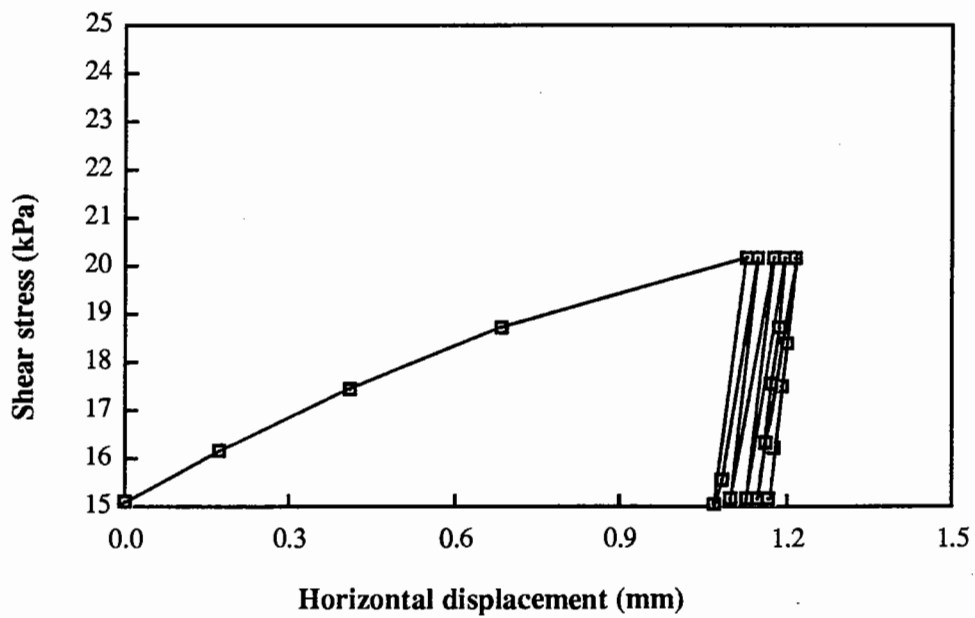
Figure 4.10 Typical deformation curve due to horizontal stress cycling (DB0.5)

4.4.4.3 Plastic strain

Figure 4.10 shows a typical deformation curve due to horizontal stress cycling. As expected, the first cycle gave the most severe plastic deformation which was many times higher than that recorded during the following cycles. The elastic recovery in each cycle was similar and the plastic strain produced in every subsequent cycle was small. For the reasons stated earlier (Section 4.4.3) the results obtained from the horizontal 15-20 kPa cycles at a vertical normal stress of 10 kPa are used for material comparison.

Figure 4.11 presents the permanent deformation generated during each shear stress cycle and Figure 4.12 enlarges the results obtained during the last four cycles. (Electronic faults developed during the test for sample DA2 and only five curves are presented.) It can be seen that the first cycle is a good indicator of the overall non-recoverable deformation and broadly ranks per cycle permanent deformation measured in subsequent cycles. This observation is in good agreement with Shenton's findings (1987).

Ranking of materials by the plastic strain developed in the first cycle is shown in Figure 4.13. When this graph is compared with Figure 4.9, fairly good agreement is found between the shear strength and permanent deformation ranking methods. Indeed, the method using the plastic strain produced by the first shear stress cycle might be better than using the ultimate shear stress approach since the results did not depend on the formation of a failure plane, which is likely to be more particle size dependent.

4.4.4.4 Elastic strain

A series of vertical repeated loads, as stated in Table 4.5, were applied to the samples and the vertical movements were recorded in order to check the resilient behaviour before the shear forces were applied. Table 4.8 details the results. Although the resilient results were lower than expected, it was noticed that the stress dependency behaviour of the materials was evident because the resilient modulus increased with the vertical stress level. The reasons for the low resilient results are not clear. Further investigation needs to be carried out. Nevertheless, the results from the samples of the same grading and degree of compaction were put together in Figure 4.14, where the axial resilient modulus (M_{ra}) is plotted against the mean vertical stress. At a low stress
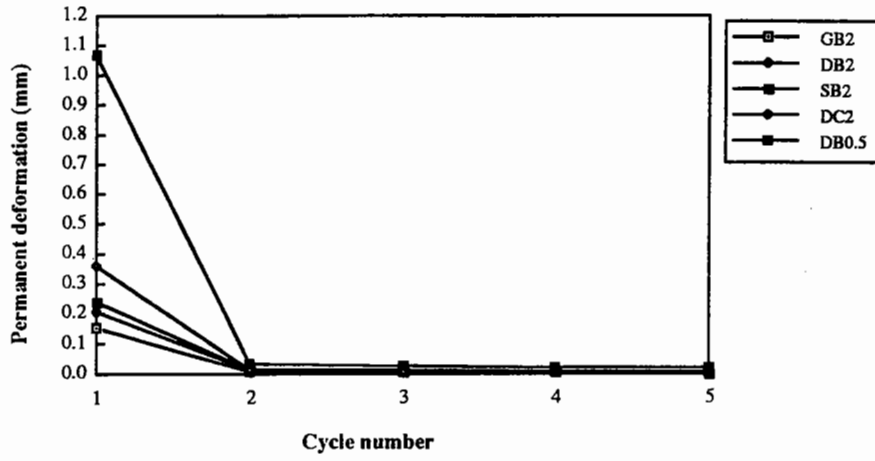
Figure 4.11 Permanent deformation during the first five cycles of horizontal loading
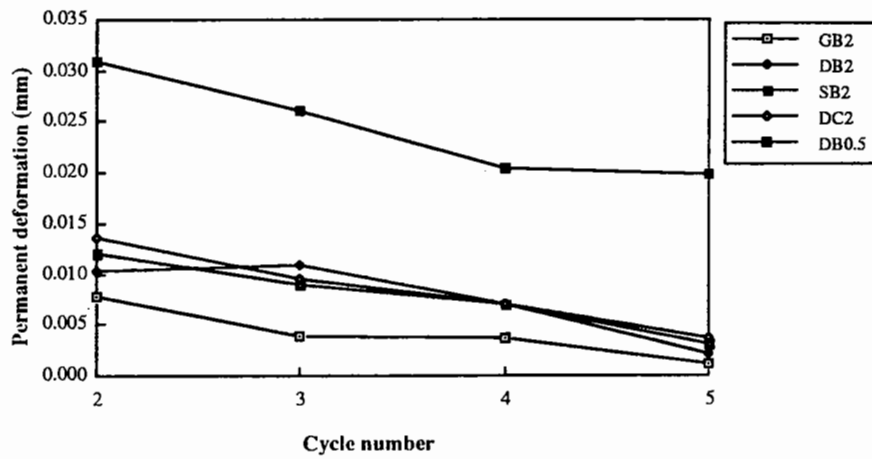
Figure 4.12 Permanent deformation of aggregates in the large shear box between cycles 2 and 5
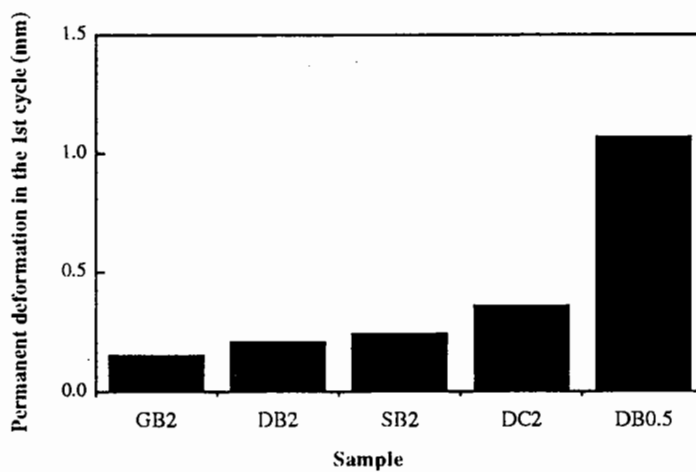
Figure 4.13 Ranking by permanent deformation observed in the 1st horizontal stress cycle (horizontal stress = 15-20kPa and normal stress =10kPa)
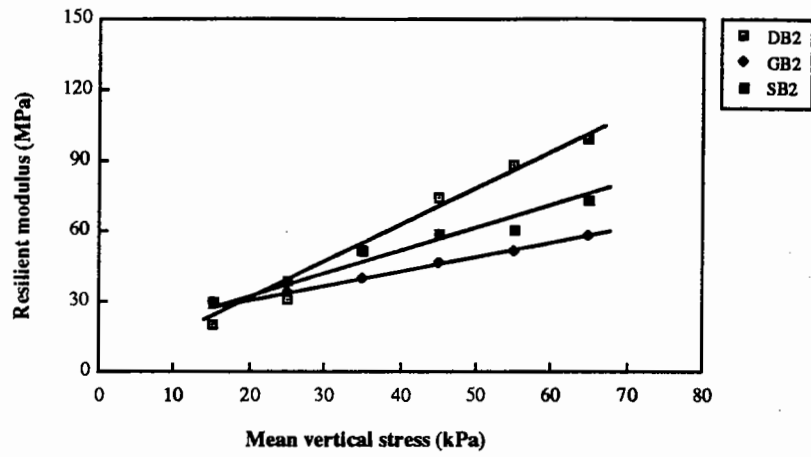
Figure 4.14 Resilient moduli of materials of different natures in the large shear box
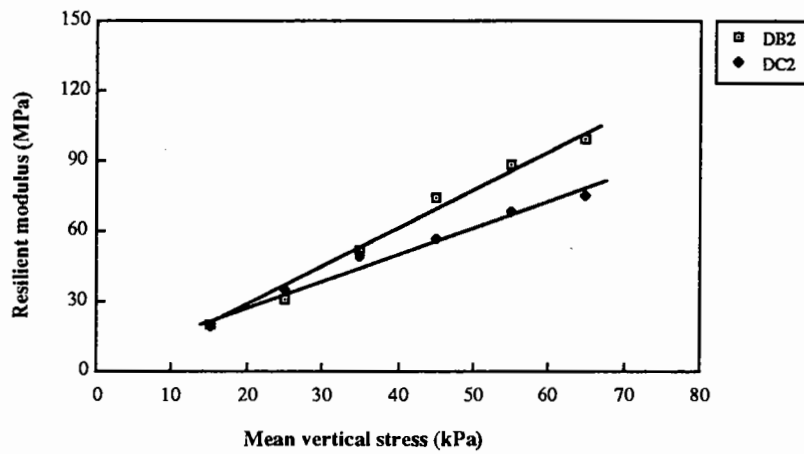
Figure 4.15 Resilient moduli of materials of different gradings in the large shear box
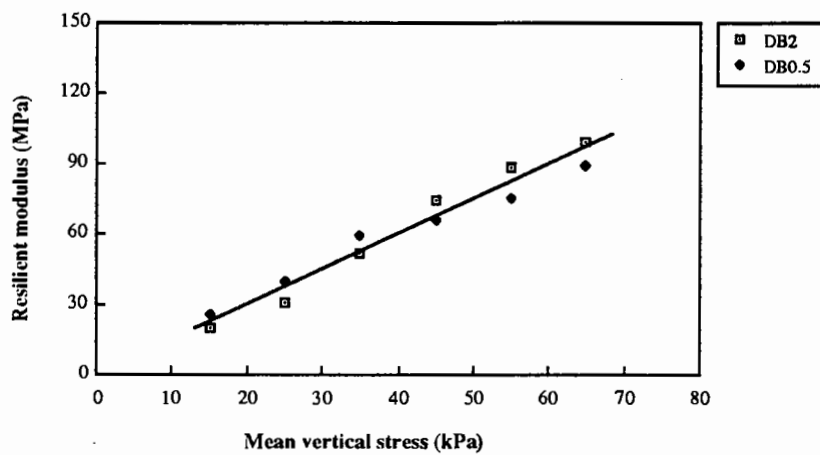
Figure 4.16 Resilient moduli of materials of different compaction efforts in the large shear box

level, the three materials behave similarly. When the vertical repeated load increases, the axial resilient modulus of the dolomitic limestone increases markedly and gives higher values than the other materials.

$$M_{ra} = \frac{\sigma_{r1}}{\varepsilon_{r1}}$$ (4.10)

where:- σ_r, and ε_r, are the repeated axial stress and the resilient strain respectively.

M_{ra} is the axial resilient modulus obtained from the large shear box.

A similar plot of the results from materials of different gradings is given in Figure 4.15. The material with the finest grading (DC2) produced a lower resilient modulus. When samples of the same material but with different compactive effort are compared, the difference between them was small (Figure 4.16). The insensitivity of the elastic properties to density of granular materials was also observed by Thom (1988).

No attempts were made to calculate the horizontal stress in the box because of the difficulty in estimating the K_o value as discussed in Section 4.4.2 and of the possible error in estimating the minor principal stress.

Since there was no direct measurement of horizontal stress on the specimen in the shear box, the full stress conditions could not be obtained. The above comparison method might give an idea of the elastic behaviour of the granular materials relative to each other but these data are far from sufficient for analytical pavement analysis.

Table 4.8 Axial resilient modulus results by using the large shear box

Axial Resilient Modulus (M_{ra})				(MPa)	
Repeated stress (kPa)	dolomitic limestone DA2	dolomitic limestone DB2	dolomitic limestone DB0.5	dolomitic limestone DC2	granodiorite GB2	sand and gravel SB2
10-20	19	20	26	19	30	30
20-30	-	31	40	35	34	39
30-40	-	52	59	49	40	52
40-50	-	74	66	57	47	59
50-60	-	88	75	68	52	61
60-70	-	99	89	75	58	73

4.5 SUMMARY

(1)   The granular materials chosen for this research were subjected to a preliminary study. The results could be used to provide an initial assessment of the performance of the newly developed 280TA.

(2)   Of the aggregates tested (dolomitic limestone, granodiorite and sand and gravel), more absorptive aggregates exhibited a lower particle strength. In general, the dolomitic limestone was the weakest and the gravel was the strongest under impact, crushing and abrasion. However, particles showing the highest crushing resistance may not possess the largest impact strength. The gravel was strongest in compression but the granodiorite showed greater ability to resist impact loading.

(3)   The dolomitic limestone was the material having the roughest surface and the gravel had the smoothest surface. Aggregates with rougher surfaces have higher surface frictions.

(4)   There was little difference in particle shape and specific gravity between the materials tested and similar densities were found when the materials at an equivalent particle grading were compacted with the same compactive effort . The angularities of the dolomitic limestone and the granodiorite were more than two times higher than that of the gravel. Since the variation of specific gravity of the three aggregate types was small, angularity and roundness do not appear to have affected density. Otherwise, there would be a significant density difference between the two crushed aggregates and the gravel (refer to samples DB2, GB2 and SB2). It appears that the shape of aggregates may be one of the dominant factors affecting material packing under compaction.

(5)   In the shear box test shear strength comparisons should only be made between aggregates of similar gradings and sizes when the particle size is big.

(6)   An aggregate ranking method using the permanent strains generated during horizontal cycling in the shear box was introduced. The advantage of this method is that it does not depend on the formation of a failure plane, hence particle size effects are minimized. Resilient performance might be checked qualitatively.

(7)   Amongst the materials having the same grading and prepared with the same compactive effort, the sand and gravel produced most permanent deformation under horizontal repeated loading in the shear box and exhibited lowest shear strength. The two crushed aggregates from quarries possessed a high shear strength and gave less plastic deformation.

(8)   The degree of compaction in the shear box has a great effect on the ultimate shear strength and resistance to permanent deformation of an aggregate. However, variation in the degree of compaction had little significance on the stiffness of the dolomitic limestone.

(9)   For well graded aggregates in the shear box, the material containing more finer particles gave a lower value of shear strength, showed lower stiffness and was more susceptible to permanent deformation under repeated loading. With the same particle grading curve dolomitic limestone was the stiffest amongst the three types of unbound granular materials tested.

(10)   Shear box testing is unable to generate enough data for analytical pavement analysis and design. Nevertheless, when used with care, it might be a convenient tool to provide qualitative information about particle interaction in terms of shear strength, susceptibility to permanent deformation and resilient performance.

CHAPTER 5

TESTING WITH THE LARGE DIAMETER REPEATED LOAD TRIAXIAL APPARATUS (280TA)

5.1 INTRODUCTION

This chapter presents the work which has been carried out in the large diameter repeated load triaxial apparatus on granular materials.

The main objective of carrying out experiments by using the large diameter repeated load triaxial apparatus was to study the performance of the newly developed apparatus when testing various types of unbound granular aggregates for use in pavement foundations. Particular attention was given to investigate the effect on measured material behaviour resulting from the simplifications which had been made to the apparatus. These included the effects of employing a manually controlled hydraulic actuator to perform resilient testing and strength testing, a drop hammer to evaluate the potential resistance to permanent deformation and using the partial vacuum method to provide the confining pressure.

A study was also included to determine the effect of the proposed compaction method on granular materials as recommended in Section 3.7.1. Before performing experiments on granular materials, it was considered sensible to carry out a test on a rubber sample to examine the performance of the proposed on-sample instrumentation technique.

Since the large diameter triaxial apparatus, 280TA, was a new device, it was considered necessary to compare the results with that of the existing repeated load triaxial device. This apparatus (150TA), which takes a specimen of diameter 150 mm, is both highly versatile and sophisticated and has been used with confidence for years. Furthermore, comparison of results between the large shear box and those of the 280TA was made.

The results of these studies were then used for assessing the suitability and the limitations of employing the 280 mm diameter triaxial apparatus for describing the characteristics of unbound granular materials for use in road foundations. Throughout this chapter, results obtained in the preliminary study of the test materials in Chapter 4

were referred to so that a better understanding of the apparatus performance and material behaviour could be made.

5.2   EQUIPMENT PERFORMANCE

5.2.1   Membrane slippage

Because the strain instrumentation is glued to the membrane, accurate readings require that there is no slippage between the sample and the membrane. It is likely that the friction between the membrane and the specimen is material dependent. Good slip resistance between the PVC membrane and crushed rock specimens, which normally have a rough surface, may be expected. Therefore, it was considered that investigation of membrane slippage should be carried out on a sample which provides a smoother surface. This would then be a worst-case experiment. A hollow cylindrical rubber sample, of 280 mm external diameter, was selected for the test.

Tests were carried out at internal partial vacuum levels ranging from 10 to 50 kPa. The repeated vertical load, which was fixed at a particular stress level, was applied by the servo-controlled hydraulic actuator at a frequency of 0.04 Hz and with a sinusoidal waveform. The results, as shown in Figure 5.1a, indicate that the vertical resilient strains, as well as the radial strains, measured by the instrument remained constant at different confining pressures. No apparent membrane slippage was observed when the vacuum level was reduced. Additional testing was carried out at 5 Hz to check whether any weakening of the slip resistance between the membrane and the sample would be created by higher frequency loading. Figure 5.1b presents the results. It shows constant resilient strain with respect to different confining pressures. No reduction of slip resistance was detected at the higher loading frequency.

5.2.2   Frequency response

Figure 5.1b, however, also shows that both the axial and radial strains from the latter test are smaller than the results obtained from the test at 0.04 Hz. A further investigation was made. It was found that there was a difference between the command signal and the response at the frequency of 5 Hz. The stress measured by the load cell was lower at the peak of the sinusoidal wave and higher at the trough than expected.
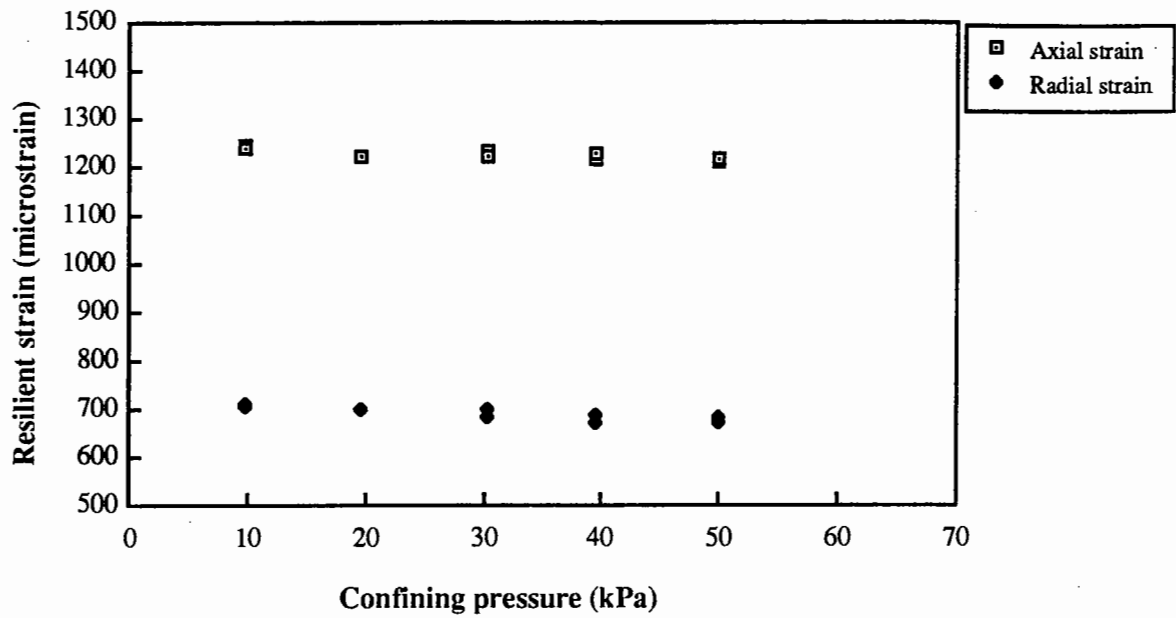
**Figure 5.1a Resilient strain on a rubber specimen at a fixed repeated load
with the loading frequency of 0.04 Hz**
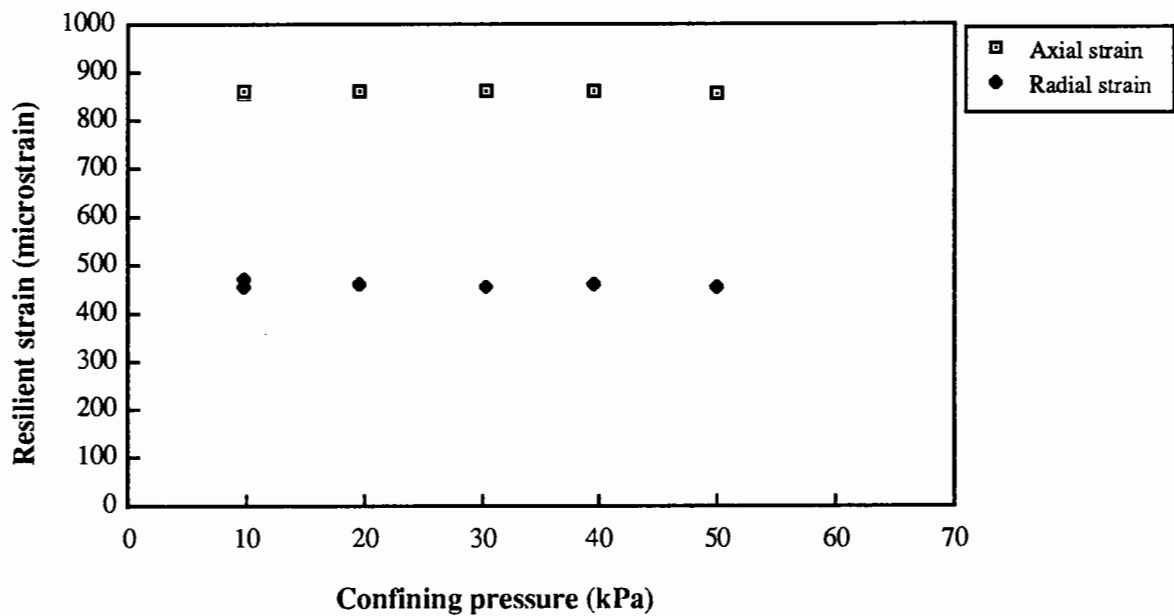
**Figure 5.1b Resilient strain on a rubber specimen at a fixed repeated load
with the loading frequency of 5 Hz**

Hence, the frequency response of the entire set-up should be checked if repeated load testing at higher frequencies is to be performed. In general, the present system is able to provide a reasonable response if the loading frequency is below 2 Hz.

5.2.3 Axial strain measurement

To check the difference between the glue-on mounting method for the LVDTs measuring vertical displacements and the traditional key-in method used on other triaxial equipment at Nottingham (Brown et al 1989), the hollow rubber sample was used again. Two sets of LVDTs were fixed next to each other over the middle third height of the specimen using the glue-on and key-in techniques respectively. The comparison test was carried out at a confining pressure of 10 kPa. Repeated loads of different magnitudes were applied at a frequency of 1 Hz. Figure 5.2 shows the results of the test. A good relationship between the two methods, with the line of equality giving a very good fit to the data, is obtained.

5.2.4 Radial strain measurement

The original design of the radial strain measurement method makes use of a set of three spring loaded LVDTs mounted horizontally on a 'Perspex' ring which in turn rests loosely on three fixed plastic blocks through three pairs of contacting steel studs (refer to Figures 3.5 and 3.6). It is a free system since the ring is free to move horizontally relative to the specimen. The free system assumes that the friction between the six contact points on the plastic blocks is negligible. However, if the friction is large and uneven, the results might be affected.

To assess the possible effect of uneven friction, a fixed mounting system was made by securing one pair of the steel studs to one plastic block with glue. The ring was no longer free and had to move with one side of the specimen. Two sets of identical resilient tests with different levels of deviator stress were carried out on three granular material specimens with the fixed and free systems respectively. The average readings from the three LVDTs for the two systems were compared. Figure 5.3 shows the comparison and no significant differences between them are noted. Therefore, the average radial strain measurement does not appear to be sensitive to the fixity of the
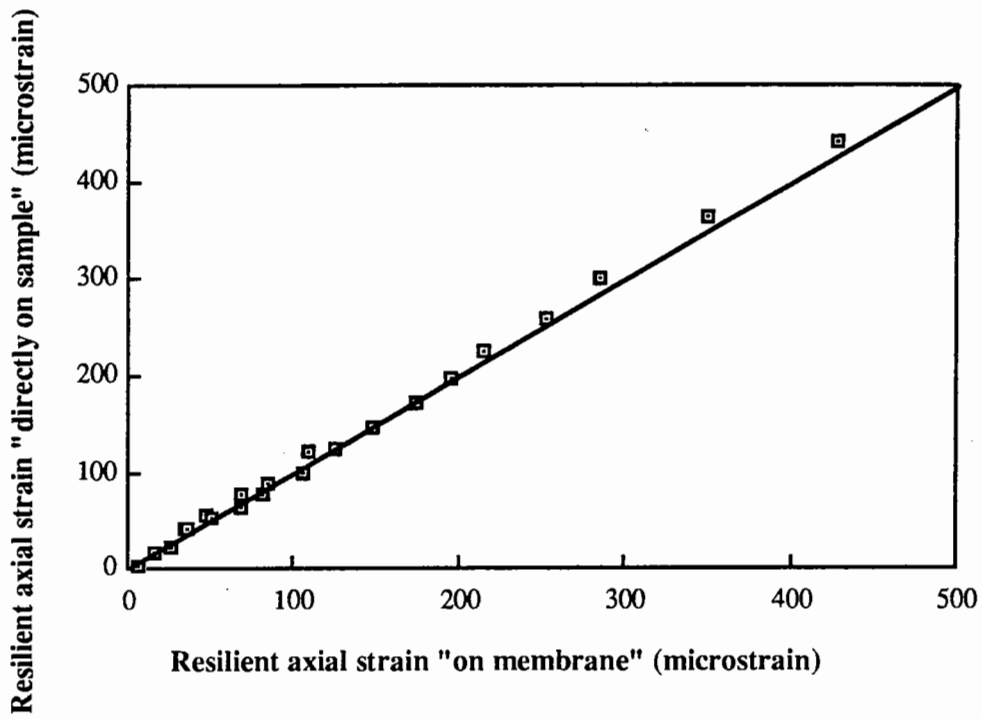
Figure 5.2 Comparison of different mounting systems for measuring axial strains (loading frequency at 1 Hz)
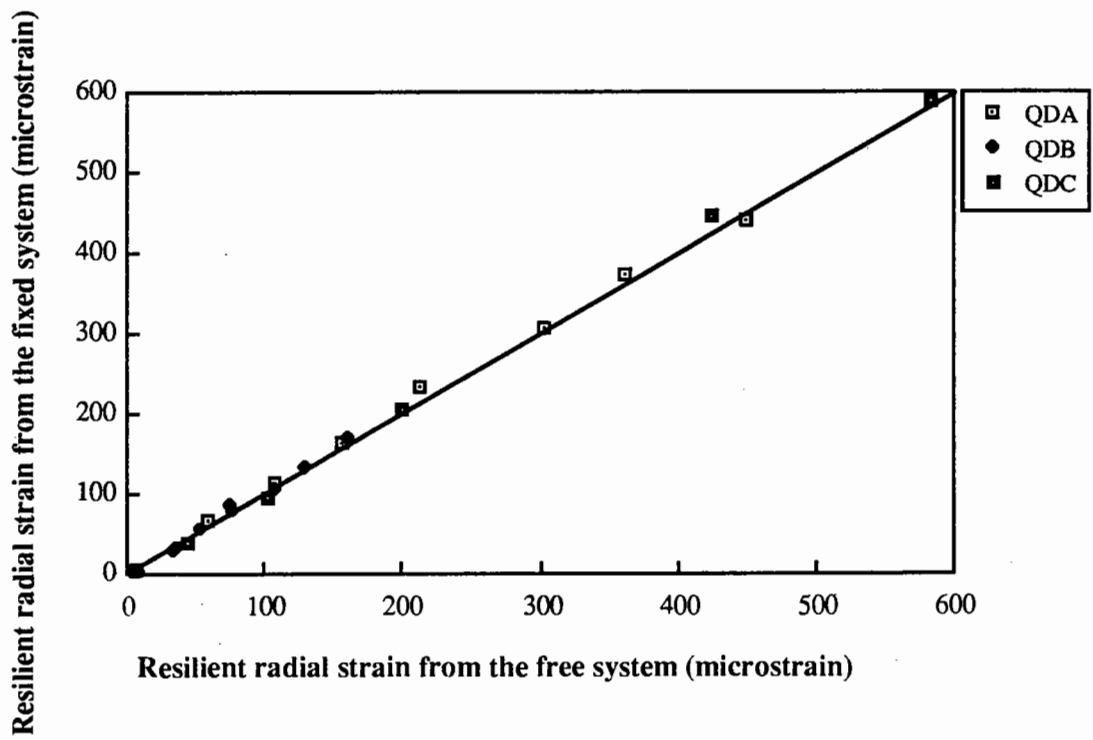
Figure 5.3 Comparison between the fixed and the free systems

ring. Application of this observation was made later in the drop hammer test for which the fixed system to hold the horizontal LVDTs was used.

An extension of this approach was considered. The ring was fixed opposite to one horizontal LVDT and the other two LVDTs were removed. The reading obtained on that instrument was taken as a direct measure of horizontal deformation and the strain computed. This would have allowed the three LVDT system to be considerably simplified to only one instrument. However, a single LVDT consistently underestimated the strains when compared with the three instrument method. This may be a function of inhomogenity in real specimens. Hence, the single LVDT system proved insufficient and the simplification was not adopted.

5.3 SAMPLES OF UNBOUND GRANULAR MATERIALS

A total of thirteen aggregate samples, excluding those used for initial apparatus assessment, have been tested by the 280TA. Amongst them, five were direct from quarries and were mixed to specified gradings. Five were from a trial site at Loughborough (Fleming and Rogers 1993) and three from another experimental site at Bothkennar in Scotland (Little 1993). At the two sites, a study of the performance of aggregates under direct trafficking was being undertaken. Materials from the Loughborough site trial were of the same origin as those coming directly from the quarries (except for the furnace bottom ash which was an additional material). For reference, the particle characteristics of the ash are summarized in Appendix E. From the Bothkennar site, two types of aggregate were used. A description of these materials has been given by Little and Dawson (1990). In summary, one of the materials was a crushed granite and the other one was a natural sand and gravel mixture obtained local to Bothkennar. The apparent specific gravities determined by Little and Dawson were 2.85 for the granite and 2.74 for the latter aggregate.

For the aggregates from the quarries, the test environment and the material conditions (such as particle grading, moisture content, density and maximum particle size) were controlled (refer to Section 3.7.2 for sample preparation details). On the other hand, simulation of in-situ conditions was made for the materials from sites. Thus a study of the performance of differing materials and their sensitivity to changing environmental conditions could be evaluated. Moreover, the limitations and the abilities of the

apparatus to describe the performance of unbound granular materials in road foundations could be studied.

The samples tested in the large triaxial apparatus are listed in Table 5.1, in which a coding system is also presented.

Table 5.1 Materials tested by the large diameter triaxial apparatus

Test series	Origin	Material	Designation
1	Whitwell quarry	dolomitic limestone	QDA
	Whitwell quarry	dolomitic limestone	QDB
	Whitwell quarry	dolomitic limestone	QDC
	Mountsorrel quarry	granodiorite	QGB
	Attenborough quarry	sand and gravel	QSB
2	Loughborough	dolomitic limestone	LDN1
	Loughborough	dolomitic limestone	LDN2
	Loughborough	granodiorite	LGN
	Loughborough	sand and gravel	LSN
	Loughborough	furnace bottom ash	LAN
3	Bothkennar	granite	BGN1
	Bothkennar	granite	BGN2
	Bothkennar	sand and gravel	BSN

Samples from quarries, that were subsequently mixed to the specified gradings, are grouped in the first test series and prefixed by a letter "Q", while the second and third series include those from Loughborough and Bothkennar sites which are denoted by an "L" and a "B" respectively. The second letter of the code represents the material type: "D" for the dolomitic limestone, "G" for the granodiorite or granite, "S" for the sand and gravel and "A" for the furnace bottom ash. The third letter indicates the particle size distribution. Grading A is a Fuller's curve (Fuller and Thompson 1907) with n = 1.5 and with a maximum particle size of 40 mm. Gradings B and C correspond to the fine end of the Type 1 sub-base envelope and the fine end of the 6F1 capping envelope

of the DoT specification (Department of Transport 1992) respectively. (These gradings have been presented in Figure 4.5.) The letter "N" indicates an as-supplied grading. The number after the three-letter code is used to distinguish specimens having the same grading and source material but of differing densities.

5.4 QUALITY OF SPECIMEN

The material conditions of each specimen are presented in Appendix F. The particle size distribution curves of the samples from the two sites are included in Appendix G. In order to understand factors which might affect the quality of a 280 mm diameter sample prepared by a particular specimen preparation method, compaction studies were carried out on the dolomitic limestones obtained directly from Whitwell quarry. The reasons for selecting dolomitic limestone for study were:-

(1)   three specimens from this material were made at different gradings, thus more information was available;

(2)   it was the material type on which the B.S. 5835 compactability test had been performed, thus comparison between different compaction efforts could be made;

(3)   dolomitic limestone is one of the softer pavement foundation aggregates, hence any effect of compaction causing degradation should be readily investigable.

The compaction results of the samples, QDA, QDB and QDC are summarized in Table 5.2.

5.4.1   Effect of compaction

5.4.1.1 Comparison with results from B.S. 5835 test

A good agreement was found between the densities obtained for the DoT Type 1 fine grading sample (QDB) from the current compaction method and from the B.S. 5835 test. However, the average dry density produced for the finest sample, QDC, was 4.5% below the value obtained by the British Standard technique, and the coarsest

grading gave a density which was 11% above it's British Standard counterpart. Hence, the 2 minute manual compaction has a greater effect on coarser materials and the effectiveness decreases as the material being compacted becomes finer. The reason, besides a certain crushing effect (which will be discussed later), may be that in full face compaction (employed in B.S. 5835) on materials containing high percentages of large particles most of the compaction energy is transmitted through the larger particles. This creates an arching effect which protects the small size particles from being compacted. Lower density, therefore, results. When random compaction is used, the application of shear loading breaks down any arches and consequently produces a higher density for coarse grading materials.

Table 5.2   Compaction results of dolomitic limestone from quarry

Sample	(a) B.S. 5835 maximum dry density kg/m^3	(b) Average dry density obtained kg/m^3	$\dfrac{b}{a}$ (%)	Uniformity coefficient (before compaction)
QDA	1835	2030	111	4
QDB	2370	2343	99	103
QDC	2300	2197	96	27

Notes:-

(1)   Detailed results from the compactibility test carried out in accordance with B.S. 5835 (1980) can be found in Appendix H.

(2)   Uniformity coefficient (U) $= \dfrac{d_{60}}{d_{10}}$

where:- d_{10} = particle size for which 10 percent of particle are finer

d_{60} = particle size for which 60 percent of particle are finer

5.4.1.2   Degradation and segregation

Figure 5.4 presents the grading curves of samples, QDA and QDB, before and after compaction. (The results for sample QDC are not available due to experimental error.) Two phenomena can be observed from the graph of the coarsest grading. The first is that the curve shifts to the left of the diagram after compaction. This means that finer sized particles have been generated due to breaking up of the larger stones. The second is that segregation has occurred with a higher percentage of smaller particles lower down in the specimen. Nevertheless, these two effects were not observed in the finer
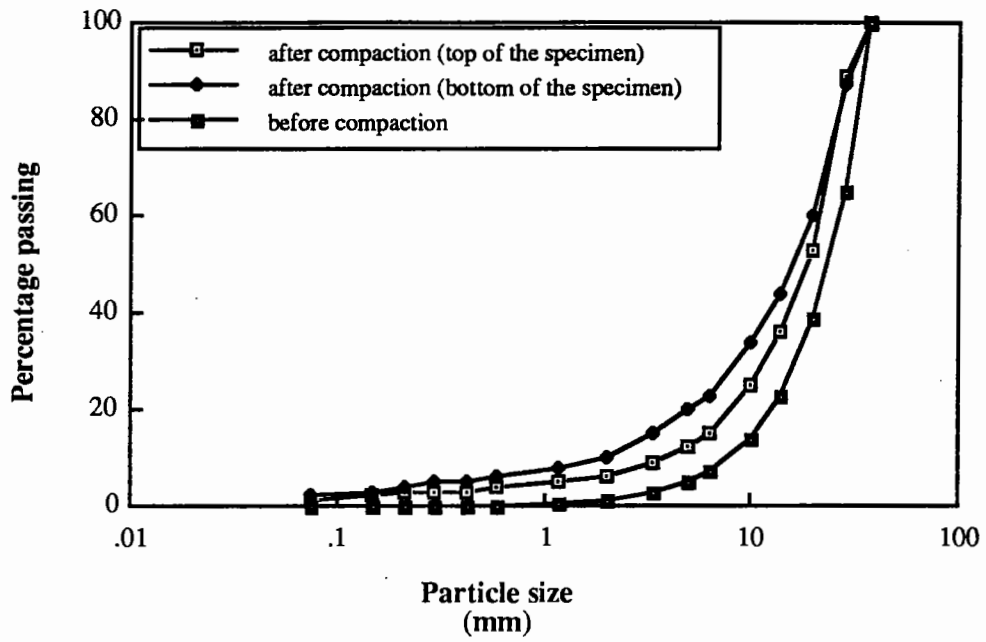
Figure 5.4a Effect of compaction on sample QDA
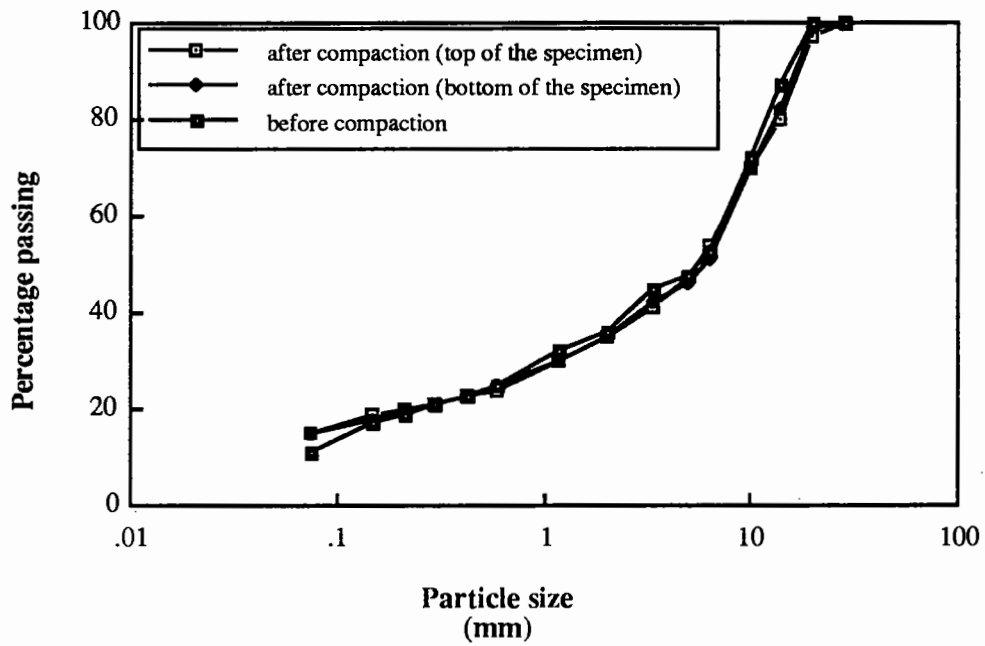
Figure 5.4b Effect of compaction on sample QDB

grading sample, QDB. It is likely that these observations also apply to the finest sample, therefore no degradation and no segregation might be expected for QDC.

5.4.1.3 Uniformity coefficient

From Table 5.2, it can be seen that the lowest maximum dry density was found in the coarsest sample. At first the density increased when the grading curve (Figure 4.5) shifted to the left on the particle distribution chart. However, it decreased when the curve shifted further to the left. Hence, the average particle size of aggregates might not provide an explanation of the density difference between materials of different gradings compacted with the same effort. In fact, this phenomenon may better be explained by the spread of the grading curve and the occurrence of voids inside the compacted samples. For the most uniform coarse sample, QDA, the average size of voids between aggregates is expected to be large because it lacks smaller particles to fill up these voids. When the range of a particle curve increases (i.e. the value of uniformity coefficient increases), more smaller particles are available and higher density can, therefore, be achieved.

Based on the limited test results from Table 5.2, a graph showing the relationship of the density and the uniformity coefficient, U, is plotted in Figure 5.5. A trend can be seen. The density of a sample of uniform grading increases greatly for a slight increase of U value when the coefficient is small. The rate of the increase of density slows down and perhaps becomes insensitive to the change of U value when the uniformity coefficient of the sample is about 100. This observation is in agreement with Chan's findings (1989), who carried out compaction tests on the same materials but in a dry condition and by a different compaction method.

5.4.2 Variation of moisture content

In the traditional triaxial test, confining pressures are provided by pressurized air, water or oil outside the specimen. In the case of a drained test, excess water generated by pore pressures due to external forces is squeezed out from the specimen. Since partial vacuum was used to provide confining pressures in the current test, more water might be removed from the specimen by suction. Table 5.3 shows the variation of moisture
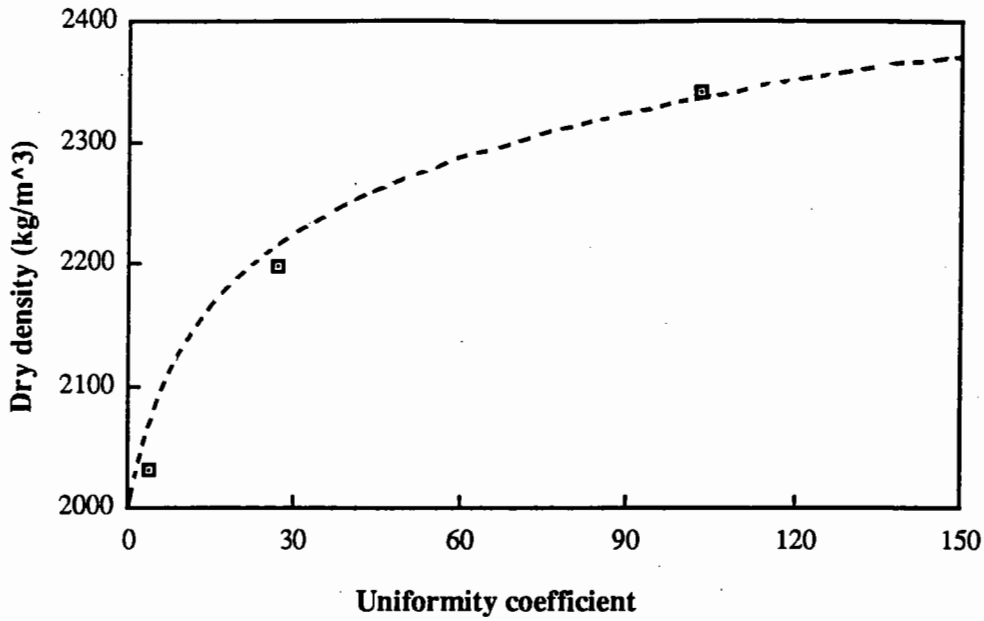
Figure 5.5 Relationship between uniformity coefficient and density (dolomitic limestone)

wheel load = 500kPa
contact diameter = 400mm

wheel load = 700kPa
contact diameter = 300mm

300mm

250mm

250mm

During construction

In-service

Bituminous material : E = 2.5 GPa, Poission's ratio = 0.4, density = 2300 kg/m^3

Granular sub-base material : density = 2100 kg/m^3, suction = 7 kPa,
parameters in Boyce's model : K1 = 3877, G1 = 4291,
β = 0.12 & n = 0.33

Subgrade soil : density = 2000 kg/m^3, Poisson's ratio = 0.5,
parameters in Loach's model : C = 1110 and D = 1.52

Figure 5.6 Flexible pavement sections for stress estimation

content before compaction and after the completion of testing the three dolomitic limestone samples.

Table 5.3 Variation of water content

Sample	Moisture Content (ω) before compaction %	ω after testing at the top of specimen %	ω after testing at the bottom of specimen %
QDA	3.2	3.0	3.3
QDB	6.3	5.2	5.3
QDC	7.4	6.3	6.3

The moisture contents before compaction were the optimum moisture contents determined by the B.S. 5835 test. In general, there were reductions in moisture content after testing. The drop was between 6 and 15 percent of the original moisture content. For the coarsest grading material, QDA, a slight variation of moisture content within the specimen, with the higher value being at the bottom, was also observed. These observations imply that there is little point in testing materials at moisture contents above optimum when a partial vacuum is used to provide the confining pressure as more significant water loss would be expected.

5.5   TEST PROGRAMME ON UNBOUND GRANULAR MATERIALS

In this section, standard test methods for describing the resilient strain behaviour, the susceptibility to permanent deformation, and the strength of the unbound granular materials are presented. In addition, test procedures which have been used to study the effects of loading by the manually operated and by the servo-controlled hydraulic actuators are included. Test procedures using the existing repeated load triaxial apparatus on a 150 mm diameter sample are also described.

A summary of the standard test procedures is included in Appendix I.

70

5.5.1 Resilient deformation test

5.5.1.1 Test Design Considerations

Since the resilient deformations of both granular materials and soils in the pavement foundation are stress-dependent and behave non-linearly, the selection of stress paths to be used on the triaxial testing is important. To estimate the stress levels in road foundations, the finite element program, FENLAP, developed by Almeida (1991) was used. The program has been designed to take into account the non-linear behaviour of pavement foundation materials.

Two flexible pavement sections representing conditions during construction and after completion as shown in Figure 5.6 were used for the estimation of stresses in the road foundation. They comprised a sub-base of 250 mm thick. For the completed pavement a 300 mm thick bituminous upper layer was provided. Non-linear models were used in the analysis:- Boyce's model (1980) for the granular sub-base material and Loach's model (1987) for the subgrade soil. The equations for these two non-linear models are as follows:-

for the granular material

$$\varepsilon_s = \frac{1}{3G_1} p^n \frac{q}{p} \tag{5.1}$$

$$\varepsilon_v = \frac{1}{K_1} p^n \left[1 - \beta \left(\frac{q}{p}\right)^2 \right] \tag{5.2}$$

for the soil

$$\varepsilon_a = C \left[\frac{q_r}{p'}\right]^D \tag{5.3}$$

where:- G_1, K_1, n, C and D are material constants.
               β is a function of G_1, K_1 and n.
               ε_s, ε_v and ε_a are the resilient shear, volumetric and axial strains respectively.

The parameters for the granular materials were extracted from Chan (1989) and those for the subgrade soil were from Loach (1987).

Figure 5.7 shows the stress distribution at the top of the granular layer calculated from the finite element program, while Figure 5.8 indicates the stresses at formation level. These stresses are expressed in terms of the stress invariants, p and q. It can be seen that, except for the q value at the top of the unsurfaced granular layer, the shapes of the stress distributions of p and q approximate to haversine curves.

Figure 5.9 shows the stress paths which can be produced by the 280TA. In p-q space, all stress paths are at a slope of 1 to 3. This is because there was no intention of varying the confining pressure whilst the vertical load was applied. It can also be argued that this is a limitation of the apparatus. Since the vacuum system was used to provide the confining pressure to the specimen, the achievable maximum value, as mentioned in Chapter 3, could be up to about 90 kPa. To prevent generation of large permanent deformation during resilient testing, the stress ratio, q/p, has to be limited to 70% of its value at failure (Brown and Dawson 1992). For most crushed aggregates the limit will be about 2. Therefore, the maximum deviator stress which can be applied is about 540 kPa.

Figure 5.9 also shows the stress paths at the top of the granular layer of the pavement as calculated by FENLAP. The computed stresses in the sub-base layers, due to trafficking of the completed pavement, are concentrated towards the left bottom corner of the graph and lie between the first two triaxial stress paths, corresponding to the confining pressures of 10 kPa and 20 kPa. For the trafficking of the unsurfaced pavement, computations of stress (particularly the horizontal stress and thus values of p) are less reliable immediately beneath the tyre. However, paths which are able to produce similar maximum values of q can be provided by the 280TA and it was recommended that these are at confining stresses of 30 or 40 kPa. Using this information the stress paths in Table 5.4 were recommended for determining the resilient properties of granular sub-base materials.
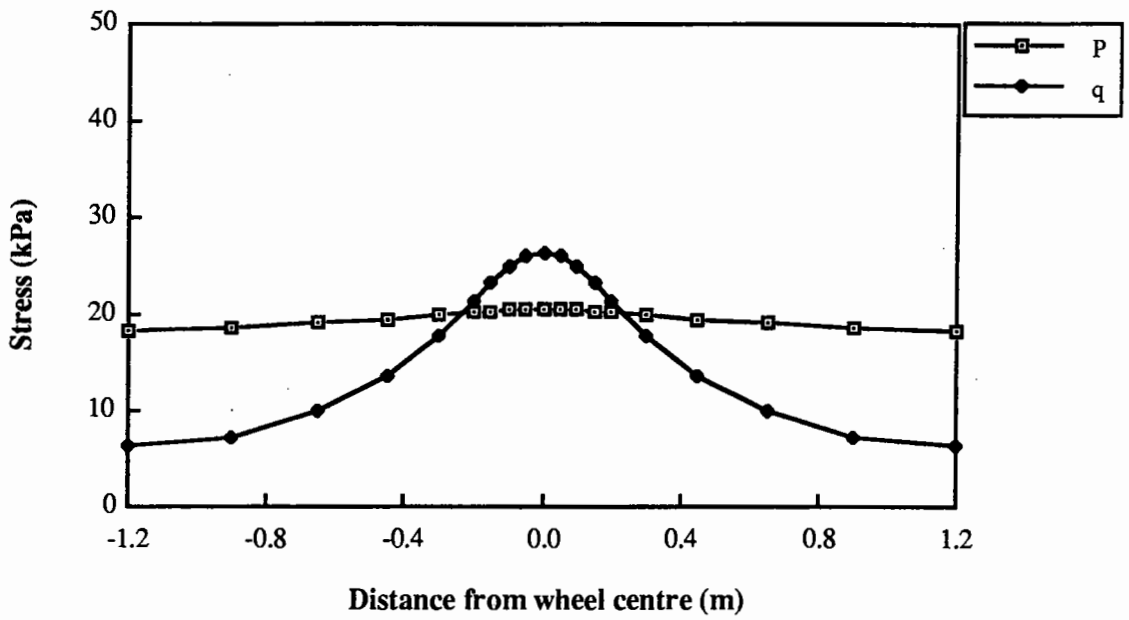
Figure 5.7a Stress distribution at top of sub-base (surfaced)
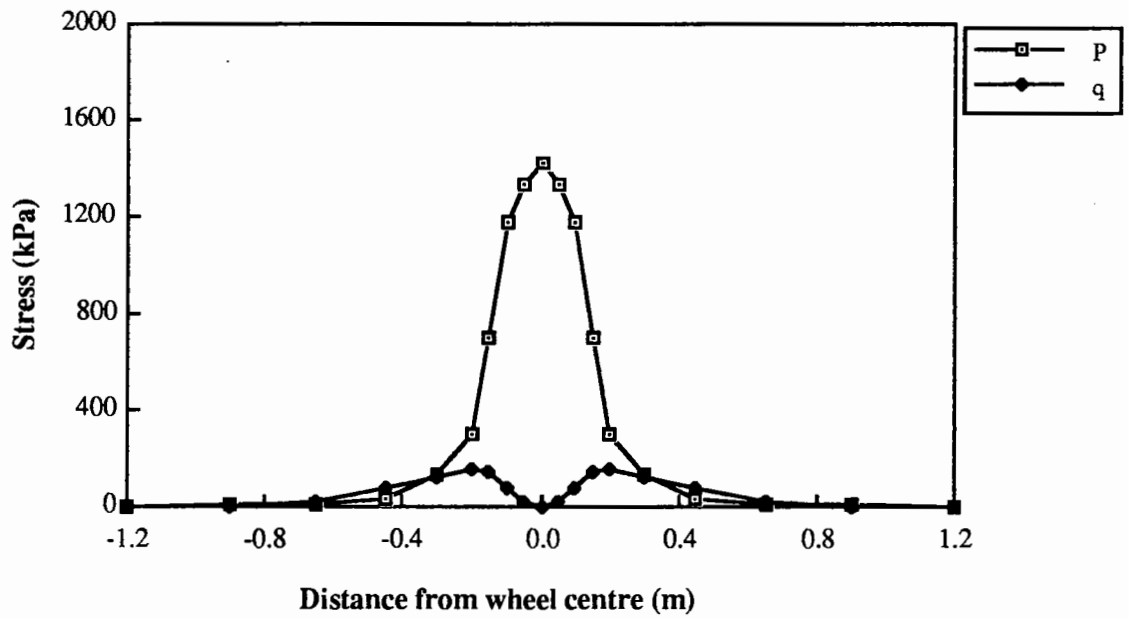
Figure 5.7b Stress distribution at top of sub-base (unsurfaced)
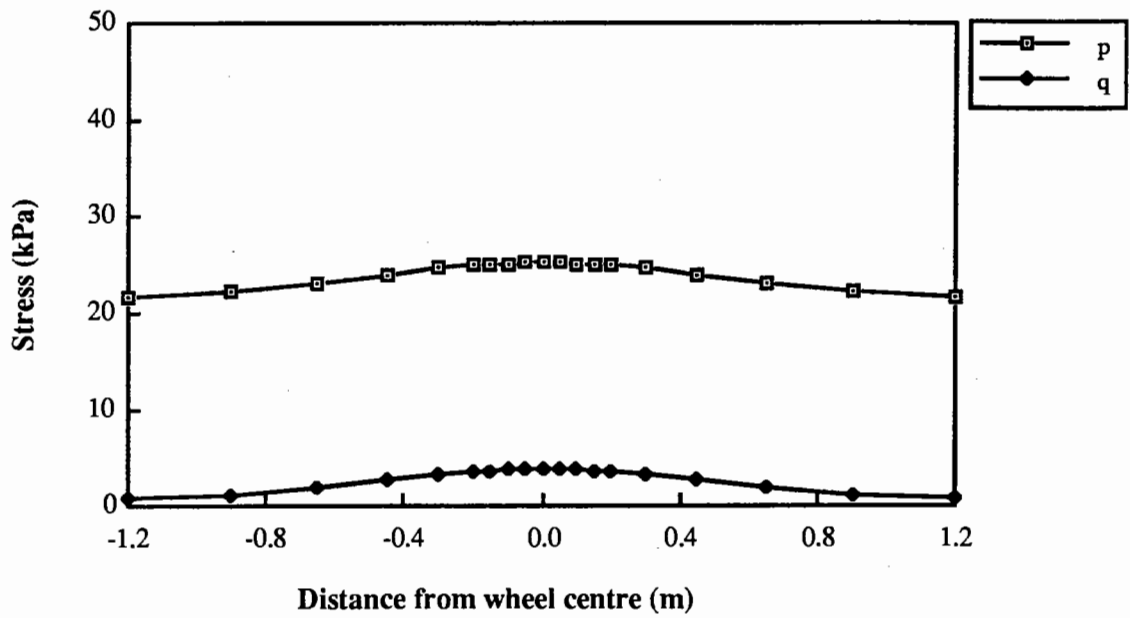
Figure 5.8a Stress distribution at top of subgrade (surfaced)
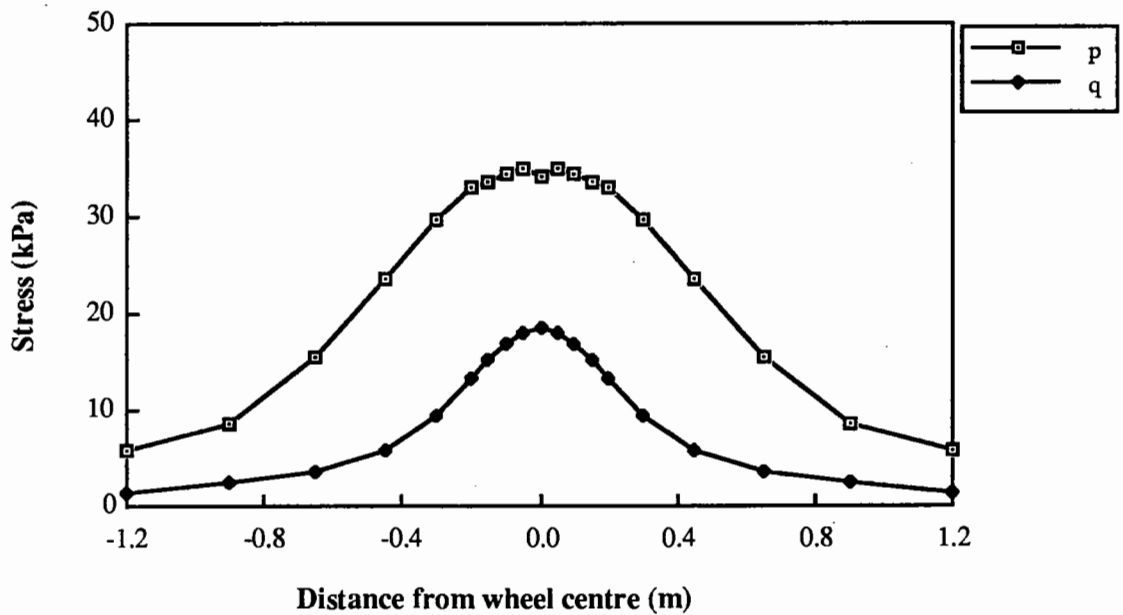
Figure 5.8b Stress distribution at top of subgrade (Unsurfaced)
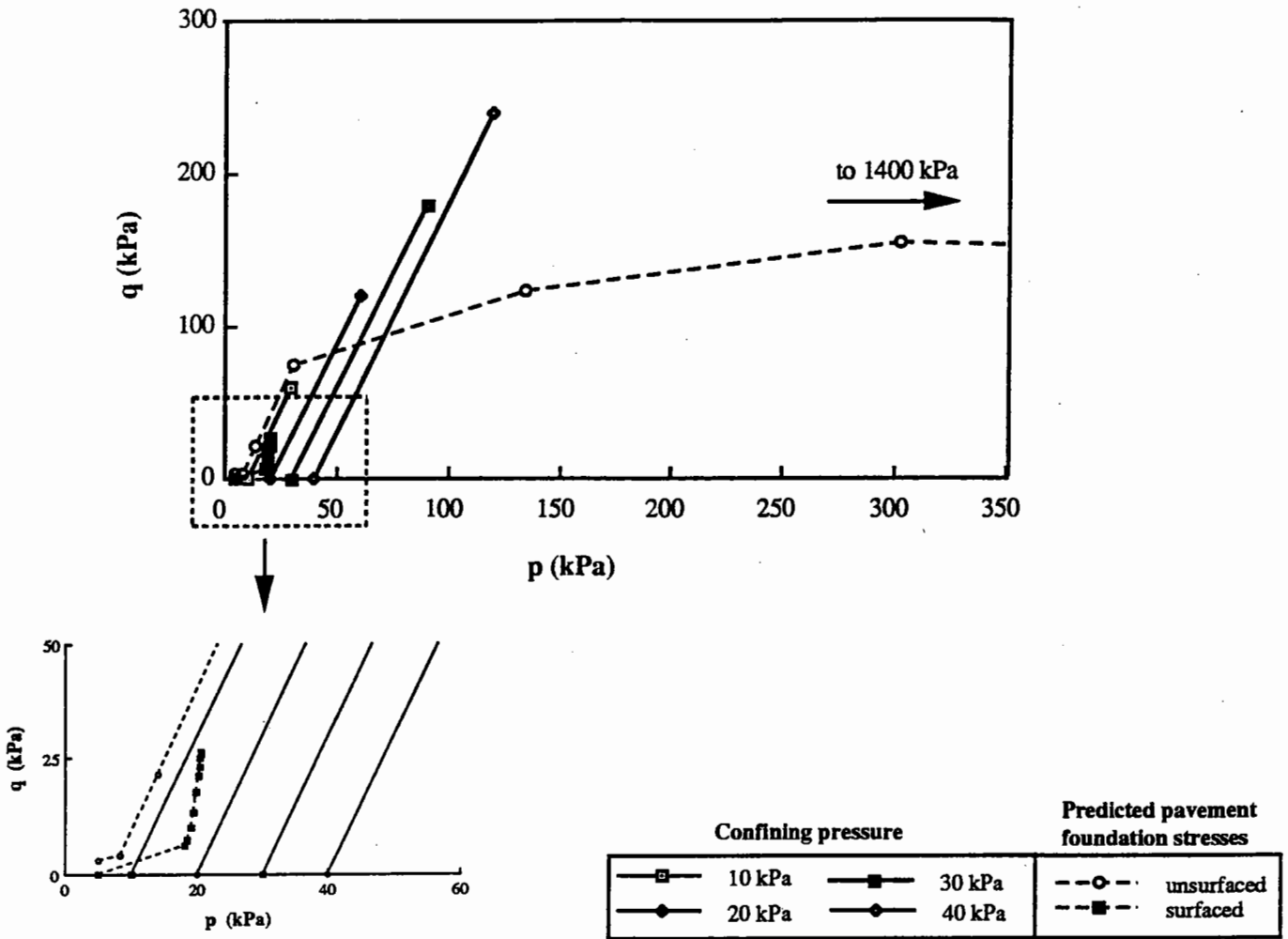
Figure 5.9 Stress paths used in aggregate testing

(predicted stresses in pavement foundations included)
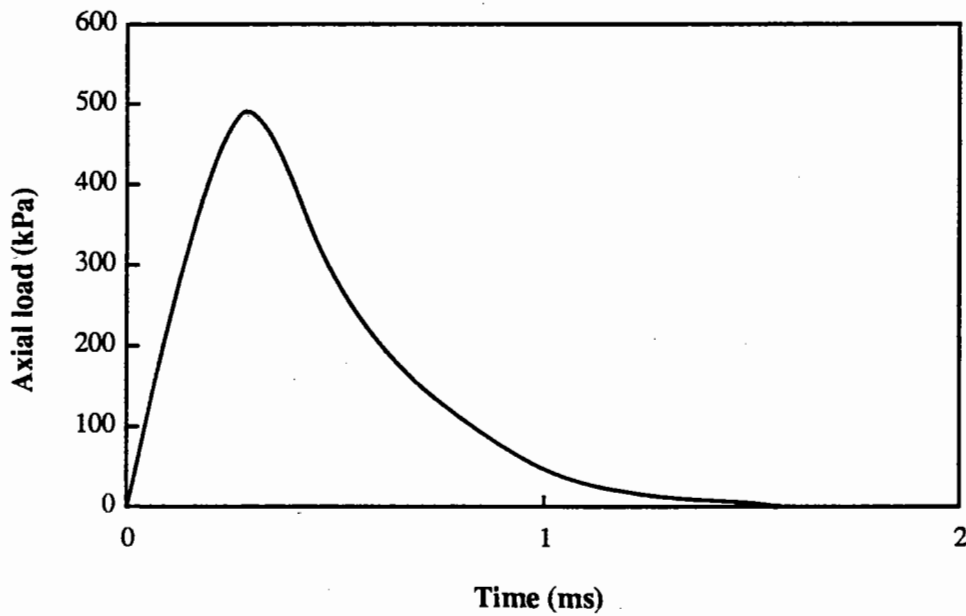
Figure 5.10 Shape of load pulse of drop hammer

Table 5.4 Stress paths for resilient strain test

Confining pressure (kPa)	10	20	30	40
maximum	30	40	50	60
vertical	40	65	90	115
stress	50	90	130	170
(kPa)	60	115	170	225
	70	140	210	280

5.5.1.2   Testing procedure

The specimens were left overnight or at least 12 hours at a confining pressure of 10 kPa after completing the installation of the displacement transducers. After this stabilisation period, vertical repeated loads, according to Table 5.4, were applied using the manually-controlled actuator. For each stress path, 10 cycles were applied before the stresses and strains were recorded. The time period allowed for the recording cycle was limited to 1 minute.

The confining pressure was increased to 20 kPa. To make sure that the partial vacuum was homogeneous inside the specimen, one of the vacuum supply lines connected to either the top or the bottom platen was turned off after the partial vacuum had been applied for 30 minutes. Readings on the vacuum gauges attached to the top and the bottom platens were then compared at 10 minute intervals. When there was no difference between the readings, the tests as stated in Table 5.4 were continued. Normally equalisation was reached in 10 minutes. As before, readings were recorded after the repeated loads had been applied 10 times.

The same procedures were repeated for confining pressures of 30 kPa and 40 kPa.

5.5.2 Permanent deformation test

5.5.2.1 Test Design Considerations

The justification for using a simple testing technique, such as a drop hammer test, to provide information about the susceptibility of unbound granular materials to permanent deformation in pavement foundations has been discussed in Section 3.3.1.

Before standardizing the testing procedure, trial testing on a sample of the DoT Type 1 grading was carried out. The 10 kg hammer was allowed to fall from a height ranging between 100 and 500 mm onto the top platen of the specimen. Load pulses were monitored by a high-speed digital oscilloscope. It was noticed that the time period of the load pulse was insensitive to the drop height of the hammer. The shape of the load pulse is shown in Figure 5.10. The pulse is similar to a skewed sinusoidal wave. The stress period is about 1.5 milliseconds. The time to reach the peak stress is about 0.5 millisecond. Hence, loading from the drop hammer might provide a constant waveform and the shape of load pulse is not too dissimilar to that produced by trafficking. However, the frequency of the load pulse is much higher than that experienced in the road foundation (refer to Section 2.2). It is known that, at these high rates of loading, inertia of the equipment and sample has a significant effect on the measured responses (Brown 1992). However, this aspect of work is outside the scope of this research and has received very limited study in this project.

The relationship between the drop height and the measured peak stress generated by dropping the hammer is presented in Figure 5.11. A non-linear relationship can be observed. The rate of increase of peak stresses declined as the height of the drop increased. As can be seen in Figure 5.11, a drop height of 300 mm is required to produce a maximum contact stress of about 550 kPa which is of similar magnitude to that from construction traffic.

Figure 5.12 shows a graph of vertical plastic strain produced by dropping the hammer onto the specimen ten times from different heights. As expected, the graph indicates that higher drop heights induce larger permanent deformations. The permanent strain produced after the whole series of tests was about 0.15%. This is very small relative to the strain produced by the traditional triaxial strength test. Furthermore, Shaw (1990) reported that the plastic strain developed under large numbers of pulse repetitions had little effect on static failure strength. Hence, the permanent deformation test itself

74
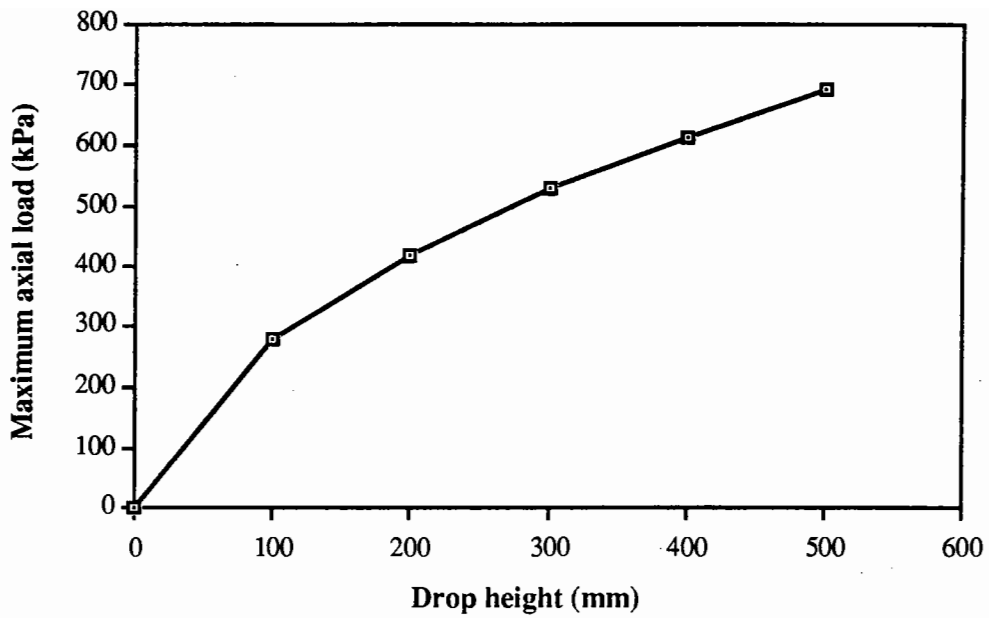
Figure 5.11 Relationship between drop height of hammer and load
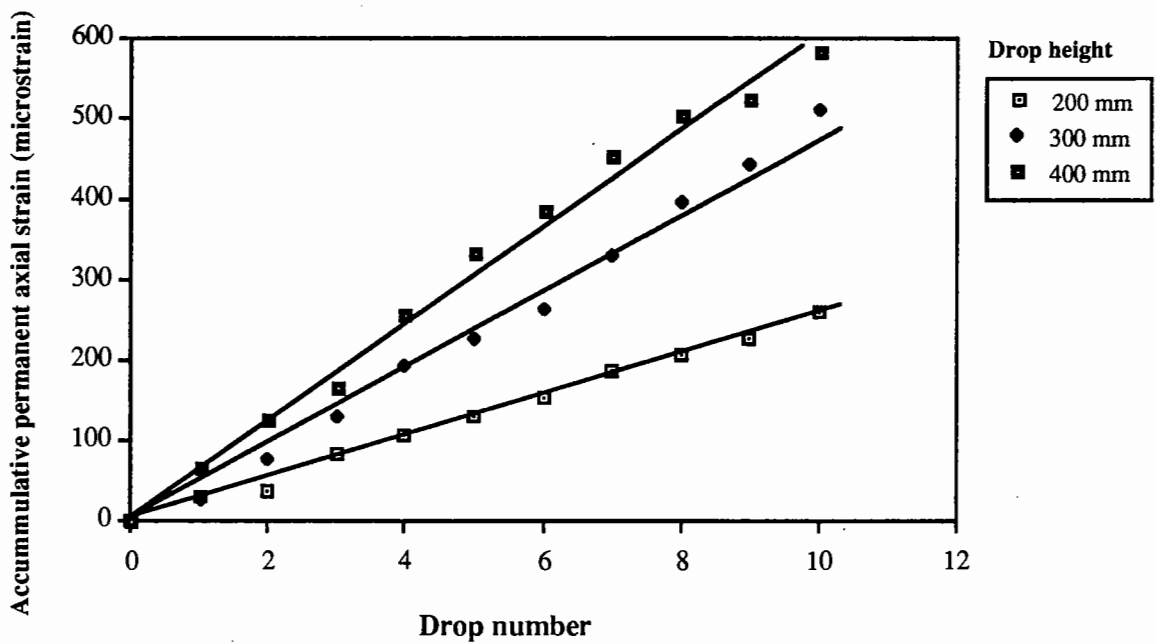
Figure 5.12 Relationship between permanent deformation and number of drop

should not have a significant effect on the subsequent strength test described in Section 5.5.3.

Another factor, which was considered, was operator fatigue. Therefore, it was recommended that the number of drops should be less than 50.

5.5.2.2 Testing procedure

In general, the permanent deformation test was performed immediately after the resilient test. Sometimes, tests to study the effects of waveforms and load frequencies (Section 5.5.4) were carried out in advance. Work by Thom and Dawson (1993) suggested that low stress excursions had little effect on permanent deformation at high stress levels.

The permanent deformation test was performed at a confining pressure of 10 kPa. To make sure that the confining pressure in the specimen was homogeneous, the same checking procedure as described in Section 5.5.1.2 was used. The number of drops chosen was 25. Before the first drop was made, readings of all displacement transducers were taken as datum values. Further data were then collected at the end of each drop. Throughout the permanent deformation test, the fixed system (as detailed in Section 5.2.4) for holding the horizontal transducers was employed.

5.5.3 Strength test

5.5.3.1 Test Design Considerations

In the traditional triaxial compression test, three identical specimens are normally required in order to establish the shear strength parameters. If the conventional procedure was adopted to perform strength tests on 280 mm diameter specimens, the time and the cost involved just to prepare specimens would be enormous. After considering the economic and practical aspects of the test, multistage triaxial testing was selected as the method to determine the strength parameters of the materials. Another benefit of employing the multistage testing technique was that the problem of variation between different samples was eliminated. Of course, it can be argued that this was also a disadvantage, in that sample variability could not be assessed or allowed for.

5.5.3.2 Testing procedure

Three stages were used to determine the strength parameters of the granular materials. Generally, the first stage of the testing was carried out at a confining stress of 10 kPa, the second stage at 30 kPa and the final at 50 kPa. Load was applied by the hand-operated jack. The maximum time period for each stage of testing was limited to 1 minute.

During the compression tests, readings were taken at half second intervals by the data acquisition system. A pen recorder was also used to provide immediate information on the vertical deformation of the specimen and the load applied. This visual device helped to prevent overstressing the sample in the first and second stages of the test. In these two stages of the test, the increment of vertical loading ceased when continued straining was observed even while the vertical load was maintained at a constant value. In the final stage, testing was carried on until the specimen could not withstand any further increment of vertical load. Horizontal LVDTs were removed at the beginning of the test to prevent possible damage which might be caused by excessive radial deformation of the specimen.

When the confining pressure was changed between the different stages of the test, the same checking procedure for assessing homogeneity of confining stress, as presented in Section 5.5.1.2, was followed.

5.5.4 Test conditions

5.5.4.1 Waveform

After the resilient strain test, a series of tests was carried out on samples QDA, QDB and QDC to check the sensitivity of material stiffness to the loading effect from different waveforms. Three types of waveform were used: square, sinusoidal and ramp. All tests were performed at a loading frequency of 0.5 Hz.

The investigation of the plastic strain development of granular materials is more difficult than that of elastic strains since permanent strains are affected by the loading history of the sample. Barksdale (1972) and Shenton (1987) suggested that the permanent vertical strain was a logarithmic function of load cycles. Very little work on the effect

76

of waveform has been carried out. To investigate the possible effects of different waveforms, two sets of repeated loading tests at a frequency of 0.5 Hz were performed on sample QDB. The first involved the square wave and the ramp wave. In the ramp wave, the applied load was increased steadily to peak and immediately reduced to zero. The second set of testing compared the performance between square wave and sinusoidal wave. Tables 5.5 and 5.6 present the details of the tests. Within each comparison test, four series of applications with the same peak to peak vertical stresses were carried out. The first and the third series were performed with square waves. The other two series were of the other waveforms. For each series, 200 applications were applied and the permanent deformation of the last 175 applications was recorded.

Table 5.5

Testing details for the effect of waveform (square and ramp)

Sequence	Frequency (Hz)	Peak to Peak Repeated Stress (kPa)	Confining Pressure (kPa)	Waveform
1	0.5	20-200	10	square
2	0.5	20-200	10	ramp
3	0.5	20-200	10	square
4	0.5	20-200	10	ramp

Table 5.6

Testing details for the effect of waveform (square and sinusoidal)

Sequence	Frequency (Hz)	Peak to Peak Repeated Axial Stress (kPa)	Confining Pressure (kPa)	Waveform
1	0.5	20-220	10	square
2	0.5	20-220	10	sinusoidal
3	0.5	20-220	10	square
4	0.5	20-220	10	sinusoidal

5.5.4.2 Frequency

To check the effect of loading frequency on the stiffness of granular materials repeated load tests on three samples, QDB, QDC and QGB, were carried out. The range of frequency used was between 0.05 and 0.1 Hz. A sinusoidal waveform was applied. Details of the frequency test are presented in Table 5.7.

Further testing to investigate the frequency and stress history effects on the development of permanent strain was performed on sample QDB. There were four steps in the test. Details of the test are shown in Table 5.8. For each step, the same peak to peak sinusoidal loading was applied. The first and the third steps of the test sequence were carried out with a frequency of 1 Hz and the others at 0.05 Hz. Two hundred load applications were applied and the results of the last 175 applications were recorded.

Table 5.7
Stress conditions of frequency tests (effect on material stiffness)

Sample	STRESS CONDITION	
	Confining pressure (kPa)	Deviator stress (kPa)
QDB	40	0 - 70
QDC	40	0 - 70
QGB	40	0 - 70

Table 5.8
Stress conditions of frequency tests (effect on plastic strain)

Sequence	Frequency (Hz)	Peak to Peak Stress (kPa)	Confining Pressure (kPa)
1	1	20-180	10
2	0.05	20-180	10
3	1	20-180	10
4	0.05	20-180	10

5.5.4.3 Creep

In addition to the waveform and frequency effect tests, experiments were conducted to study the effect of a constant static loading. The test was carried out on sample QDB at a confining pressure of 10 kPa. A static vertical load of 180 kPa was maintained for a period of thirty minutes and then released quickly. The change in the vertical creep strains was monitored during the loading period and for another half hour after the axial load had been removed.

5.5.4.4 Loading with a manually-controlled actuator (MCA)

Since a Manually-Controlled Actuator (MCA) was chosen to apply the vertical loads, tests to study the effect of loading with this device, which is unable to produce a definite waveform and loading frequency, were necessary. Therefore, a series of resilient tests on four different samples were carried out using both the MCA and the servo-controlled hydraulic actuator. A sinusoidal waveform at a frequency of 0.5 Hz was applied when the servo-controlled loading device was used.

5.5.4.5 Time of equilibrium

Since the provision of the confining pressure was achieved by applying partial vacuum to the specimen, the time required for the partial vacuum inside the specimen to reach equilibrium state had to be assessed. This time period depends on the porosity, the degree of saturation and the grading of the sample. It varies between specimens.

Tests were carried out on the three dolomitic limestone samples, QDA, QDB and QDC from Whitwell quarry. This provided the opportunity to study the equilibrium periods required by differently graded materials at their optimum water contents as defined by the B.S. 5835 compactibility test. A standard repeated load with a peak stress at 50 kPa was applied by the MCA at different time intervals after the partial vacuum supply had been changed from 10 to 20 kPa, and the variation in the resilient vertical strains was monitored.

5.5.4.6 Tests in the existing triaxial apparatus (150TA)

A brief description of the existing triaxial apparatus for a specimen size of 150 mm diameter has been given in Section 2.5.2. There are several fundamental differences between the existing and the new devices.

(1) The sizes of the specimens are different. This has a direct effect on the specimen to particle size ratio even when materials of the same grading are used in both apparatuses.

(2) Normally, the existing apparatus uses external pressures to provide confining stresses to the tested specimen.

(3) The electronic control system, on-sample instrumentation units, and data acquisition system are different.

Therefore, testing a sample in the existing apparatus means testing under new conditions.

To study the effect of specimen to particle size ratio on material behaviour, the grading selected for the test was the fine end of the DoT Type 1 envelope, which the maximum aggregate size was limited to 20 mm. The sample used was QGB. Identical testing procedures as recommended in Table 5.4 were used in the tests on both apparatuses. These tests were carried out with a sinusoidal waveform at a frequency of 0.5 Hz. Confining pressures used in both apparatuses were supplied by partial vacuum.

In addition, further testing was performed using the existing triaxial apparatus to study the possible difference in material behaviour when the confining stress was supplied by the traditional method in which external pressures are used. The same stress paths as described in Table 5.4 were used.

5.6 RESULTS AND DISCUSSION OF TESTS ON GRANULAR MATERIALS

5.6.1 Introduction

Results of the granular material tests are grouped into two main sections. The first section presents results of tests which have aimed at studying the effect of different test conditions. Effects on material behaviour due to loading frequency, waveforms, history and confining pressures provided by partial vacuum are included.

The second section consists of results from the standard tests for investigating the resilient characteristics, the susceptibility to permanent deformation and the strength of different material types.

5.6.2 Test conditions

5.6.2.1 Waveform effect

In order to observe any effects of different waveforms on resilient strains generated by repeated loads, experimental data obtained from the square wave stress and from the ramp wave are plotted against those from the sinusoidal wave tests in Figure 5.13. The recoverable strains produced by the square waves were consistently higher. On average, they were about 10% above those of the sinusoidal wave. On the other hand, there were no significant differences between the results from the sinusoidal and the ramp waves.

Typical hysteresis loops from the sinusoidal wave and the square wave are shown together in Figure 5.14. It is clear that they produce different amounts of resilient strain at the same deviator stress.

The softening effect due to the square wave may be explained by the change of frictional resistance between particles. During resilient cycling with the sinusoidal and the ramp waves at 0.5 Hz, friction similar to that of the static frictional resistance between particles might be applied. However, dynamic frictional resistance might be more appropriate in the case of square wave during loading and unloading because there are sudden displacements of particles in a very short period of time at the beginning and at the end of the wave.
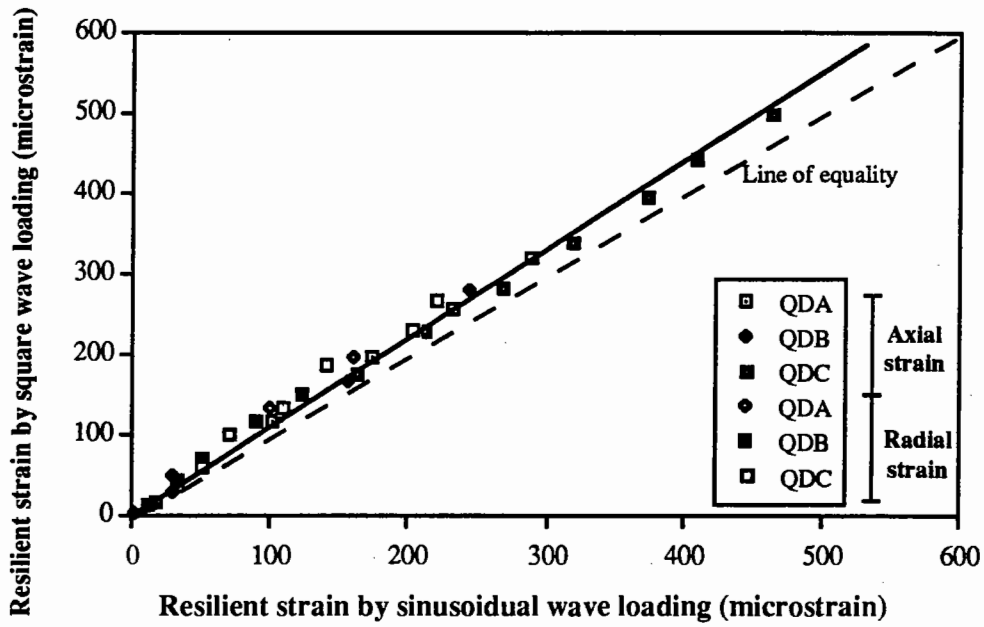
Figure 5.13a Comparison between square and sinusoidual wave loading
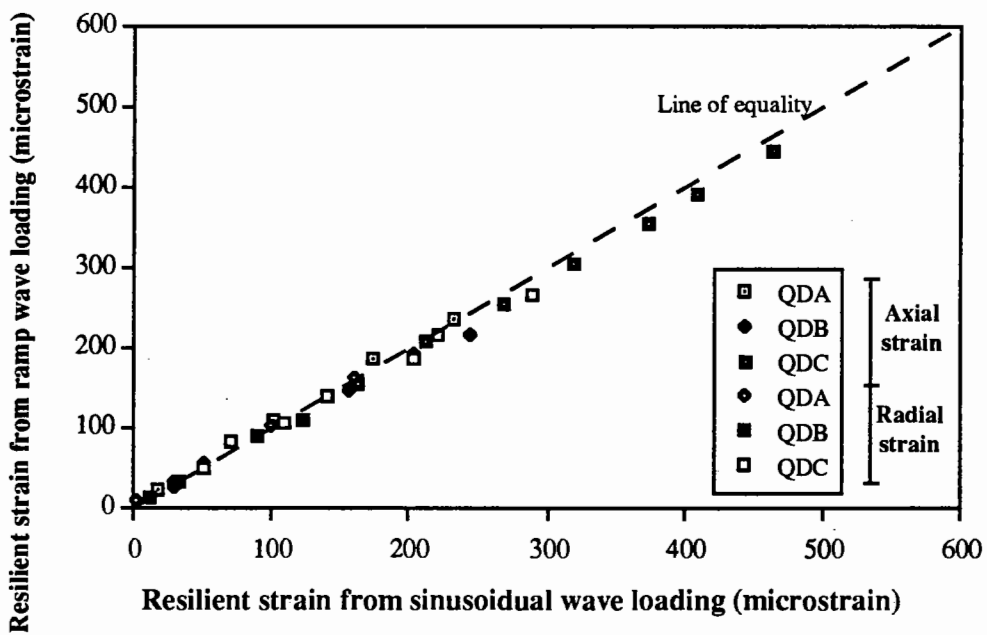
Figure 5.13b Comparison between ramp and sinusoidual wave loading
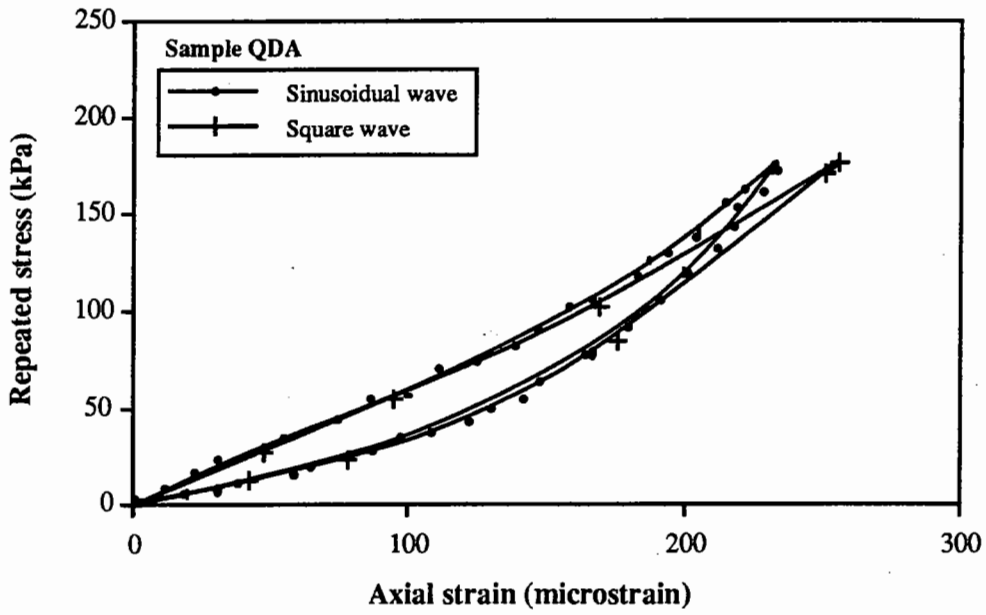
Figure 5.14 Typical hysteresis loops from different waveform loading
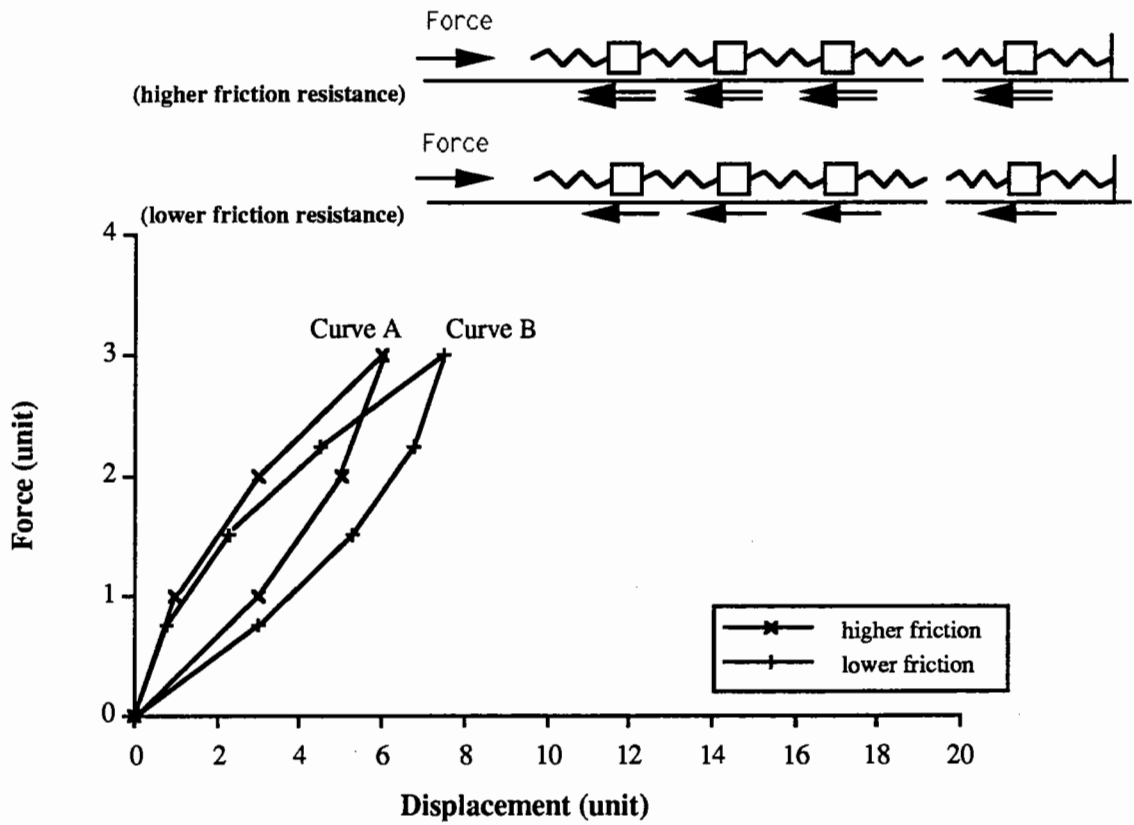
Figure 5.15 Effect of surface friction on resilient behaviour (based on Zytynski model)

The theoretical model developed by Zytynski et al (1978) was chosen to study the effect of reducing frictional resistance. Pappin (1979) had found a favourable explanation to the stress-strain hysteresis behaviour of granular materials by using the model. O'Reilly (1985) used the same model to explain the energy loss in repeated loading tests. Zytynski's model, as shown in Figure 5.15, consists of a series of blocks and springs. A lower coefficient of friction is used to represent the smaller frictional resistance in the square wave. Curve A in Figure 5.15 shows the predicted hysteresis loops representing those obtained from sinusoidal and ramp wave loading. Curve B, which contains higher resilient strains, represents the results of the square wave. It can be seen that the softening effect from the square wave can be explained by the reduction in surface friction.

To fully understand the very interesting softening phenomenon in unbound granular materials, certainly, there are many other aspects, such as inertia effects created by the sudden loading from the square wave or visco-elastic properties of the tested material etc, to look into. However, modelling of the waveform effect is outside the scope of the current research.

Figure 5.16a compares the permanent deformation results obtained from the repeated load triaxial testing due to the square and to the ramp waveforms. Figure 5.16b compares the results from the square and the sinusoidal loading. It was noticed that permanent deformation produced in sequences 1 and 3, in which square waves were used, were higher than the others. The finding was especially apparent when the results of the second and the third sequences of the tests were compared. In both figures, the later sequences incur higher value of strain. Hence, higher permanent deformation produced by the square wave is evident. Reduction of frictional resistance, as discussed above, may be one of the reason to explain the observation. It may also be due to the fact that a waveform with longer time period at or near peak stress produces higher plastic strain because of creep-type displacements (visco-plastic behaviour). Furthermore, it is noticeable that the difference in permanent deformation generated between the square and the ramp waves (Figure 5.16a) is much higher than that between the different waveforms in Figure 5.16b. It appears that the sinusoidal wave produces higher permanent strain than the ramp. This observation supports the second observation given above, that a waveform which has a longer time period at or near the peak stress generates more permanent strains.
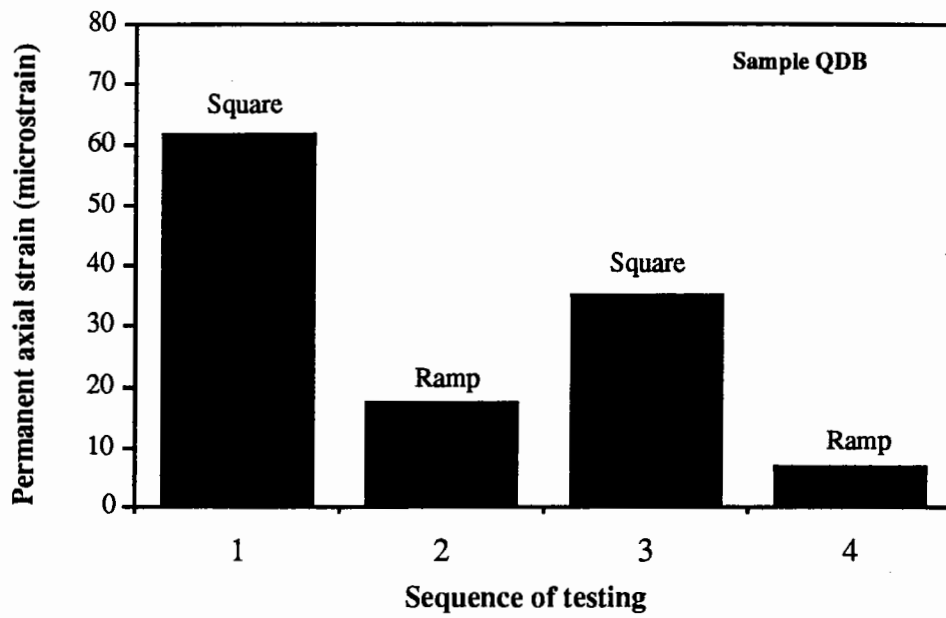
Figure 5.16a Comparison of permanent deformation from square and ramp
waveform loading
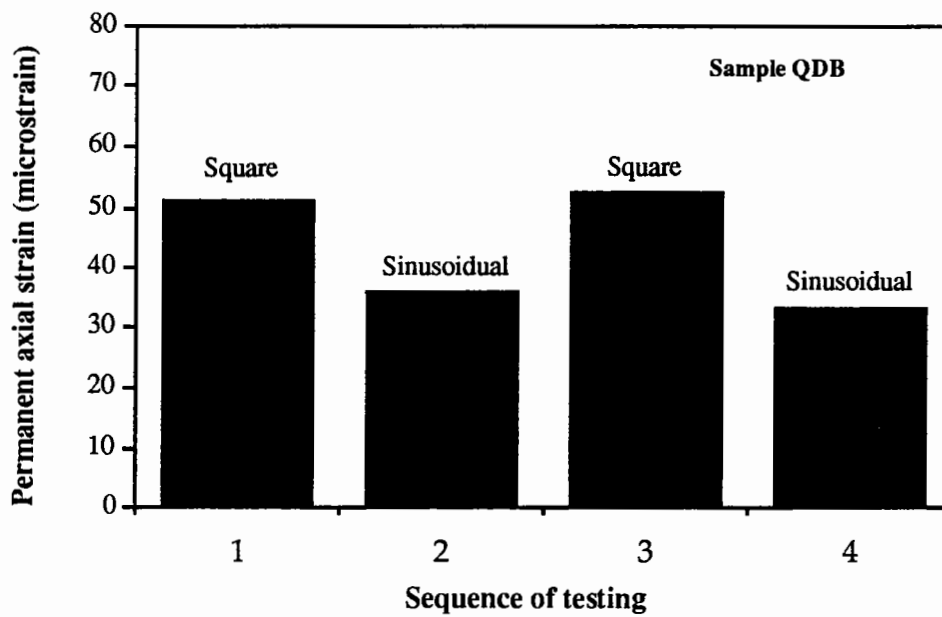
Figure 5.16b Comparison of permanent deformation from square and
sinusoidual waveform loading

5.6.2.2 Frequency effect

The stiffness results of samples tested at different frequencies are plotted in Figure 5.17. A horizontal line represents data obtained from testing sample QGB. Thus the loading frequency has no effect on the behaviour of granodiorite at this particular grading.

A scattering in the data is noticed for the other two samples of dolomitic limestones with different grading curves. There is a trend of increasing stiffness as the loading frequency increases. A 100 fold increase in frequency raised the stiffness by approximately 3% and 5% for QDB and QDC respectively. Since the degrees of saturation of the two samples were not high, 72% for QDB and 63% for QDC (refer to Appendix F), reduction of effective stress due to generation of pore water pressure inside the sample during testing should be negligible. From the limited test results, it is suggested that the effect of loading frequency on resilient behaviour may be material dependent. Nevertheless, even when there is a frequency effect, the influence is rather small.

The permanent vertical strains generated from the repeated loading tests at different frequencies are illustrated in Figure 5.18. It shows that the largest plastic strain was produced in the second sequence of the test in which repeated loads were applied at a frequency of 0.05 Hz. The test at 1 Hz in the third sequence gave the smallest amount of permanent strain.

When the results obtained from the two test sequences performed at the same frequency of 1 Hz were isolated for further investigation, the former sequence, as expected, gave higher plastic strain than the latter test. The same observation could be made for the tests at a frequency of 0.05 Hz. This confirms that the number of previous cyclic loads applied on granular materials affects the subsequent permanent deformation behaviour.

If the generation of non-recoverable strains in granular materials is only affected by the previous number of load applications, and assuming that the effect of varying frequency is negligible, the first sequence of the test should have produced the largest amount of permanent deformation, less in the following sequence and the least in the last sequence. Obviously, the results do not follow this hypothesis. By comparing the results of the first and the second sequences, it was noticed that the 0.05 Hz test gave higher permanent deformation even though the test was performed after the 1 Hz test.
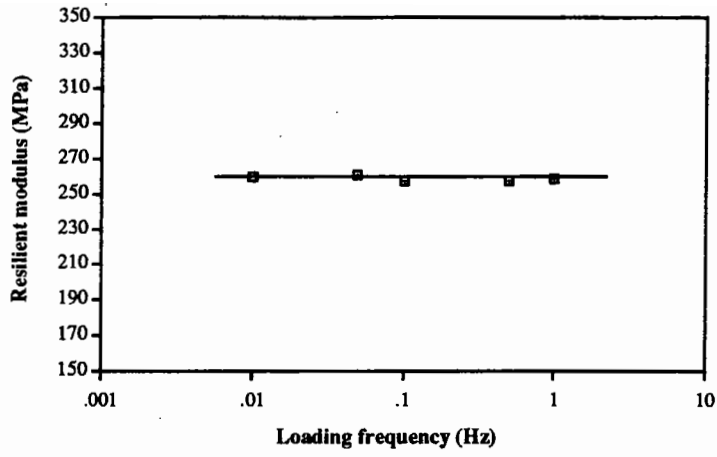
Figure 5.17a Frequency effect on sample QGB
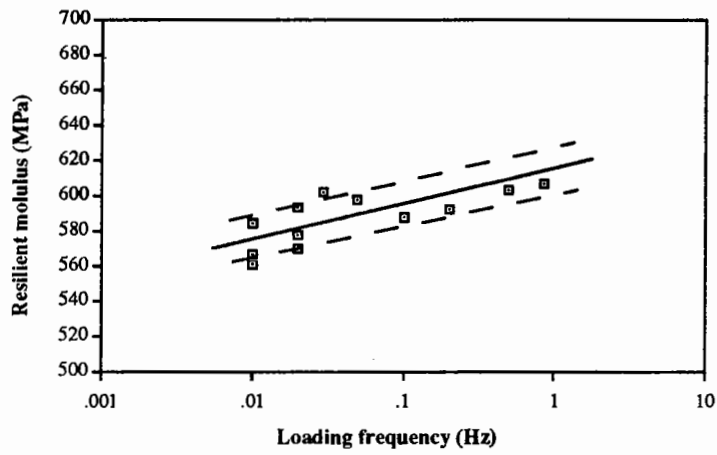
Figure 5.17b Frequency effect on sample QDB
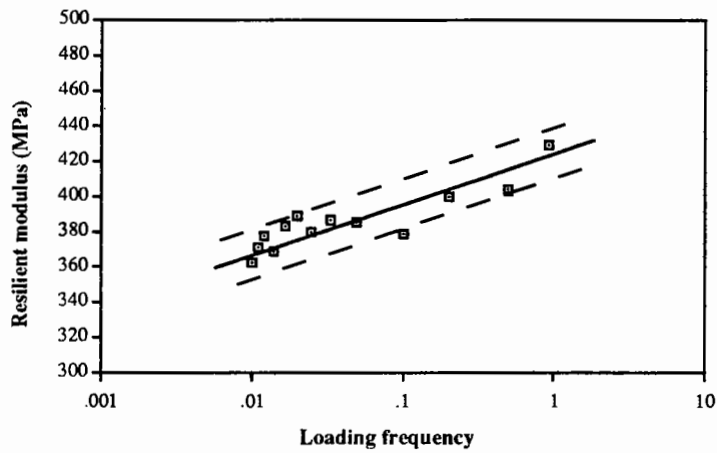
Figure 5.17c Frequency effect on sample QDC
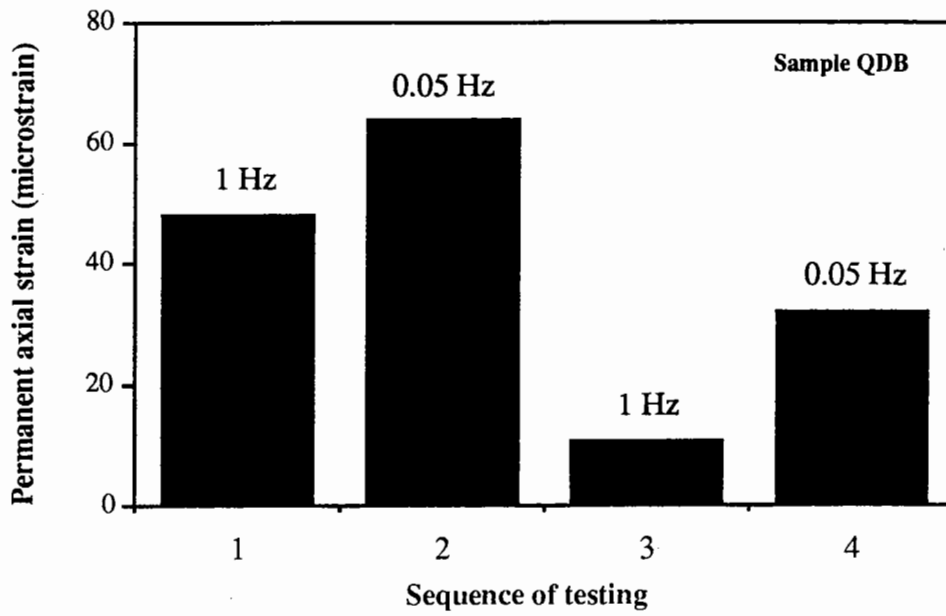
Figure 5.18 Effect of load pulse length (loading frequency) on aggregate permanent deformation
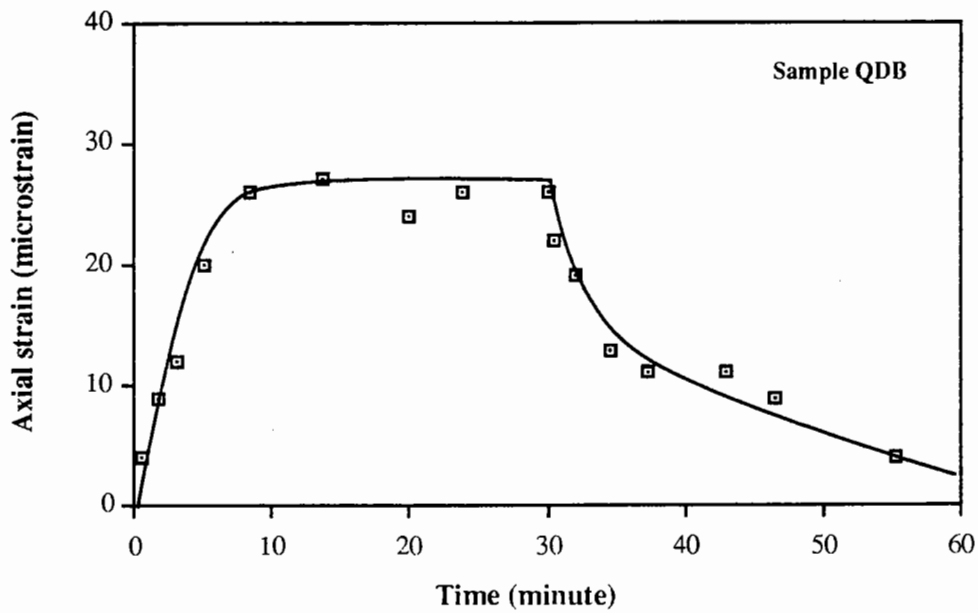
Figure 5.19 Creep behaviour of unbound granular material

(Strain is measured from the end of loading and end of unloading)

The observation is confirmed by the results obtained from the third and the fourth test sequences. Hence, repeated loading at a lower frequency produces a larger amount of plastic strain in granular materials. This observation provides further confirmation that a load pulse which has a longer time period near the peak stress produces more plastic deformation.

Good control of stress paths is, therefore, essential for tests of permanent deformation in order to give a consistent result. Since the MCA is unable to produce repeated loads of standard waveforms and of exact frequency, it is not appropriate as the loading device to perform permanent deformation tests.

5.6.2.3   Creep

The effect on the deformation behaviour of granular materials caused by holding a static load for a time period of 30 minutes is presented in Figure 5.19. The figure shows the development of the vertical creep strain in the specimen when the peak load is on and after the vertical load is released. The specimen crept rapidly in the first 10 minutes after the peak load was applied and then slowed down quickly. Similarly, most of the recovery took place in the first few minutes after unloading. However, only about 85% of the full creep was recovered even after 30 minutes of unloading.

Hence, strains in a wet granular material are still developing even after the increase of applied stresses has stopped. Most of the strains take place at the very beginning after the designed peak stress has been reached and very little further increment of strain is developed later. The majority of the creep strain produced is recoverable. Thus, creep which occurs due to the application of a constant static load away from the failure stress of the material may consist of two parts. The major part is elastic and the minor part comprises the permanent deformation. This observed creep behaviour goes some way to explaining the frequency and waveform effects noted in the two preceding sections. More time, during a load pulse, spent at high stress levels is likely to cause more strain (some of it recoverable) and thus softer and more easily deformed specimens.

Therefore, when prolonged stresses, such as those produced by the manually-controlled actuator, are applied, elastic creep will probably be generated during the test. The effect is that the resilient modulus obtained may be lower than at a frequency more representative of traffic loading.

5.6.2.4 Loading with a manually-controlled actuator

A typical stress-time curve obtained by the MCA as the axial loading mechanism for resilient strain testing is shown in Figure 5.20. A relatively smooth curve for both loading and unloading can be seen. This indicates that a simple hand-operated actuator is able to provide reasonable control of axial loads. Figure 5.21 gives a comparison of the resilient axial and the radial strains produced by the two loading systems. It is noted that there was not much difference between the results of the samples, QSB and QGB. However, the axial and radial strains generated by the MCA for the samples, QDB and QDC, were about 10% higher than those produced by the servo-controlled actuator. In fact, the results agree with the previous observation on the frequency testing (Section 5.6.2.2) and confirm that the frequency effect on the resilient behaviour of aggregates is material dependent. Nevertheless, using the resilient strain results obtained by the MCA loading method will produce a slightly conservative pavement foundation design by underestimating the real stiffness value.

5.6.2.5 Time of equilibrium

The vacuum meters connected to the top and the bottom platens showed that equilibrium of the material with the coarsest grading, QDA, was reached almost immediately after the suction was altered. Hence, only the two finer specimens required checking. Figure 5.22 shows the results of testing. The curves in both figures are similar in shape. As expected, the stiffnesses of the materials continue to increase with time after the partial vacuum has increased and before the equilibrium state is reached. It took half an hour for sample QDB to reach equilibrium. On the other hand, about 12 hours were required for the finest graded sample, QDC.

5.6.2.6 Tests in the existing triaxial apparatus

The results shown in Table 5.9 indicate that the average dry density of the specimens (of QGB) tested in the new and the existing apparatuses were similar. Therefore, direct comparison of the two sets of testing results may be made.
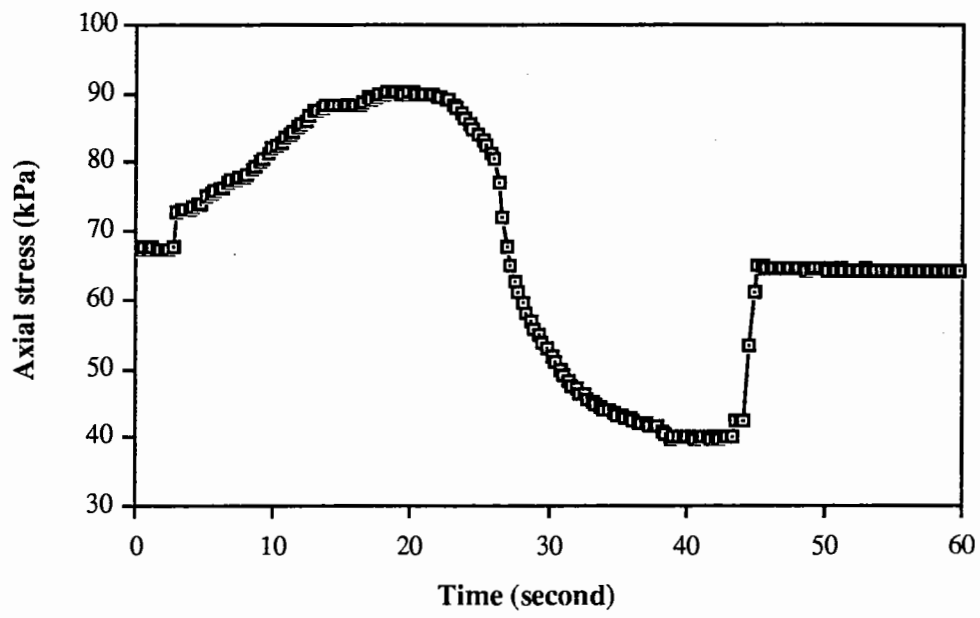
Figure 5.20 Typical stress-time curve by hand jack
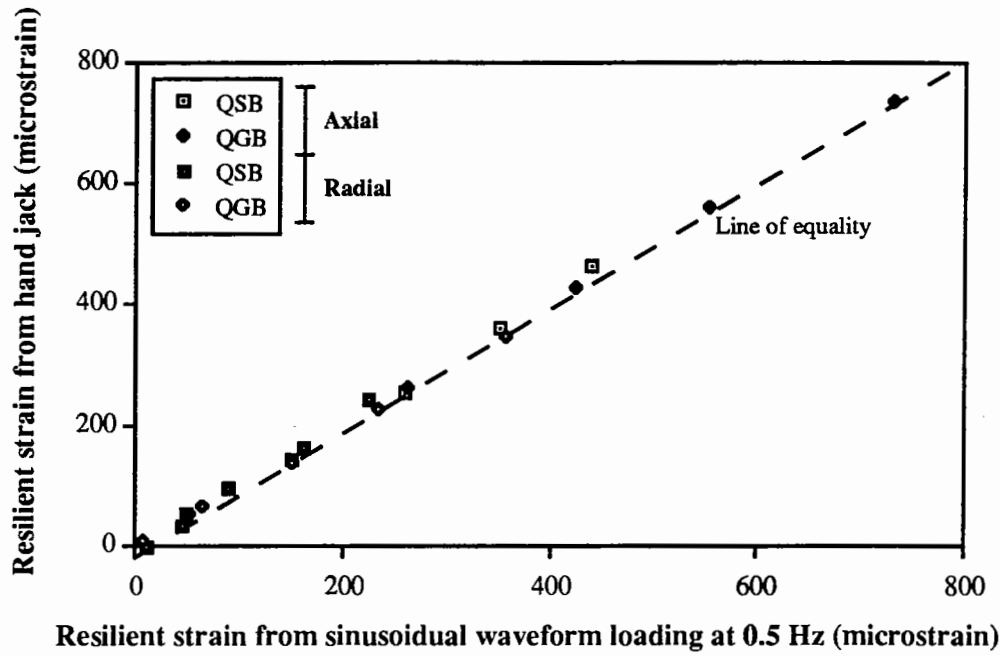
Figure 5.21a Comparison of resilient strains produced by different loading methods
(Samples QSB and QGB)
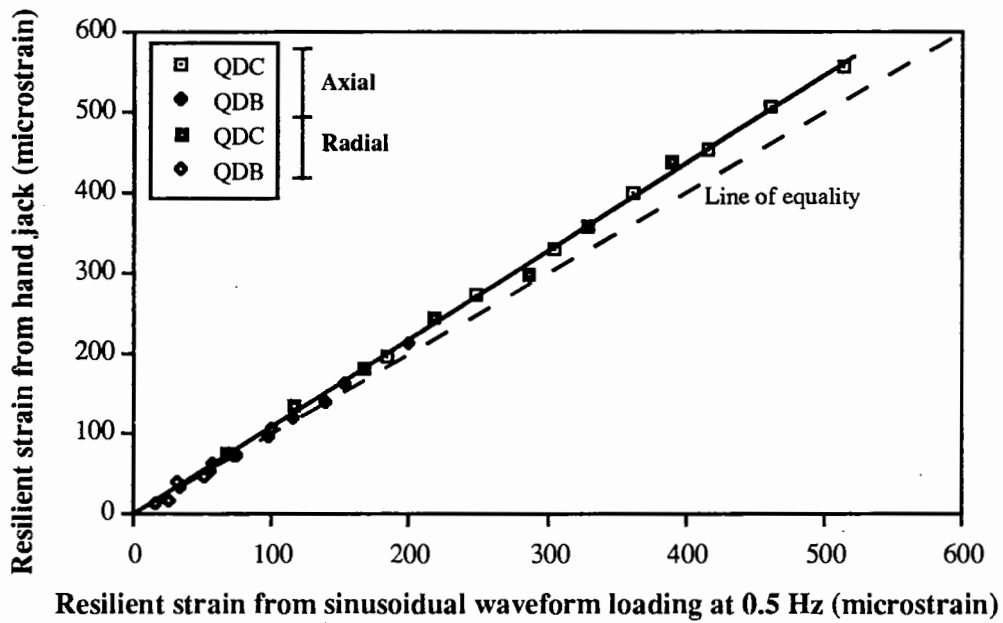
Figure 5.21b Comparison of resilient strains produced by different loading methods
(Samples QDB and QDC)
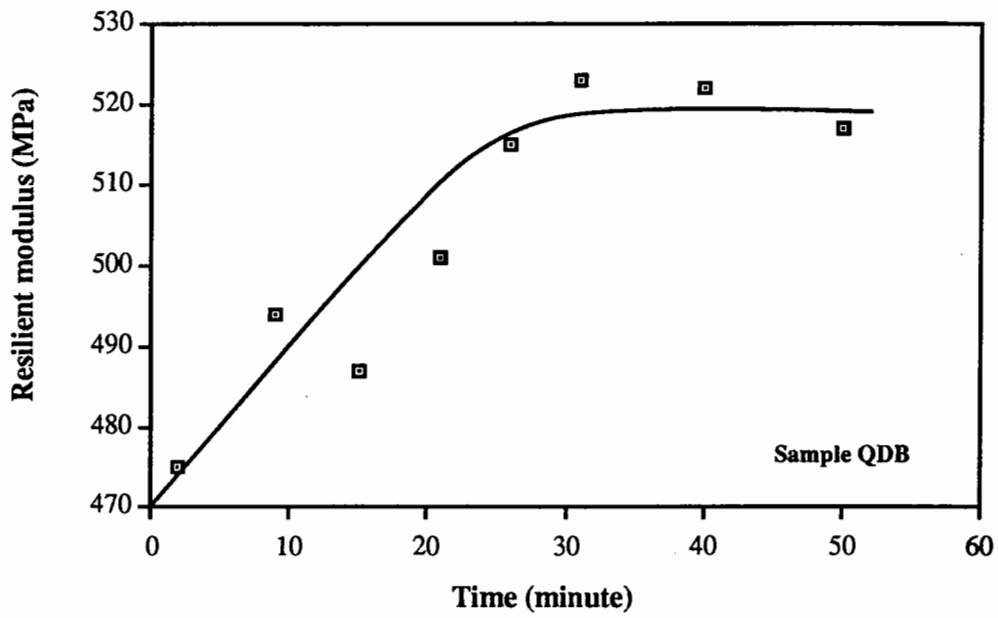
Figure 5.22a Equilibrium time for aggregates of particle envelope of DoT Type 1 fine side
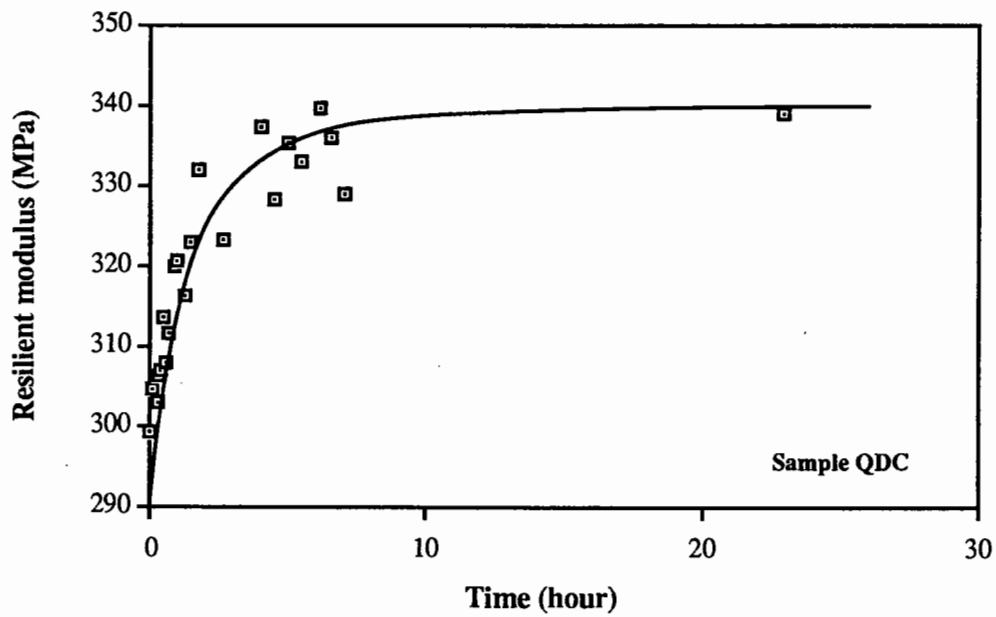
Figure 5.22b Equilibrium time for aggregates of particle envelope of DoT Capping 6F1 fine side

Table 5.9
Conditions of the 150 mm and 280 mm diameter specimens

Specimen diameter (mm)	Dry density of the specimen (kg/m^3)	Degree of saturation (%)
150	2335	70
280	2317	70

In Figure 5.23, the resilient axial and radial strains obtained from the two apparatuses are compared. Lines of equality are inserted to help to identify their relationship. In the graph showing radial strains, although more scattering is noticed, the deviation is considered acceptable in comparing two completely different systems. Hence, the differences due to changing instrumentation, specimen size and the possible effect of particle size are not significant.

The implication of the observation is that:-

(a)   The particle to specimen size ratio of 7.5 currently used for the 150 mm diameter QGB specimen in the 150TA is sufficient since it gave results similar to those from a ratio of 14 in the larger diameter (280 mm) specimen in the current comparison tests. Thus, the ratio of 7 (Section 3.2), which has been recommended for the new triaxial apparatus to test granular materials, is likely to be sufficient.

(b)   The overall performance of the on-sample instrumentation used in the existing and the newly developed triaxial apparatuses is comparable.

Comparison was also made for the resilient axial strains and the radial strains obtained from tests by the two methods of supplying confining pressures to the 150 mm diameter specimen. The results are shown in Figure 5.24. Data are scattered closely around the line of equality. Since water was allowed to drain away during the load applications and the granular samples were far from saturation (Table 5.9), the build-up of positive pore water pressure inside the sample should be negligible. Hence, the increment of confining pressure by both methods should be approximately equal to the increment of effective pressure and there should be a good match between the two sets
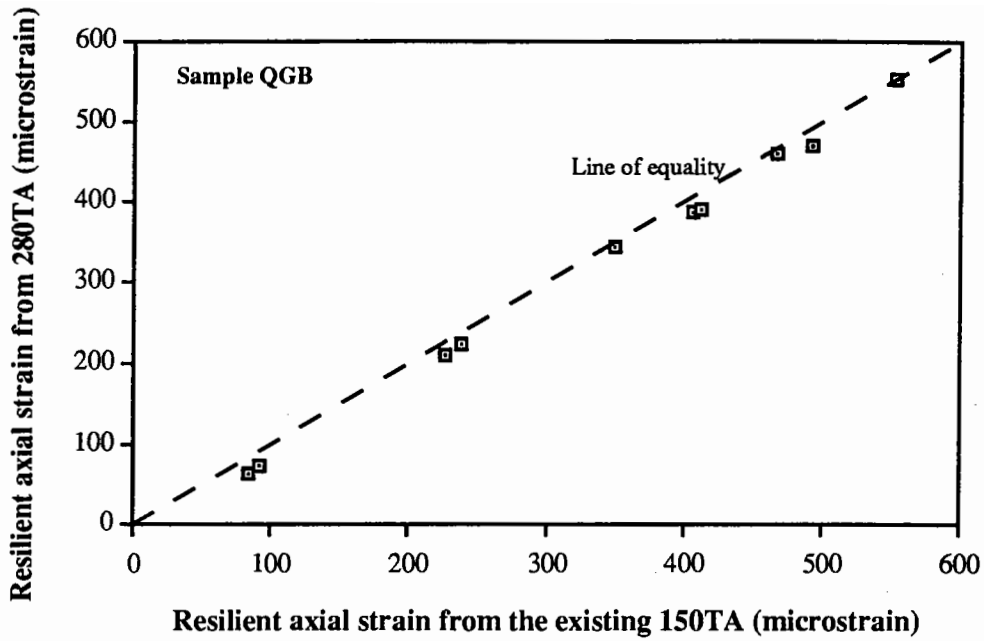
Figure 5.23a Comparison of resilient axial strains produced by different repeated load triaxial apparatuses
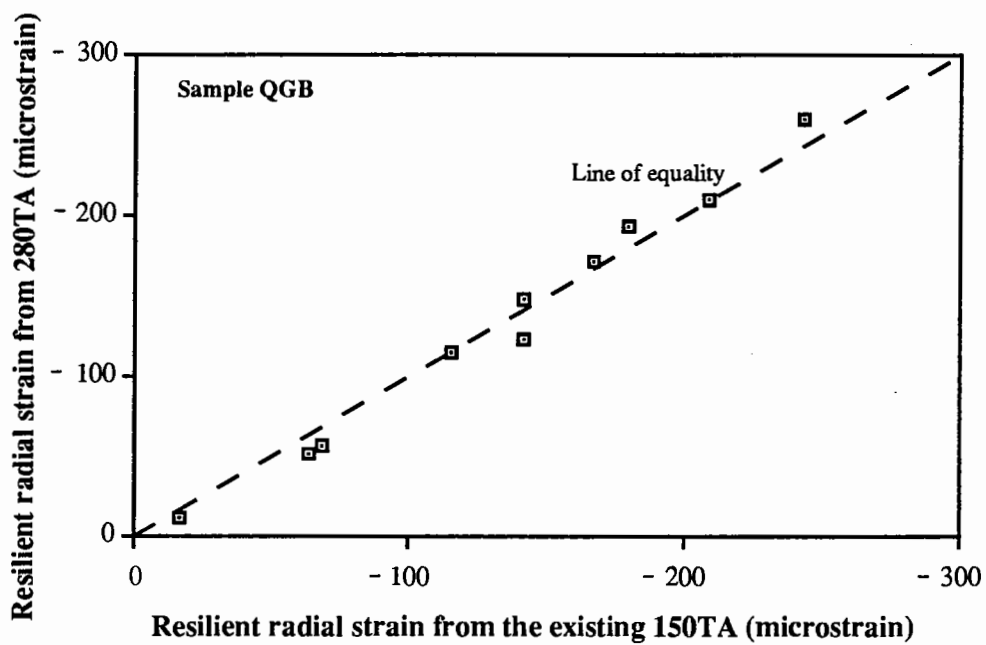
Figure 5.23b Comparison of resilient radial strains produced by different repeated load triaxial apparatuses
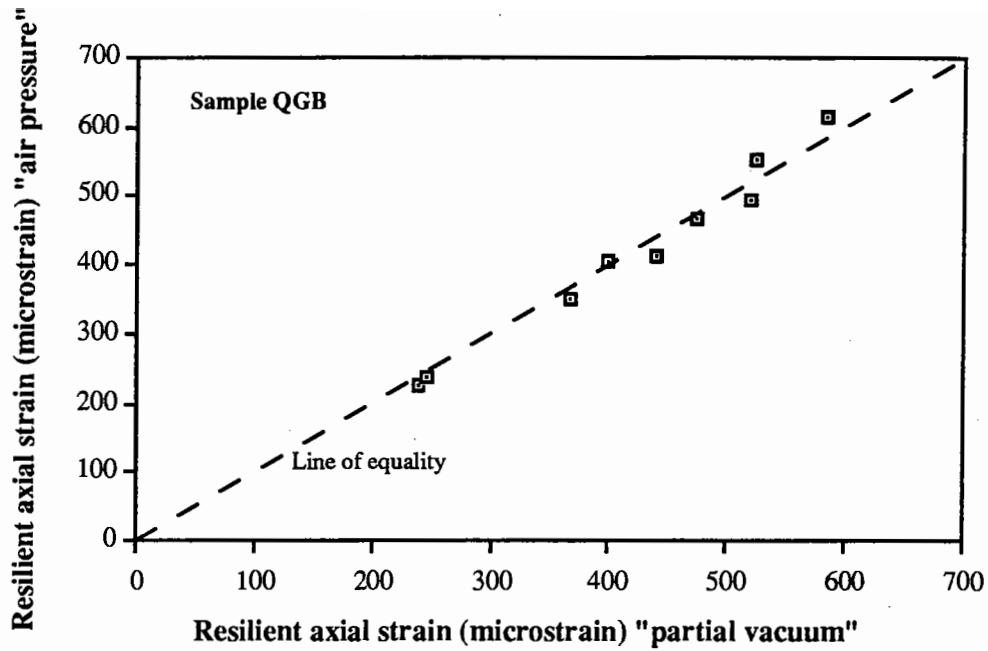
Figure 5.24a Comparison of resilient axial strains produced in tests of different means of confinement
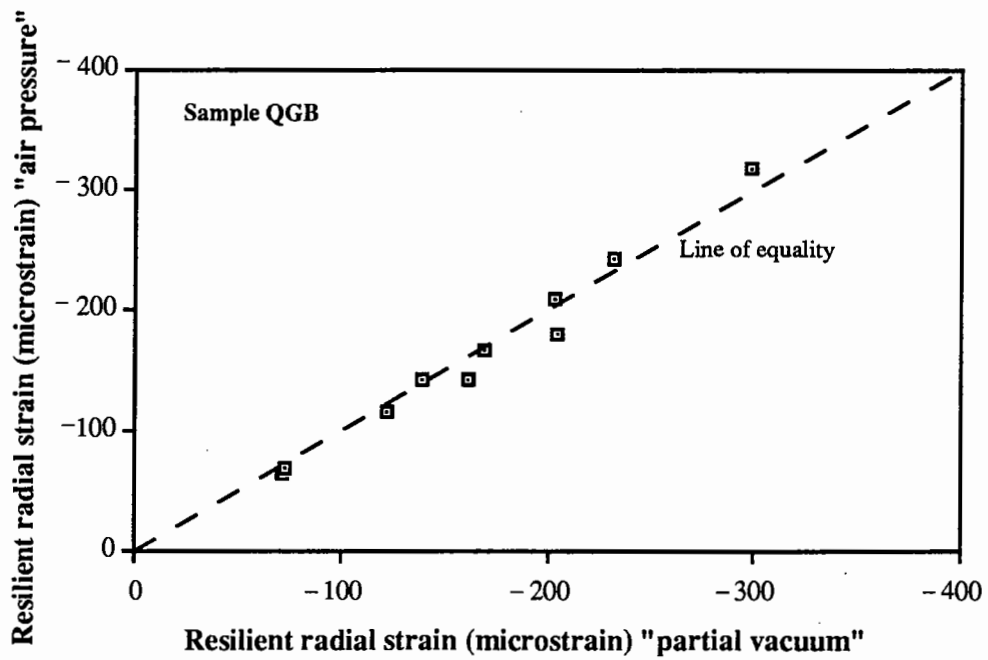
Figure 5.24b Comparison of resilient radial strain produced in tests of different means of confinement

of testing results. This is found to be the case for materials a long way from saturation and illustrates the acceptability of the partial vacuum confining pressure method.

Hence, provided that the specimen to particle size ratio is kept above the recommended value, high quality resilient strain results are obtainable from the new test method.

5.6.3 Standard test

This section presents and discusses results obtained from the standard tests. Where comparison is made, the emphasis is to compare results within each series. Particular attention is also given to the effect of the different constituent particles, which have been carefully examined in the preliminary tests (Chapter 4). When results showed obvious errors, they were discarded.

5.6.3.1 Elastic behaviour

Loading and unloading hysteresis

Figure 5.25 shows the typical response of granular materials to changes in deviator stress at the mid-height of a specimen when using the manually-controlled actuator (MCA). The non-linear behaviour of the unbound granular materials is evident. The changes in material strains in both axial and radial directions are not linearly proportional to the change in applied stresses. For instance, as indicated in Figure 5.25a, the rate of change of vertical strains near the peak deviator stress are much smaller than that at the low stress level. A higher stiffness is, therefore, expected when the deviator stress increases. Brown and Dawson (1992) suggested that a high resilient modulus was appropriate for the sub-base unbound layer during the construction period. The figure they proposed was four times higher than that appropriate for the in-service pavement.

Hysteresis loops due to the difference between loading and unloading strain paths were also observed. This is in agreement with those found by previous researchers (Boyce 1976, Pappin 1979 and O'Reilly 1985).

Though modelling of the non-linearity of the aggregate is outside the scope of this project, further study of the resilient stress-strain response was attempted so that

87

understanding of the pavement performance under wheel loads might be improved. For all the materials tested, the vertical and radial strain curves during unloading were of a similar shape although their shapes during loading were not the same. As shown in the graphs of Figure 5.25, the unloading curves are concave upward.

Another way of presenting the elastic behaviour of the granular material is to plot radial strains against axial strains (Figure 5.26). The slope represents the tangent Poisson's ratio. When it is compared with the secant Poisson's ratio, the tangent value is always larger during loading, while both of them become approximately the same during unloading. (When the secant Poisson's ratio is above 0.5, net material dilation is expected.) Another special feature noticed is that the slope of the unloading curve, and thus of Poisson's ratio, is almost constant. Figure 5.27 shows a graph presenting the resilient secant Poisson's ratio. The curve in the figure can be divided into two sections. The first section shows that the Poisson's ratio increases with deviator stresses during loading. However, it is nearly a constant, at almost 0.5 in this case during unloading. This response during unloading was confirmed by tests carried out on the other materials.

These observations highlight the complexity of analyzing the pavement structure (even in two dimensions) because of the difference in elastic response between loading and unloading. Graphs in Figure 5.28 are used to illustrate the effect. A moving wheel and four elements at the same depth of a pavement are shown in Figure 5.28a. Figure 5.28b represents the general stress-strain relationship. Element A is far away from the wheel so it is only subjected to the dead load from the over-burden. The resilient strain is zero. Element C is directly below the wheel. Peak resilient strain is expected. Elements B and D are of equal distance from the wheel. If the load is stationary, the elastic strains at B and D should be same. However, this will not be the case when they are under a rolling wheel even though the vertical stresses on both of them are identical. Element B has just experienced a stress-strain path from point A to B in Figure 5.28b and the path for element D has been from A to D through C. The net strain at D is d which is higher than b for the element B. The consequence of this unloading effect, as far as the granular material is concerned, is the formation of an asymmetrical deflection bowl as shown in Figure 5.28c.
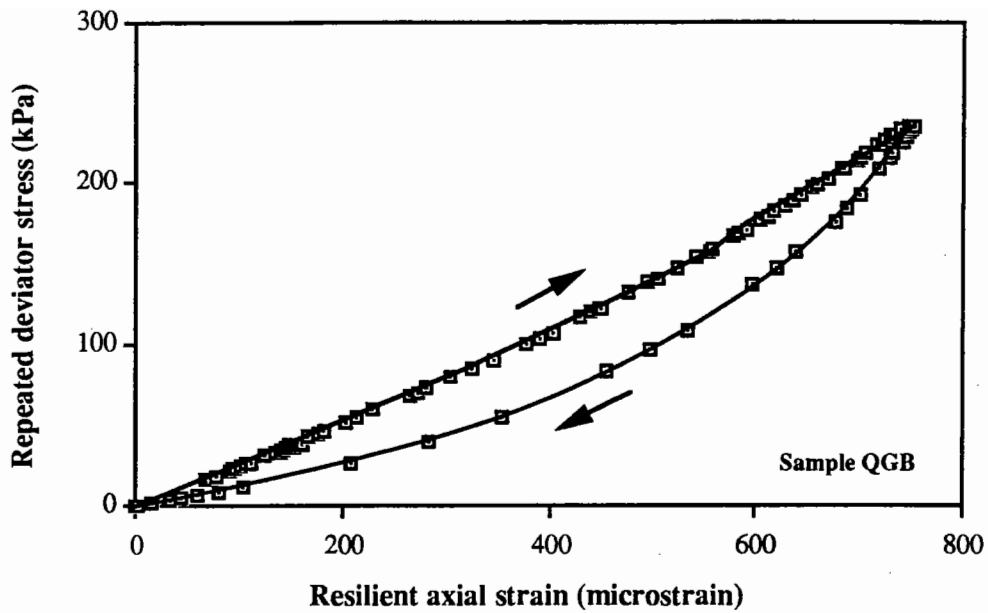
Figure 5.25a Typical hysteresis loop under loading from manually-controlled actuator (axial strain)
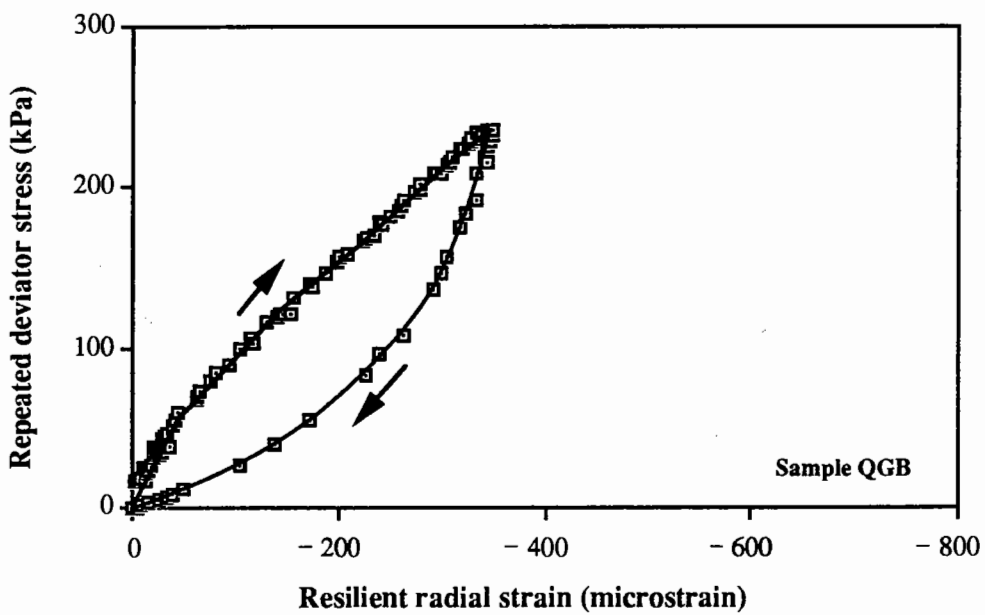
Figure 5.25b Typical hysteresis loop under loading from manually-controlled actuator (radial strain)
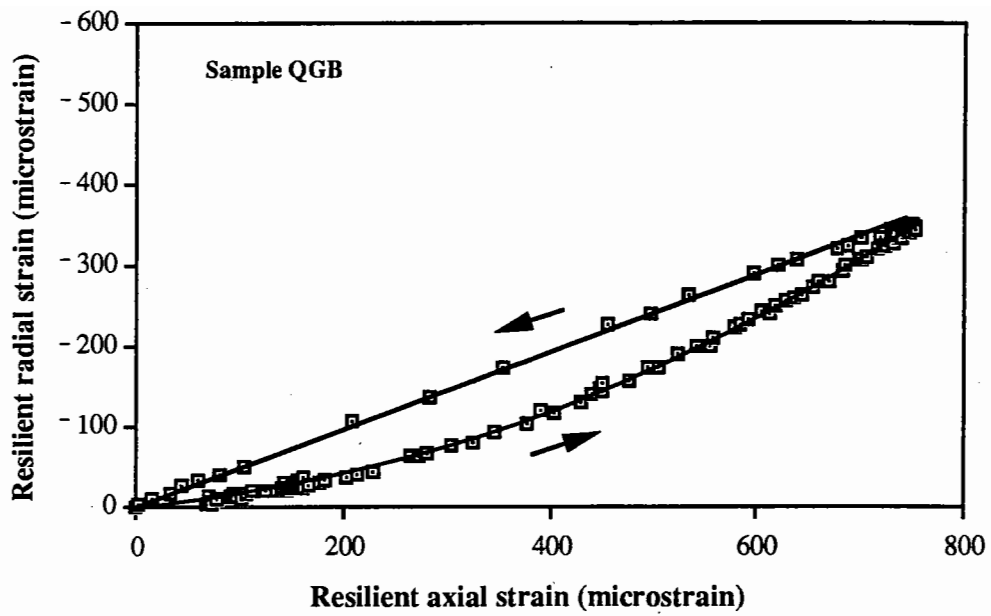
Figure 5.26 Relationship between radial and axial strain
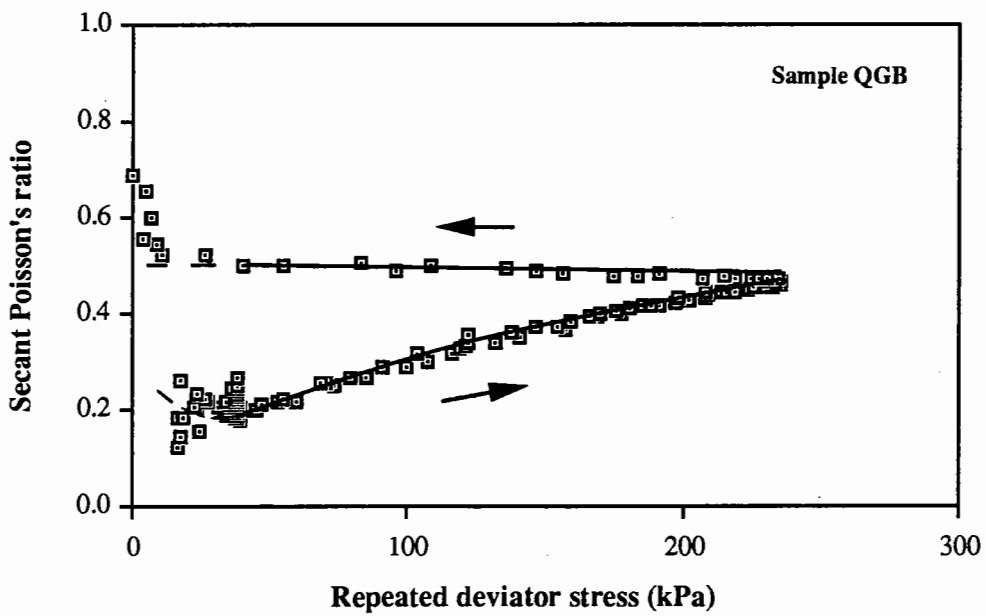
Figure 5.27 Variation of Poisson's ratio due to repeated loading
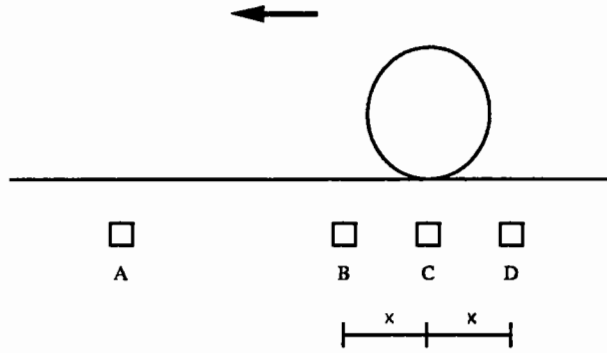
Figure 5.28a Elements at the same depth under a moving wheel
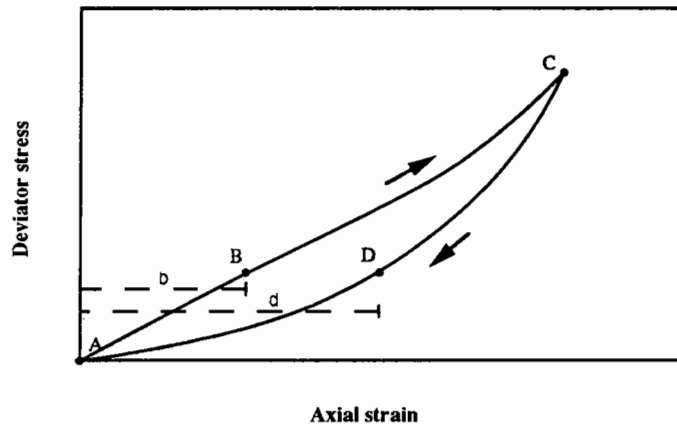
Figure 5.28b Typical stress-strain relationship of unbound granular material
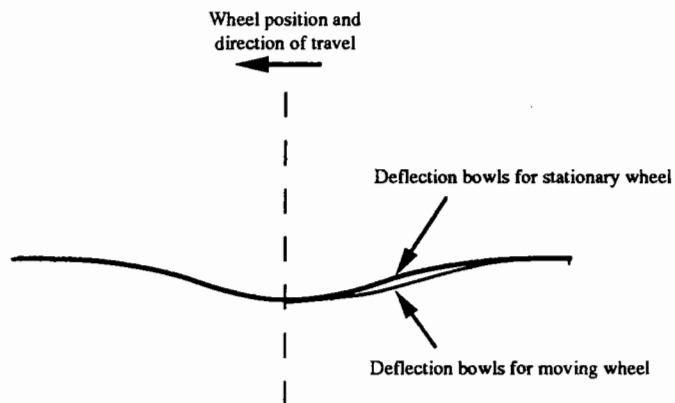
Figure 5.28c Deflection bowls for stationary and moving wheels

<u>Resilient strain</u>

To study the performance of individual samples, the K-theta model and Boyce model have been tried. It was noticed that the former model did not give a full description of the materials. Only behaviour in the vertical direction is described. This is overcome by the Boyce model, which possesses multiple parameters, but interpretation of these parameters and defining their effects is not straightforward. Furthermore, little information will be obtained if comparison of materials is carried out at a particular stress level when they behave non-linearly. After considering several alternatives, it was decided to present the full stress-strain pattern of each test in terms of shear and volumetric strains. Figures 5.29 and 5.30 show the typical results of resilient shear and volumetric strains respectively. Generally, resilient shear strains radiate from the origin. Within a particular confining pressure, shear strain increases almost linearly with increasing deviator stress in most of the crushed-stone samples. The deviator stress has little effect on the shear modulus. When the confining stress increases, higher stiffness results.

As shown in Figure 5.30, a series of curves is recorded for the volumetric strain. The material is experiencing compression when stress levels are below the peak volumetric strain value. Expansion begins when the peak is reached. Equation 5.4 shows the relationship between the deviator and the normal stresses in a triaxial specimen.

$$\Delta p = \frac{\Delta q}{3} \tag{5.4}$$

It is because q is increasing at a much faster rate than the increase in p in the triaxial specimen, that volume expansion can occur though the mean normal stress is increasing. Another observation made is that the higher the confining pressure, the greater the maximum compressive volumetric strain (Fig. 5.30) - as might be expected.

The results of the resilient deformation test are summarized in Appendix J.

- First test series -

Figure 5.31 presents results from the three samples of dolomitic limestone in the first test series. Figure 5.31a shows the resilient shear behaviour of the tested materials. The fine material, QDC, had the lowest stiffness while the performance of the other two, QDA and QDB, was similar. The relationship between resilient volumetric strains and normal stresses are plotted in Figure 5.31b. For the stress regíme applied, QDB

89
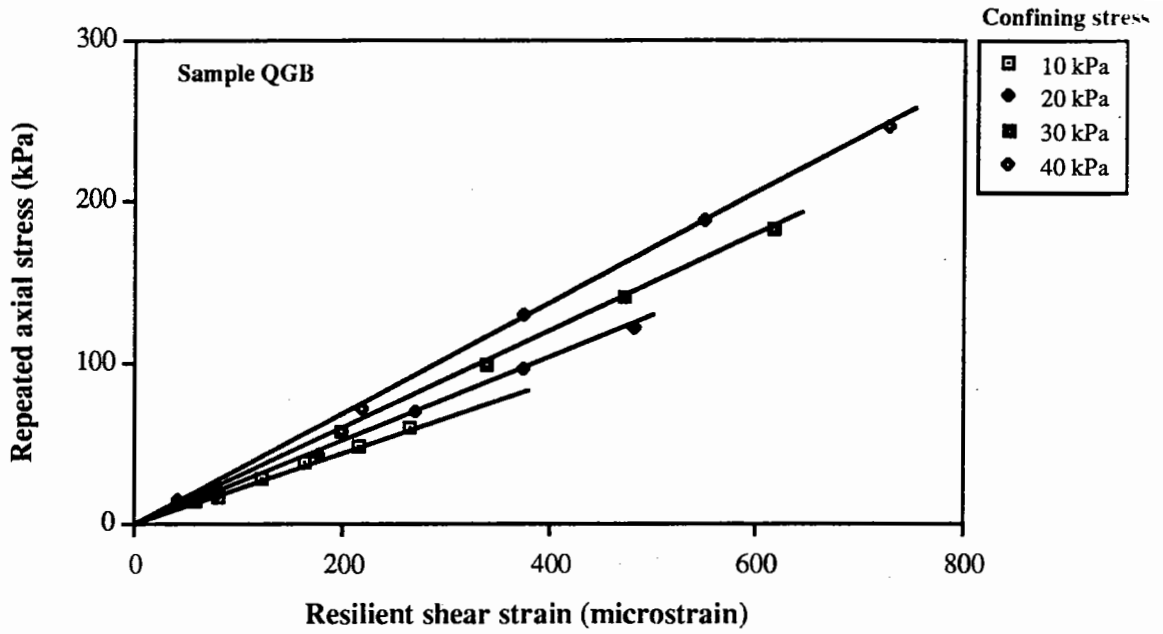
Figure 5.29 Typical resilient shear strain plot of granular material
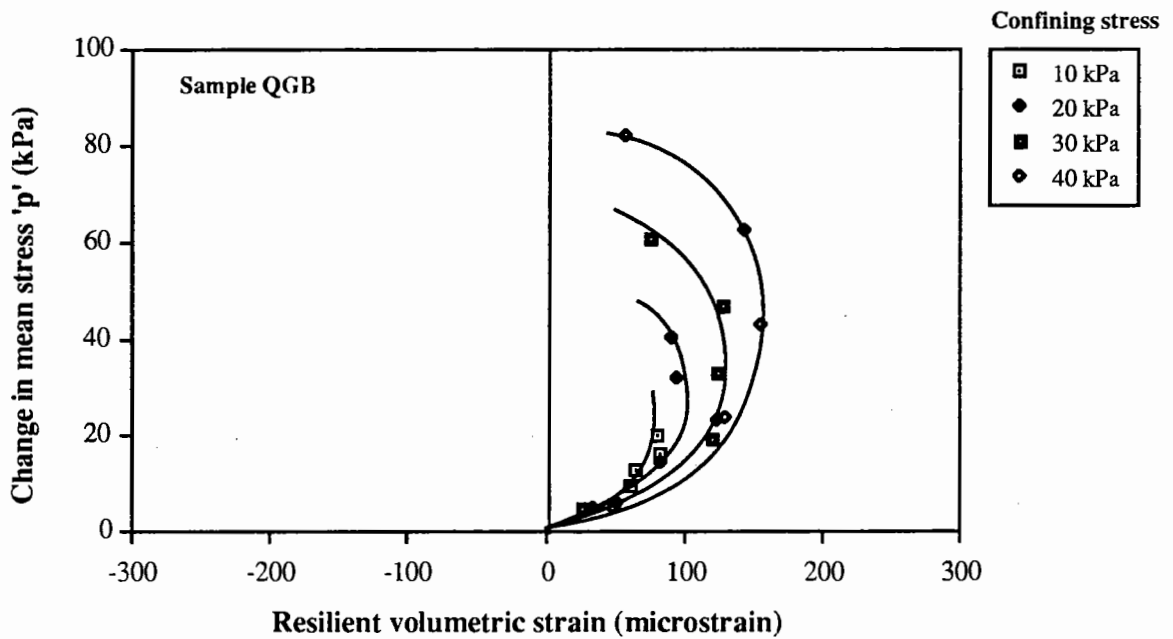
Figure 5.30 Typical resilient volumetric strain plot of granular material
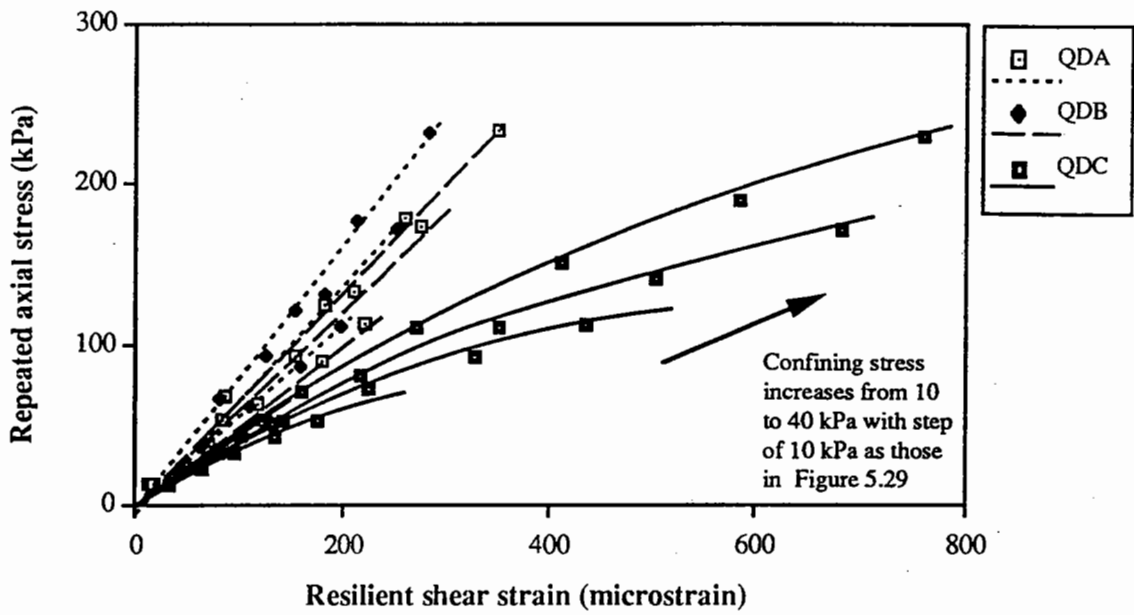
Figure 5.31a Resilient shear strain graph (comparison of different gradings)
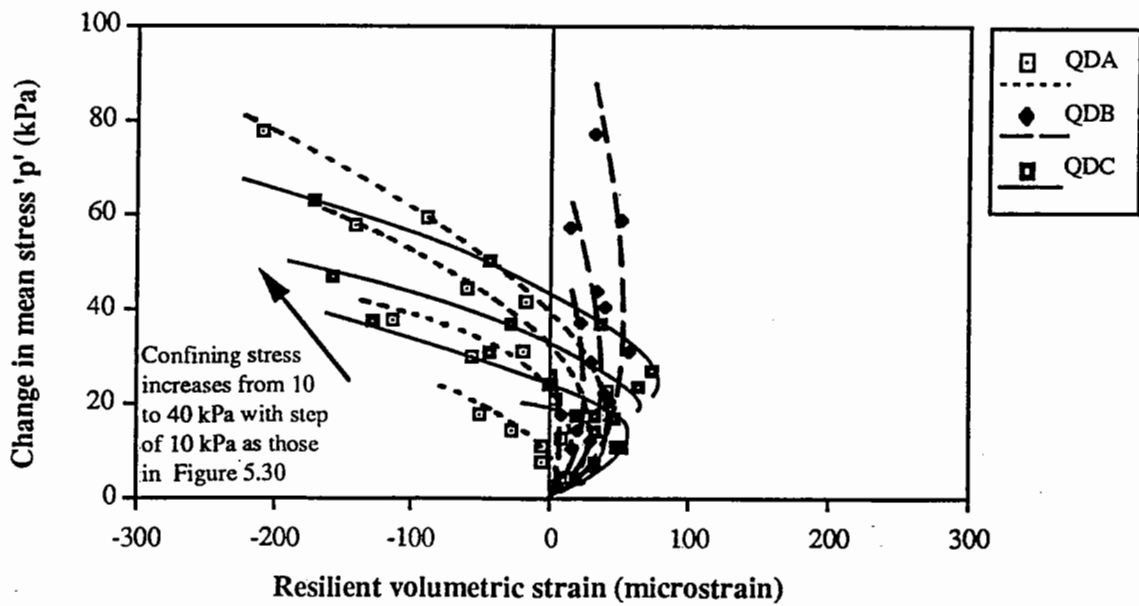
Figure 5.31b Resilient volumetric strain graph (comparison of different gradings)

did not dilate. Both the finest and the coarsest materials, QDC and QDA expanded into the dilation zone at higher stresses, and the dilation of QDC was more than that of QDA. Hence, the use of high fine content materials in the pavement sub-base should be avoided not only because of the potential drainage problem (Grace 1981) but also their bad resilient performance both in terms of shear and volumetric components.

To compare materials of different origins, the results of QDB, QGB and QSB are presented in Figure 5.32. All these materials were of the same grading and were compacted to their refusal densities. It is noted that although the granodiorite and the gravel was of different particle angularity and surface texture, their resilient shear behaviour was similar. Both of them produced more strain than the dolomitic limestone. Preliminary test results in Chapter 4 have shown that the particles of the limestone possess a high surface friction resistance. This might be the reason that the limestone produced less shear strains. This phenomenon was also observed by Thom (1988).

The resilient volumetric strains plotted in Figure 5.32b indicate that curves of the sand and gravel dip into the dilation zone when stresses are increased. On the other hand, both crushed rock materials are well within the compression zone. Based on the limited data, it appears that materials consisting of rounded particles are more likely to be susceptible to dilation. This observation supplements Thom's suggestion (1988). He noted that , broadly, materials of rounded particles, such as sands and gravels, were concentrated at the lower end of his ranking chart for volumetric strains, showing that, as a general rule these materials are more susceptible to volumetric strain.

- Second test series -
Figures 5.33 to 5.34 show the resilient strain testing results on the materials from the Loughborough site. For clarity, results of a maximum of three samples are presented in each figure.

The resilient shear strains of the granodiorite and the furnace bottom ash are almost linear over the range of applied axial repeated loads (Figure 5.33a). Nevertheless, the granodiorite is about 30 to 50% stiffer than the furnace bottom ash (LAN). The higher stain recorded for LAN might be due to the fact that this sample was made of weak porous aggregates (for details refer to Appendix E and Table 4.3 in Chapter 4). A considerable amount of resilient deformation might have been produced within the

90
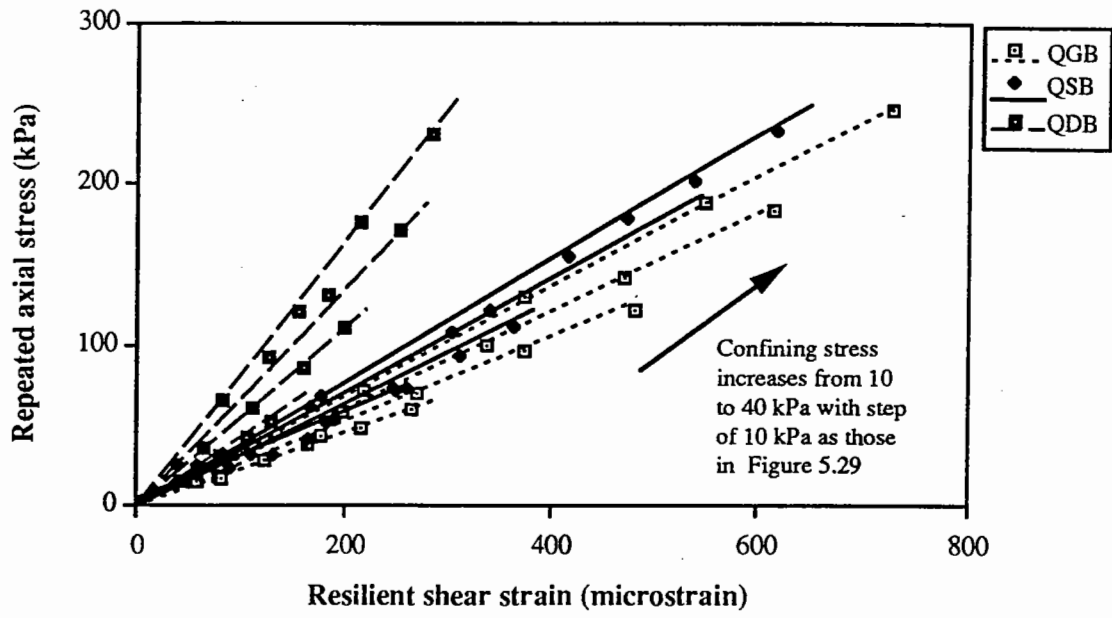
Figure 5.32a Resilient shear strain graph (comparison of different materials)
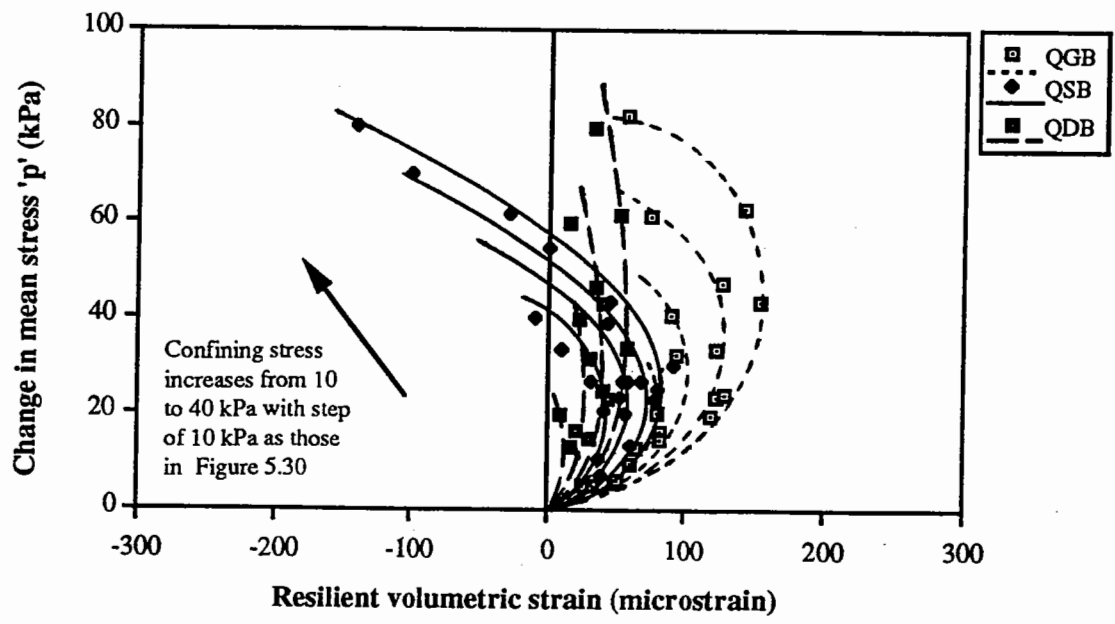
Figure 5.32b Resilient volumetric strain graph (comparison of different materials)
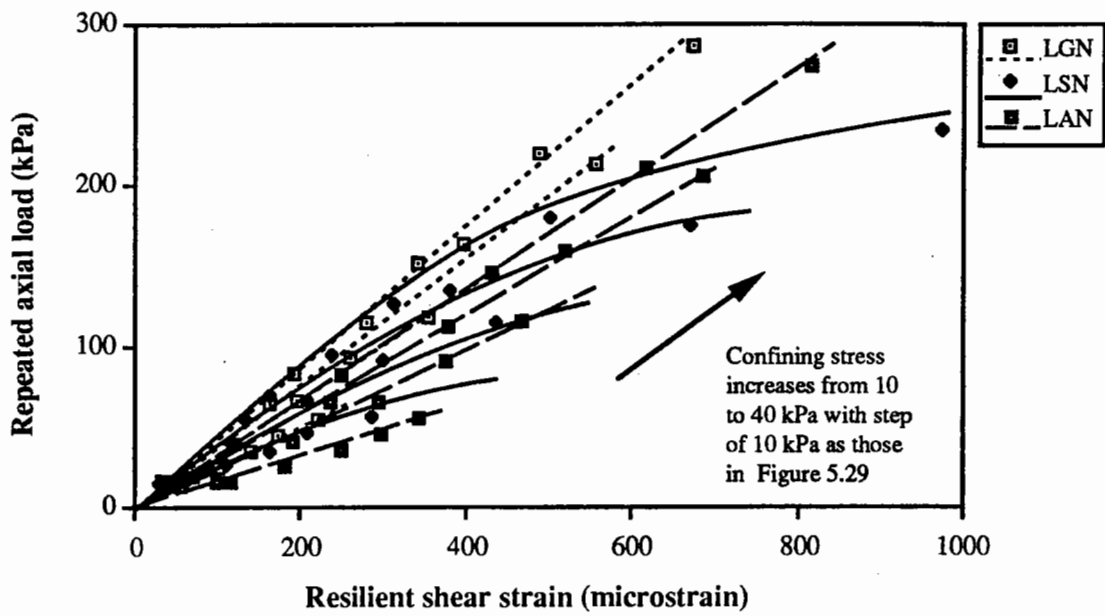
Figure 5.33a Resilient shear strain graph (comparison of different materials from the Loughborough trial)
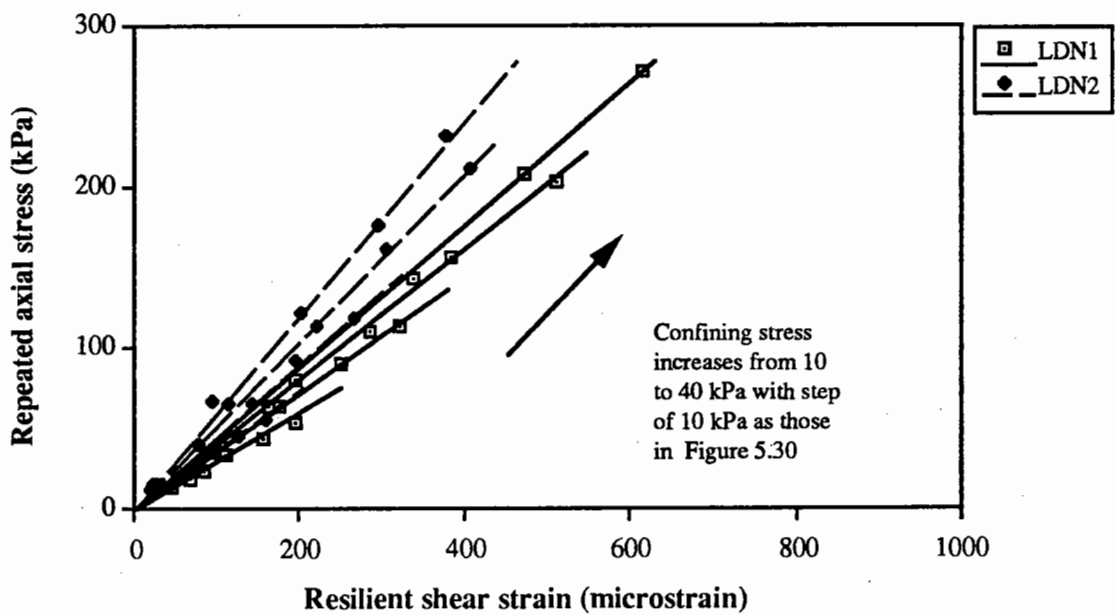
Figure 5.33b Resilient shear strain graph (comparison of different materials from the Loughborough trial)
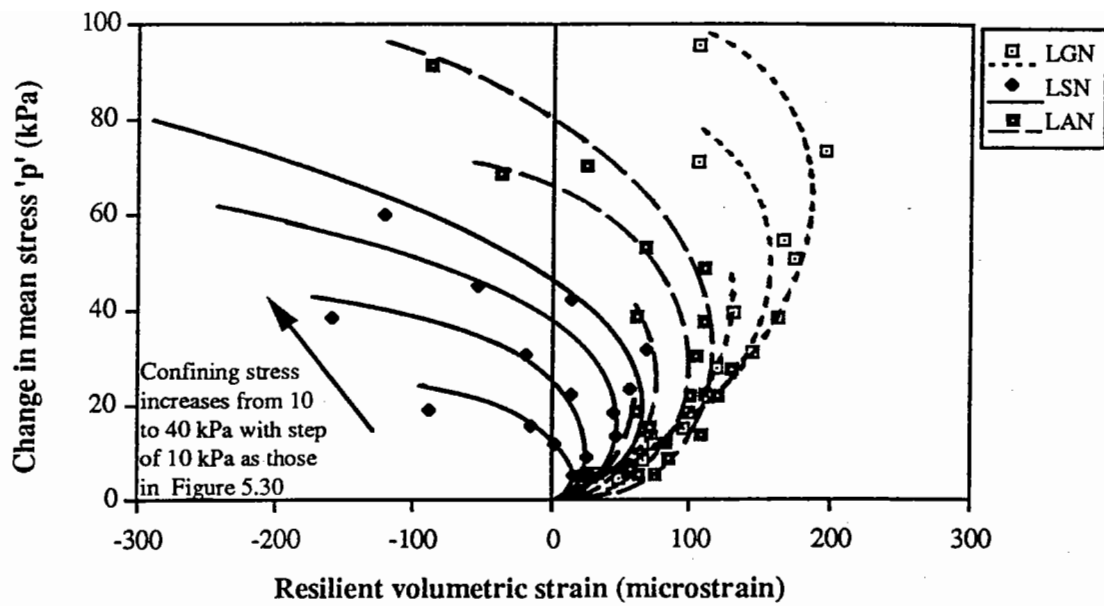
Figure 5.34a Resilient volumetric strain graph (comparison of different materials from the Loughborough trial)
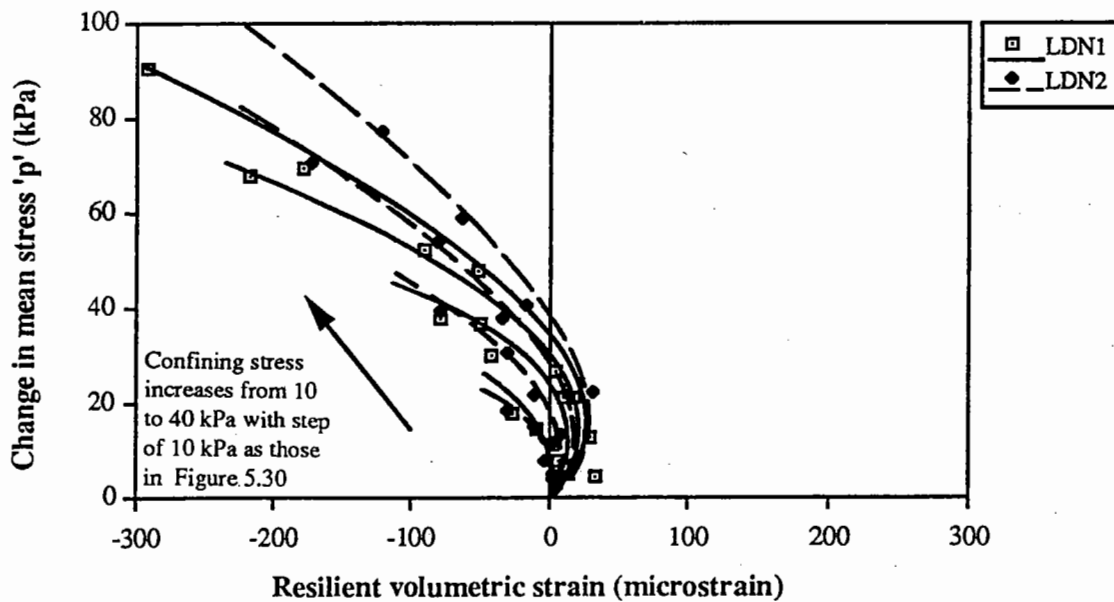
Figure 5.34b Resilient volumetric strain graph (comparison of different materials from the Loughborough trial)

particles themselves. The resilient shear strain behaviour of the granodiorite and the sand and gravel (LGN and LSN) are very similar at low deviator stress, but when the stress increases, the resilient shear strain development of the two samples diverges. While the rate for the granodiorite is still quite constant, the strain rate for the sand and gravel increases showing reducing shear modulus for the material.

The resilient shear strain results of the two samples of dolomitic limestone, as shown in Figure 5.33b, indicate that LDN1 is softer than LDN2 by about 25 to 40 %. Since the two samples were of the same particle size distribution and of the same moisture content, but of different solid contents (Appendix F), the probable cause of the softer response may be the lower density of the former sample. When the two graphs in Figure 5.33 are viewed together, it is noticed that LDN2 was the stronger sample in terms of resilient shear behaviour and, LDN1 and LGN were performing similarly.

Results of the resilient volumetric strains of the samples, LGN, LSN and LAN are presented in Figure 5.34a. Large dilation was observed for the sand and gravel sample (LSN). On the other hand, dilation was recorded for the furnace bottom ash (LAN) at high stresses and no dilation was noted for the granodiorite (LGN). Figure 5.34b shows the volumetric results for the samples, LDN1 and LDN2, again the less dense sample produced the greater strains (dilative in this case).

- Third test series -
The effect of density on the resilient strains of granular materials was further observed in the testing results of the materials from the Bothkennar site. Figure 5.35a shows that for the same material type, BGN2 produced less resilient shear strain than that of BGN1, for which a lower density was recorded. BGN2 has a 60 to 90% higher shear modulus than BGN1. Furthermore, for BGN1, the material dilated when the stress ratio (q/p) was at high magnitude (Figure 5.35b). However, no dilation was observed for the denser granite sample.

When the shear strain results of the two samples, BSN and BGN2, of different material types were compared, little difference was noted. The resilient volumetric behaviour of BSN was found to be similar to those in the other test series for other sand and gravel samples - dilation was observed.
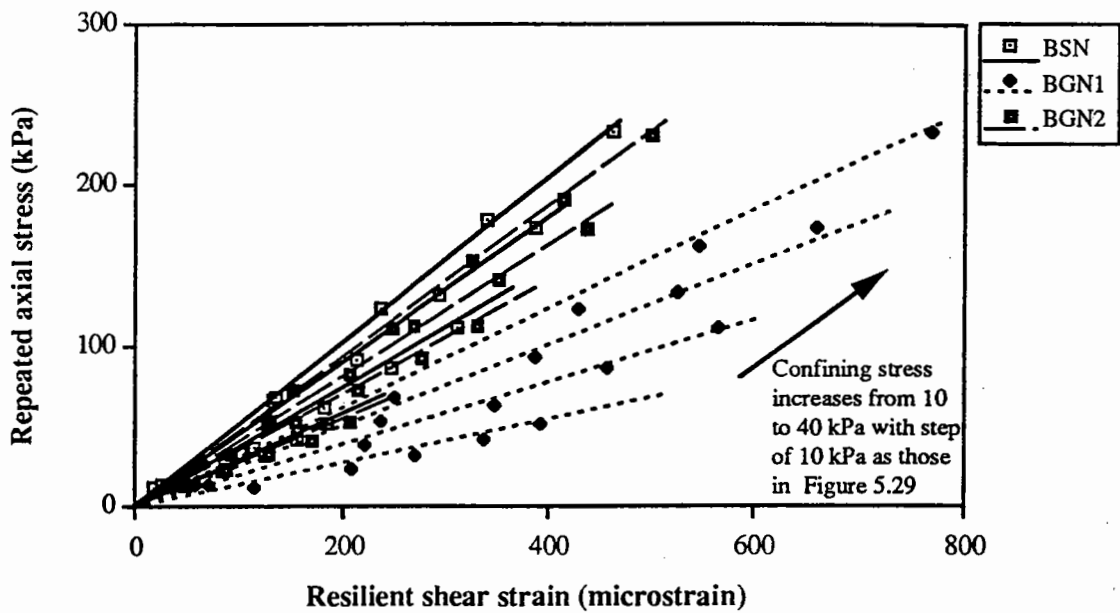
Figure 5.35a Resilient shear strain graph (materials from the Bothkennar trial)
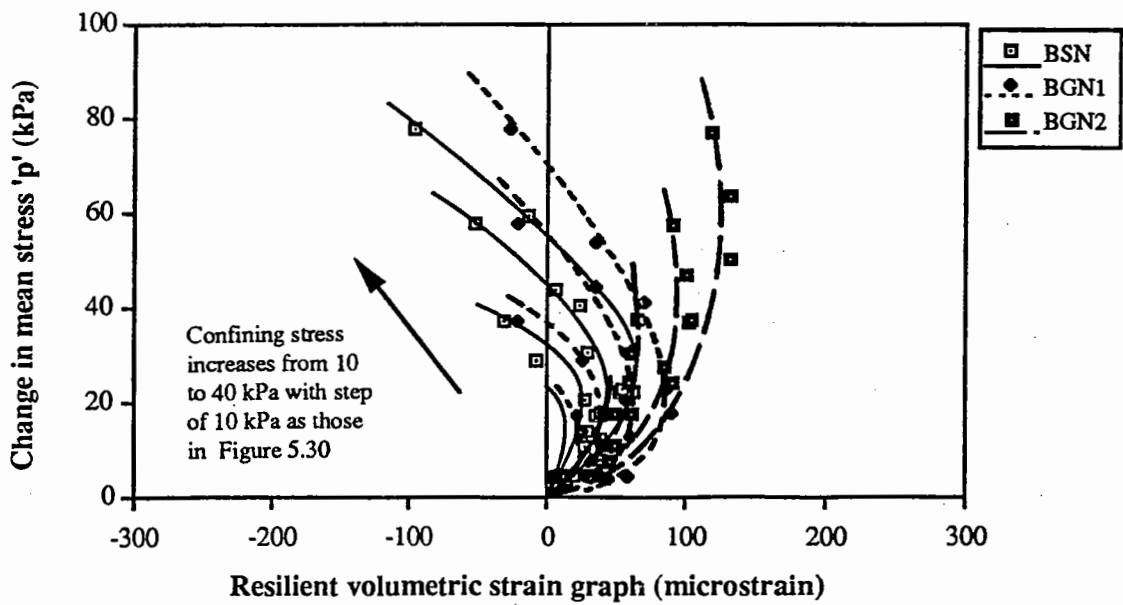
Figure 5.35b Resilient volumetric strain graph (materials from the Bothkennar trial)

5.6.3.2 Permanent deformation

Figure 5.36 shows the axial and radial responses of aggregates obtained from the drop hammer test in the first test series. The results are also typical of the other two series. In general, the development of the axial plastic deformation can be approximated to being linear. For the radial plastic strain, the rate of strain increment generally decreases with the blow number. Curved lines are more appropriate to fit these data. Nevertheless, it is observed that higher axial strains are related to higher radial strains. In the following sections, the use of the drop hammer results as a tool to compare the permanent deformation susceptibility of different aggregates is demonstrated. Table 5.10 presents a summary of the results of the permanent deformation developed after dropping a 10 kg hammer for 25 times through a height of 300 mm on the top of the specimens.

Table 5.10 Drop hammer results (25 blows)

Test series	Material	Designation	Solid content (%)	Permanent	
				Axial strain (micron)	Radial strain (micron)
1	dolomitic limestone	QDA	72	2077	-1993
	dolomitic limestone	QDB	83	619	-725
	dolomitic limestone	QDC	78	1245	-1017
	granodiorite	QGB	87	428	-725
	sand & gravel	QSB	88	1067	---
2	dolomitic limestone	LDN1	77	2004	-1131
	dolomitic limestone	LDN2	80	---	-591
	granodiorite	LGN	79	1160	-1152
	sand & gravel	LSN	78	14055	-16304
	furnace bottom ash	LAN	55	1345	-3540
3	granite	BGN1	68	2401	-1500
	granite	BGN2	75	1290	-1250
	sand & gravel	BSN	76	486	-692

- First test series -

Results from the dolomitic limestones in the first test series indicate that there appears to be an optimum grading to resist permanent deformation. The fine (QDC) and the
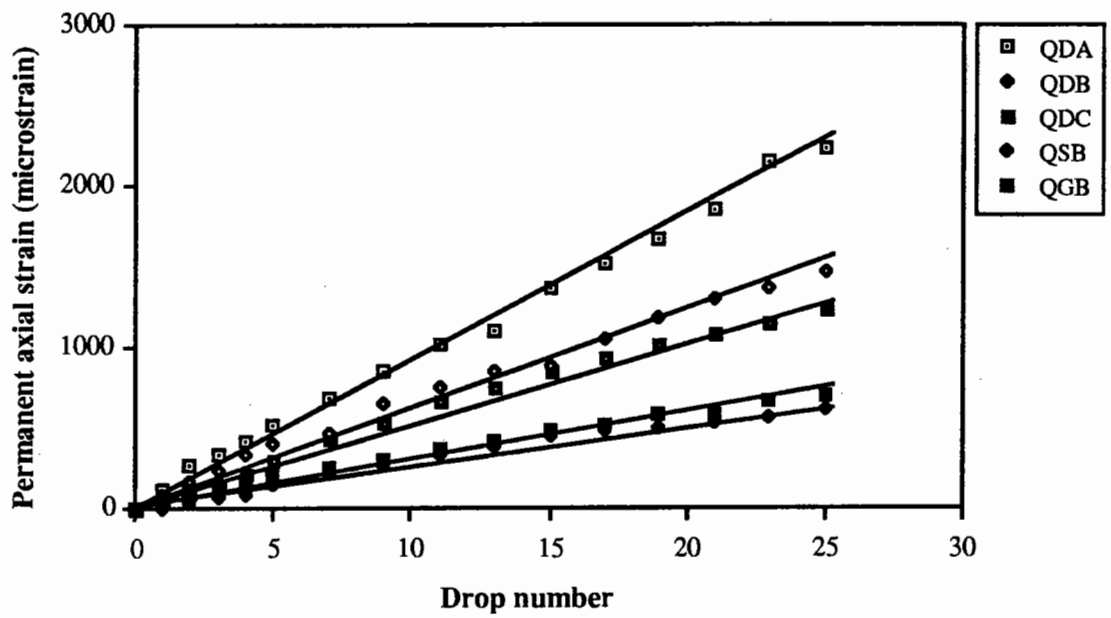
Figure 5.36a Permanent axial strain in drop hammer test
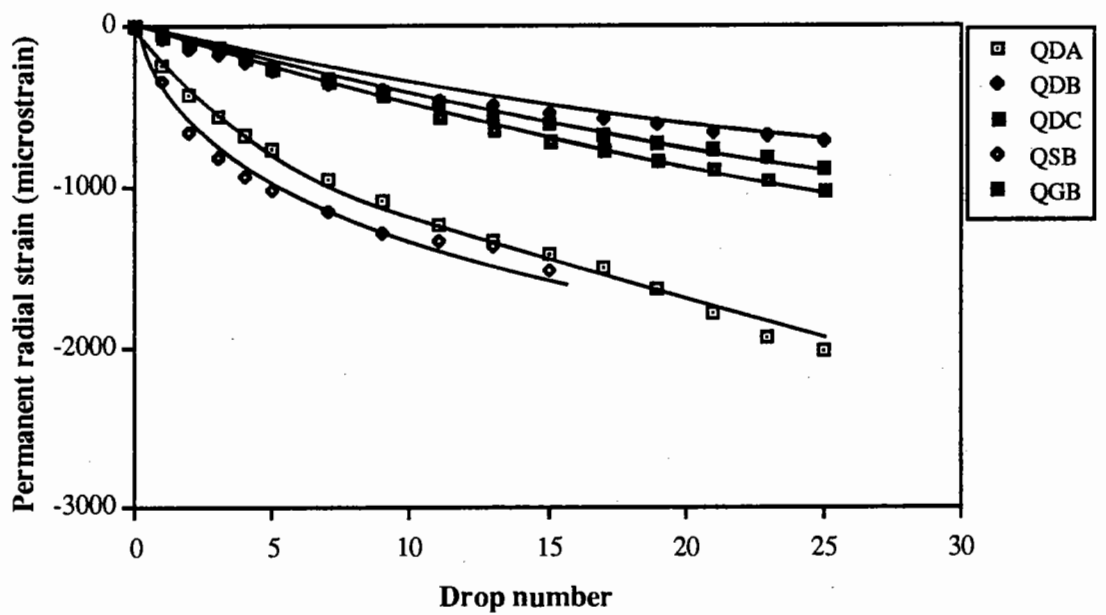
Figure 5.36b Permanent radial strain in drop hammer test

coarse (QDA) gradings were away from the optimum. The middle grading (QDB) gave the highest resistance to permanent deformation. In fact, the optimum may be related to the solid contents of the tested samples. Solid content is defined as:

$$\text{solid content} = \frac{\text{oven-dry density of the sample } (kg/m^3)}{\text{specific gravity of particle X 1000 } (kg/m^3)} \text{ X } 100\% \quad (5.4)$$

Figure 5.37 shows graphs of the plastic strains generated from the three dolomitic limestones plotted against the solid content. These limited results indicate that materials of low solid contents (or of high void ratio) produce more permanent strains. QDB had the highest solid content, and gave minimum plastic strains. The importance of producing high density materials, by appropriate choice of particle size distribution, to reduce the formation of plastic strains is highlighted.

Attempts were also made to study the relationship between the solid contents and the non-recoverable strains of materials from different sources but mixed to the same grading curves and compacted with the same compaction effort. For these, correlation between solid content and permanent deformation is not apparent. However, these results do provide a basis for observing the effects of physical properties of the constituent particles. (The particle properties have been studied by various preliminary tests in Chapter 4.) The dolomitic limestone, QDB, and the granodiorite, QGB, had similar physical properties (angularity and roundness), but the latter material possessed a higher solid content. As anticipated, QGB generated less axial deformation (Table 5.10) after 25 drops of the hammer although both samples developed the same amount of radial strain. The sand and gravel, QSB, possessed a low angularity value and a high roundness number. In spite of the fact that the solid content of QSB was higher than those of the crushed aggregate samples, the plastic strains created were about double those of the other two materials. Therefore, it appears that particle angularity is another major factor affecting the permanent deformation response of aggregates.

-Second test series -

Results of the second test series, as shown in Table 5.10, indicate that after 25 drops of the hammer, both the axial and radial plastic strains produced in the sand and gravel, LSN, were on average, ten times more than those for other samples in the same test series. Hence, LSN must be very susceptible to permanent deformation. In fact, there was a 10% drop in solid content of the same material type between the sample QSB in the 1st test series and LSN in the 2nd series. The effect of low particle angularity
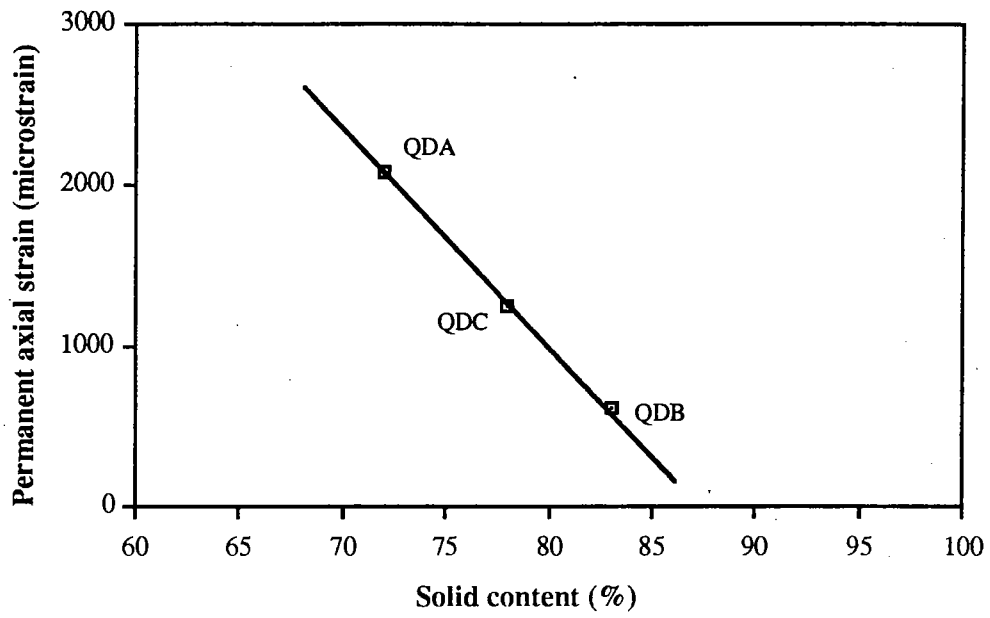
Figure 5.37a Effect of solid content on permanent axial strain
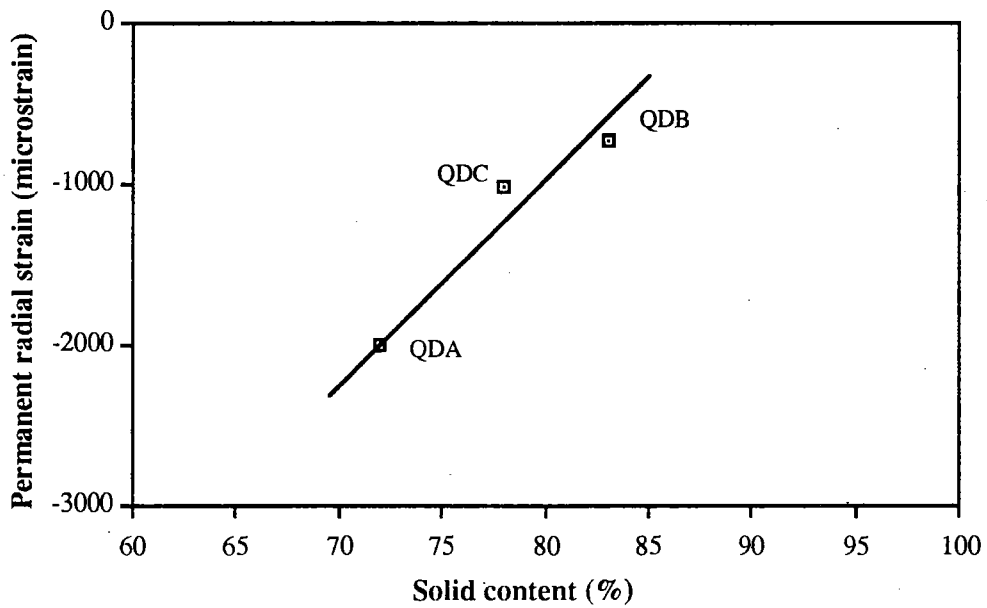
Figure 5.37b Effect of solid content on permanent radial strain

coupled with low solid content were demonstrated. When LDN1 and LDN2 were compared, the sample with the higher solid content again generated less plastic strain. Although the furnace bottom ash sample, LAN, which consisted of the weakest particles, did produce similar axial strains when compared with the results from the crushed rock samples, this was not the case with regard to radial strain. In fact, the radial permanent deformation of the furnace bottom ash was much higher than those of the crushed rocks. This might be due to the fact that the weak particles of LAN (Appendix E) were susceptible to breaking into smaller particles under loading and caused expansion in a highly compacted specimen. Hence, high radial measurements were obtained.

- Third test series -

The solid content effect was further confirmed in the third test series when results of BGN1 and BGN2 were compared. The sample which had been subjected to less compaction and had lower solid content produced higher plastic strain.

It is, however, interesting to note that the non-crushed sand and gravel sample, BSN, possessed the highest resistance to plastic strain under repeated loading. Since detailed particle studies have not been conducted for aggregates obtained from the Bothkennar site, the main cause of such a good resistance was not clear. Nevertheless, the solid content of BSN was the highest among the three samples in the third series. This might be one of the reasons for this observation. Furthermore, this result agrees with the findings of Earland and Pike (1985). They reported that some sands and gravels could be good materials for resisting permanent deformation under repeated trafficking.

5.6.3.3   Multistage triaxial testing

A typical plot of the multistage strength test using the Manually-Controlled Actuator is presented in Figure 5.38. As expected, strain recovery at the end of the first and the second stages is observed. In general, the rate of the vertical strain developed is quite constant at the beginning of each stage. The rate gradually increases when the peak strength value is approached. Finally, the specimen continues to deform after the peak value has been reached. Strengthening effects due to increasing of the confining pressure are also evident. The maximum axial load at each stage increases with the confining pressure.
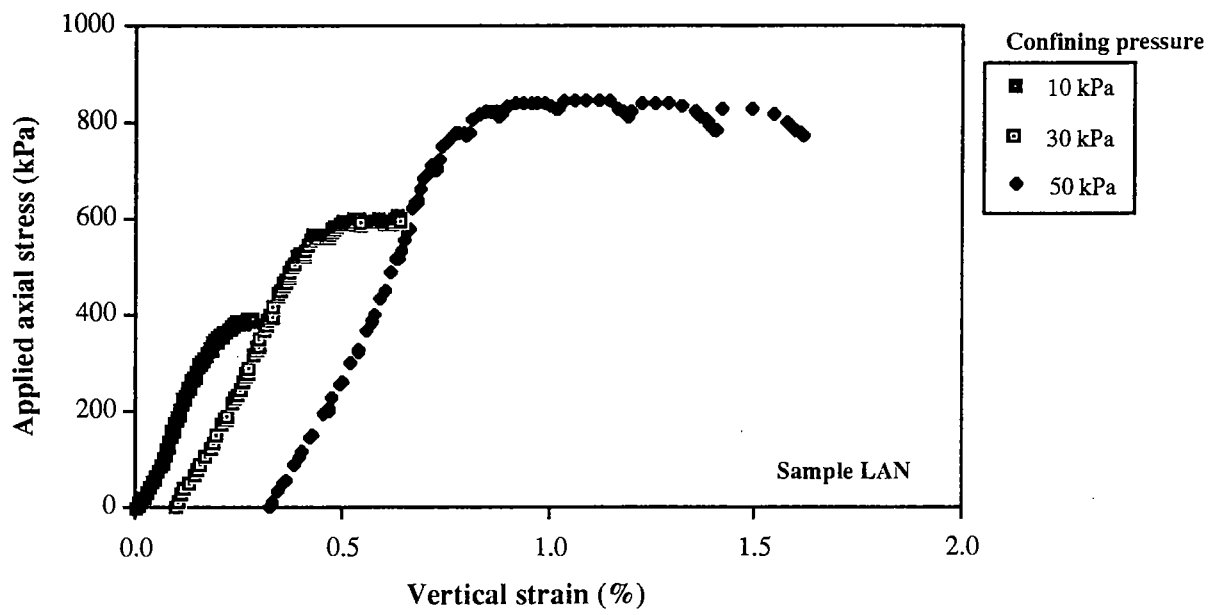
Figure 5.38 Typical results of the multistage triaxial testing

A summary of the multistage triaxial testing results is presented in Table 5.11. The corresponding apparent angles of shearing resistance, ϕ, and the values of τ intercept, c, are also included.

Table 5.11   Results of multistage strength tests

Material designation	Peak axial stress at confining pressure of			Apparent friction angle (ϕ)	τ intercept (c)
	10kPa	30kPa	50kPa		
	(kPa)	(kPa)	(kPa)	(degree)	(kPa)
QDA	471	621	726	46	86
QDB	1518	—	—	—	—
QDC	667	—	—	—	—
QGB	1550	—	—	—	—
QSB	481	825	1125	63	35
LDN1	406	558	745	51	53
LDN2	637	779	$1282_{(66)}$	62	54
LGN	439	648	1016	53	46
LSN	99	180	348	48	6
LAN	420	644	906	57	37
BGN1	382	425	500	32	93
BGN2	460	$790_{(40)}$	$1080_{(70)}$	56	53
BSN	625	$750_{(20)}$	---	61	57

Note:- Letters in the subscript bracket indicate the specific confining pressures used in that particular stage when this differs from the column heading.

ϕ and c

Figure 5.39 shows the multistage triaxial testing results in p-q plots for the three series of tests. Since a few specimens were required to establish the technique for carrying out multistage testing successfully, most samples in the first test series finished the first stage of the strength test only. In these p-q plots it is noticed that straight lines can be used to join the results of different stages together for all samples.
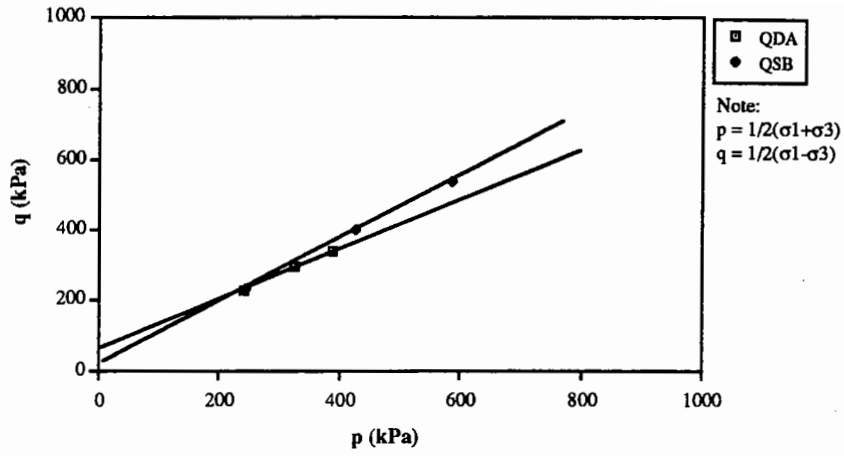
Figure 5.39a p-q plot for materials from quarry
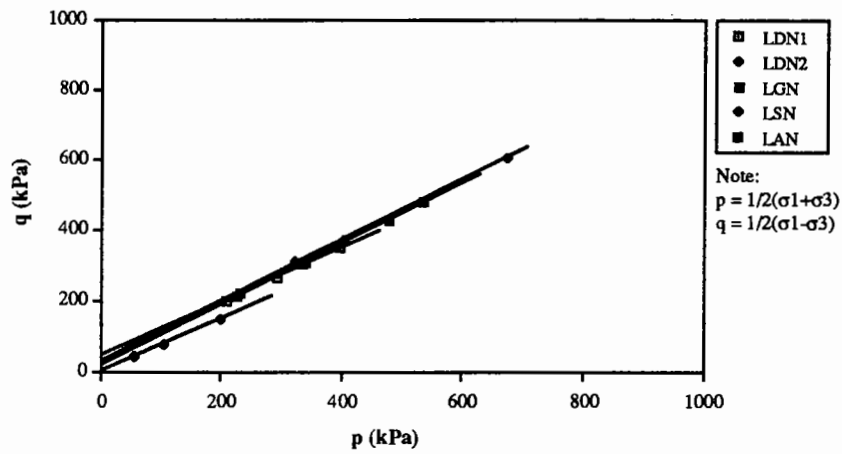
Figure 5.39b p-q plot for materials from the Loughborough trial
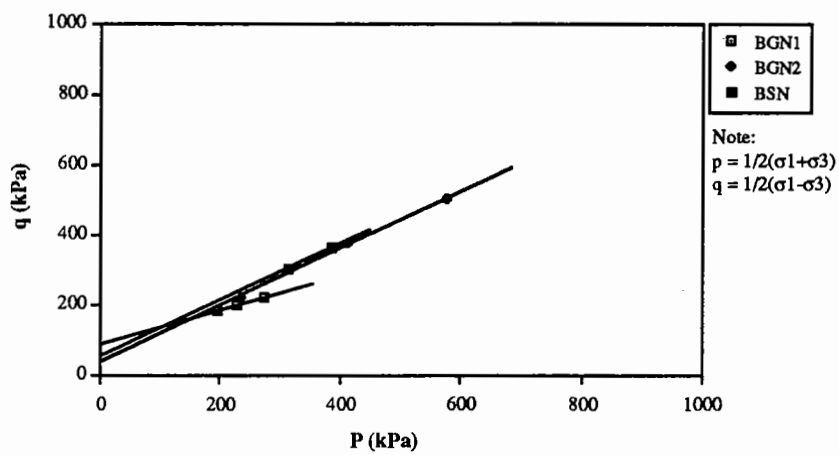
Figure 5.39c p-q plot of materials from the Bothkennar trial

The τ intercepts, c, which are known as the apparent cohesion in traditional soil mechanics, obtained for the aggregate samples were between 6 and 93 kPa (Table 5.11) with most of the results at about 50 kPa. For cohesionless materials, the τ intercept value should be equal to zero. It may not be true for heavily compacted granular materials or moist samples since compaction may generate locked-in stresses, the packing arrangement of stones may provide further stability and inter-particle moisture creates negative pore pressures which hold particles together. Thom (1988) observed that the unconfined compressive strength (with membrane on) of dry granular materials could be as high as 30 kPa. He also compared results from testing both dry and moist samples of identical materials. He concluded that pore suction in moist samples could increase the compressive strength by another 25 kPa. Hence, the combined effect of the locked-in stresses due to compaction, the particle interlocking and the pore suction may cause an apparent cohesion of as much as 55 kPa. In general, the results in Table 5.11 support Thom's observations.

A particle angularity effect on the value of the τ intercept is apparent. Generally, higher τ intercept values were found in the crushed rock samples, which were of particles with high angularity values (refer to preliminary test results in Chapter 4). The values were between 46 and 93 kPa while the range was between 6 and 57 kPa for the sand and gravel samples, QSB, LSN and BSN. Due to the limited available results, relationships between the τ intercept value and other surface characteristics of particles have not been established.

On the other hand, particle angularity might have no influence on the apparent friction angle of aggregates. The results in Table 5.11 show that the ϕ values for the crushed rock aggregates and for the sands and gravels were of similar ranges. For the crushed rock aggregates the ϕ values varied from 32° to 62° while for the sands and gravels, they were between 48° to 63°.

When comparing samples made of the same materials but with different solid contents, it is evident that apparent friction angles increase with increasing solid contents. The solid content of LDN2 was 4% higher than that of LDN1, a corresponding 22% rise in ϕ value was observed (Table 5.11). A greater increase of ϕ value was found in BGN2, which had a solid content about 10% higher than that of BGN1. Figure 5.40 presents a graph showing the relationship between the friction angle and the solid content. The result for the furnace bottom ash has not been included because of the porous nature of its particles, which give a very low solid content even though it had been heavily
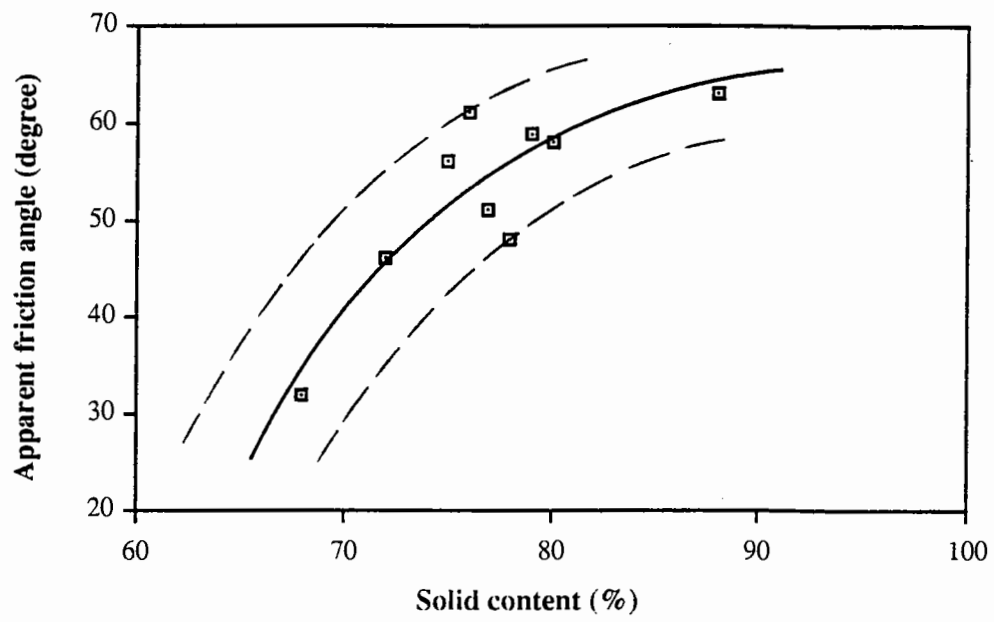
Figure 5.40 Relationship between solid content and apparent friction angle

compacted. A curved line is used to represent the data points. Due to the great difference between the nature of the tested samples, as expected, a scattering of results can be seen. However, a trend can still be seen. At low solid contents the increment of friction angle value with increasing solid content is large. The increment gradually reduces at higher levels of solid content. Finally, when the solid content of aggregate is at about 90%, there is very little increase in the ϕ value.

Effect of c on permanent deformation

In order to study the inter-relationship between permanent deformation under repeated loads and material strength, the vertical and the horizontal plastic strains generated by the drop hammer test at a confining pressure of 10 kPa are plotted against material strength parameters (c and ϕ) obtained in the multistage triaxial test in Figures 5.41 and 5.42. Figure 5.41 shows graphs of the shear intercept value, c. No simple correlation could be found between the c value and the plastic strain generated under repeated loading. However, it was noted that LSN, which possessed an extremely low c value, produced exceptionally high plastic strains estimated at more than 10 times the average values for the rest of the samples in both the axial and radial directions. It is, therefore, likely that a critical c value, below which excessive permanent deformation will develop, may exist. Since the performance of aggregates is stress dependent, it is in the author's opinion that the critical c value should vary with the magnitude of the deviator stress of the repeated loads and more work will be needed to define the critical c value. Nevertheless, the results have demonstrated that aggregates of very low c value are poor in providing resistance to permanent deformation at the low confining stresses required by pavement foundations.

Effect of ϕ on permanent deformation

Figure 5.42a plots the axial plastic strains formed after performing the standard drop hammer test against the apparent friction angle. A general trend, indicating that there is a direct non-linear relationship between the plastic axial strains generated under repeated loading and the ϕ values of aggregates, can be obtained. The result of LSN was not included in the figure because it was believed that the effect of the extremely low c value of LSN would overshadow the plastic strain to friction angle relationship. A similar plot showing the effect of the apparent friction angle on the plastic radial strain of aggregates is presented in Figure 5.42b. It was noticed that very high radial strain was obtained from LAN, constituted of very weak particles (Appendix E) although the

97
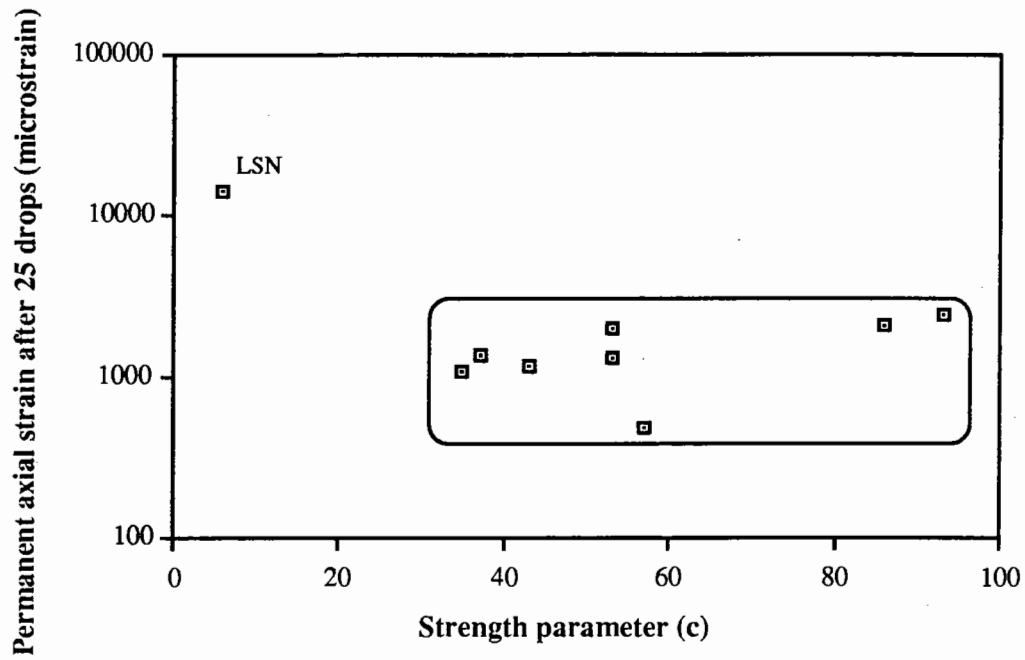
Figure 5.41a Plotting of permanent axial strain results of drop hammer test against strength parameter (c)
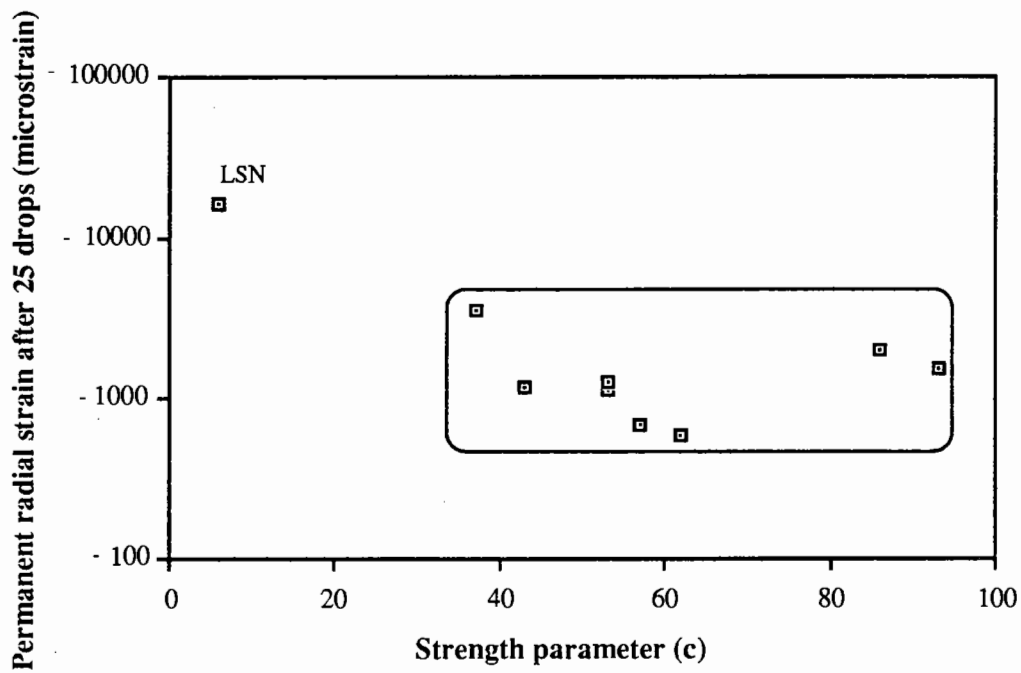
Figure 5.41b Plotting of permanent radial strain results of drop hammer test against strength parameter (c)
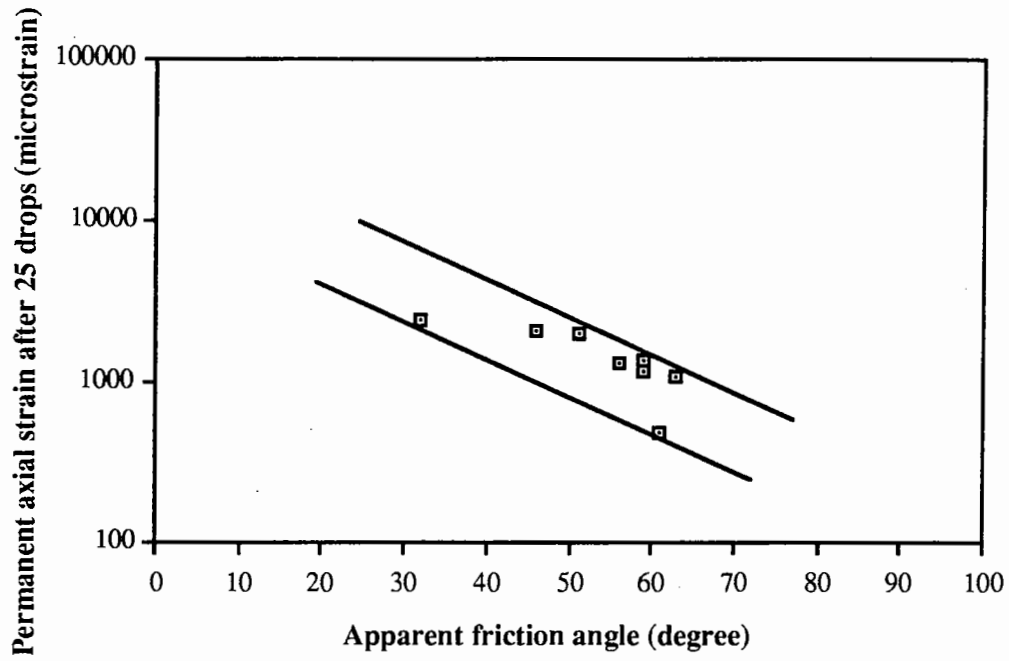
Figure 5.42a Plotting of permanent axial strain results of drop hammer test against apparent friction angle
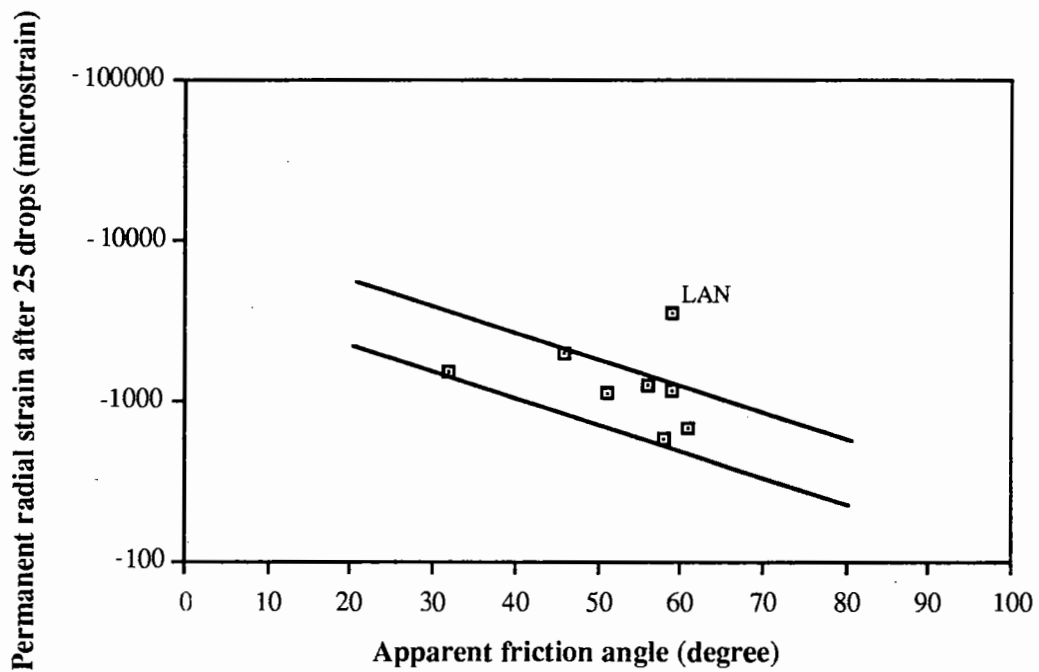
Figure 5.42b Plotting of permanent radial strain of drop hammer test against apparent friction angle

ϕ value of the aggregate could be considered as high. As mentioned in Section 5.6.3.2, expansion due to breaking of weak particles into smaller ones might be the cause of the extremely high plastic radial measurement. If the result of LAN can be excluded, then a similar trend to that of the axial plastic strain as shown in Figure 5.42a can be seen. Therefore, the permanent deformation resistance of aggregates generally increases with increasing friction angle. As a result, aggregates with the highest possible apparent friction angle should be used in road foundations to provide better resistance to permanent deformation under repeated trafficking.

5.6.4   Comparison with results from the large shear box text

Some of the sample types (the first series in Table 5.1) tested in the newly developed 280TA have also been tested by the large shear box (Section 4.4). Results from both devices may be compared. Since the testing condition, the compaction method and the moisture content used in the two tests were different, only general comparison was allowed.

It was noticed that both devices, in general, ranked materials of different strengths in a similar way. For materials with identical particle grading and the same compaction effort within their own series (two minute compaction in the shear box and compacted to refusal densities for the triaxial samples), both tests found that at low confining pressure, samples made of sands and gravels (SB2 (Table 4.7) in the shear box test and QSB (Table 5.11) in the triaxial test) possessed low strength. Conversely, samples of crushed stones gave high strength values.

However, the large shear box test generally ranked the samples in accordance with the size of the constituent aggregates. For samples of the same material type and compaction effort, but of different grading envelopes, the one with the highest amount of fine particles possessed the lowest strength and vice versa. The effect of particle size on the test results did not appear in the strength tests performed by the 280TA. QDA, the sample with a high percentile of large particles, but with a low density and a high void ratio, and QDC, the sample with a high fines content, were found to be of low strength. The highest strength was obtained from QDB, which was of DoT Type 1 grading envelope and the highest compacted density.

Figure 5.43 shows the range of the results obtained from the multistage triaxial test and the shear box test in the current study. Results of Pike (1973) for DoT Type 1 sub-base grading materials from using a 300 mm square box are also included for comparison. Since the axial normal stress used in the current shear box tests was small, 10 kPa, the results obtained were at the lower end of Pike's. However, it is clear that results from the shear box tests from Pike gave extremely high apparent angles of shearing resistance, ϕ, which were between 60° and 85°. It has been noticed that (Section 4.4.4.2) shear strengths measured by the shear box increase with the particle size of the tested aggregates. The insufficiency of the apparatus to particle size ratio of the 300 mm shear box for testing pavement foundation materials has been highlighted. Therefore, the results from the triaxial test should give a more realistic description of the material strength of aggregates used in road sub-bases.

Comparison between permanent deformation results from the drop hammer test (Table 5.10) on triaxial samples and those from the repeated horizontal loading (Figure 4.13) in the shear box test has also been made. Based on the material types and gradings, four sets of results were identified for comparison. They were results for GB2, DB2, SB2 and DC2 from the shear box test and results for QGB, QDB, QSB and QDC from the triaxial test. Figure 5.44 shows the comparison. Identical ranking was obtained by the two methods. Samples of the material with the finest particle grading (DC2 and QDC) exhibited the least resistant to permanent deformation. They were followed by SB2 and QSB, samples consisting of sands and gravels of round particles. As expected, materials made of crushed rocks and with the DoT Type 1 grading envelope had the highest resistant to permanent deformation.

Attempts had been made to compare stiffness results from the shear box test and the repeated load triaxial test as well. It was realized that such comparison might not be meaningful since the resilient behaviour of granular materials are very much stress dependent. Comparison of material stiffness should be made under similar stress condition. Furthermore, the horizontal stress induced by the vertical normal stress in the shear box test was uncertain. Estimation of the horizontal stress, such as by using elastic theory, will lead to great error and inaccurate interpretation of the results.
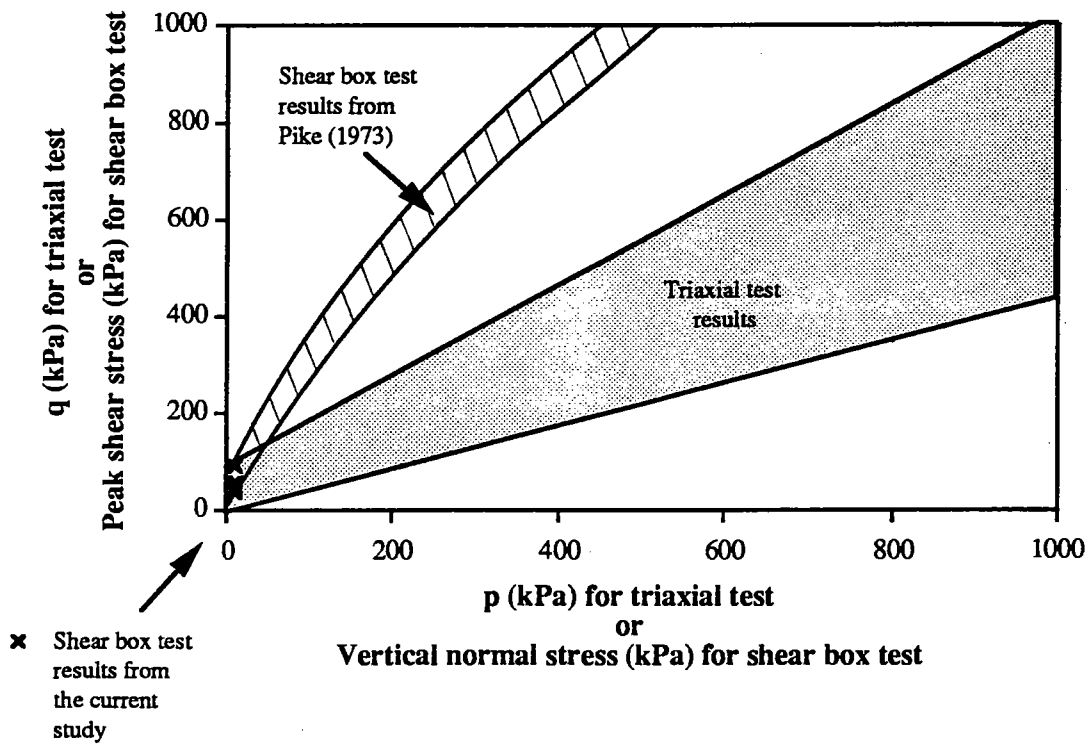
Figure 5.43 A summary of results from the multistage triaxial test and from the large shear box test
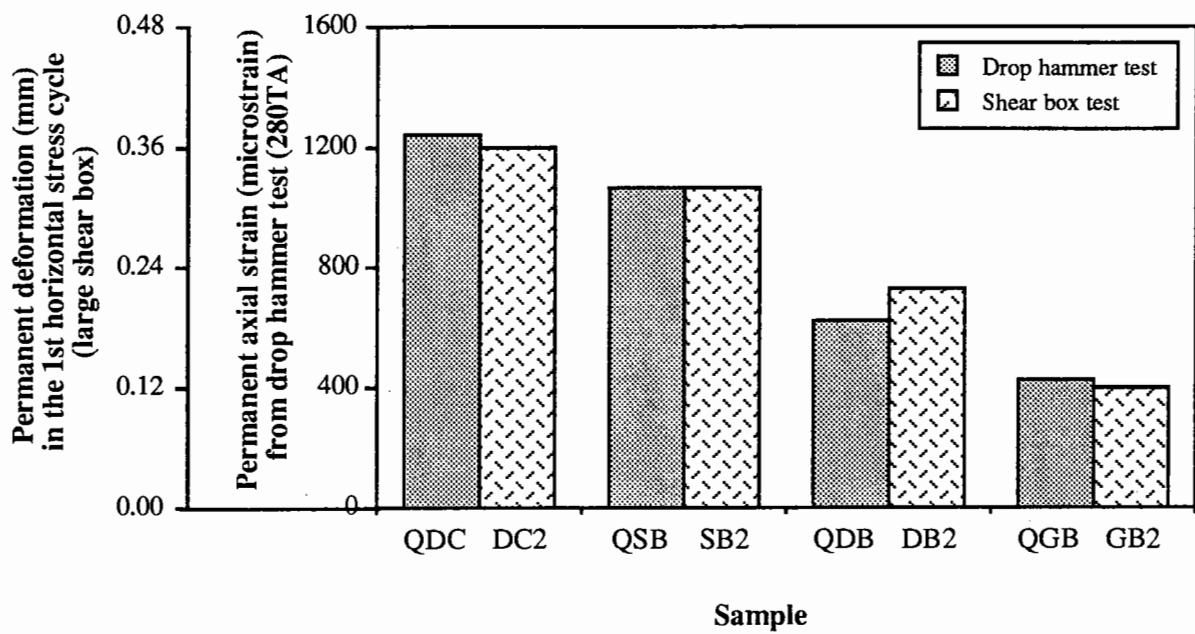
Figure 5.44 Comparison of permanent deformations measured by the drop hammer test in the 280TA and by the 1st horizontal stress cycle in the large shear box

5.6.5 Summary

Apparatus

(1) Comparable results were obtained from the glue-on and the key-in on-sample instrumentation methods for measuring the axial strain of the specimen under repeated loads. Results from examining the free and fixed systems for supporting the horizontal LVDT's showed that both systems produced similar horizontal displacement measurements.

(2) The compaction method used in this study was able to produce densities of unbound granular materials similar to those on site and to those produced in the B.S. 5835 compatibility test for the DoT Type 1 graded aggregates.

(3) A specimen to particle size ratio of 7 was found to be sufficient to avoid the particle size effect for repeated load triaxial testing.

(4) A routine testing procedure which had the ability to describe the resilient strain behaviour, the permanent deformation susceptibility and the strength of unbound granular materials by using simple loading methods was developed.

(5) Resilient strains produced by using a Manually-Control Actuator were found to be only slightly higher than those from a sophisticated servo-hydraulic actuator.

(6) No apparent difference in resilient strain results was observed whether the confining pressure was applied by the partial vacuum method or by the external pressurized air technique.

(7) A certain length of time to reach internal equilibrium was found necessary when the confining pressure was provided by the partial vacuum method. A period of half an hour should be enough for materials of DoT Type 1 grading.

(8) The use of the partial vacuum method generally decreased the material moisture content during testing although the drop was small. For materials compacted at the optimum moisture content, a drop of 0.3 % to 1.1 % moisture content was observed.

(9)   Comparison between the results obtained from the new repeated load apparatus tests and the large shear box tests indicated that the latter method had serious drawbacks. The shear box test gives unrealistic shear strength parameters and it is not able to provide sufficient data for describing the resilient behaviour of granular materials.

Material behaviour

(1)   Compaction results on wet samples confirm that the shape of aggregates is a crucial element controlling the material density. There is also a relationship between the density and the uniformity coefficient of materials.

(2)   In general, load pulses of different shapes of waveform can be expected to produce similar resilient strains. However, a waveform such as a square wave, which consists of a sudden increase and decrease of loading, will generate more resilient strains.

(3)   The effect of loading frequency on resilient behaviour appeared to be small and material dependent.

(4)   Both the shape of stress waveforms and the load pulse frequency were found to have a significant effect on the permanent deformation development under repeated loads and could not be ignored.

(5)   Under constant static vertical loads, both recoverable and non-recoverable creep can be developed.

(6)   Decreasing resilient shear strains were found with increasing surface friction of aggregate particles.

(7)   However, besides surface friction, it appeared that very weak particles (i.e. porous aggregates) had a significant effect on the formation of resilient shear strains under repeated loading. Otherwise, the bottom furnace ash which possessed the highest surface friction should have produced the least amount of shear strains.

101

(8)   Materials consisting of rounded particles appeared to be more susceptible to resilient dilation.

(9)   Excessive resilient shear and volumetric strain responses were observed in aggregates containing a high fines content.

(10)   Resilient shear strains obtained from samples of the same material but different densities showed that a lower density sample produced more strain. This contradicts the observation made on another material in the preliminary study in which no significant difference in stiffness was found in samples of varying compacted densities. Thus it appears that the effect of density on resilient stiffness is material dependent.

(11)   Asymmetrical pavement deflection due to the difference between the loading and unloading effects of a moving wheel was highlighted.

(12)   In general, for aggregates of the same grading, the one with particles of lower angularity and of higher roundness are expected to give higher plastic strains under repeated loading and to give a lower compressive strength.

(13)   High solid content (or low air void) is an important factor in reducing the formation of plastic strains due to repeated loading and in increasing the apparent friction angle, ϕ, and hence the strength, of the granular material.

(14)   Aggregates with a high roundness value are likely to give lower shear intercept values and vice versa. Furthermore, aggregates of very low c value are susceptible to permanent deformation under repeated loads at low confining stress.

(15)   In general, the permanent deformation resistance of aggregates increases with increasing ϕ value.

PART C

ASSESSMENT TESTS FOR SOILS

CHAPTER 6

DEVELOPMENT OF A REPEATED LOAD TRIAXIAL
APPARATUS FOR COHESIVE SOILS (100TA)

6.1 INTRODUCTION

The development of a new repeated load triaxial apparatus to test cohesive soils in pavement foundations, together with the specimen preparation procedures, is described in this Chapter. The design of the apparatus was based on the requirements for soil characterization as described in Section 2.6.3.

The repeated load triaxial apparatus for soil testing in Nottingham was first developed by Lashine (1971), and modified by Parr (1972), Hyde (1974), Austin (1979), Overy (1982) and Loach (1987). A servo-controlled hydraulic system was used. It is able to provide accurately controlled cyclic axial and cell pressures to a 75 mm diameter specimen. Although this piece of apparatus is very versatile, it is too sophisticated and expensive to be used in routine engineering laboratories. For this reason, a new simplified version of repeated load triaxial apparatus was developed in order to obtain the relevant soil parameters for the analytical design of road foundations. Plate 6.1 shows the equipment arrangement.

In essence, the equipment consists of four units:-

(1)   A self-contained loading frame with a removable triaxial cell.
(2)   An "on-sample" instrumentation system for measuring specimen displacements.
(3)   A pneumatic loading system to provide axial loads and confining stresses.
(4)   A computerized control and data acquisition system.

In developing the new apparatus, a particular effort was made to use:

(a)   A conventional triaxial cell size (which is normally of 170 mm internal diameter) suitable for a 100 mm diameter specimen, so that the design can be directly adapted for a commercially available apparatus with minimum cost.
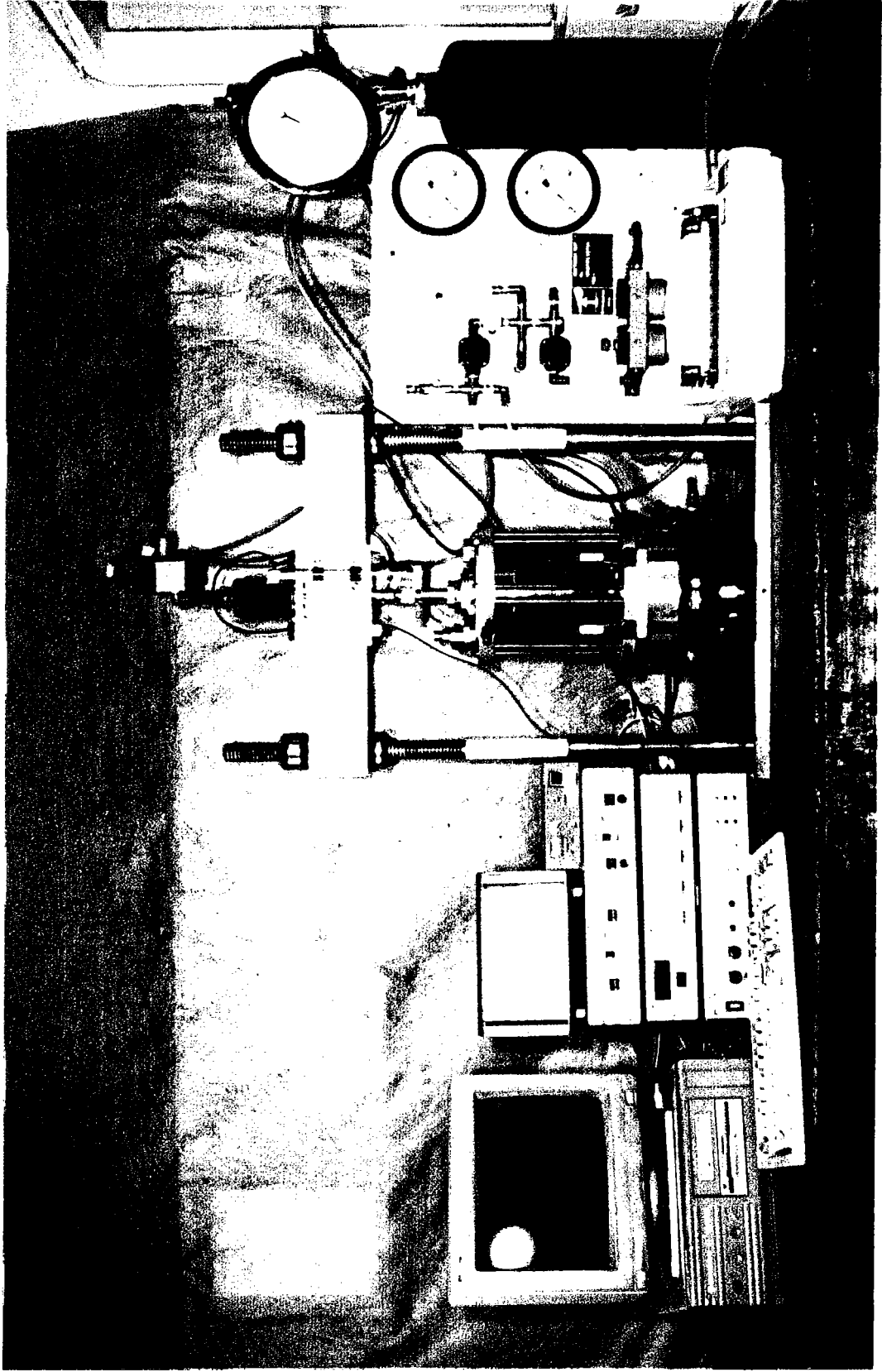
Plate 6.1 General arrangement of the repeated load triaxial apparatus (100TA) for soils

(b)   Conventional 100 mm diameter soil samples allowing them to be sourced from normal "U100" samples, and prepared using typical sample preparation methods.

This led to the development of "on-sample" instrumentation (to measure axial and radial strains) that was able to fit into the limited space between the cell wall and the specimen.

The adoption of compressed air as the loading medium has eliminated the need for heavy machinery (such as a large hydraulic actuator and a big pump). It should be possible for the apparatus to be easily installed in any commercial soil laboratory, including site laboratories. This apparatus is referred to as the 100TA in this thesis.

6.2   SIZE OF SPECIMEN

Static triaxial testing of cohesive soils is traditionally carried out on a 37.5 mm diameter by 75 mm high specimen or a 100 mm by 200 mm specimen. The vertical displacement due to the applied load is measured outside the triaxial cell. The radial strain of the specimen is estimated from the volume change of the confining fluid when water or oil is used to provide the cell pressure. However, it has been well documented by Bishop and Henkel (1962) that friction between the end platens and the specimen induces inhomogeneous strain and stress conditions, especially at both ends of the specimen. A comparison between the movement at the end platen and the displacement directly measured on a tested specimen by Moore et al (1970) indicated that the former method could overestimate the actual axial strain by 100%. Symes and Burland (1984) recommended the use of an on-sample measurement method to avoid the undesirable end effects of load platens. Since accurate measurement of the small axial and radial strains under repeated loads is the essential element for describing soil behaviour in road foundations, the traditional measuring method was considered inappropriate. Thus on-sample strain measurement method was chosen.

To ensure the provision of enough gauge length for the on-sample instrumentation, the height of soil specimen currently used in the existing repeated load triaxial apparatus in Nottingham is 150 mm and the diameter is 75 mm. Good quality results were recorded by Loach (1987). However, this size of specimen may not be a convenient dimension for routine purposes. Normally, for undisturbed samples, a "U100" sampler (100 mm

diameter) is used. Hence, the final specimen diameter chosen for the new apparatus was based on this 100 mm standard to take account of the practical aspect. As recommended in Section 3.2, a ratio of height to diameter of 2 was used. Taking into consideration the dimension tolerance of the U100 tube, the exact size of the soil specimen for the 100TA is 103 mm diameter by 206 mm high. Slight variations can be accommodated and a 100 mm diameter sample can also be accepted. A facility has also been incorporated into the design to allow 150 x 75 mm samples to be tested so that direct comparison of testing results can be made between the new device and the existing repeated load triaxial apparatus.

6.3 LOADING SYSTEM

The arrangement of the loading frame and the triaxial cell can be seen in Plate 6.1. The loading frame consists of a crossbeam made of a rectangular hollow steel section, two steel columns and a steel base plate. The columns are threaded, thus the crossbeam can be lowered or raised to the required height by turning the adjustable locknuts on the columns. The base plate has a groove in it, cut from the edge to the centre. The sample may be set up in front of the loading frame and the cell is placed over it. The groove then allows the whole of the triaxial cell, with the specimen set up inside, to be slid into the loading position without causing sample disturbance due to transporting.

Axial repeated load is provided by directly connecting the piston rod of an air cylinder to the load ram which rests on the top platen of the specimen. The load platen, with a central cone recess to receive the end of the load ram, is made of aluminium to reduce the dead weight acting on the specimen. Figure 6.1 illustrates the schematic diagram of the pneumatic system. A single air pressure source is used. A filter is fitted at the inlet to remove dirt from the supply and a lubricator is provided to condition the air. After air conditioning, the main line is subdivided into two streams:- one for the confining stress, and the other for the axial load. To prevent interference between the two streams within the system, an air reservoir is installed upstream of the axial load regulator. The apparatus is protected by pressure limiters and 'pop'-valves to prevent over-pressurization of any part of the system. If the supply pressure exceeds the pre-set values, the air valves will be activated and excess pressurized air will be released through them. A computer commanded electro-pneumatic regulator is used to regulate air pressures into the load actuator to which it is closely fitted (to avoid line losses). Maximum air pressures, beneath the upper limit of 700 kPa, to the inlet of the electro-
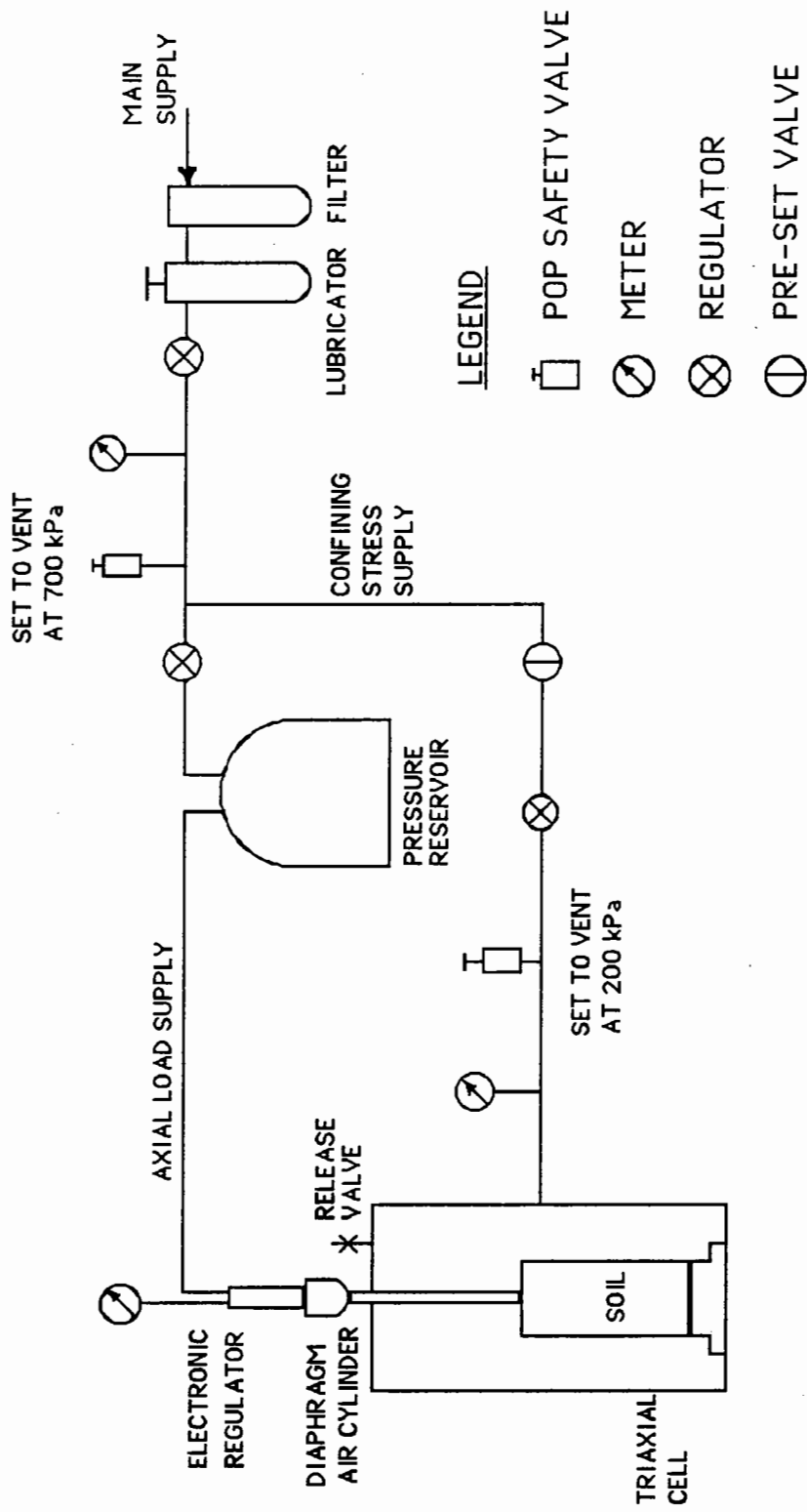
Figure 6.1 Pneumatic system of the repeated load triaxial apparatus for cohesive soils

pneumatic regulator can be preset by a manual regulator. The load actuator for the 100TA, which converts air pressure to axial load, is a diaphragm air cylinder with an effective loading area of 2580 mm^2. For the present arrangements an axial load up to 200 kPa on a 103 mm diameter sample is possible.

Stress analysis, with the finite element program FENLAP (Almeida 1991), has been made in Section 5.5.1.1. For the top of the subgrade of a typical flexible pavement, the analysis suggested that little variation in horizontal stress would be expected in the soil layer due to in-service trafficking. Although the variation can be higher during the construction stage, the application of constant confining stress was considered to be an appropriate compromise between realism and test complexity. Hence, it was deemed unnecessary to use an automated control system for the confining stress. The regulation of the confining stress for the tested specimens is made manually. A maximum cell pressure of 200 kPa is permitted in the current design.

To provide the physical boundary to maintain the confining stress and to support the tested specimen, the existing triaxial cell (originally designed by Austin (1979)), which is of the same internal diameter as that of the conventional cell for a 100 mm diameter specimen, is used. It comprises three main parts :-

(1)   A cell top made of aluminium,
(2)   A cell wall of 'Perspex' material, and
(3)   A base of epoxy resin.

'O' rings are fitted at both ends of the cell wall to ensure air-tightness between the wall and the top and base. It is anticipated that other similar size commercially available triaxial cells can be used with little modification.

Since the specimen diameter is 103 mm, but the existing (standard diameter) cell was designed for an instrumented specimen of diameter 75 mm and height 150 mm, the cell was modified to suit the new specimen. Plate 6.2 shows the modification to the cell base. An aluminium sleeve is added to enlarge the base for the larger specimen. The sleeve is held by an aluminium plate which, in turn, is fixed by three screws onto the epoxy resin base. To accommodate the extra height of the taller specimen, an aluminium ring of 50 mm high has been made to extend the existing cell wall. All the associated bolts which lock the cell wall to the base have been replaced by longer ones.

Plate 6.3 Frame to hold the proximity transducers (100TA)

Plate 6.2 Modification to the cell base (100TA)

The base is provided with sealed sockets into which the instrumentation cable can be connected. This allows the instrumentation to be separated from the cell wall.

6.4 SEALING SYSTEM

Latex membrane is commonly employed in triaxial testing to provide the enclosure for specimens when the confining fluid is water or oil. However, latex is susceptible to air penetration. The permeability of a 1 mm thick sheet at an air pressure difference of 1 kPa is 11.49×10^{-9} cm^3/s/cm^2. This is approximately equivalent to 10 cm^3 of air penetration per hour at a confining stress of 100 kPa for the 103 mm diameter specimen. Since the confining stress to the specimen is provided by pressurized air, membranes made of neoprene, which are impermeable to air, are chosen to eliminate air penetration. However, a dry neoprene membrane may absorb water from the soil specimen. Membranes are thus immersed in de-aired water for 24 hours before being used. The sealing system is completed by the usual method in which two pairs of rubber 'O' rings are used to seal up the ends of the membrane at the top and the bottom platens.

6.5 INSTRUMENTATION

A total of seven transducers are employed for the testing:

(1)   A pair of strain loops for measuring axial movement up to 2 mm (3% strain),

(2)   A pair of proximity transducers for horizontal movement up to 2 mm (4% strain),

(3)   A LVDT for vertical movement up to 50 mm (25% strain),

(4)   A pressure transducer for monitoring cell pressures (0-700 kPa), and

(5)   A load cell for axial stresses (0-1000 kPa).

Details and functions of all electronic devices for the repeated load triaxial apparatus for testing subgrade soils are described in Appendix K.

Axial strain

For measurement of axial strain it was considered that the "glue-on" technique to fix the "on-sample" instrumentation, as designed for the 280 mm diameter specimen (Section 3.5), might not be suitable for the 100 mm diameter soil specimen because relative

107

movement between the soil specimen and the soft rubber membrane could be expected (especially when the test was carried out at zero confining pressure). The current "key-in" fixing method (Loach 1987) used in the existing repeated load triaxial apparatus for soil testing to measure vertical displacements seemed to provide the solution to this problem. However, Loach's method required four LVDTs and was considered to be too complicated for routine testing.

To provide accurate, but simple "on-sample" measurement of small resilient and permanent axial deformations, free from the end effects of the platens, a new measuring device was designed. There were three major considerations in designing the on-sample instrument for measuring the vertical displacements:-

(a)   Weight of the device,

(b)   Measuring range,

(c)   Limited space between the specimen and the cell wall.

It is important to minimize the weight of the "on-sample" measuring unit to avoid creating undesirable local distortion of the specimen, especially when soft clays are tested. This could have been achieved by making the smallest possible device. However, usually the smaller the monitoring device, the smaller would be the measuring range. After taking into account these factors, two light-weight loops, each 12g, were made.

The device is detailed in Figure 6.2. Each loop consists of two locating studs, a pair of rubber bands and an open ended loop. The studs are made of aluminium, so that each of them is only 3g in weight and they are resistant to corrosion. The studs connect the loop to the specimen. At one end of the locating stud, a cross-headed pin provides an anchorage into the soil. At the other end, a square block with a sharp recess at the centre provides a precise fixing point to support the loop. Connection between the square block and the loop is achieved by providing a pin-tailed location screw which fits into the recess of the block. A rubber band is used to provide the fixation. Since the screw is adjustable, setting of an initial reading can be made after the loop has been installed. Once the initial setting is finished, the screw is locked in its final position with the loop by a nut to prevent relative movement during testing.

For the loop, 5 mm diameter hollow brass tube sections of length 46 mm are used at both ends in order to reduce the weight of the instrument. A 5 mm wide by 0.56 mm

thick phosphor bronze strip mounted with strain gauges forms the active centre part of the loop. The use of the thin phosphor bronze strip prevents the development of any significant spring force which may be induced by the loop to the specimen. A calculation has been made to find out the effect. A maximum of 25.6 gram-force, which can be considered as having minimum effect, was estimated. Detailed calculation can be found in Appendix L. The device records axial movements over the middle third of the specimen. Calibration has been carried out and results are detailed in Appendix M. The linear measurement range of the loop is 2 mm. This is equivalent to 3% over a gauge length of 68 mm. Because of electronic restrictions, the precision value for the present arrangement is limited to 28 microstrain.

The design allows the loop to be placed parallel to the specimen, therefore the device can easily be fitted into the limited space provided between the specimen and the wall of the triaxial cell. Two loops are needed for axial strain measurement. They are placed on two opposite sides across the diameter of the tested specimen.

Although the adjustable screws of the loop can allow re-setting to prevent over-ranging whenever necessary, the measuring range of the loops is not sufficient for triaxial compressive strength testing. The upper limit recommended by B.S. 1377 (1990) for testing soil strength is 20% axial strain. Hence, a second axial displacement measuring device is provided. It is a large LVDT clamped onto the load ram outside the triaxial cell. This transducer is able to provide a linear measurement of axial deformation up to a range of 50 mm, which is equivalent to 24% of the height of the specimen. The precision is limited to 53 microstrain (again an electronics rather than a sensor restriction) over a gauge length of 206 mm. Details of calibration can be found in Appendix M.

Radial strain

The non-contact position measurement method used by the existing repeated load triaxial apparatus for soil testing at Nottingham (Brown et al 1980) for recording the radial displacement of the specimen was considered an appropriate method for the new apparatus. For the new repeated load triaxial apparatus two proximity transducers (part no. 2UB) supplied by Kaman are used to monitor the radial strain of the soil specimen. The proximity transducers are placed at the mid-height of the specimen and at right angles to the strain loops across the diameter. The measuring device consists of three main parts:-

(1)   Conductive target,

(2)   Sensor, and

(3)   Signal conditioning unit.

When the target moves away from the specimen, it causes an impedance change in the coil of the sensor. The signal conditioning unit then converts this change to a voltage. The voltage is proportional to the displacement of the target. A holding frame, as shown in Plate 6.3, supports the proximity transducers, hence, the instrument exerts no force onto the tested specimen. The transducer selected is of a very thin body, only 6.3 mm in thickness, and with the core cable coming from the side of the sensor. It allows the transducer to be placed in the limited space between the specimen and the cell wall. Fixing details of the proximity transducer onto the supporting frame are shown in Figure 6.3. They comprise an external case and an adjustable component to allow the sensor to travel up to 10 mm. To prevent interference to the magnetic field in front of the sensor, the holding materials within the sensing zone of the transducer are made of non-metallic medium. The target of the transducer is an aluminium foil, of thickness 0.07 mm and 30 mm square. It is affixed to the surface of the specimen and enclosed between the membrane and the sample. The maximum measuring range of the proximity transducer is 2 mm, which is equivalent to 4% strain across the radius of the specimen, and the precision is 10 microstrain for a specimen of 103 mm diameter. More details of the calibration can be referred to Appendix M.

Pore pressure

In considering the provision of a pore pressure transducer to the specimen, previous work carried out at Nottingham was reviewed. A degeneration in response of the pressure transducer installed at the base of the soil specimen was reported by Overy (1982) when the frequency of cyclic loading was higher than 0.005 Hz. Loach (1988) planted pore pressure transduces in the base and the centre of specimens. He noticed that the centre probe was able to follow the change of pore pressure up to a cyclic loading frequency of 10 Hz. Nevertheless, different results were recorded by the two probes at high stress levels. He suggested that the difference might be due to the inhomogenity of stress and pore pressure distribution caused by the end restraint from the bottom platen. Therefore, it seems that the provision of a pore pressure transducer at the bottom of the specimen cannot provide accurate measurement of pore water pressure. On the other hand, it is unlikely that pore water pressure measurements at the centre of the specimen will be readily accepted by any routine laboratory because of the

ROTATABLE
COLLAR FOR
ADJUSTMENT

NON-METALLIC
BLOCK TO CARRY
TRANSDUCER
(IN 3 PARTS)

NOTE:-
MATERIAL IS BRASS EXCEPT WHERE NOTED

14 mm

FRAME

TRANSDUCER

SUPPORTING POST
7 mm DIAMETER

SECTION

PLASTIC GRUB
SCREW TO
CLAMP COLLAR

33 mm

38 mm

CABLE
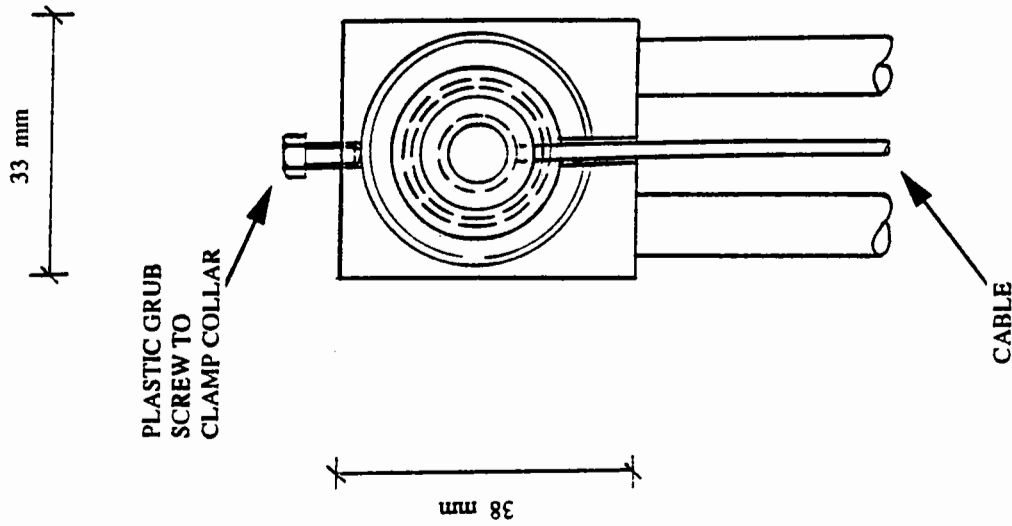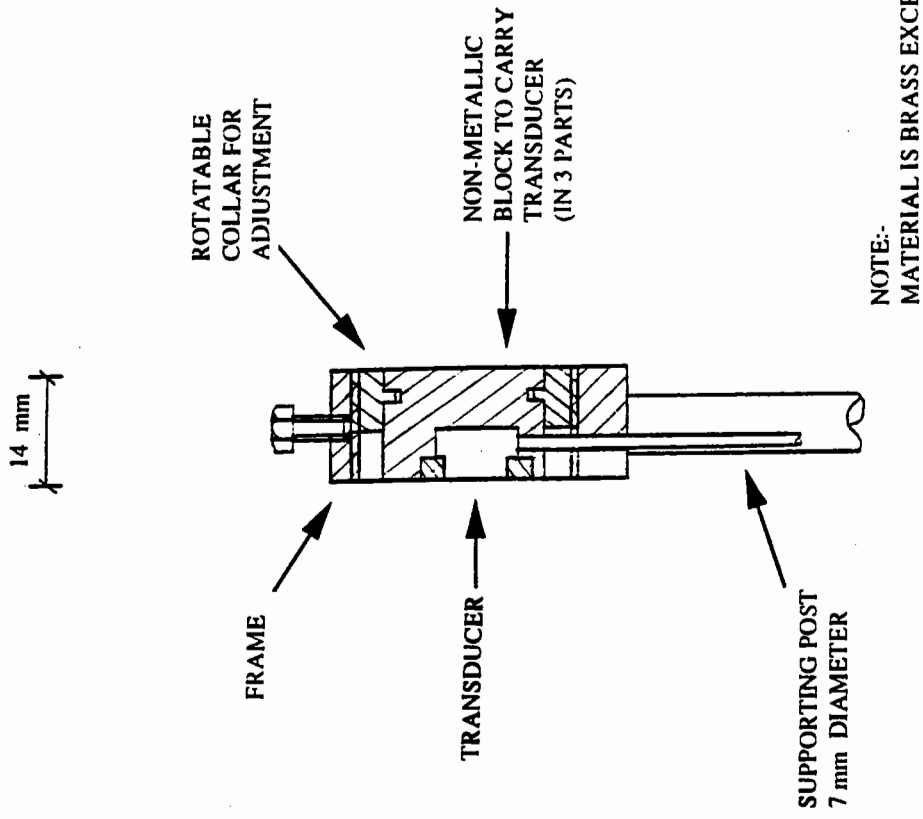
ELEVATION

Figure 6.3 Proximity transducer of the repeated load triaxial apparatus for cohesive soils

complexity of installation. From these considerations it was decided that the new repeated load triaxial apparatus would not be equipped with a pore water pressure measuring unit. This limits its ability to provide direct measurement of the pore water pressure but this is not expected to be an undue limitation especially in resilient testing which involves stress paths at low magnitudes. Furthermore, estimation of the pore water pressure of partially saturated soils can be made by making use of the soil suction test suggested by Croney (1977). Fuller details of the test can be found in Section 7.4.

Axial load

Axial load to the specimen is measured by the load cell originally designed by Austin (1979). It is able to provide measurement to 8 kN. The load cell is made of two pairs of strain gauges which are attached to the surface of the load ram at a point where its cross sectional area has been reduced. This measuring unit is situated inside the triaxial cell, thus ensuring that friction between the load ram and the top of the triaxial cell does not affect the measurement of applied loads. The precision of the load cell, as indicated in Appendix M, is 0.4 kPa for a 103 mm diameter sample.

Confining stress

Finally, the existing strain-gauged silicon transducer, type PDCR 10/F, made by Druck Limited, with a measuring range from 0 to 700 kPa is used to monitor the confining stress. Since the transducer is installed inside the triaxial cell, errors arising from attenuation in the piped system are eliminated. The precision of the cell pressure transducer is 0.4 kPa (Appendix M).

6.6 CONTROL AND DATA ACQUISITION SYSTEMS

Figure 6.4 shows the interrelationship between the electronic units which form the control and data acquisition systems.

The same 386 SX AT computer as described in Section 3.6 is used as a multi-purpose central unit to issue command signals, collect data and process results. Communication between the computer and other units, including all transducers and the electro-pneumatic regulator, is made possible by a CIO-AD16 Board which is capable of converting analogue to digital signals and vice versa for up to 16 channels. Electronic

111
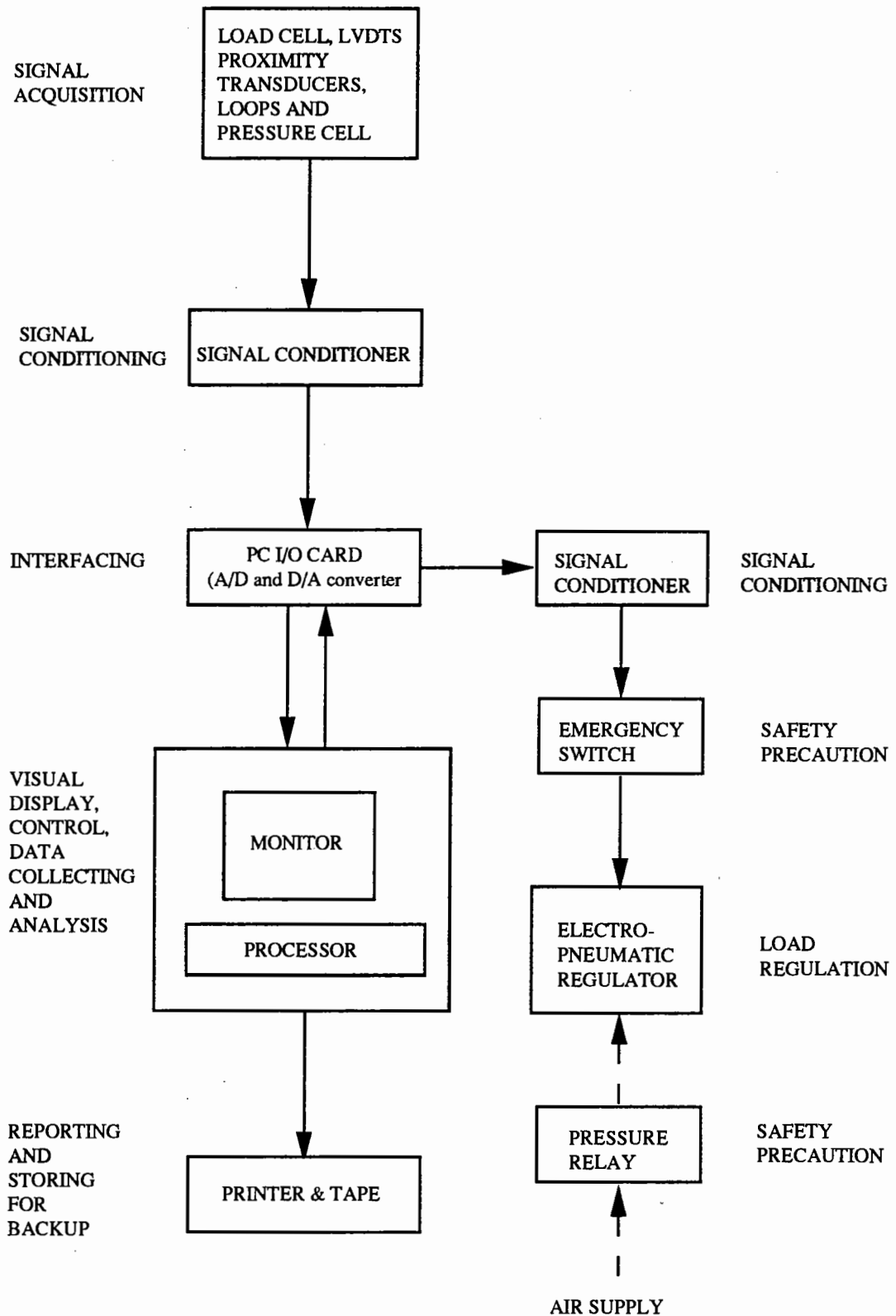
Figure 6.4 Electronics block diagram of the repeated load triaxial apparatus for cohesive soils

units from Peter Goss Associates provide the main signal conditioning for all signals except for those from the proximity transducers which possess their own integrated conditioning electronics. The hardware comprises:-

(1)   A five channel transducer signal conditioning unit and,

(2)   A command signal conditioning unit capable of handling eight control channels.

With the associated DCS (1990) system software, the system is able to generate signals to control the frequency and magnitude of the required load pulses. At the same time, electronic signals from all transducers and from the command channels can be viewed on the computer monitor and stored in the hard disk. The control software runs under the Microsoft Windows environment and is very 'user-friendly' (the software has been specifically written for the repeated load testing of pavement and geotechnical materials). To provide paper print-out of graphs and results, a dot-matrix printer is used. A tape is used to store back-up copies of test data.

It was found that the electro-pneumatic regulator, which supplied regulated pressure to the load actuator, was susceptible to failure if the device was energized before pressurization. To prevent damage, safety devices consisting of a pressure relay and a emergency stop have been installed. The pressure relay ensures that electrical power to the regulator will be connected only when the supply air pressure is on. The emergency stop will immediately terminate a test in progress without interrupting the data acquisition and result processing units by removing the regulator's energization.

6.7   SPECIMEN PREPARATION

6.7.1 Sample compaction

Soil excavation and filling are the principal processes in highway construction prior to pavement construction. In a fill section, soils are normally taken from a local source. These materials are laid and compacted in layers to a high density and receive moderately heavy compaction. Therefore, the soils are in a largely remoulded state. In the cut section of the highway, soils above the formation level are removed. The surface of the subgrade is then levelled. Further compaction by rollers is seldom required. Good practice requires that after the levelling of the formation, sub-base materials are immediately laid to protect the soils from deterioration. Although

relatively high stresses will be generated by the site traffic during the construction period, disturbance of the protected subgrade soils should be limited. Hence, the soils in the subgrade may remain relatively undisturbed.

On this basis it appears that undisturbed samples from cut sections do not need further treatment before carrying out repeated load triaxial testing. However, the unloading effect in the cut sections may cause significant immediate pore water pressure depression followed by subsequent long term pore pressure equalisation as water is sucked in from the adjacent water table. The unsaturated compacted soils in fill sections may also absorb water in the long term (depending on the depth of the water table). Thus for representing the subgrade soils in pavement foundations, there are at least four kinds of soil conditions:-

(1)   Fully remoulded,
(2)   Undisturbed (and, possibly, overconsolidated),
(3)   Remoulded and soaked,
(4)   Undisturbed and soaked.

Conditions (1) and (2) are of interest to pavement engineers immediately after compaction and excavation respectively. Cases (3) and (4) represent soil conditions after dissipation of any induced pressures or suctions. To permit these varieties of soil condition to be incorporated into routine soil assessment, a sample preparation mould was constructed for soil compaction and conditioning to produce specimens to the four possible soil conditions. The mould, as shown in Figure 6.5, can be divided into three sections. The first section is a connection piece between a 'U100' sample tube and the main body of the preparation mould. Through the connection piece, undisturbed soils in the sample tube can be directly extruded into the main body of the mould, which is a long aluminium cylinder. Once the soil is in the main body, the first section can be removed and replaced by the third piece - the base plate. On the inside surface of the main body, a layer of pervious plastic filter material is fitted. This filter can be connected to an external water source and it allows water to readily enter (or leave) the soil sample (thus simulating a real water flow regíme for subgrade soils). The third section is a metal collar fitted internally with a removable piston. Specified axial loads, simulating the overburden, may be applied to the piston when the sample is conditioning. For remoulded soils, the main body of the mould is fitted to the base plate at the start of compaction which then takes place in the mould.
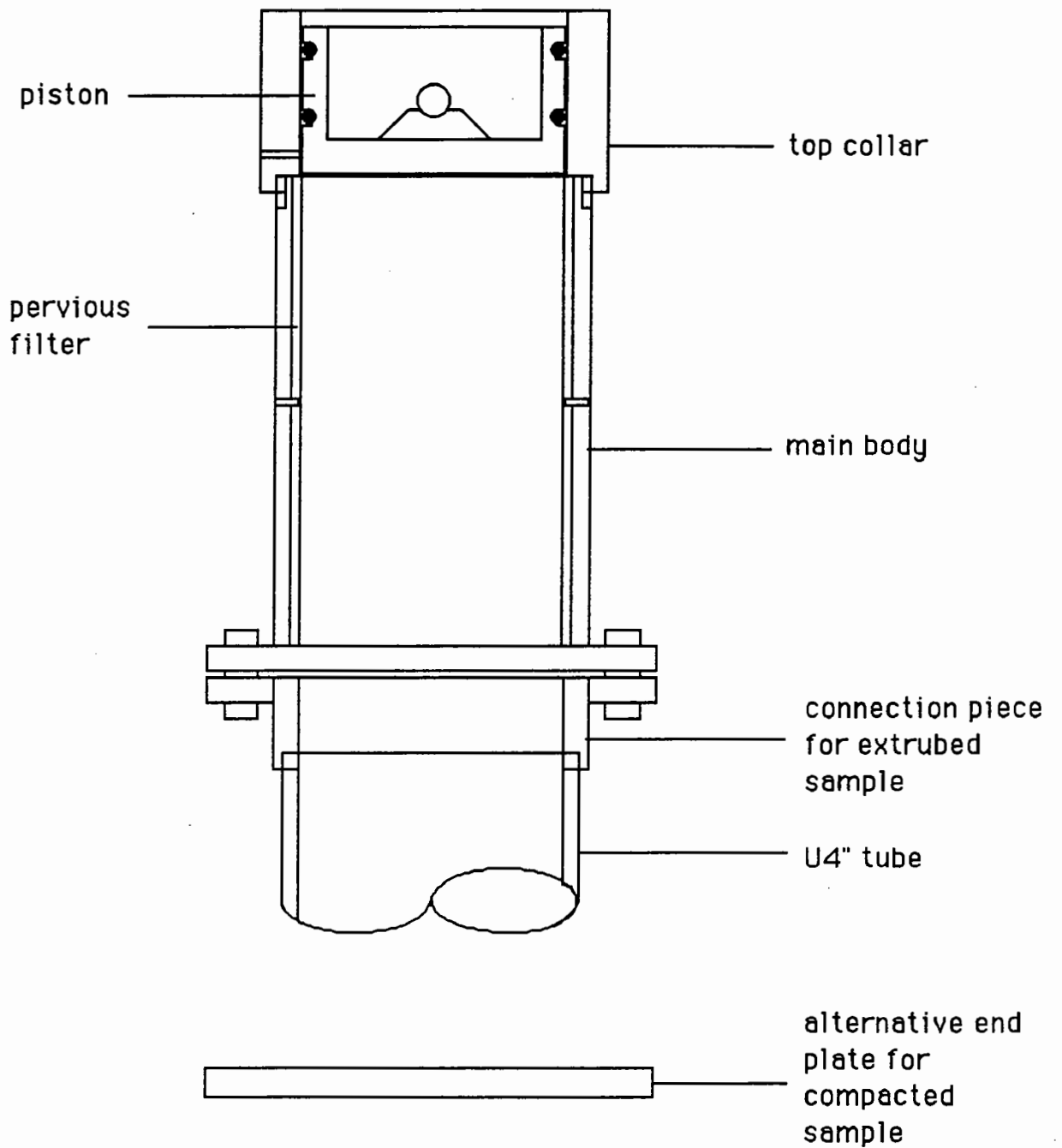
Figure 6.5 Soil preparation mould for repeated load triaxial testing

Despite the ability of the apparatus to permit pore-pressure equalisation, because of the time limit, it was decided to concentrate efforts on testing remoulded specimens without soaking.

Seed et al (1962) had shown that the method of sample compaction affects the resilient properties of a soil. They noticed that the resilient behaviour of soil specimens prepared to high degrees of saturation by kneading compaction in the laboratory was similar to the soil compacted to the same degree of saturation with rollers on site. Degrees of saturation above 85% were defined as high. In the U.K. , when remoulded clay soils are properly compacted, they normally possess high degrees of saturation. The kneading compaction method is, therefore, considered appropriate for preparing remoulded samples of clay for testing.

Compaction effort, similar to that required by B.S. 1377: Part 4 (1990), is used. Since the sample preparation mould has an internal height of 206 mm and a diameter of 103 mm, the specimen is compacted in five equal layers. For each layer 27 blows from a 2.5 kg rammer, dropped from a height of 300 mm, are applied.

6.7.2 Routine set-up procedure

For remoulded samples soils obtained from sites are left in metal trays to dry at room temperature. These air-dried materials are passed through a crushing machine so as to break them into small pieces. A mechanical grinder is then used to turn the soils into powder form. Lumps of soils bigger than 2 mm are removed by sieving and returned to the machine for further grinding. When a sufficient amount of soil for a specimen, usually 5 kg, is ready, the water content of the sample is increased to the required level by adding de-aired water into the soil powder. This process is carried out with a soil mixer. However, it is important to determine the residual water content of the soil powder before water is added to them. A residual water content as high as 5 % has been recorded. The sample is allowed to mix for 30 minutes. The mixed soil is then quickly transferred into air-tight containers and is ready for compaction. The compaction method as described in the previous section is used to produce remoulded samples.

Having finished the sample compaction, the specimen is extruded from the cylinder and trimmed to the exact length. Load spreaders which were made by cutting a tube, of an

internal diameter equivalent to the size of the soil sample, into three equal longitudinal sections have been found very useful for handling the soft specimen without causing damage to the sample. After the soil is transferred to the base of the triaxial cell, the exact locations of the fixing points on the specimen for the "on-sample" instrument are marked using a rig and a needle. They are shown in Plate 6.4. The main features are:

(a)   Two sets of diametrically opposite guide rods fixed between top and bottom rings, and

(b)   Two sliding blocks.

To make the marking, the blocks are allowed to slide to the pre-set height, the needle is then pushed through the hole at the centre of the block. When the marking procedure is finished, the vaned studs for supporting the strain loops are inserted by hand into the specimen at the marked locations.

The two pieces of aluminium foil, used as the target for the proximity sensors, are prepared. They are put at the mid-height of the specimen and are placed, in plan, 90 degrees away from the studs.

A standard membrane stretcher is used to place the neoprene membrane, which has been soaked in water for 24 hours, onto the specimen. When the membrane is on, the top platen is positioned. To seal the sample, two pairs of rubber O-rings are rolled into the grooves on the top and bottom platens.

A hot soldering iron is used to puncture the membrane over the studs. The blocks, which support the strain loops, are then screwed through the membrane into the studs and the loop hooks on (see Figure 6.2). Between the membrane and the block, a small "O" ring is used as a seal. To fix the loops onto the blocks, rubber bands are employed. Finally, the frame fitted with the two proximity transducers is bolted onto the base of the triaxial cell and this completes the routine specimen preparation and on-sample instrumentation. Plate 6.5 shows the specimen before the cell is installed. A minimum of 24 hours is allowed for pore pressure equilibrium before testing is started.

If a 150 mm high by 75 mm diameter sample is to be tested, provision of two 25 mm thick spacer blocks, one at the top and one at the bottom of the tested specimen respectively, is needed. Furthermore, a slight modification consisting of shifting the

external case, which holds the proximity transducer, 12.5 mm towards the centre of the cell, as shown in Plate 6.6, is required.

6.8   SUMMARY

(1)   A simple load frame and a modified triaxial cell, with the flexibility of being semi-portable, has been designed to provide the rigidity to withstand the required loads during soil testing.

(2)   Accurate measurement of the small axial movements under repeated loading is made using a pair of light-weight, highly sensitive strain loops across the middle-third height of the specimens. Although these loops look delicate, given reasonable care in handling, no replacement has yet been needed. For large axial displacements in triaxial static strength tests, off-sample measurement is provided. Radial movement is measured at mid-height of the specimen by a pair of proximity transducers which provide non-contact, high resolution output.

(3)   Special attention to "on-sample" instrument size has enabled a typical triaxial cell to be of sufficient size to contain these additional devices.

(4)   The equipment permits "on-sample" instrumentation to be installed on the apparatus, thus reducing the opportunity for sample disturbance.

(5)   The pneumatic system developed is able to apply axial load pulses or axial static stresses simultaneously with the application of a constant confining stress to soil specimens. Regulation of constant air pressures for confining stresses is controlled manually, while static axial loads or vertical load pulses are regulated by an automated computer-based control.

(6)   A computerised data acquisition system is incorporated into the equipment. It enhances automation of data acquisition and minimizes data processing errors.

(7)   To provide a simulation of the soil conditions prevailing in pavement subgrades, a sample preparation mould has been developed. It allows soils to
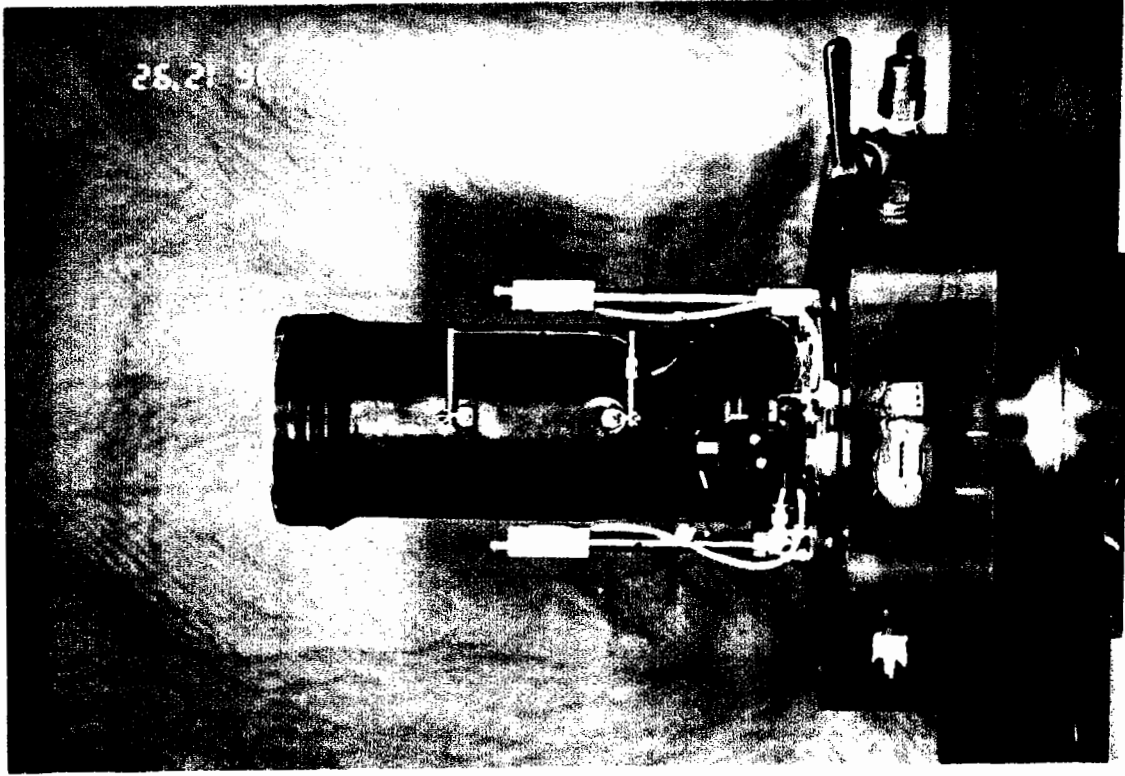
Plate 6.5 Soil specimen with 'on-sample' instrumentation (100TA)
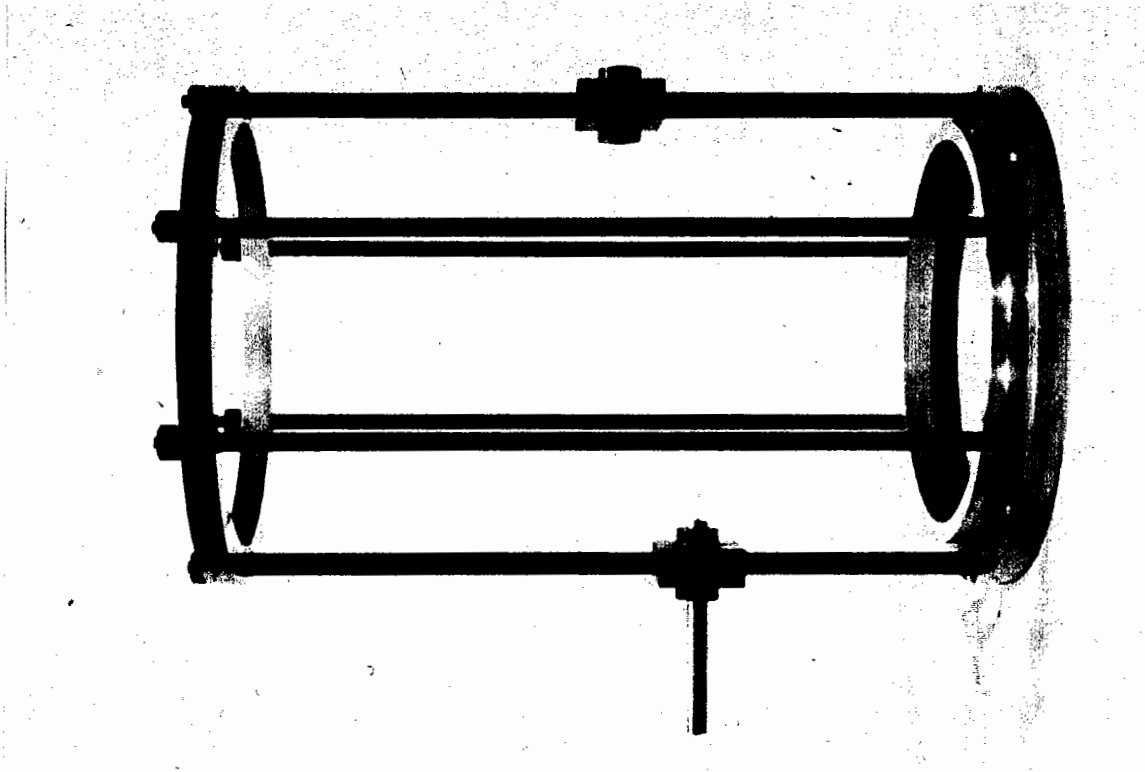
Plate 6.4 Marking rig for soil specimens

be compacted and has been designed to permit both remoulded and undisturbed samples to be conditioned by swelling and consolidation.
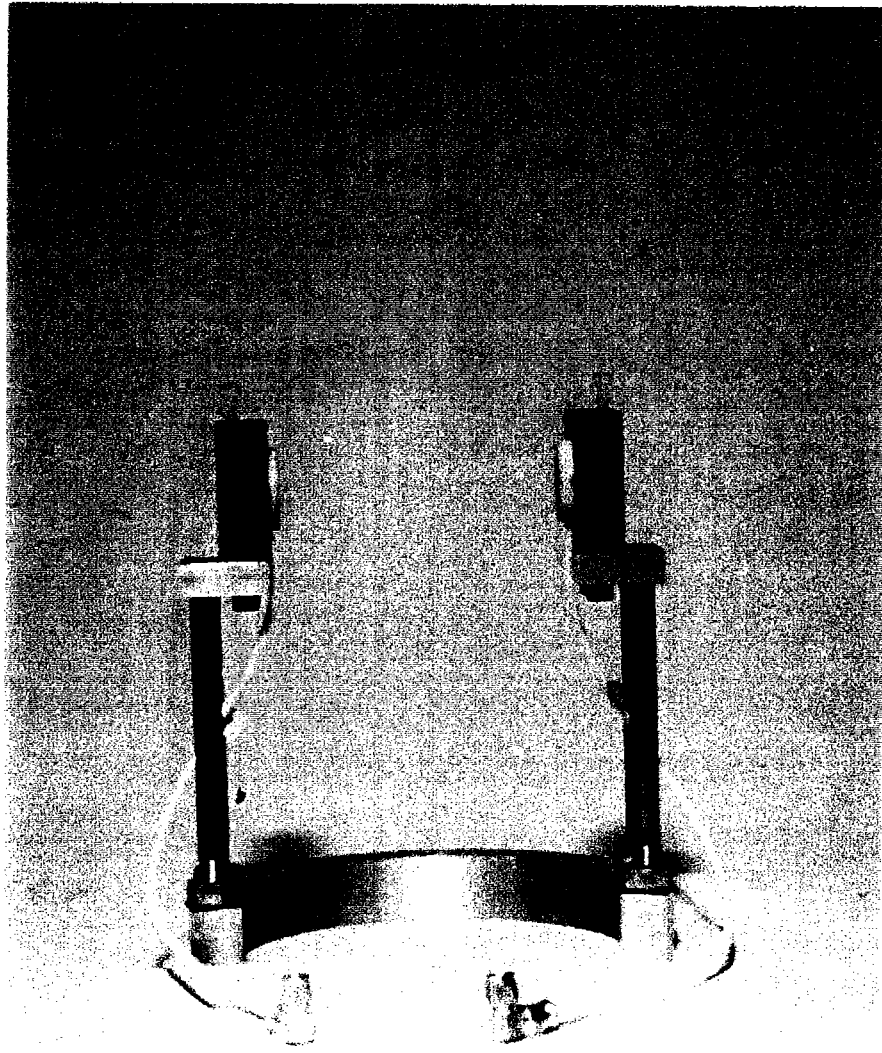
Plate 6.6   Modification to the supporting frame for 75 mm diameter
            specimens

CHAPTER 7

PRELIMINARY STUDY OF TEST MATERIALS

7.1 INTRODUCTION

A preliminary study of the test materials was carried out before the repeated load triaxial tests were performed in the newly developed 100TA. The study mainly involved three kinds of testing:- soil classification, soil suction evaluation and permanent deformation development under wheel loading. This section presents the work and the results from the preliminary study.

Classification testing to describe the physical nature of the soils included determination of the soil plasticity, the particle size distribution and the specific gravity of the solid content. The influence of the deviator stress, suction, plasticity and soil type were investigated by Loach (1987). He found that the deviator stress and the suction were the principal factors affecting the load spreading ability of the subgrade soil under repeated loading. Therefore, following the classification testing, the suction behaviour of soils was studied using a rapid suction apparatus (Dumbleton and West 1968). To observe the permanent deformation development in soils under wheel loading, materials were tested by the Soil Rut Testing Facility (refer to Section 2.5.7 for details) developed in Nottingham. This study provided valuable preliminary information about the possible factors which might affect the plastic strain resistance of soils.

The results from the preliminary tests provide a characterization of the soils against which the performance of the new equipment described in Chapter 6 may be assessed and better understanding of soil behaviour under repeated loading may be made.

7.2 MATERIALS

Since much of the area of the U.K. is covered by clayey soils, three types of cohesive soils were chosen for testing in this research as being representative. These were Keuper Marl, a Bothkennar clay and a London clay.

The London clay was kindly provided by the TRL and originated from the Summerlease clay pit located near Colnbrook, Buckinghamshire. This clay had been

used in an experimental retaining wall project by Symons (1989). Keuper Marl was supplied in the form of wet unfired brick by a brick manufacturer (Butterley Brick Limited) from Ollerton, Nottinghamshire. This is a Triassic age soil and had been used extensively by previous researchers, Hyde (1974), Overy (1982) and Loach (1987) at Nottingham. The Bothkennar clay came from an experimental site of the Science and Engineering Research Council about two miles from Kincardine in Scotland. At this site, a parallel project was undertaken by Nottingham University to study the behaviour of a haul road in a full scale trial (Little 1993).

7.3 SOIL CLASSIFICATION

7.3.1 Particle size distribution

One of the methods used in this study to classify soils is the particle size distribution (PSD) test described in B.S. 1377 (1990). A combination of wet sieving and sedimentation (pipette) tests were performed.

The test results for the three soil types are presented in Figure 7.1. Among the soils, the London clay was the soil with the highest clay content (74%), followed by the Bothkennar clay (29%) and Keuper Marl (22%). On the other hand, the results indicates that the Bothkennar clay possessed the highest silt content (68%), Keuper Marl is in the middle (55%) and the London clay has the lowest (23%). Only trace amount of sand (about 3%) were found in the London clay and Bothkennar clay while Keuper Marl included 23% sand. Therefore, of the selected soils, Keuper Marl had the coarsest grains and the London clay the finest.

7.3.2 Plasticity

The soil's plasticity was determined in accordance with B.S. 1377 (1990) and was expressed in terms of Liquid Limit (LL), Plastic Limit (PL) and Plasticity Index (PI). A greater plasticity index generally means a greater clay content. The results are summarized in Table 7.1 and Figure 7.2.

The solid "A" line in Figure 7.2 separates silts (below the line) from clays (above the line). As shown in Figure 7.2, all the soils under investigation lie above the A line,

119
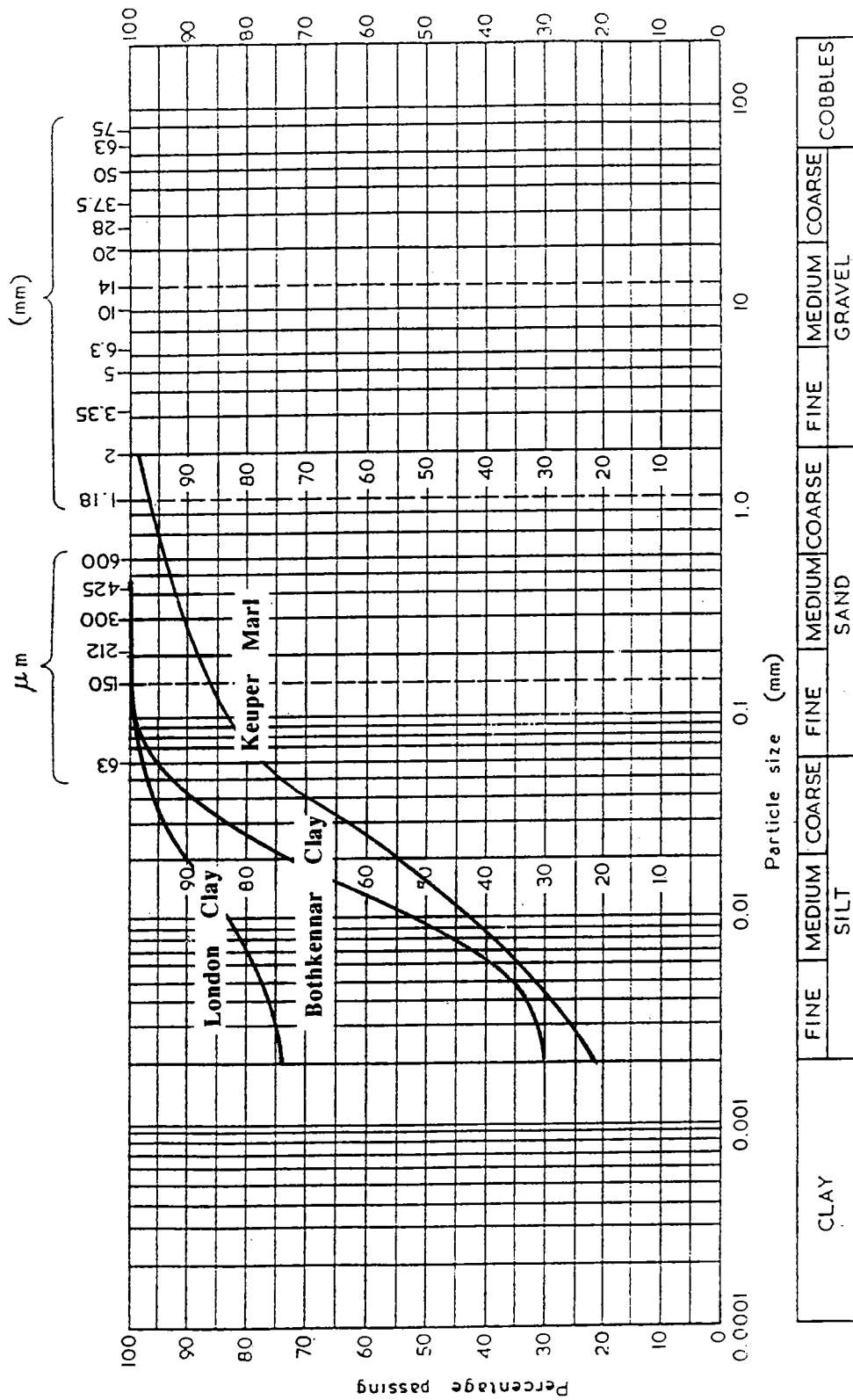
Figure 7.1 Particle size distribution of soils

hence, they are classified as clay soils. The plasticity of the London clay, the Bothkennar clay and Keuper Marl is described as very high, high and low respectively. Also shown in Figure 7.2 is a dotted line described by the equation,

$$PI = 0.838(LL) - 14.2 \qquad (7.1)$$

suggested by Clare (1948) for a wide range of cohesive soils in the U.K., is shown. It is noted that the plasticities of the selected soils follow Clare's line. It follows that the selected materials are generally representative of British soils.

Table 7.1 Plasticity of soils

	Keuper Marl	Bothkennar Clay	London Clay
Liquid Limit (%)	33.7	54.3	76.0
Plastic Limit (%)	17.6	25.1	25.2
Plasticity Index (%)	16.1	29.2	50.8
Plasticity	Low	High	Very high

7.3.3 Specific gravity (G_s)

Table 7.2 lists the results of specific gravity determinations made according to B.S. 1377 (1990). The measurements obtained in this study represent normal values for soils, except the London clay which is greater than usually expected. Nevertheless, a similar value was obtained by Symons et al (1989).

Table 7.2 Specific gravity of soils

	Keuper Marl	Bothkennar Clay	London Clay
Gs	2.72	2.72	2.80
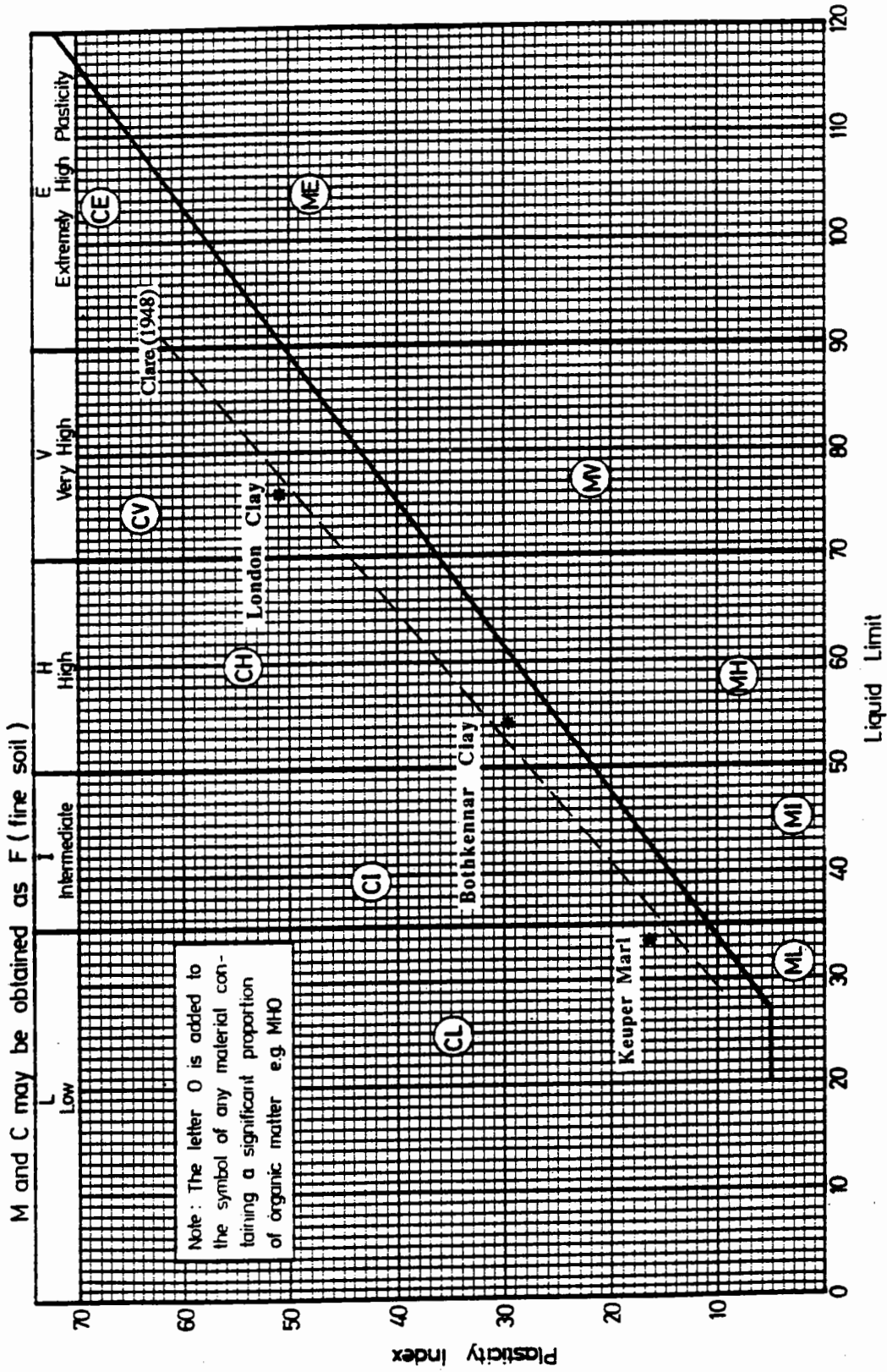
Figure 7.2 Plasticity chart of the cohesive soils

7.4 SOIL SUCTION

The term "soil suction" generally refers to the negative pressure, with respect to the atmospheric pressure, generated from the surface tension at the soil-water interface and from the surface absorption in a soil mass not subjected to any external stresses. Effects of soil suction on material stiffness have been reported by different researchers (Sauer and Monismith (1968), Dehlen (1969), Richards and Gordon (1972), Fredlund et al (1975) and Loach (1987)). Their observations show that resilient modulus increases with increasing soil suction. Loach proposed a model to describe the relationship between suction, deviator stress and soil stiffness. The predicted values derived from his model were found to be within ±20 % of the measured values from repeated loading tests.

In this study, the apparatus developed at the Transport Research Laboratory (Dumbleton and West 1968) was used to determine the suction of soils at various moisture contents. Other suction determination methods such as the suction plate method and the osmotic method normally require a long equilibrium time. The time needed for the current method is short because it involves a very small soil sample, and during the test there is little water movement. It is for this reason that the test device is named the "rapid suction apparatus". A schematic diagram of the apparatus is given in Figure 7.3. It consists of a small bore glass tube at one end of which a fine sintered glass suction plate is attached. It allows water flow but restricts air entry. The other end of the tube is connected to a hand vacuum pump. The tube is filled with de-aired water continuously from the suction plate to about 80 mm from the other end. During the test, a soil sample is placed on the suction plate, which has been saturated with de-aired distilled water, and a partial vacuum is applied to the soil through the tube. The water begins to flow into or out of the sample until the applied negative pressure is the same as the suction of the soil, then the water meniscus on the glass tube will stop moving. Further preparation details were described by Dumbleton and West (1968). The apparatus is also equipped with a steel chamber for providing confining pressure to the soil sample.

In carrying out the suction test in this study, sufficient soil was dried at room temperature and ground into powder. De-aired water was then added to the soil so that the desired lowest moisture content was attained. The wetted soil was mixed thoroughly and compacted into a metal cap of 55 mm in diameter and 40 mm deep. The mixed sample was stored in an airtight container for a day before being used. A small
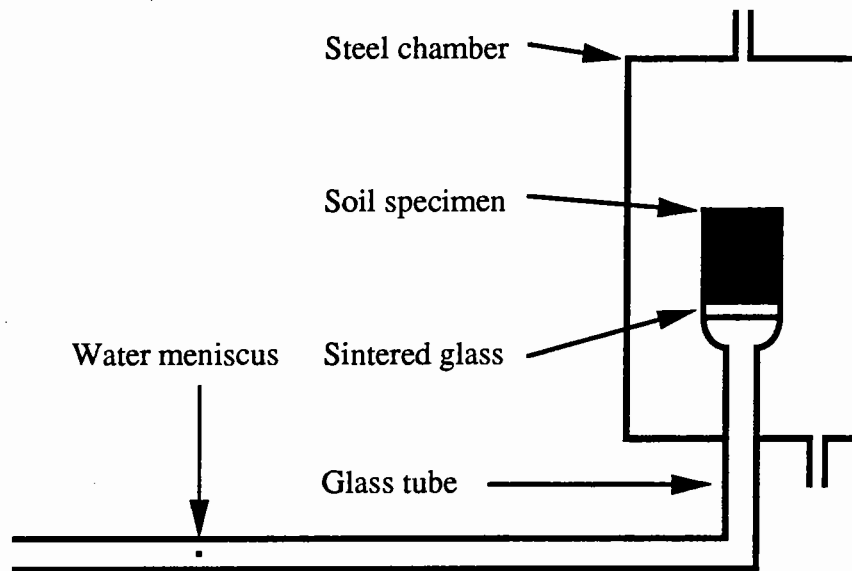
Figure 7.3a Schematic diagram of the rapid suction apparatus
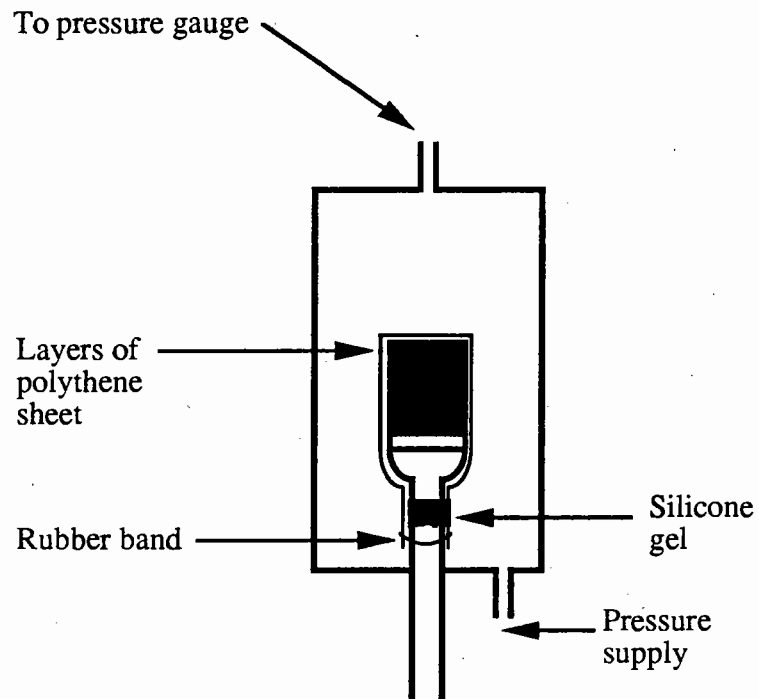
Figure 7.3b Arrangement for a pressurized specimen in the rapid suction apparatus

piece of sample was cut out by a 12 mm diameter tube with a sharp cutting edge. The height of the sample was trimmed to approximately 10 mm. The resulting specimen was then placed on the sintered glass plate and its suction determined. Furthermore, suction tests were also performed on soils cut directly from specimens of SRTF after wheel tracking testing, as described later in Section 7.5.

After the suction of the specimen had been found, its moisture content was determined. A small amount of water was then added to the remaining soil to increase the moisture content and the same sample preparation procedures were repeated for the successive tests.

The soil suction curves obtained from this study for Keuper Marl, the Bothkennar clay and the London clay are presented in Figure 7.4. The suction is expressed in terms of pF which is the logarithm of the pressure in centimetres of water. The results show that the suction of soils increased with decreasing moisture content. At the same moisture content, materials of higher plasticity and finer grading were found to possess a higher suction value. It was also observed that the sensitivity of the suction to change in moisture content decreased with increasing plasticity of materials (this aspect is discussed in the next paragraph). Hence, the London clay was the least sensitive among the soils and possesses the shallowest slope in the figure. Furthermore, test results obtained either from samples prepared in a metal cap or cut directly from the specimens of SRTF follow the suction curves with respect to their soil types. Hence, soil suction was insensitive to the sample preparation methods used in this study. Also in Figure 7.4, the suction curve of Keuper Marl as determined by Loach (1987) is included. It is very obvious that his curve is of a different shape from the one obtained by the author for Keuper Marl. This may be due to the difference between the wetting and drying suction curves (Black and Lister 1979). Soils were found to have a higher suction when they were drying. The results of this study represent the wetting curve of Keuper Marl. A lower suction was found. However, Loach's soils were in an uncertain state since he added dry samples into wet samples to adjust the moisture content. The state of his soil can be considered both as a wetting up of dry samples and as a drying up of wet samples.

It has been noticed that the relationship between suction and moisture content is related to the plasticity of the tested soils (Figure 7.4). This phenomenon was also observed by Russell and Mickle (1970) and Loach (1987). Therefore, investigation was made to find their possible inter-relationship. It was found that when the moisture content was
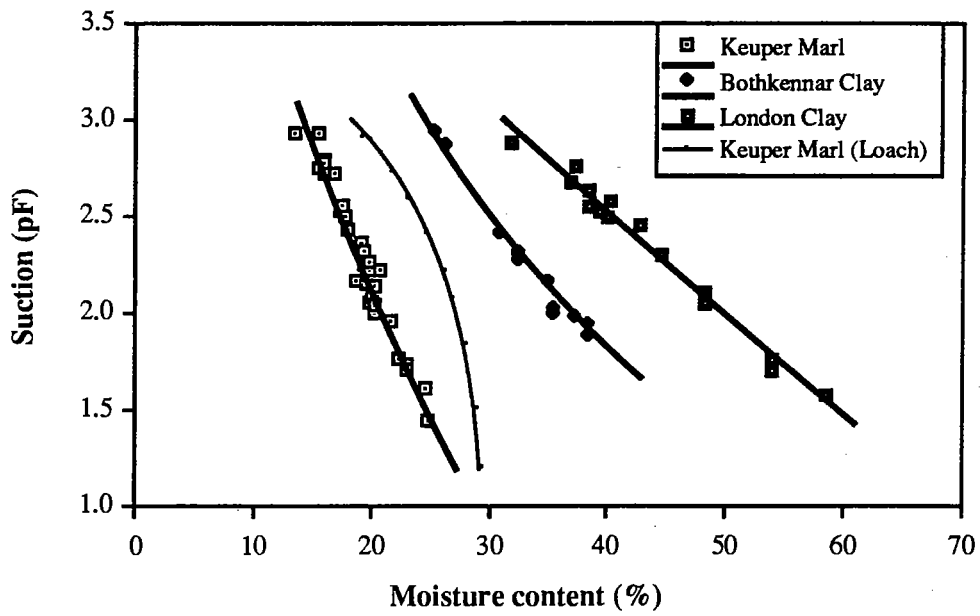
Figure 7.4 Suction curves of soils
(wetting curves except for Loach's)
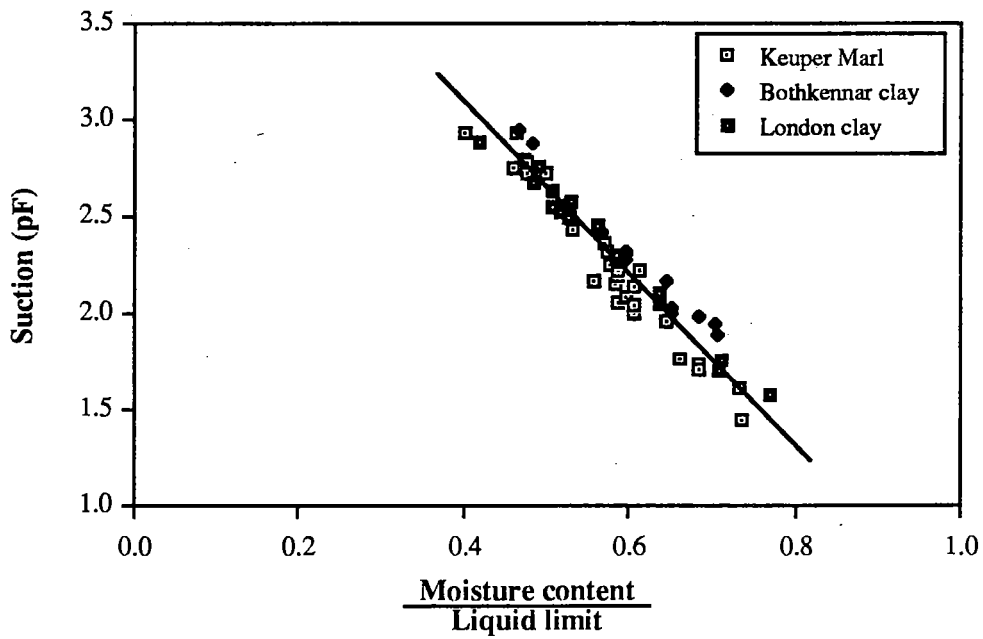
Figure 7.5 Relationship of suction and normalized moisture content of soils

normalized by the liquid limit of the soil, all suction results from the three soil types fell into one line. This is shown in Figure 7.5. The expression of the resulting relationship is:-

$$S = R\frac{\omega}{LL} + I$$ (7.2)

where: The constants R and I are -4.54 and 4.91 respectively.

ω is the moisture content of the soil sample.

S is the soil suction.

7.4.1 Soil compressibility factor

The soil compressibility factor, α, is defined as the ratio between the change in pore water pressure and the applied confining pressure. Croney and Croney (1991) suggested that soils of different plasticities possess different values of compressibility factor. An increase in resilient stiffness of compacted soils was observed by Loach (1987) when he raised the confining stress to his samples tested under repeated loading. He believed that the increase in the soil stiffness was due to lowering of pore water pressure in the samples.

To determine the soil compressibility factor of the selected soils, the rapid suction apparatus was again used. Since air was used to provide the confining pressure to the soil element, to prevent air from entering the soil specimen under confining pressure, three layers of thin polythene sheet were employed to cover the soil and sealed as shown in Figure 7.3 using silicon gel and a rubber band. Finally, the steel pressure chamber was installed.

Figure 7.6 shows the variation of the soil suction due to change in the confining air pressure for the three chosen materials. The relationship between the measured suction and the confining pressure is linear. Their corresponding soil compressibility factors, α, are included in Table 7.3. The α value increases with the plasticity of soil. A similar observation was reported by Croney and Croney (1991).
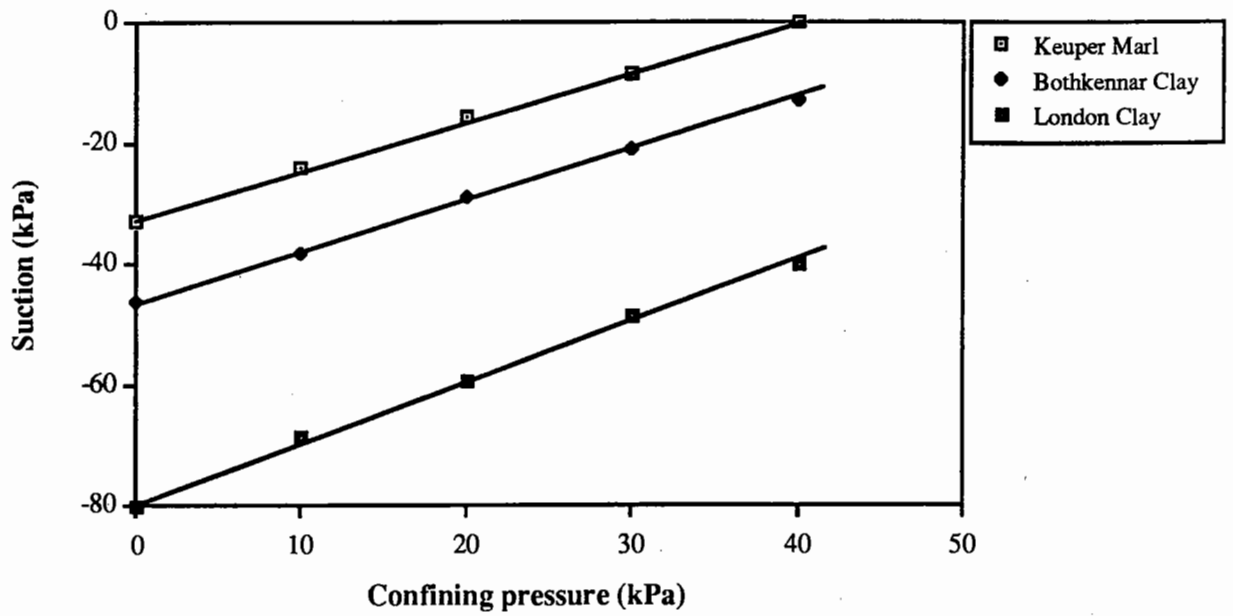
Figure 7.6 Effect of confining pressure on soil suction
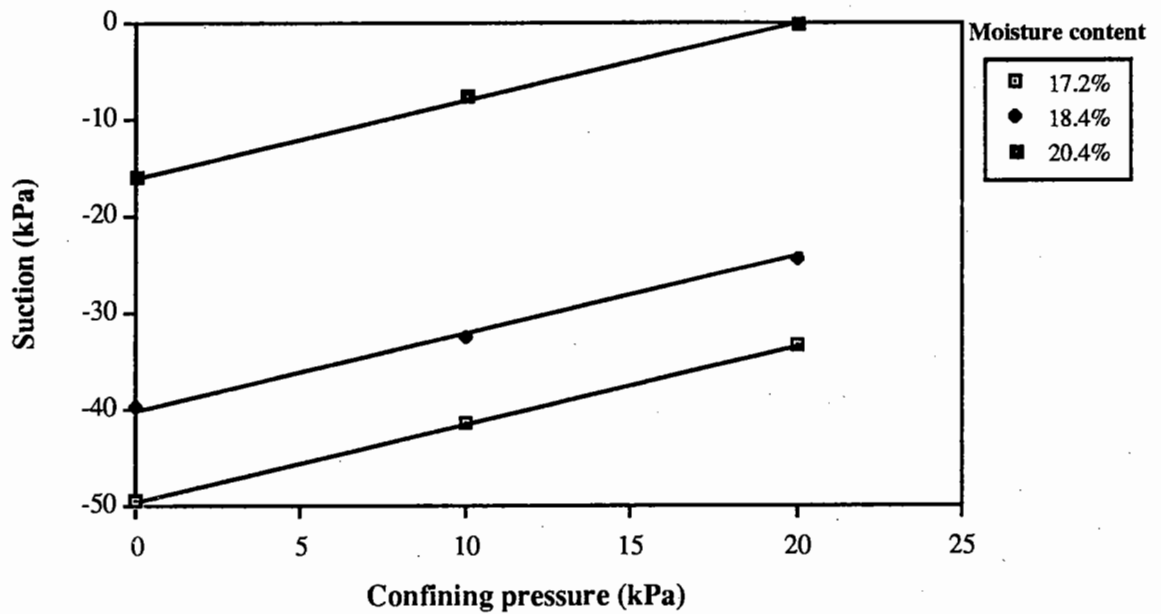
Figure 7.7 Effect of confining pressure on soil suction at different moisture contents
(Keuper Marl)

Table 7.3 Soil compressibility factor (α) of the selected soils

	Keuper Marl	Bothkennar Clay	London Clay
α	0.78	0.87	1.00

Figure 7.7 presents the results from testing Keuper Marl at three different moisture contents. It is worth noting that the three lines are of similar gradient. This suggests that the rate of change of soil suction with respect to confining pressure is unaffected by the moisture content.

7.5   WHEEL TRACKING TESTS

7.5.1 Introduction

The permanent deformation characteristics of soils under wheel loading were examined using the Soil Rut Testing Facility (SRTF) at Nottingham. Description of the facility can be found in Section 2.5.7. The factors which influence the permanent deformation characteristics of soils can be numerous (Section 2.4.1.2). In this study, particular attention was directed to the development of plastic strain with respect to the number of load cycles. Consideration was also given to the effect of material conditions and soil types. To further the understanding of the formation of plastic strain under different modes of loading, a simple test which included dropping a standard weight repeatably from a standard height onto a soil surface, was performed.

7.5.2 Preparation

The source soil was cut into small pieces of volume about a cubic centimetre and air dried at room temperature for a few days. The moisture content was then determined and de-aired water was added until the desired moisture content was reached. The watered soils were mixed for 20 minutes in a mixer and sealed in heavy duty polythene bags. These soils were then stored in a high humidity room.

When sufficient quantity of material was prepared, soils were compacted into the test trays in four layers. Compaction was by a hand rammer weighing 1.8 kg and 1000 strokes were applied to each layer. The compacted samples were then sealed to prevent loss of moisture and the samples were left for at least seven days in a high humidity room to allow variations in pore pressure to equalize. Immediately before testing, excess soil above the level of the top of the tray was trimmed. Two layers of microwave plastic film were then laid on the specimen to prevent change of moisture content during the test.

7.5.3 Testing

A total of twelve samples were tested in the SRTF. Six of them were Keuper Marl, three were Bothkennar clay and the last three London clay. It was intended that the test materials should be at various moisture contents. However, due to an error, some of the Bothkennar clay samples and London clay samples were prepared at similar moisture contents to each other. However, this did provide a good opportunity to check the repeatability of the test. The moisture content of each sample is presented in Table 7.4.

Table 7.4 Moisture contents of the test specimens

Material	Sample number	Moisture content (%)
Keuper Marl	K1	12.8
	K2	15.0
	K3	17.3
	K4	18.6
	K5	20.3
	K6	21.3
Bothkennar clay	B1	33.0
	B2	35.9
	B3	36.5
London clay	L1	39.4
	L2	39.9
	L3	42.5

The main test was performed by running the soil specimen under a wheel for 1000 passes at a pre-set speed and an initial contact pressure. The rut depth produced by the wheel was measured with a dial gauge, capable of reading to an accuracy of 0.01 mm, at three locations near the middle of the tray. The travelling speed was predetermined from a preliminary trial (Cheung and Dawson 1990). A test speed of 90 metres per hour was selected. It was the highest travelling speed that could be achieved without causing excessive rebound of the wheel when it travelled between trays of soil specimens. It followed that the travelling time on the surface of each specimen was about eight seconds. The wheel load and the contact pressure were also set after the preliminary trial. If a low wheel load (hence a low contact pressure) was used, a measurable rut depth might take a long time to form. On the other hand, a high load could distress the specimen in a single pass. For this study, the chosen reference contact pressure on a rigid surface was 300 kPa and the wheel load used was 2.6 kg.

The condition of the soil was checked by moisture content determination, strength testing using a shear vane and by a soil suction test at the end of the wheel tracking test. Finally, sufficient material was cut from the test specimen for CBR testing according to the procedure in B.S. 1377 (1990). After the completion of the CBR tests, the penetration (development of dent depth) under repeated drop-hammer loading was investigated. This was done by dropping a weight onto a metal plate of 32 mm diameter, which rested on the surface of the soil specimen. The mass of the drop weight was 1.82 kg and the height of free fall was 30 mm. The dent depth formed after the tenth drop was recorded.

7.5.4 Results and discussion

Plate 7.1 shows the typical soil surface conditions for different rut depths. For soft samples, significant rutting was formed directly under the wheel and heaving at both sides of the wheel path could be observed. Table 7.5 summarises the test results showing the strength of each material and the rut depths formed after 1000 passes (RD 1000) of a rolling wheel. The permanent deformations (DD10) obtained after dropping a weight on a plate resting on the top of a CBR specimen, as detailed in the previous section, are also included. It was evident that the permanent deformation resistance of soils was a function of material strength. The higher the strength of the soil, the lower the permanent deformation generated under repeated loading.

RUT DEPTH
= 0.5 mm

RUT DEPTH
= 2 mm

RUT DEPTH
= 2.7 mm
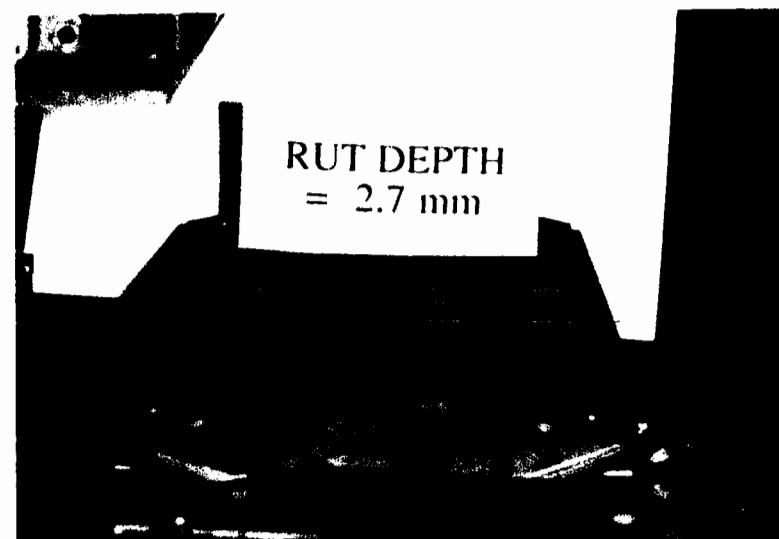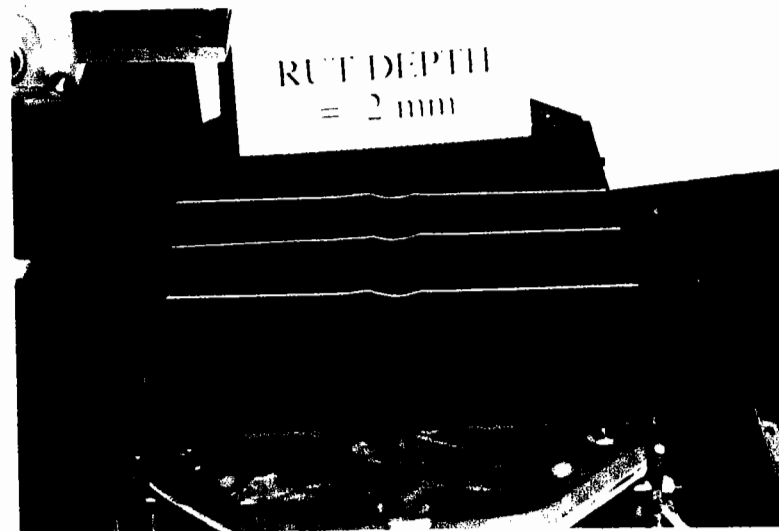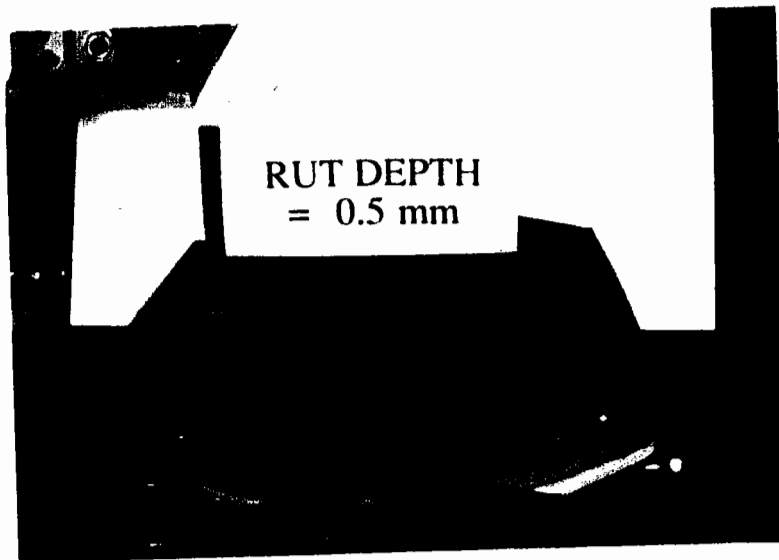
Plate 7.1   Typical soil surface condition at the end of the wheel
tracking test

Table 7.5 Results of the wheel tracking tests

Sample number	CBR (%)	Vane shear strength (kPa)	Suction (kPa)	RD1000 (mm)	DD10 (mm)
K1	13	>120	-	0.07	1.02
K2	5	>120	-	0.37	2.33
K3	2	91	32	0.74	5.19
K4	1	49	21	2.11	8.54
K5	0.5	26	12	3.65	16.54
K6	0.5	22	9	4.93	22.91
B1	1	41	17	1.73	9.34
B2	0.5	24	10	2.97	19.48
B3	0.5	22	9	3.28	22.92
L1	2	37	32	0.99	9.76
L2	2	37	31	1.26	10.17
L3	2	29	22	1.64	12.70

The rut development of Keuper Marl, the Bothkennar clay and the London clay specimens is plotted in Figure 7.8. The formation of the rut depth is rapid at the beginning but the rate decreases as the number of passes increases. For strong soils, samples K1 to K3 of shear strength more than 90 kPa (Figure 7.8a), the rate of rutting approached zero after 1000 passes. Figure 7.9 presents the rut development of the soils against the number of passes on a log scale. Except for the very soft samples of Keuper Marl, K5 and K6, a semi-log function between the accumulated rut depth and the number of passes may generally be observed. Similar observations were made by Parr (1972) and by Loach (1987). Both of their observations were made on repeated loading tests on triaxial samples. It follows that the additional stress condition, the continuous rotation of principal stresses induced by a travelling wheel, may not change the essential mode of permanent deformation development.

Acceleration of rutting was found in tests carried out on K5 and K6 of very low shear strength (being lower than 30 kPa). This might be partly explained by the observation made by Brown et al (1987) in their repeated load triaxial testing. They reported that when the deviator stress applied exceeded a certain limit (about 1 to 3 times the static strength of the soil), excessive permanent deformation development could occur. However, it was interesting to note that though the strength of samples B2 and B3 of
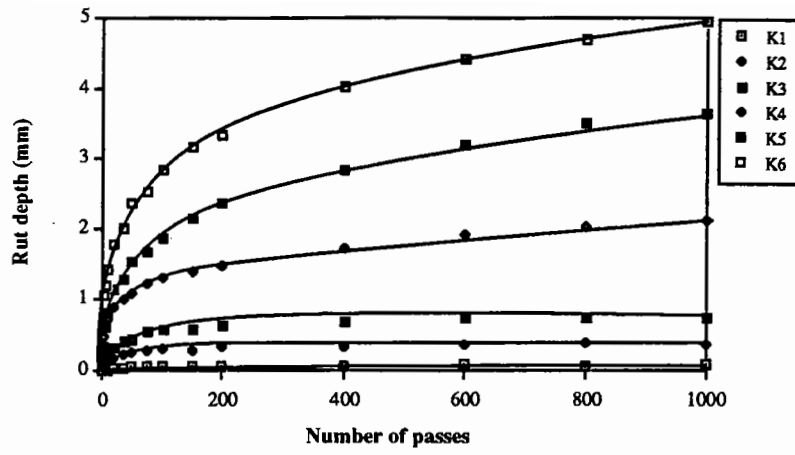
Figure 7.8a Rutting of Keuper Marl under direct wheel load
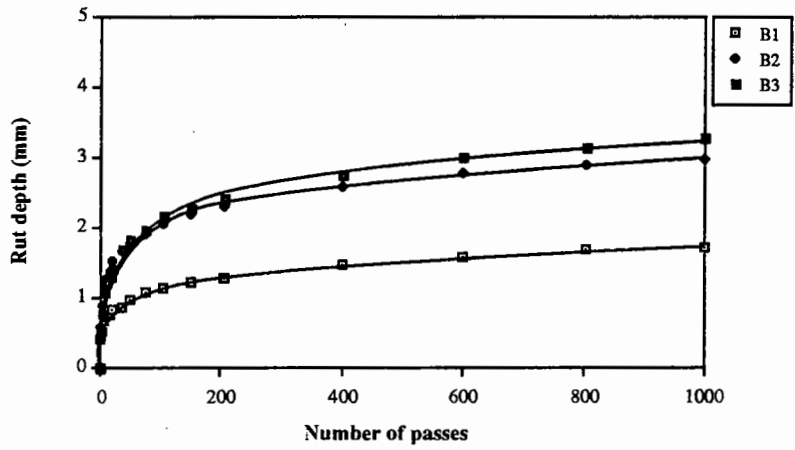
Figure 7.8b Rutting of Bothkennar clay under direct wheel load
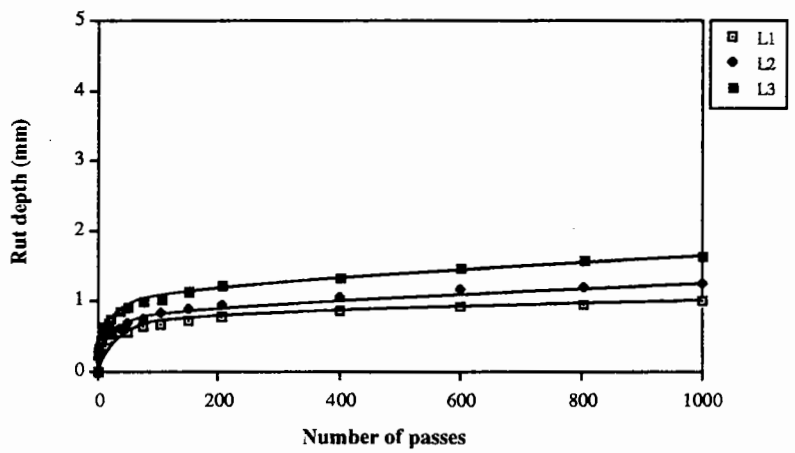
Figure 7.8c Rutting of London clay under direct wheel load
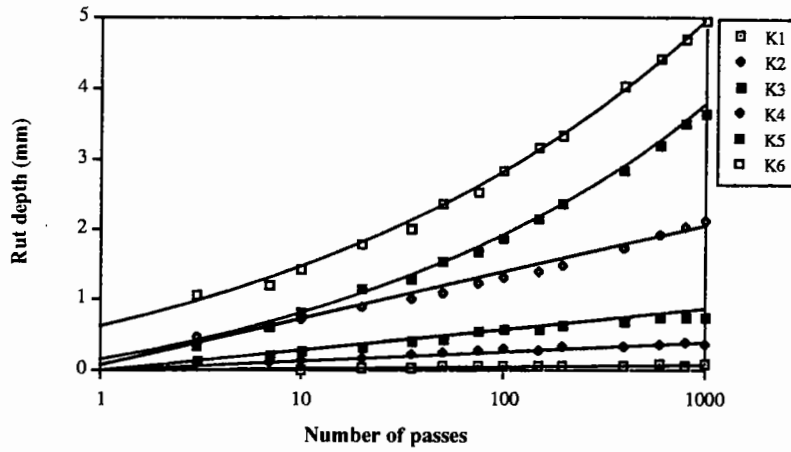
Figure 7.9a Semi-log plot of rut development of Keuper Marl under direct wheel load
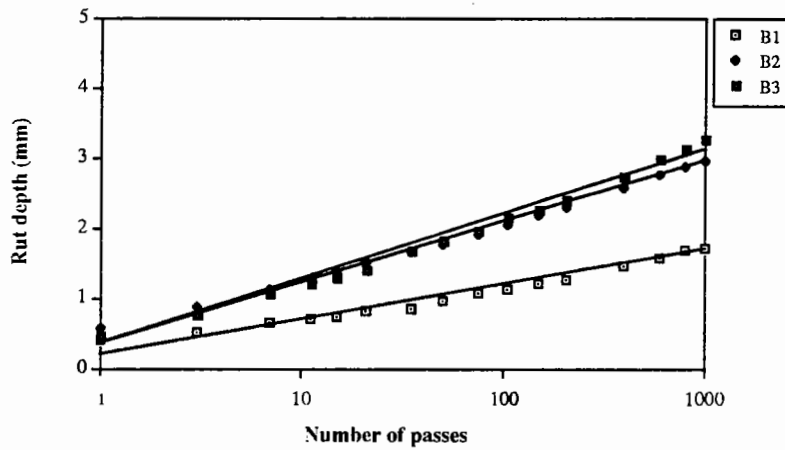
Figure 7.9b Semi-log plot of rut development of Bothkennar clay under direct wheel load
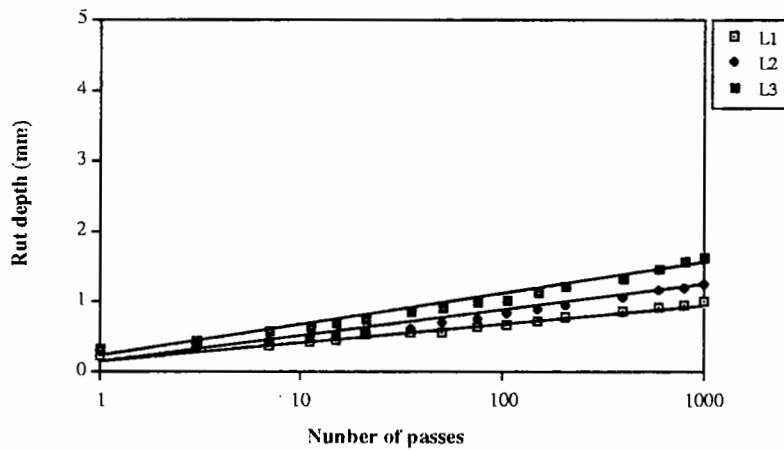
Figure 7.9c Semi-log plot of rut development of London clay under direct wheel load

the Bothkennar clay and L3 of the London clay were all of low strength, below 30 kPa, acceleration of rutting was not found in these two soil types of higher plasticity. Hence, besides the strength of soils which affects the plastic strain performance, for soils of the same strength, materials of a higher plasticity seem to perform better in resisting permanent deformation due to repeated loading.

Figures 7.10 to 7.12 show the rut depths formed after 1000 passes compared against strength related parameters (undrained shear strength, CBR value and suction respectively). Linear log-log relationship are apparent between RD1000 and the strength related parameters. All results indicate a logical trend, materials of low strength or small soil suction produce high rut depths and vice-versa. It was also noticed that these relationships might be material dependent. In Figure 7.10, where the shear strength results are plotted, the results of Keuper Marl, which had the lowest plasticity among the three materials tested, are near to the upper bound of the trend. The London clay, of the highest plasticity, forms the lower bound suggesting that materials of the same shear strength but of lower plasticity may be more susceptible to permanent deformation under wheel loads. However, such a material dependent phenomenon is not obvious in the plot of RD1000 against suction (Figure 7.12). Although most of the Keuper Marl's results are at the upper bound of the trend, one of the data points is, in fact, at the lower bound. In addition, the Bothkennar clay's results, but not those of the London clay, lie towards the lower bound. Furthermore, Figure 7.11 shows considerable scatter of RD1000 results at 2% CBR for the London clay. Therefore, general trends between rut depth developments and strength related parameters are evident, but the effect on the detail (due to difference in the test methods to obtain the strength parameters) is unclear.

Figure 7.13 presents a graph showing the permanent deformation results of RD1000 against DD10. A linear relationship between them can be observed. This observation suggests that uniaxial repeated loading may be able to reflect the permanent deformation characteristics of soils under wheel loads. Again, within the linear band (Figure 7.13), different lines might be drawn for each material type. The cause of the variations might be due to one or a combination of the following reasons:- (i) the use of different stress regimes in the two tests on the stress dependent materials even though repeated loads had been used in both tests and, (ii) different material types.

Finally, Figure 7.14 presents the rut depth (RD1000) against conditions of the tested soils (such as moisture content, void ratio and dry density). With the limited data
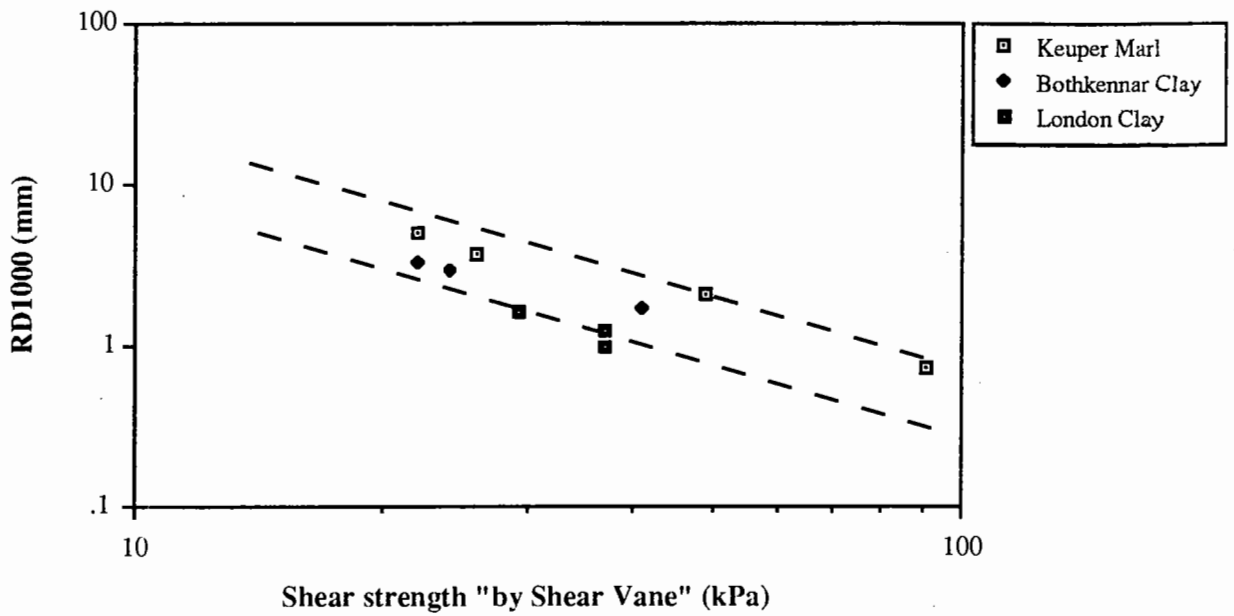
Figure 7.10 Relationship between rut depth after 1000 numbers of direct wheel loading and shear strength of soils
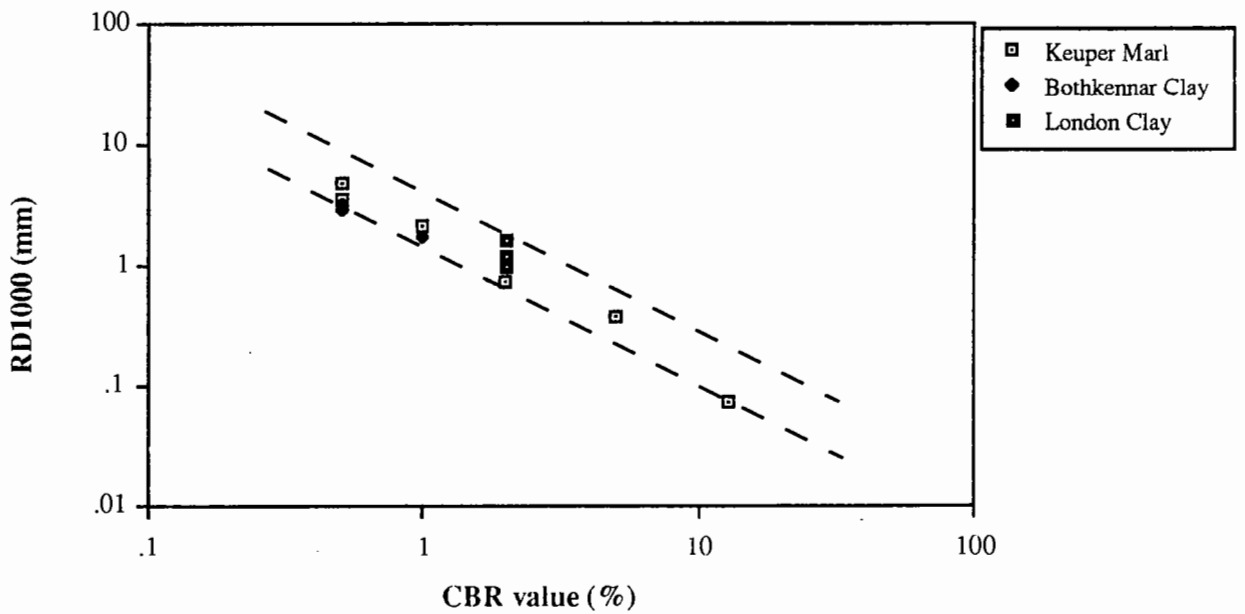
Figure 7.11 Relationship between rut depth after 1000 numbers of direct wheel loading and CBR value of soils
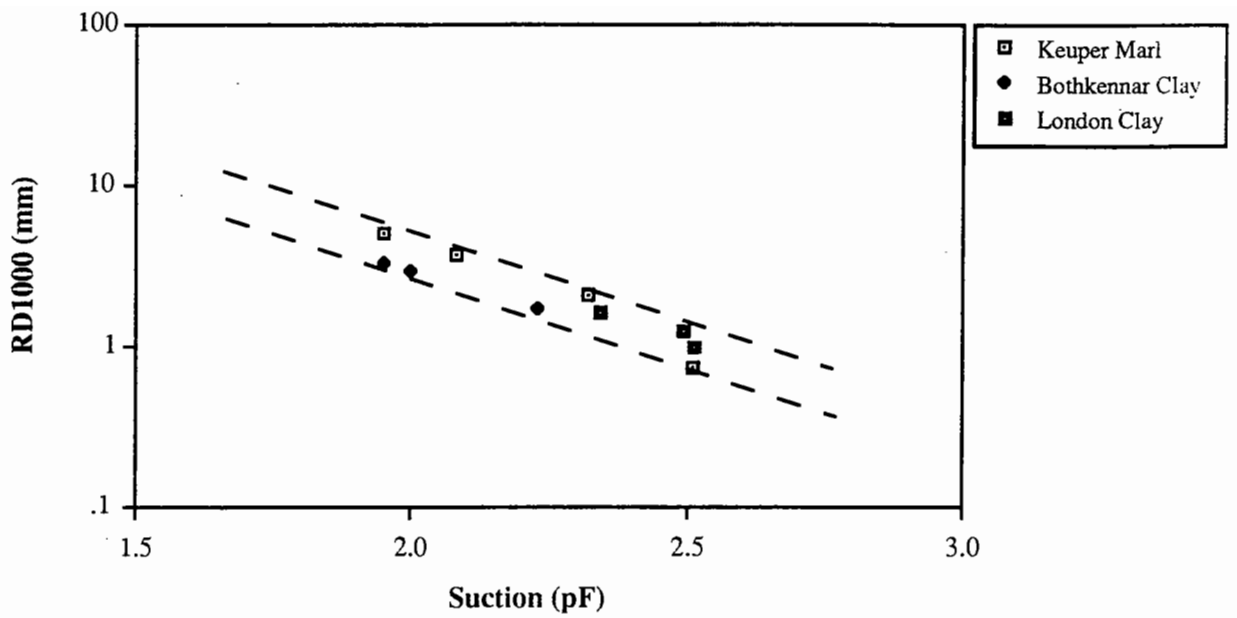
Figure 7.12 Relationship between rut depth after 1000 numbers of direct wheel loading "RD1000" and suction of soils
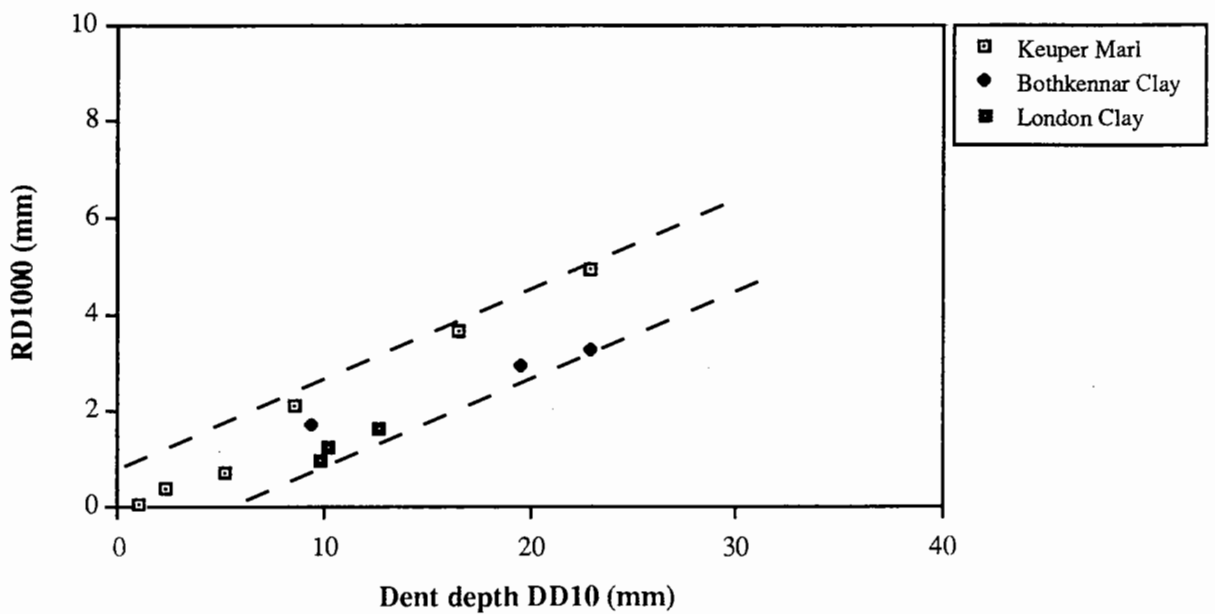
Figure 7.13 Relationship between rut depth "RD1000" and dent depth created by dropping a weight on soil surface for 10 times
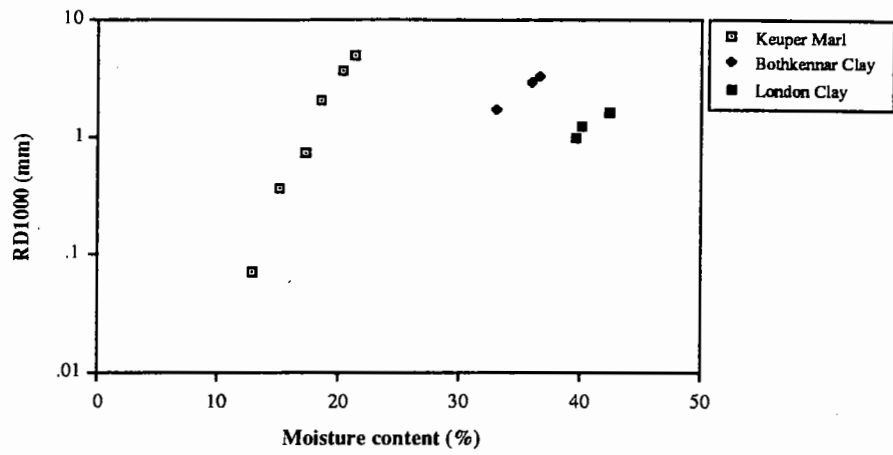
Figure 7.14a Relationship between rut depth "RD1000" and moisture content of soils
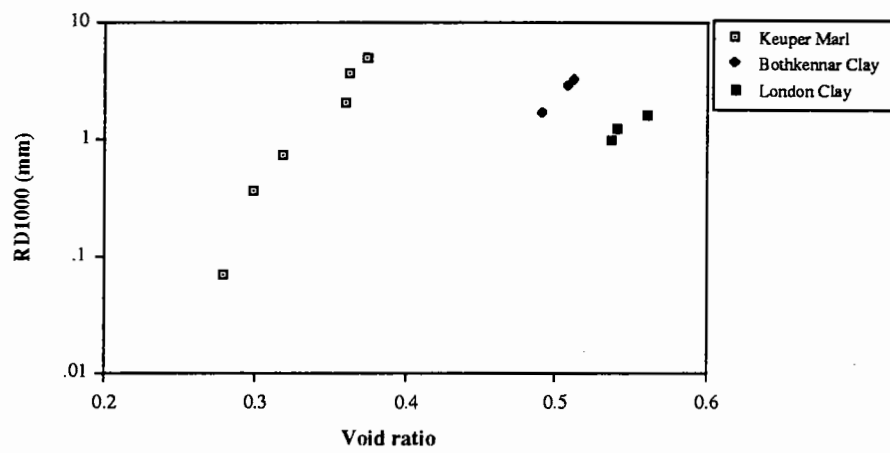
Figure 7.14b Relationship between rut depth "RD1000" and void ratio of soils
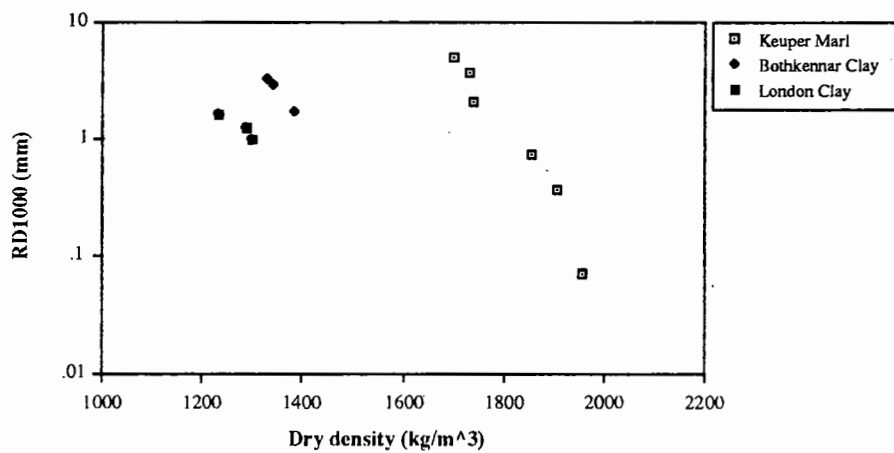
Figure 7.14c Relationship between rut depth "RD1000" and dry density of soils

available relationships between the logarithm of rut depth and these soil conditions may be established. Identical patterns are shown in both plots of RD1000 against moisture content and against void ratio while the dry density plot shows the mirror image of the pattern. In general, the higher the moisture content (or void ratio) of a samples, or the lower the dry density, the more the soil ruts.

7.6 SUMMARY

(1)   From the classification test results, it was found that the chosen materials were typical British soils.

(2)   The soil suction and moisture content relationships of the soils were established. Materials having a higher plasticity index possessed higher suction values at any given moisture content.

(3)   Liquid limits may be used to normalize moisture contents of different soils for predicting suction, and an equation has been proposed.

(4)   Variation of water content has little effect on the soil compressibility factor. However, the compressibility factor depends on the plasticity of the soil.

(5)   Results from wheel tracking tests showed that:-

(a)   The mode of rut development under wheel loading, when there is a rotating principal stress field, can be modelled with a semi-log function (similar to permanent deformation formed in uniaxial repeated load tests).

(b)   In general, there are log-log relationships between the permanent deformation characteristics of soils and the strength related parameters (such as undrained shear strength, CBR value, and soil suction).

(c)   The soil conditions expressed as dry density, moisture content or void ratio were found to affect the permanent deformation behaviour of soils.

129

CHAPTER 8

TESTING WITH THE NEW REPEATED LOAD TRIAXIAL APPARATUS (100TA)

8.1 INTRODUCTION

The testing work which has been carried out using the newly developed repeated load triaxial apparatus (100TA) is presented in this chapter.

The chief purpose of performing tests using the 100TA was similar to the reason for testing with the 280TA. It was to study the ability of the new apparatus to test pavement foundation materials, specifically, in the case of the 100TA, to test subgrade soils. The reliability of the device was checked against the existing repeated load triaxial apparatus for testing soils, 75TA, which has been used with some confidence at the University of Nottingham for many years. Details of that apparatus have been reported by Loach (1987). Results from the preliminary study (Chapter 7) of the selected soils are used in this chapter to check the ability of the new apparatus to test soils in road foundations and to further the understanding of soil behaviour under repeated loading.

Two particular test methods were developed to study the subgrade soils. The test procedure of the first involved only one sample for each soil condition. It was a multi-purpose test. The test procedure (summarized in Appendix N) was designed:-

(a)   To provide a suitable pre-conditioning.
(b)   To determine the permanent deformation behaviour.
(c)   To determine the resilient behaviour.
(d)   To obtain the undrained unconfined shear strength of the soil specimen.

As the permanent deformation behaviour of soils is influenced by the loading history (as mentioned in Chapter 2), a second test procedure was developed to further the understanding of permanent deformation development. This involved the application of repeated loads on five identical specimens with each specimen receiving a different level of deviator stress.

Models to describe the resilient strain behaviour and the permanent deformation development of compacted soils were developed on the basis of the test results.

8.2 EQUIPMENT PERFORMANCE

Generally, individual instruments, including the proximity transducers, the strain hoops, the load cell, the pressure cell and the LVDTs, performed reasonably well with respect to their precisions which have been presented in Section 6.5. This section, therefore, is concerned with the overall performance of the 100TA. The capability of the loading system to cope with repeated loading and the ability of the instrumentation to monitor repeated loads are reported. Comparative results from both the newly developed 100TA and the existing repeated load triaxial apparatus for soil testing are also included.

8.2.1 The loading system

The performance of the loading system depends on many factors. The obvious ones are the capacity of the actuator, the stability of the primary air supply, the sensitivity of the electro-pneumatic valve and the mechanical efficiency of all the moving parts. Although every part was carefully designed, the response of the entire system when all components worked together needed to be examined before tests could reliably be performed on soil samples.

The examination was done by sending a series of repeated sinusoidal command signals of the same peak to peak value to the electro-pneumatic regulator at different frequencies, while the tip of the load ram was resting on a solid surface. Readings were taken at the load cell near the end of the load ram. Results are shown in Figure 8.1. At loading frequencies below 3 Hz a stable maximum loading was recorded. Degeneration of load response was found when the frequency was above this upper limit. Hence, repeated loading tests should be conducted at a frequency not exceeding 3 Hz. To ensure adequate performance a frequency of 2 Hz was used for soil testing by the 100TA.

Figure 8.2 presents a plot showing the typical response signals of the load cell under repeated loading on soil specimens. Five consecutive cycles are included in the plot.
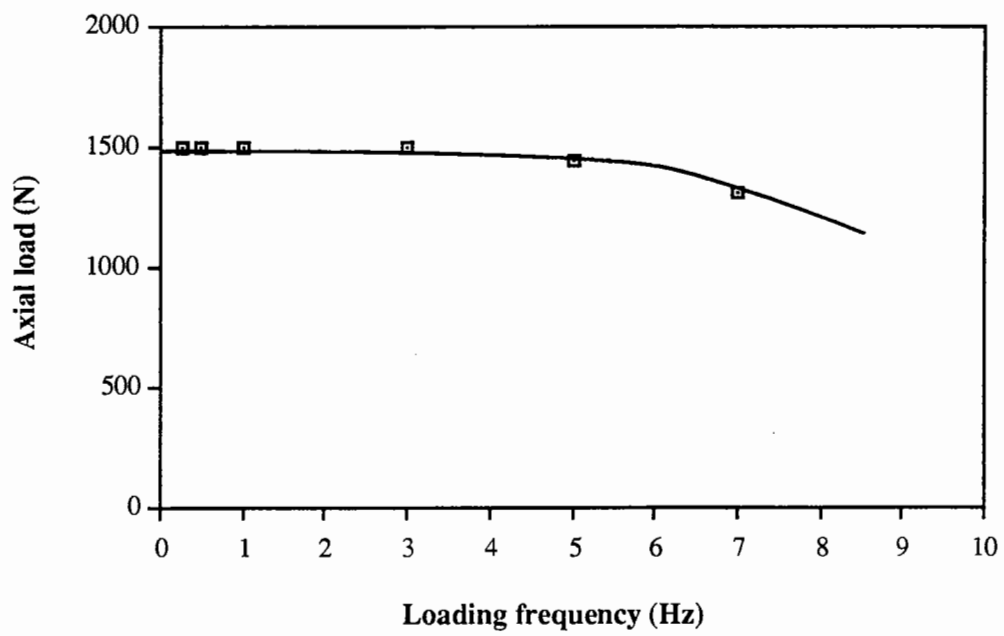
Figure 8.1 Effect of loading frequency on the axial load response
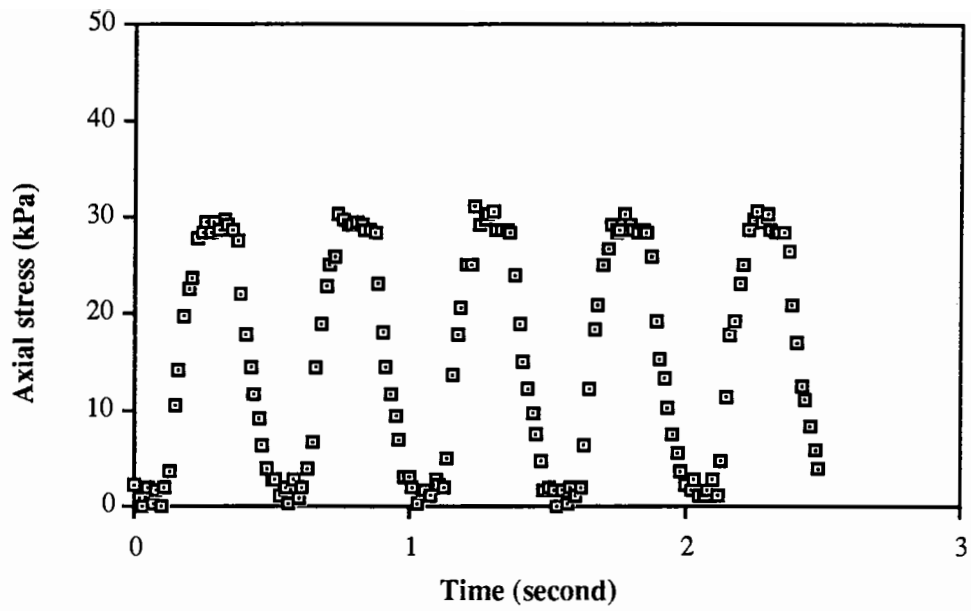
Figure 8.2 Typical record of loading at a loading frequency of 2 Hz
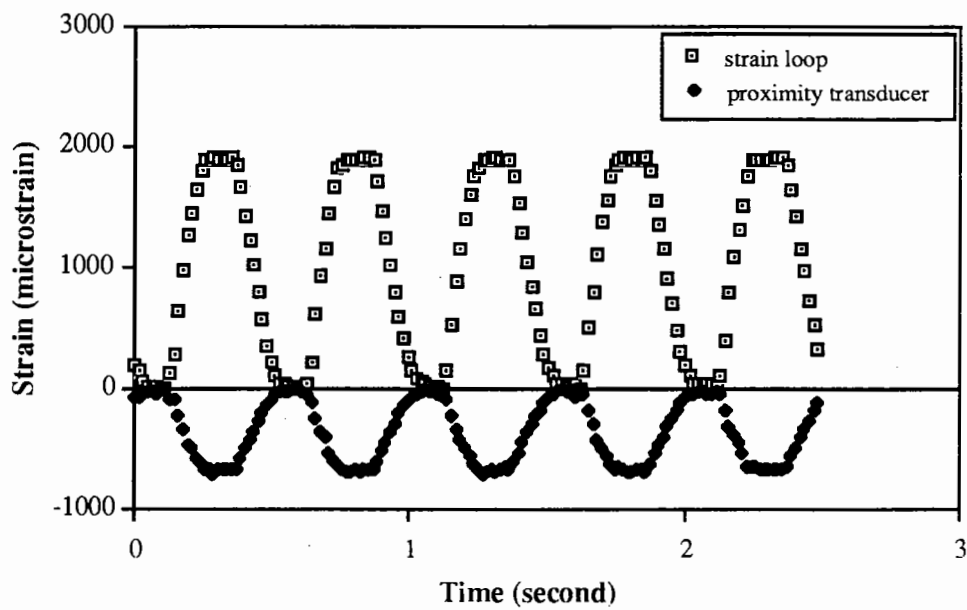
Figure 8.3 Typical record obtained from the strain loop and proximity transducer

at a loading frequency of 2 Hz

The control command used was a series of sinusoidal waveforms at a loading frequency of 2 Hz and with a maximum deviator stress of 30 kPa. Slight degeneration of the sinusoidal waveforms into trapezoidal waveforms can be observed. Nevertheless, the sinusoidal shape of each pulse could generally be maintained. Furthermore, the difference between consecutive load pulses was insignificant. This demonstrated that the apparatus was able to produce consistent and repeatable load pulses. Hence, the suitability of employing the current pneumatic loading system for producing axial load pulses to simulate traffic loads was indicated.

8.2.2 Instrumentation

Similar pulse signals can be found in Figure 8.3 for the axial and radial displacement measurements recorded by the LVDTs and the proximity transducers respectively. These signals were also found to correspond with the shape and length of the load pulses. Hence, the capability of the displacement transducers used in the 100TA was evident.

It was noticed that once the instruments were set up and a period of approximately 30 minutes was allowed for the electronic components to warm up, stable signals could be obtained. Nevertheless, interference from the other equipment operating in the same laboratory sometimes occurred. The system was thus improved by replacing all signal transmitting wire with shielded cables and by making necessary re-wiring. The occurrence of interference was then reduced down to once a month on average. Because of the time limit, further improvement to the electronics of the apparatus was not carried out.

8.2.3 Tests in the existing triaxial apparatus

To gain further confidence in using the newly developed 100TA, the apparatus was checked against the existing repeated load triaxial apparatus (Loach 1987).

There are considerable difficulties in producing consistent soil specimens which will give the same results under the same repeated loading test, even though strict control of the soil moisture content and density is observed. Gillett et al (1991) compared the performance of repeated load triaxial apparatuses in four countries - England, France,

the Netherlands and Portugal. In that study, in order to reduce the natural variability of soil samples, solid specimens of a synthetic material were used. For the study in this research project, the specimen selected was made of rubber.

The existing apparatus (75TA) can only test specimen of 75 mm in diameter and 150 mm in height, therefore a rubber sample of this size was used. Since the new apparatus was originally designed to test cylindrical specimens of size 100 mm by 200 mm, modifications to the proximity transducer supporting rig (as presented in Section 6.7.2) were made and spacer blocks were provided at both ends of the specimen.

Two similar series of vertical load pulses of a sinusoidal shape with increasing deviator stresses at a loading frequency of 2 Hz were applied to the rubber specimen by the two apparatuses. Fifty cycles were given and the results of the last five were recorded. Figure 8.4 shows the resilient axial strains and Figure 8.5 presents the resilient radial strains. Good agreement between the axial strains produced by the two apparatuses was observed. The radial strains obtained from the new apparatus were, on average, 9% higher than those from the existing one. Nevertheless, such a discrepancy might be expected when comparing two apparatuses with completely different instrumentation systems. In fact there is more scatter in the axial and radial strain results obtained from the older apparatus. This tends to suggest that the results of the older apparatus are less reliable.

8.3   SAMPLES OF COHESIVE SOILS

A total of twenty-six samples have been tested by the 100TA. Three of them were undisturbed samples extruded from 'U100' sample tubes. Others were compacted samples prepared by the preparation method described in Section 6.7.2.

There were three types of compacted soil:- Keuper Marl, London clay and Bothkennar clay. Details of these materials have been presented in Chapter 7. All of them were clay soils with low, very high and high degrees of plasticity respectively.

Undisturbed samples were taken from the subgrades of the Loughborough trial site and the Bothkennar site. Details of the Loughborough samples are given in Appendix O. In brief, the soil was a Boulder clay and could be described as a silty clay with occasional gravel. The undisturbed samples obtained from Bothkennar were of the
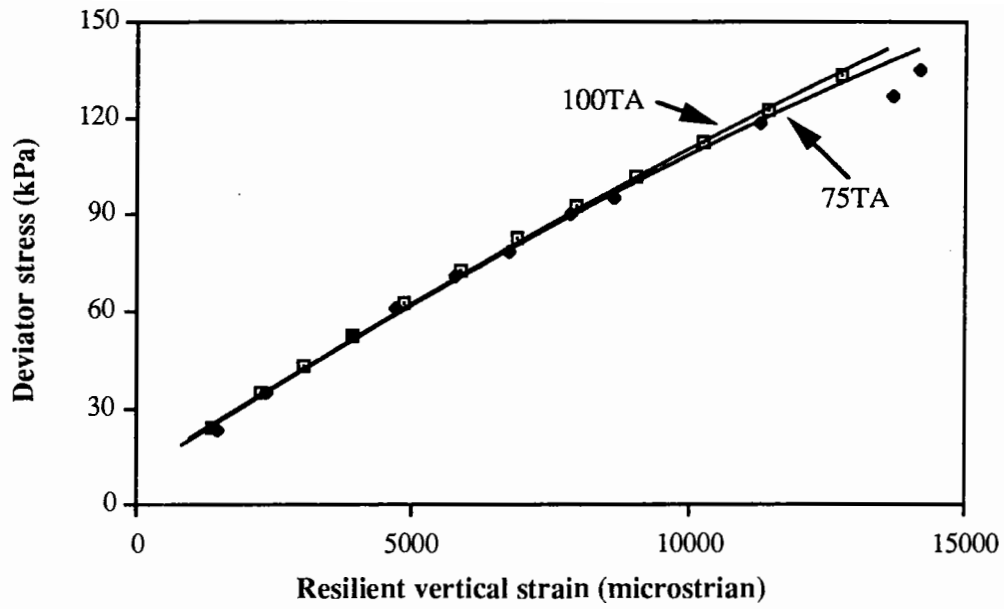
Figure 8.4 Comparison of vertical strains measured by the 100TA and the existing 75TA
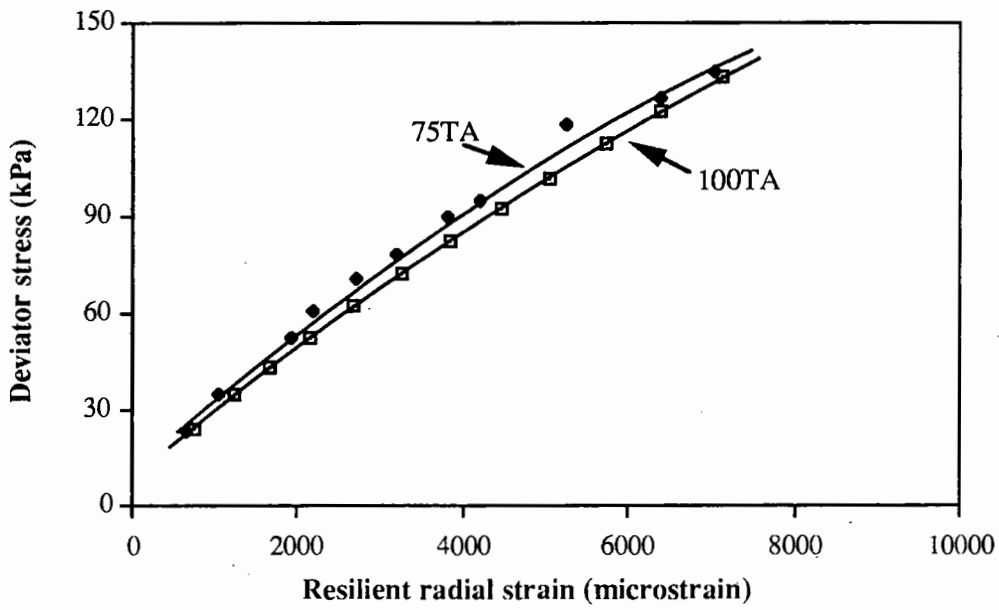
Figure 8.5 Comparison of radial strains measured by the 100TA and the existing 75TA

same origin as those used for compacted samples. Hence, details of the soil can be found in Chapter 7.

The samples which were tested by the 100TA can be divided into two main groups according to the test procedures they underwent. The first group refers to samples subjected to multi-stress path testing (Sections 8.4.1, 8.4.2 and 8.4.3), the second group to the single-stress path test (Section 8.4.4). Codes used to represent these samples are listed in Table 8.1.

The first letter of the code indicates the type of material: "K" for Keuper Marl, "L" for the London clay, "B" for the Bothkennar clay and "O" for the boulder clay from the Loughborough site. The nature of the sample is shown by the second letter, of which "C" is for compacted samples and "U" is for undisturbed samples. For the first group a number is given next to the letters to distinguish samples of the same material but with different moisture content or density. The number in the second group denotes the sequence of testing. Finally, a letter "Q" is suffixed to the samples in the second test group.

Details of the tested specimens by their dry density, percentage air void and degree of saturation are presented in Appendix P. For the compacted samples, the degrees of saturation were within a narrow range between 0.89 to 0.96. With the same compaction effort, it was noted that the higher the plasticity of the material, the higher the air voids. The Keuper Marl specimens possessed the minimum air voids ranging between 1 and 3%. Air voids more than 3% were found in the Bothkennar clay. The air voids in the London clay specimens were between 3.5 and 5.5%. Although the phenomenon of changing air void content with plasticity is interesting, it was not within the scope of this project and was not pursued further.

8.4 TEST PROGRAMME ON COHESIVE SOILS

In this section, standard test procedures used in this research project to determine the permanent deformation susceptibility, resilient strain behaviour and shear strength of cohesive soils from a single sample are presented. In addition, a test method which has been used to further the understanding of the permanent deformation behaviour of subgrade soils is described.

Table 8.1   Samples tested in the 100TA

Group	Nature	Material	Designation
1	compacted	Keuper Marl	KC1 to KC7
1	compacted	Bothkennar clay	BC1 to BC3
1	compacted	London clay	LC1 to LC3
1	undisturbed	Boulder clay	OU1
1	undisturbed	Bothkennar clay	BU1 to BU2
2	compacted	Keuper Marl	KC1Q to KC5Q
2	compacted	London clay	LC1Q to LC5Q

8.4.1   Permanent deformation test

8.4.1.1   Test design consideration

The stress history of pavement foundation materials has a great effect on their subsequent elastic strain development (as mentioned in Section 2.4.2). This is a particularly important aspect of behaviour for weak materials such as soft clays. If it is desirable to destroy this stress history effect, then prior application of permanent deformation tests will 'swamp' any earlier stress history 'knowledge' carried by the soil. Prior application also has the effect of overcoming thixotropic stiffening of soils which takes place after compaction (refer to Chapter 2 for further details). This permanent deformation testing will then take the place of conditioning (AASHTO 1986). On this basis, it was considered justifiable to study the plastic strain characteristics of cohesive soils before performing other test stages.

Preliminary tests were carried out on four Keuper Marl triaxial specimens, KC1, KC2, KC3 and KC4, of different moisture contents, to define a testing procedure which could serve the two purposes:-

(a)   Determining the pre-conditioning procedure for resilient strain tests.

(b)   Investigating the plastic strain behaviour.

135

These samples were subjected to axial repeated loads at different stress levels in increasing magnitude. For each stress level, 1000 load repetitions were applied. Typical results are shown in Figure 8.6. In the figure, the data points indicate the accumulated permanent deformation strains produced at the end of each stress level for the beginning of the test. It is noticed that the strain accumulation rate is slow when the deviator stresses are small. However, when the stress level increases, the plastic strain grows at an exponential rate.

Preliminary analysis to get a rough estimation of the plastic strains formed at different depths within the subgrade layer were performed using Almeida's (1991) finite element program and by making use of the results obtained from the preliminary tests.

For the analysis a pavement structure consisting of a 200 mm thick granular sub-base material lying on top of the subgrade was used. The wheel diameter was 400 mm and the contact stress was 500 kPa. Figure 8.7 shows the deviator stress distribution and the estimated permanent deformation in the subgrade based on the test results presented in Figure 8.6. It is noticed that most of the permanent deformation is generated in the top 500 mm of the subgrade. This zone provides more than 85 percent of the total strain. In this top layer, the initial confining stresses from the overburden are rather low, varying from 4 kPa to 14 kPa if a K_0 value of 1 is assumed. Therefore, it is considered appropriate to determine the plastic strain behaviour for soils in road pavements at low confining stress. For a conservative design, testing at zero confinement is suggested.

To protect the sample from damage due to excessive deformation, the total amount of plastic strain allowed during permanent deformation testing has to be limited. Bishop and Henkel (1962) reported that for most clay soils the total strain at failure in a compressive test usually exceeded 4%. A ceiling of 1% plastic strain, which is well below the minimum failure strain value, may be appropriate.

8.4.1.2 Testing procedure

The specimens were tested at least 24 hours after the setting-up procedures, as described in Section 6.7, had been completed. Each test was performed at zero confining pressure and in drained condition. In general, 1000 repetitions of a deviator stress of 5 kPa were first applied. Sometimes a deviator stress of 2.5 kPa was used if
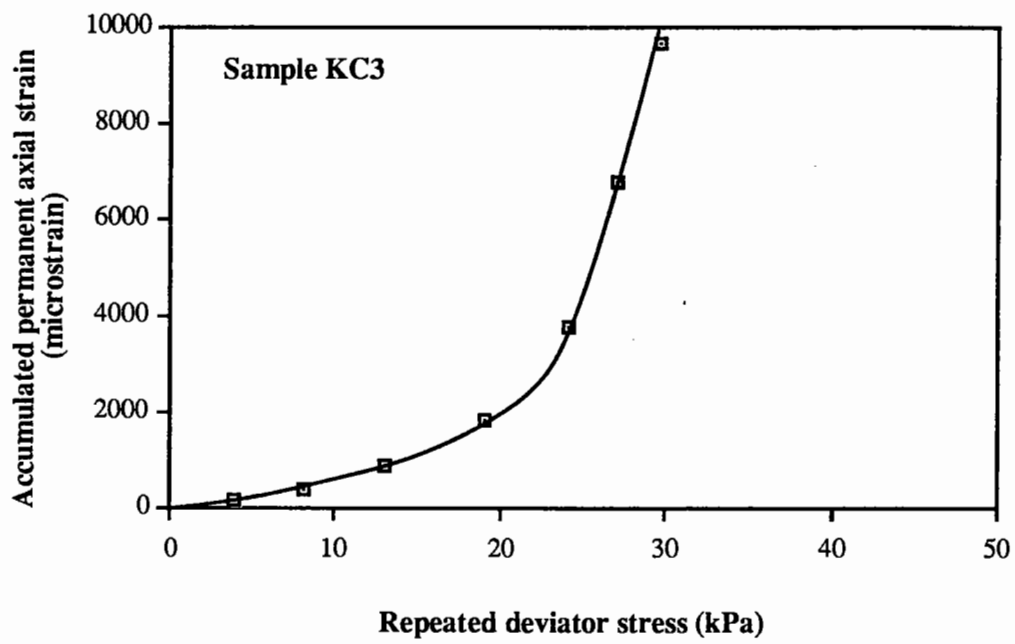
Figure 8.6 Typical accumulated permanent strain of a cohesive soil under repeated loading
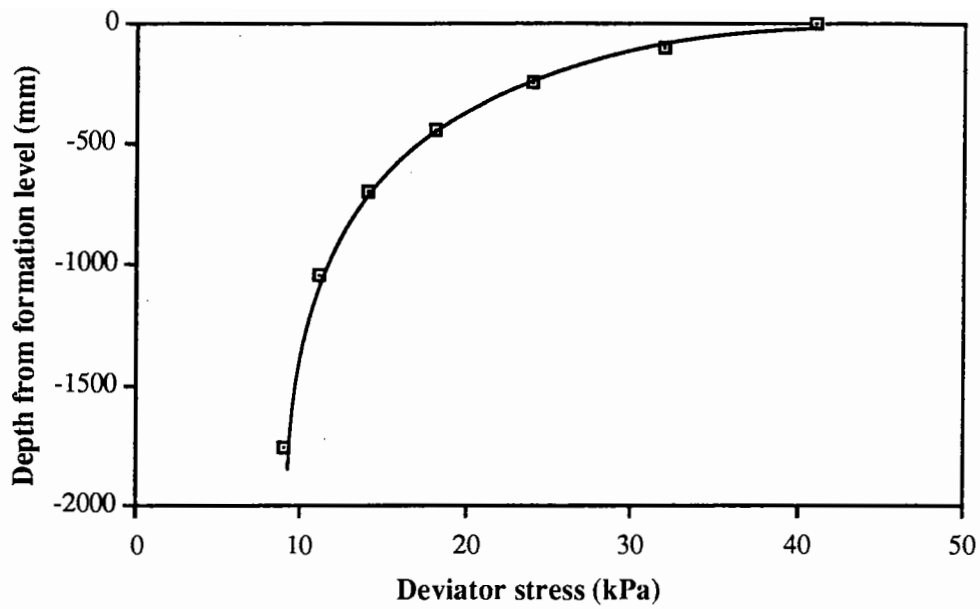
Figure 8.7a Estimated deviator stress distribution in subgrade at the centre of wheel path
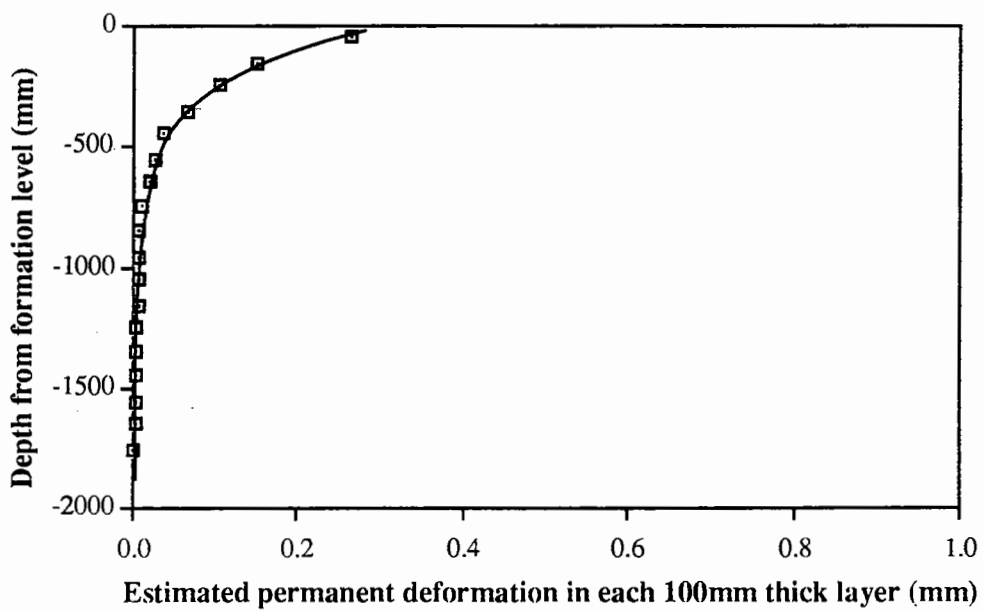
Figure 8.7b Estimation of permanent deformation (after 1000 passes of wheel loads)

beneath subgrade surface

very soft samples were being tested. The load pulses were of a sinusoidual waveform and the loading frequency employed was 2 Hz. The permanent deformation generated after the completion of cycling was recorded. Then the second series of cycling followed. This comprised another 1000 repetitions of deviator stress at a magnitude 5 kPa higher than the previous value. The same loading frequency and waveform were used. Again the permanent deformation at the end of cycling was taken. The same testing procedure was repeated until the accumulated axial plastic strain was at, or just above, 1%.

8.4.2   Resilient deformation test

8.4.2.1   Test design considerations

Unlike the imported unbound granular materials used in pavement foundations which have normally undergone some selection processes before being used, there is almost no chance to choose the nature of the subgrade soils (except those in fill sections or soils in treated sections). Hence, much variation in soil nature must be expected. Some soils may be very strong, others can be rather weak. If a fixed standard set of stress paths is used to determine the resilient behaviour of soils, it will suit only a small range of materials. The stress paths may not be sufficient for testing stiffer materials. On the other hand, some soils may fail before a test is finished. It is thus difficult to find a standard set of stress paths to suit all cases.

However, the stress value determined at an accumulated axial plastic strain of 1%, which is named 'q_t' in this thesis, in the permanent deformation test may be used to give a guide for setting the stress paths for the resilient testing of a particular soil. For a properly designed pavement, excessive permanent deformation should not develop in the subgrade. Therefore, the elastic response of soils at stress levels beneath this stress is of greatest interest. For determining the resilient behaviour of cohesive soils, stress paths as shown in Table 8.2 were used.

Table 8.2   Loading procedure for resilient strain test

Magnitude of deviator stress (kPa)	Cell pressure (kPa)	Number of pulses at each deviator stress level	Frequency (Hz)
$\dfrac{q_t}{6}, \dfrac{q_t}{3}, \dfrac{q_t}{2}, \dfrac{2q_t}{3}, \dfrac{5q_t}{6}$	90	50	2
$\dfrac{q_t}{6}, \dfrac{q_t}{3}, \dfrac{q_t}{2}, \dfrac{2q_t}{3}, \dfrac{5q_t}{6}$	60	50	2
$\dfrac{q_t}{6}, \dfrac{q_t}{3}, \dfrac{q_t}{2}, \dfrac{2q_t}{3}, \dfrac{5q_t}{6}$	30	50	2
$\dfrac{q_t}{6}, \dfrac{q_t}{3}, \dfrac{q_t}{2}, \dfrac{2q_t}{3}, \dfrac{5q_t}{6}$	0	50	2

Estimation of the stress levels in road foundations, during and after construction, by the finite element program, FENLAP, has already been presented in Chapter 5. The magnitudes of the estimated stresses at the formation level can be found in Section 5.5.1.1. Figure 8.8 shows these stress paths together with those of Table 8.2 (assuming that the q_t is 30 kPa). It can be noticed that the stresses induced by the traffic at the top of subgrades at different stages are well covered by the stress paths of the triaxial testing except that the slopes are different. The stress paths at the higher confining pressures, 60 kPa and 90 kPa, are used to cover soil conditions deeper in the subgrade where high confining stresses occur. Deviator stresses deeper in the subgrade are much smaller than those near the formation level. The highest deviator stress level, $\dfrac{5q_t}{6}$, as recommended in Table 8.2, could be reduced. However, in consideration of the consistency of the test procedure used in a routine test, the use of a maximum deviator stress of $\dfrac{5q_t}{6}$ for each confining pressure throughout the test was considered appropriate. Since constant confining pressures are employed in the triaxial test, stress paths at a slope of 3 to 1 on a p-q plot, similar to those in tests carried out by the 280TA, are inevitable. Nevertheless, the limitation of using a constant confining stress to test subgrade soils has been considered justifiable as an appropriate compromise between realism and test complexity.

8.4.2.2   Testing procedure

The resilient strain test was carried out immediately after the permanent deformation test (see Section 8.4.1.2) on the same specimen in accordance with Table 8.2. The waveform of the load pulse was sinusoidual and the loading frequency was 2 Hz. For
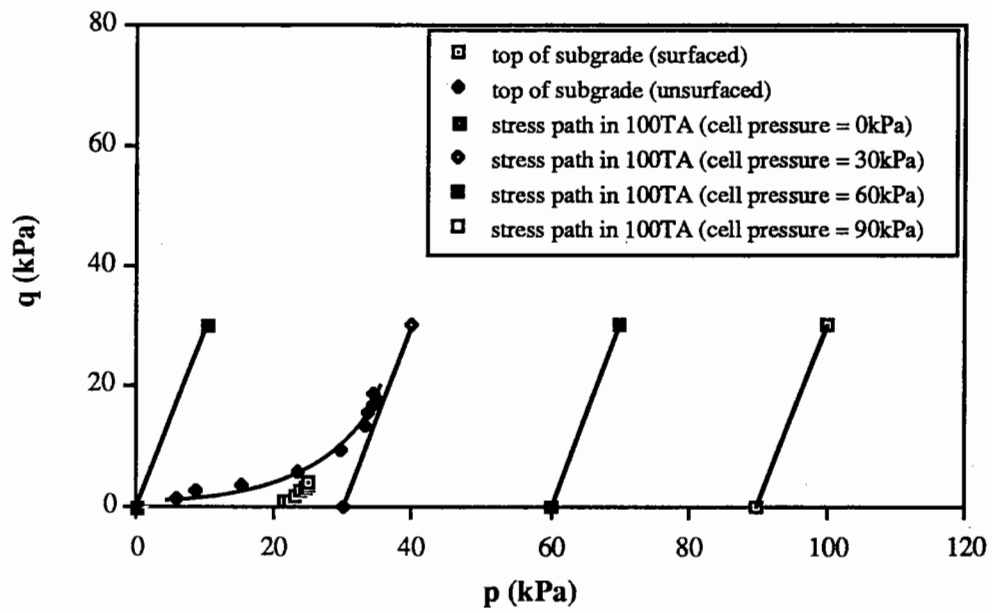
Figure 8.8 Stress paths in the subgrade of pavement and in the 100TA

each stress path, 50 cycles were applied and readings were taken during the last 5 cycles.

8.4.3 Strength test

8.4.3.1 Test design considerations

Subgrade soils should be strong enough to support trafficking both before and after completion of construction. This requirement is particularly important during the construction period when there is little or no protection from the top layers and heavy plant and lorries are being used. Therefore, it may be useful to have a measure of subgrade strength. Furthermore, results from the preliminary test (Chapter 7) have shown that strength testing may be a means of obtaining an index for rutting susceptibility.

8.4.3.2 Testing procedure

To eliminate unwanted membrane effects at large strains the rubber membrane was removed before the strength test was carried out. In addition, the "on-sample" instrumentation was taken off.

During the strength test, no confining pressure was used. Vertical axial stresses at an increasing rate of 10 kPa per minute were applied. After the unconfined strength test, additional measurements of strength were performed using a 19 mm shear vane and a 6.5 mm diameter hand penetrometer. The moisture content was determined at the end of all tests.

8.4.4 Single stress-path tests

8.4.4.1 Considerations

Determination of the permanent deformation behaviour of soils as described in Section 8.4.1.2 is a useful guide to guard against premature failure of road pavements due to subgrade permanent deformation. However, the plastic strain characteristics of the soil

in the latter part of the test may have been affected to an indeterminable amount by the preceding load pulses at lower deviator stresses. In order to assess the effect of these preceding repeated loads applied at lower stress magnitudes, a new specimen for each different repeated deviator stress level is required.

8.4.4.2 Testing procedure ("quick" test)

The test to further the understanding of the permanent deformation behaviour of soils and particularly to find the preceding loading effect was carried out on five identical specimens. Each individual specimen can be quickly tested hence the procedure is described as the "quick" test in this thesis. The testing procedure is given in Table 8.3.

Table 8.3 Testing procedures for "quick" test

Specimen number	Deviator stress	Cell pressure (kPa)	Number of cycles
1	q_t	0	1000
2	2 times q_t	0	1000
3	3 times q_t	0	1000
4	4 times q_t	0	1000
5	5 times q_t	0	1000

Again testing was carried out after the specimen had been set up for 24 hours and the test condition was drained. Only the external LVDT was used because the strains measured were relatively large. For the first specimen, load pulses of the stress equivalent to the q_t value were applied. Pulses of magnitude twice as large as this initial level were applied to the second specimen, three times as large to the third and so on. The number of load pulses for each test was 1000. Records were taken at intervals during the test. After the application of cycling, to keep a record of the material quality, the soil strength was checked by a shear vane and a pocket penetrometer. Finally, the moisture content of the material was determined.

8.5 Results and Discussion of Tests on Cohesive Soils

In this section the results obtained by the 100TA are presented and discussed in two main sub-sections. The first sub-section concentrates on results produced in the multi-stress path test in which the permanent deformation behaviour, the resilient behaviour and the strength of soils were studied. The second sub-section deals with results obtained from the single-stress path or "quick" tests. Test data showing obvious errors has been discarded. Since most of the samples tested were remoulded, unless otherwise specified, the following description is for compacted soils. Furthermore, in the following sections comparison of results obtained from the repeated load triaxial test with those of the soil rutting test from the preliminary study (Chapter 7) are frequently made.

8.5.1 Multi-stress path tests

8.5.1.1 Permanent deformation

Typical plastic strain development of a cohesive soil under repeated loading as described in Section 8.4.1.2 is given in Figure 8.9. In the figure, each point indicates the accumulated permanent deformation from the beginning of the test. Points in the upper part and the lower half of the graph show the development of the axial and the radial strains respectively. It is evident that the permanent deformation of the cohesive soils relates to the applied stress non-linearly. Similar to the results obtained from the preliminary test performed on Keuper Marl (Figure 8.6), the shape of the typical axial strain curve (Figure 8.9) is concave upward confirming that the rate of the plastic strain accumulation of cohesive soils escalates exponentially when the stress level increases. This is, in fact, in agreement with the observations made in the soil rutting tests (Section 7.5.4) where non-linear relationships between the permanent deformation characteristics and the strength related parameters have been reported.

Figure 8.10 presents the development of permanent deformation obtained from three different soil samples, LC2, BC2 and KC3 at similar levels of soil suction (42 to 47 kPa). It is worth noting that the rates of plastic strain development of the three soil types are different. This suggests that the permanent deformation behaviour of the soils may be material dependent.

141
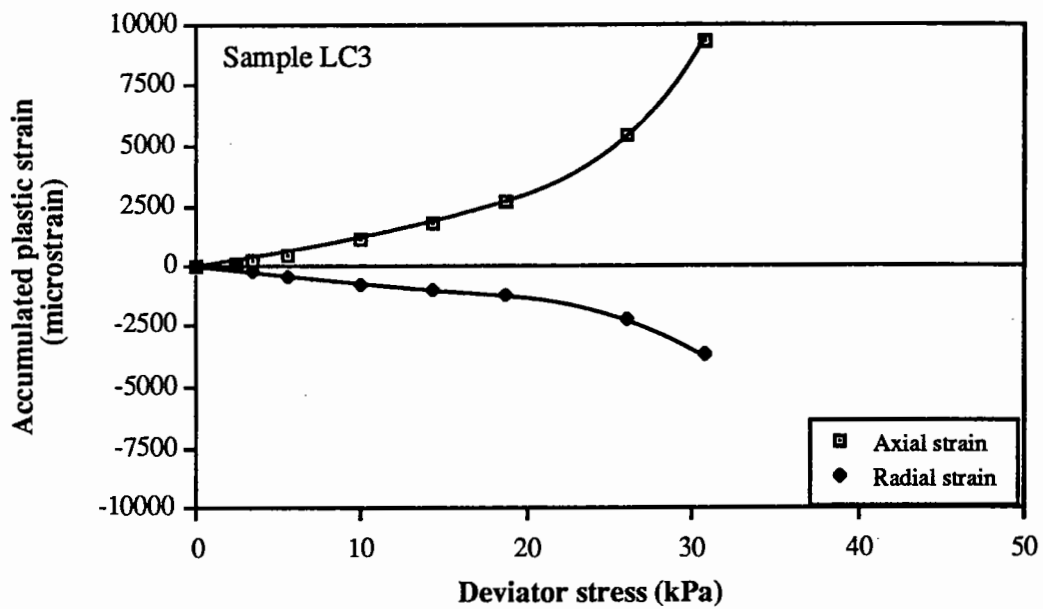
Figure 8.9 Typical plastic strain development of cohesive soil during the multi-stress path test
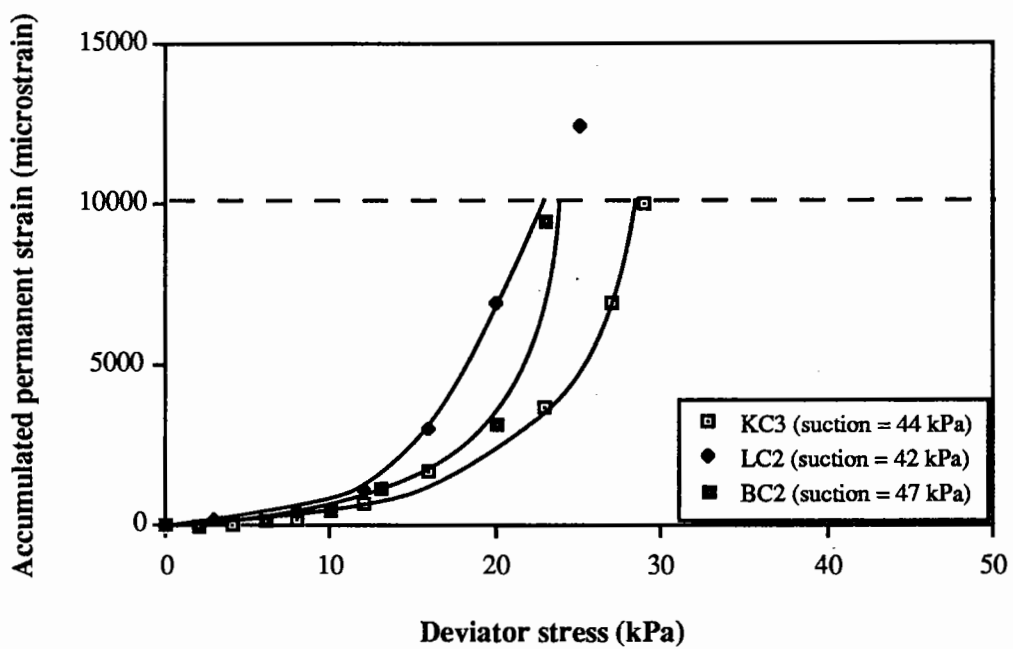
Figure 8.10 Permanent strain development of different soil types but of similar soil suction

To enable a sensible comparison of samples of the same material type at different soil suctions, the deviator stress value, q_t, derived from the permanent deformation test presented in Section 8.4.1 was used. Together with the corresponding suction values, the q_t values of the tested samples are listed in Tables 8.4 and 8.5. Soil suction was determined in the manner described in Section 7.4. It is noticed that the observation made in the soil rutting test (Section 7.5.4), in which permanent deformation resistance of soils increased with soil suction, can also be seen in the two tables. For each material type, the higher the suction of the soil, the greater the q_t value obtained.

Table 8.4 Deviator stress at 1 % permanent deformation (compacted samples)

Sample number	Soil suction (kPa)	q_t (kPa)
KC1	20	20
KC2	27	23
KC3	44	30
KC4	59	52
KC5	7	6
KC6	36	27
KC7	63	47
BC1	33	12
BC2	47	22
BC3	79	29
LC1	25	15
LC2	42	21
LC3	63	30

Table 8.5 Deviator stress at 1 % permanent deformation
(undisturbed samples)

Sample number (kPa)	Soil suction (kPa)	q_t (kPa)
OU1	39	21
BU1	21	34
BU2	3	22

Figure 8.11 is used to show the relationship between q_t and the suction value in graphic form for the three types of compacted soils. Despite a certain degree of scatter (and limited data available for the London clay and the Bothkennar clay), in general, for each soil type, the results can be represented by a straight line passing through the origin. Hence, the accumulation of permanent strain, ε_p, under the repeated loading regíme described earlier could be a function of deviator stress to soil suction ratio. The general expression should be as follows:-

$$\varepsilon_p = fn \left(\frac{q_r}{S}\right) \tag{8.1}$$

where:- q_r is the repeated deviator stress (kPa)
S is the soil suction (kPa)
fn = a function of

Since the lines are of different slopes (F = 0.8, 0.42 and 0.5 for Keuper Marl, the Bothkennar clay and the London clay respectively), this confirms that the permanent deformation characteristics of soils are material dependent.

Effect of soil conditions
Figures 8.12 and 8.13 show the plots of q_t against compacted density of the soils and q_t against the moisture content respectively. For each type of soil, samples of higher density were found to be more resistant to permanent deformation. On the other hand,
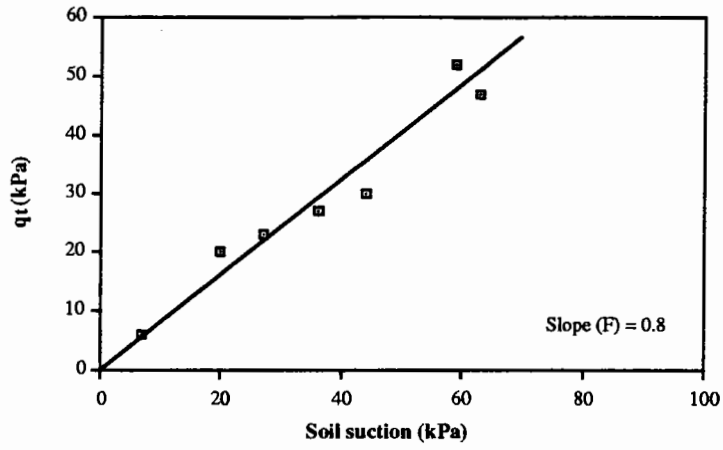
Figure 8.11a Relationship between q_t and soil suction for the Keuper Marl samples
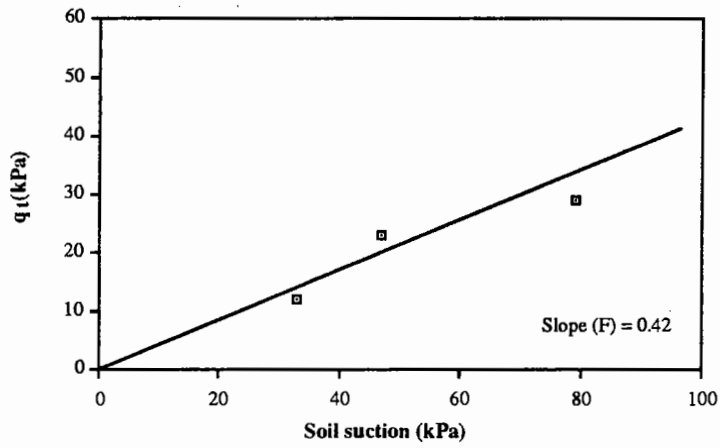
Figure 8.11b Relationship between q_t and soil suction for the Bothkennar clay samples
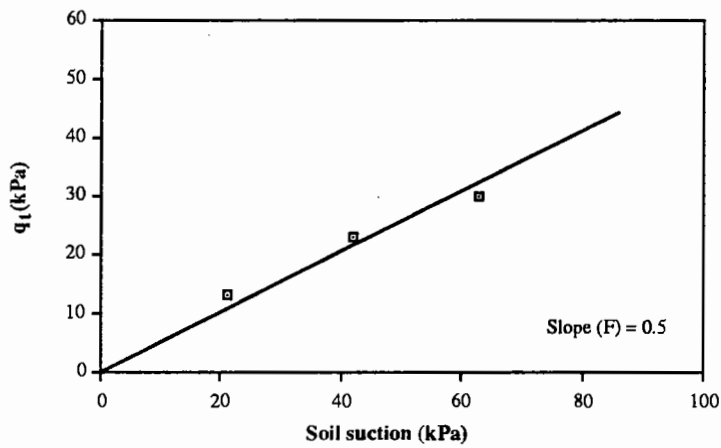
Figure 8.11c Relationship between q_t and soil sucion for the London clay samples
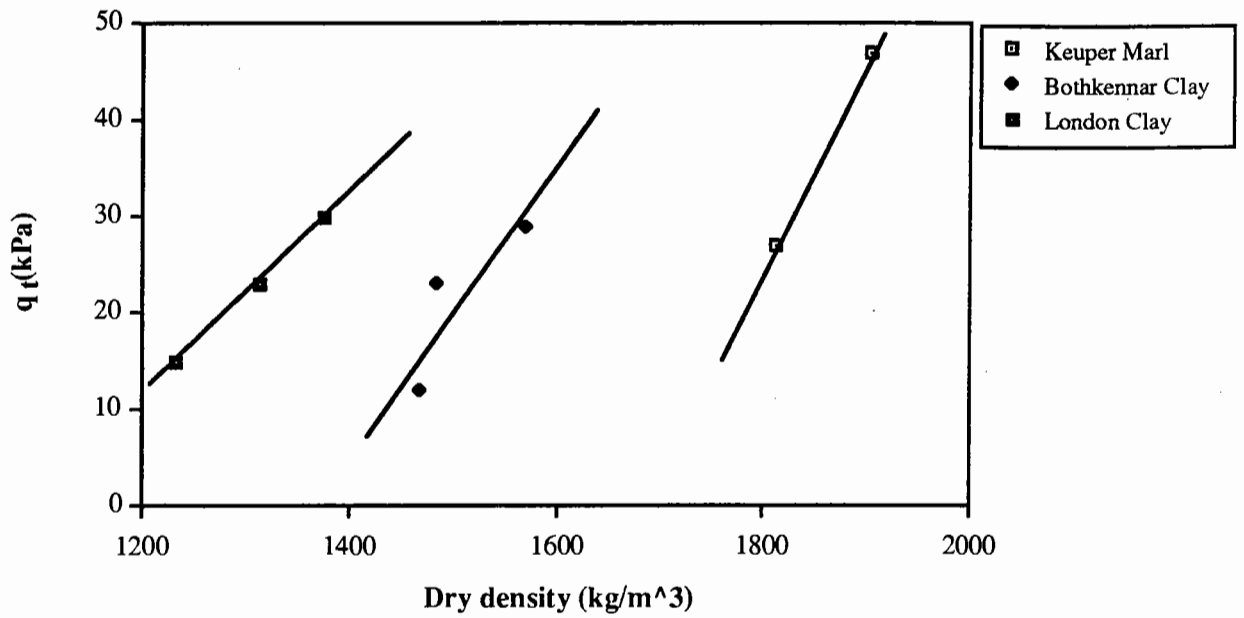
Figure 8.12 Effect of dry density on the value of q_t for the recompacted cohesive soils
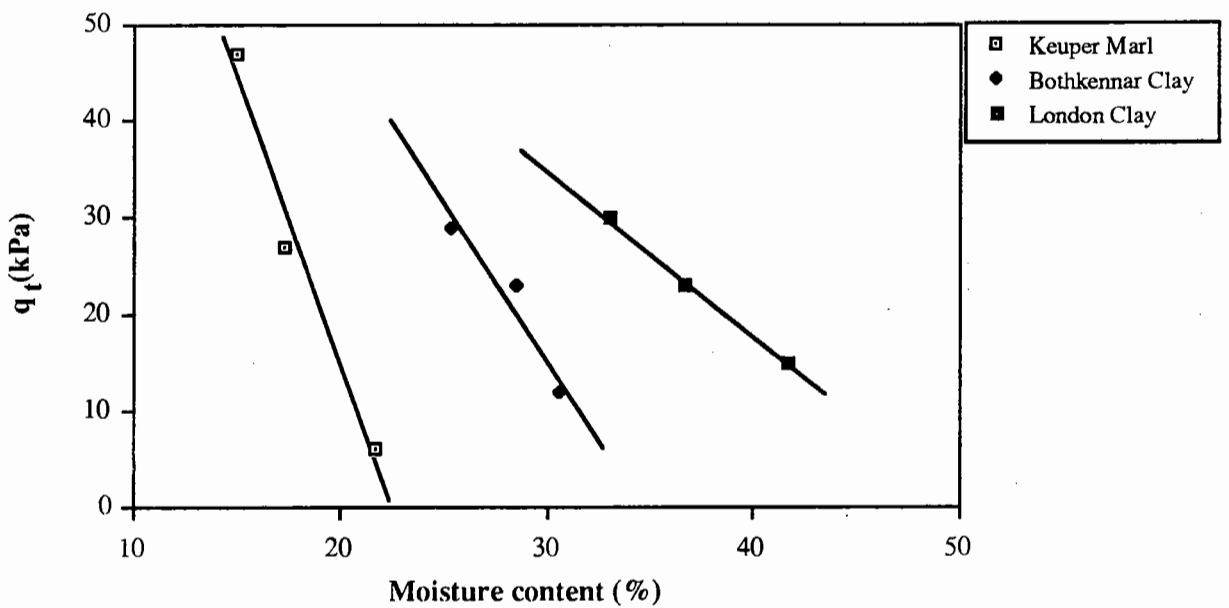
Figure 8.13 Effect of moisture content on q_t for the compacted cohesive soils

samples of higher moisture content were more susceptible to permanent deformation. This is in agreement with the observation made in the soil rut testing (Section 7.5.4).

Further discussion of the permanent deformation test results is made in Section 8.5.2 where the results from the "quick" tests are presented.

8.5.1.2 Resilient Deformation

In the following presentation, results obtained from the resilient tests with zero confinement will be discussed first. Discussions of the tests with non-zero cell pressure follow. The results of all the resilient deformation tests are summarized in Appendix Q.

At zero confinement

Figure 8.14 shows a typical plot of resilient strain produced under different magnitudes of deviator stresses at zero confining pressure. As expected, both the axial and radial strains increased non-linearly with the deviator stress. In Figure 8.15, the radial strains are plotted against the axial strain and a linear relationship between them is observed. Hence, the Poisson's ratio is unaffected by the deviator stress. However, it was observed that the Poisson's ratio decreased slightly when the suction of the compacted soil increased. Figure 8.16 shows the Poisson's ratio for the compacted samples. A general trend of decreasing Poisson's ratio with increasing suction, S, is seen. The equation to represent the trend is shown as follows:-

$$v = \beta S + \gamma \qquad (8.2)$$

where:- $\qquad \beta = -0.003$

$\qquad \qquad \gamma = 0.524$

$\qquad \qquad v = \text{Poisson's ratio}$

Too few samples were tested to assess the sensitivity of Poisson's ratio to deviator stress on the undisturbed soils.
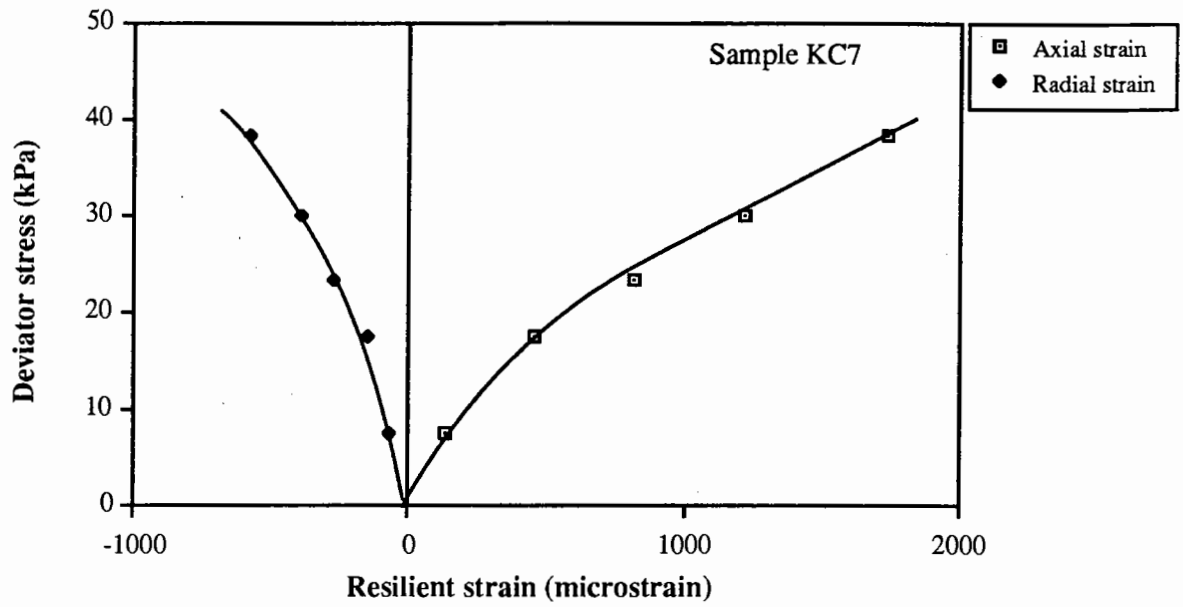
Figure 8.14 Typical resilient strain plot at zero confining pressure
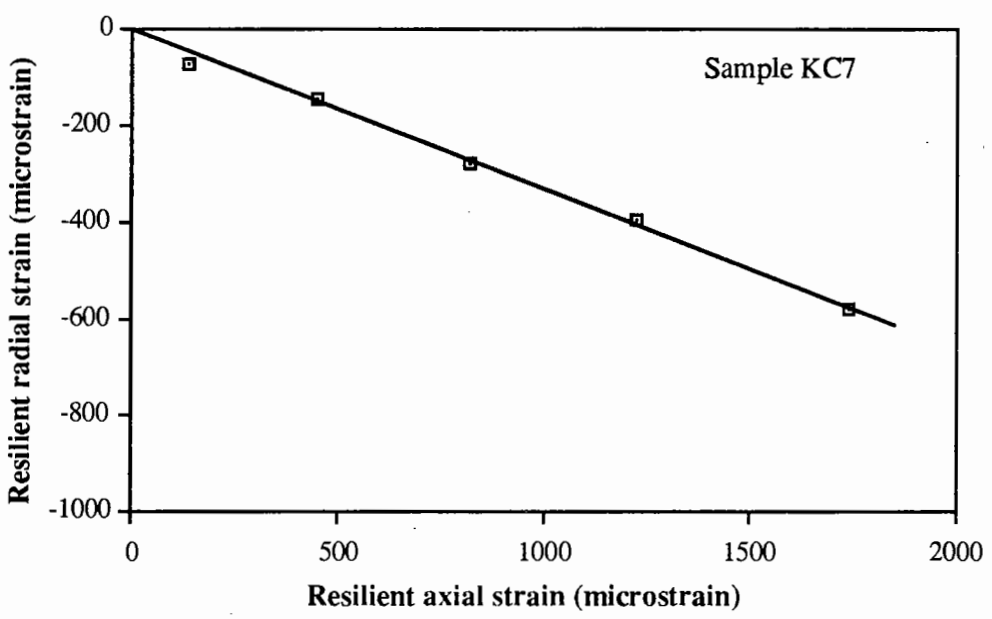
Figure 8.15 Typical relationship between resilient axial and radial strains
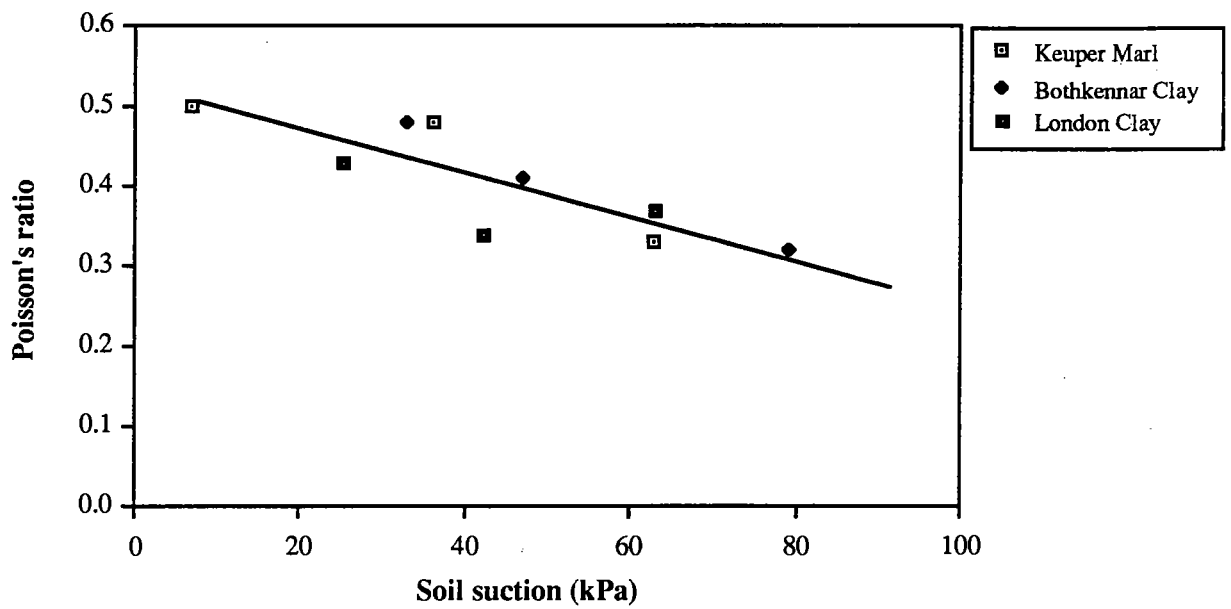
Figure 8.16 Relationship between the Poisson's ratio and the soil suction of the compacted samples

Figure 8.17 shows the axial strain contour plots for the three types of compacted soils. Linear contour lines radiating from a displaced origin seem to give the best fit to the data.

The general formula for such a relationship is:

$$\varepsilon_a = A(\frac{q_r}{S-C})^B$$

(8.3)

where:-　　　　A and B are dimensionless material parameters.

C is the value of the x-intercept in units of pressure.

ε_a is the resilient axial strain.

q_r is the magnitude of the repeated load.

This equation appears to be an improvement on that proposed by Loach (1987) in which, effectively, C equalled zero. Use of his equation was found to give a high level of scatter between predicted and observed axial strain (Figure 8.18).

The material constants of the compacted soils to suit Equation 8.3 are given in Table 8.6. The ability of Equation 8.3 to estimate the axial resilient response is shown in Figure 8.19. This is clearly an improvement over the Loach prediction.

Table 8.6　Material constants for resilient axial strain

Material	A	B	C (kPa)
Keuper Marl	4027	1.55	-4.7
Bothkennar Clay	13532	1.81	-15
London Clay	7319	1.63	-11.7
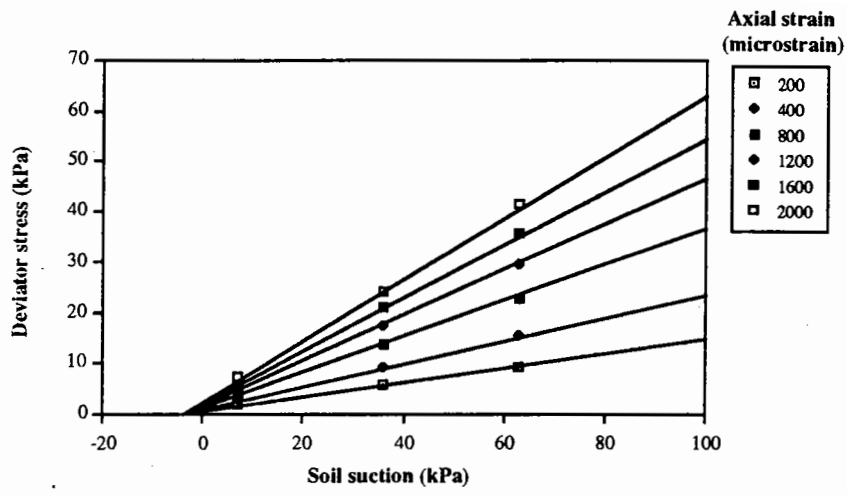
Figure 8.17a Strain contour plot for the Keuper Marl samples
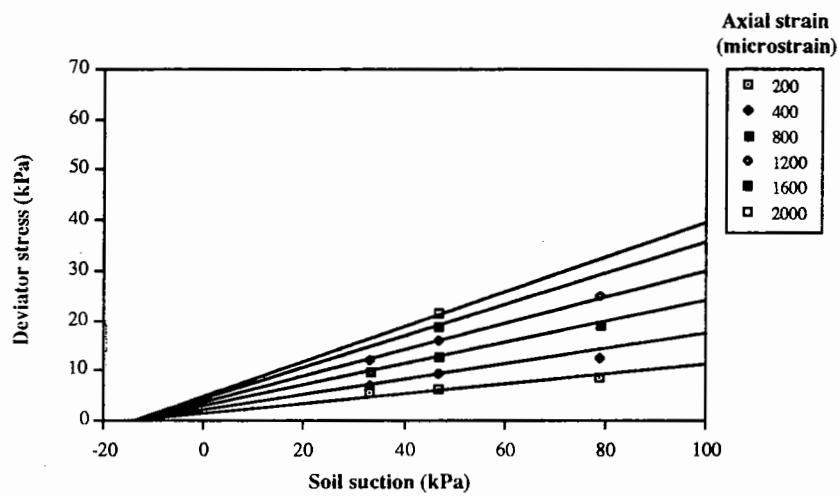
Figure 8.17b Strain contour plot for the Bothkennar clay samples
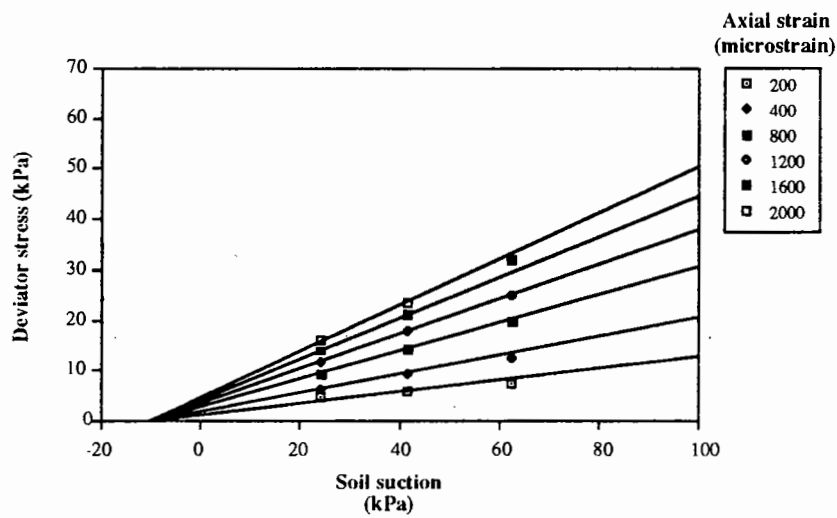
Figure 8.17c Strain contour plot for the London clay samples
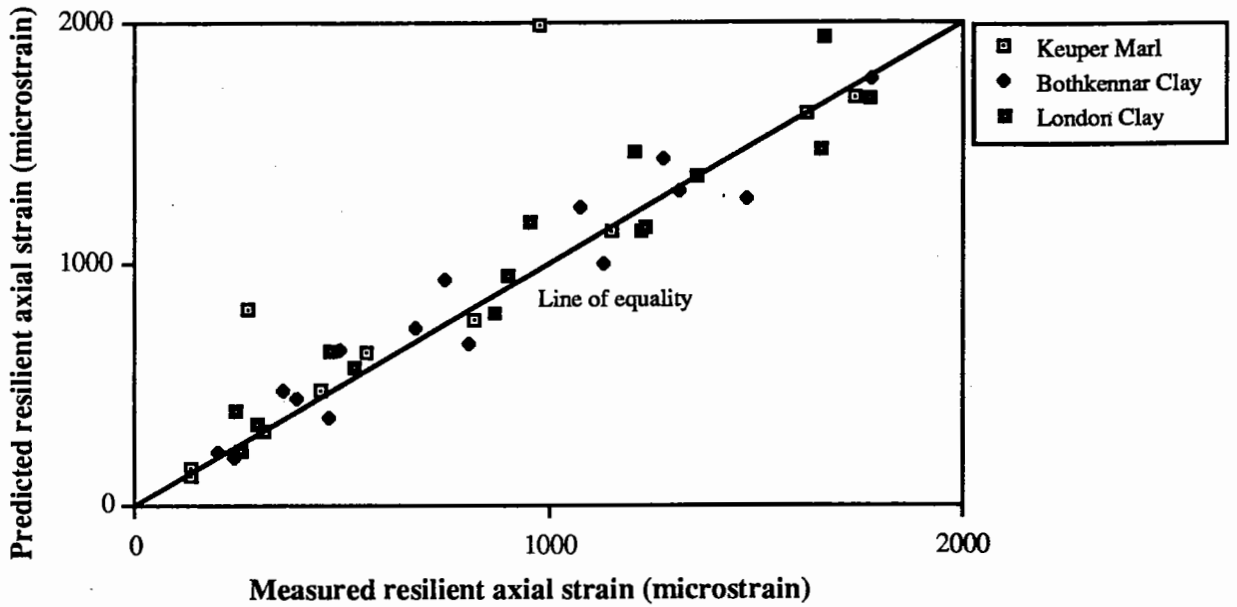
Figure 8.18 Comparison between the predicted (by Loach's equation) and

the measured resilient axial strains
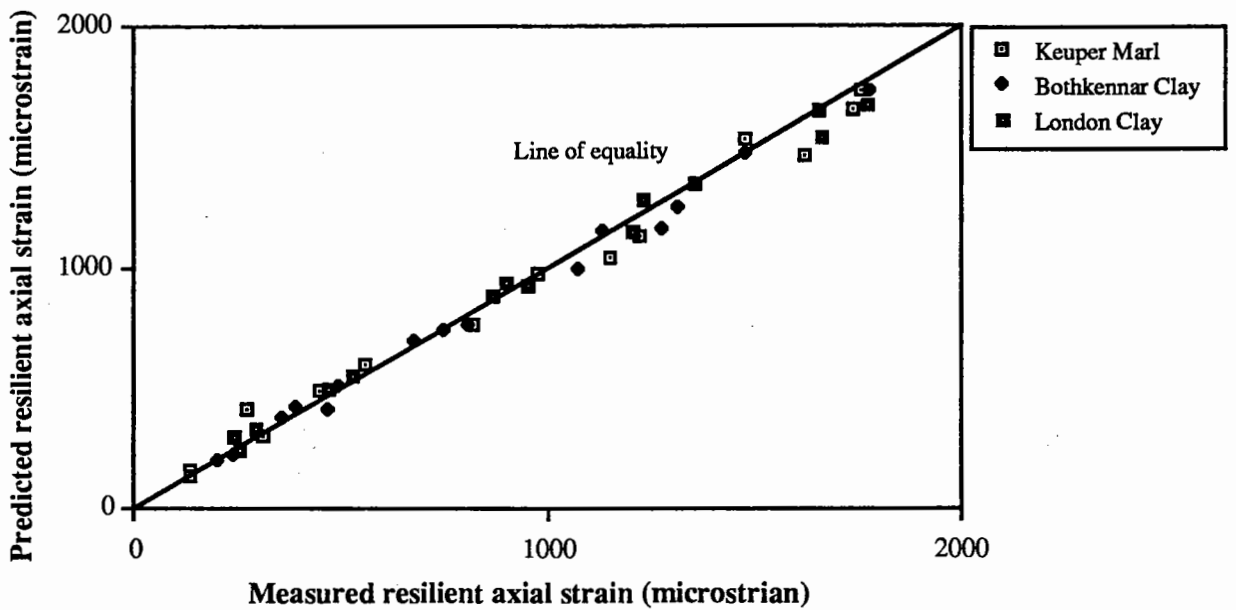
Figure 8.19 Comparison between the predicted (by Equation 8.3) and

the measured resilient axial strains

Since Equation 8.2 has provided a general relationship between the axial and the radial resilient strain, Equation 8.4 may be used to describe the resilient radial response of soils under load pulses.

$$\varepsilon_r = A(\frac{q_r}{S-C})^B \nu \qquad (8.4)$$

where:- ν is a variable Poisson's ratio determined from Equation 8.2.

ε_r is the radial resilient strain.

Figure 8.20 shows the predicted and actual resilient radial strains for the compacted materials. The data points scatter $\pm 20\%$ about the line of equality.

The constants recommended for the undisturbed materials are shown in Table 8.7. The values of A, B and C obtained from both the compacted and undisturbed soils were of similar magnitudes. Average Poisson's ratio of 0.5 and 0.47 were obtained for the materials from the Loughborough and the Bothkennar sites respectively.

Table 8.7   Constants for the undisturbed samples from sites

Material	A	B	C (kPa)	ν
Loughborough Clay	4083	1.73	-10	0.5
Bothkennar Clay	19352	1.21	-80	0.47

With non-zero cell pressure

Typical resilient axial and radial response of Keuper Marl, the London clay and the Bothkennar clay to repeated deviatoric stress pulses at different cell pressures are presented in Figure 8.21. For the Keuper Marl sample, the higher the cell pressure, the smaller the strain produced under the same deviator stress. The same phenomenon can be observed on the graph for the Bothkennar clay (Figure 8.21b) but the difference is smaller. For the London clay sample, there is even less effect of the cell pressure, all data points seems to merge into a narrow band although there is a slight increase of stiffness when the confining pressure increases.
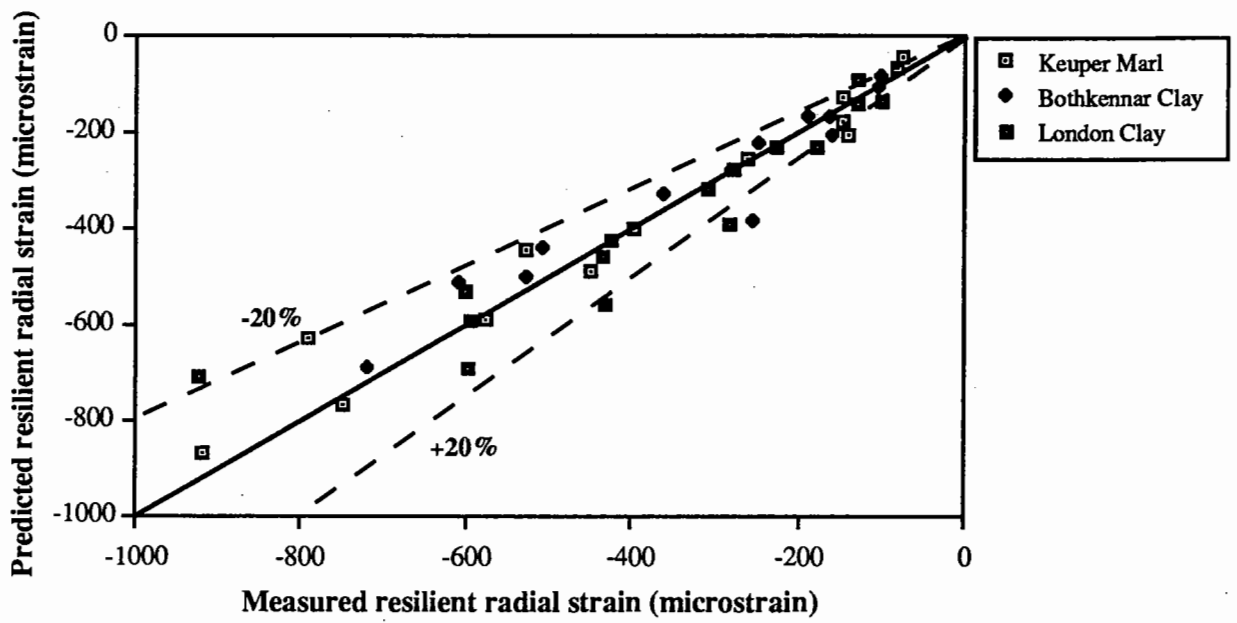
Figure 8.20 Comparison between the predicted (by Equation 8.4) and the measured radial strains
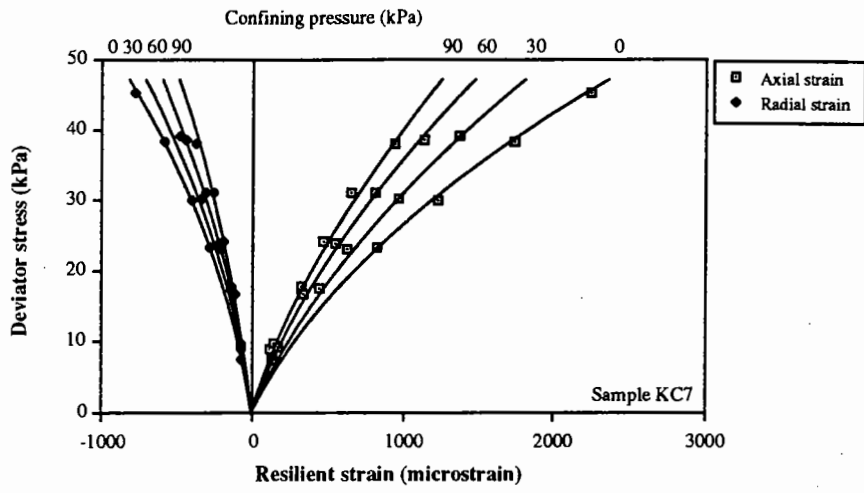
Figure 8.21a Typical deviator stress-resilient strain relationship at different constant confining pressures for Keuper Marl
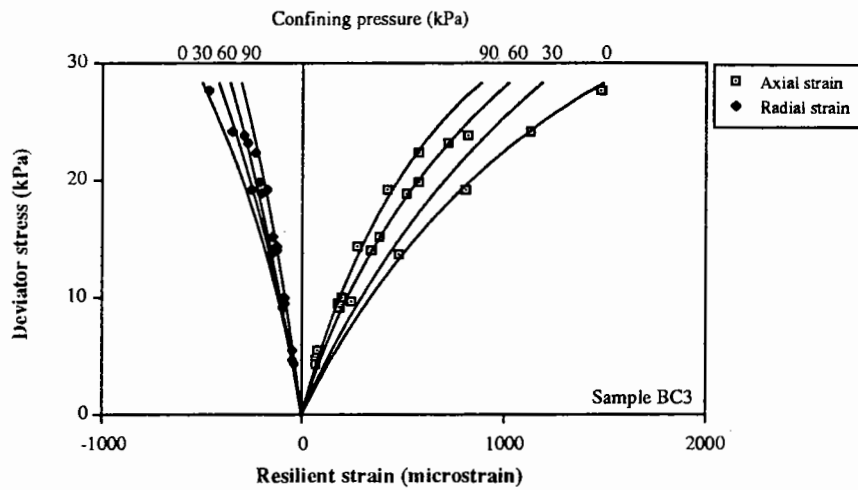
Figure 8.21b Typical deviator stress-resilient strain relationship at different constant confining pressures for the Bothkennar clay
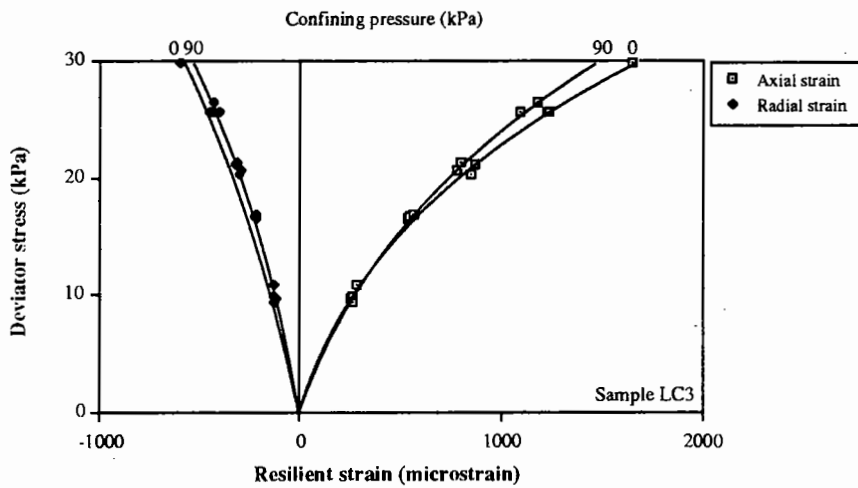
Figure 8.21c Typical deviator stress-resilient strain relationship at different constant confining pressures for the London clay

A plausible explanation can be made in terms of the effective stress theory. When the cell pressure increases, the normal effective stress in an unsaturated undrained sample will also increase. The relationship between the change of effective stress and the confining pressure has been discussed in Chapter 7. To derive the effective stress of the samples, which is the summation of the original soil suction and the change of suction due to the increase of the confining pressure, the soil compressibility factors (from Section 7.4.1) determined by the rapid suction apparatus were used.

The graphs showing the relationship between resilient strain and the derived effective stresses for the three types of compacted soils are presented in Figure 8.22. The contour lines used in Figure 8.17 for each soil type are superimposed onto these graphs. The results, in general, follow the related contour lines. Nevertheless, some of the results are found lying above the recommended contour lines particularly at high deviator stress levels. This may be attributed to a disproportionately smaller air volume being present in the suction test sample causing a slight over-estimation of the soil compressibility factor for samples of much larger quantity. For example the determined compressibility factor for the London clay was unity, yet Figure 8.21c clearly shows that there is a small compressibility effect. Taking into account the possible difference induced by the trapped air in the samples, these contour lines in the figures may be used to represent the test results when the confining pressures were applied. To include the effect of confinement, general formulae for resilient strains under repeated loads as shown from Equations 8.5 to 8.7 are suggested.

$$\varepsilon_a = A(\frac{q_r}{S-C+(1-\alpha)\sigma_3})^B \qquad (8.5)$$

$$v = \beta(S+(1-\alpha)\sigma_3)+\gamma \qquad (8.6)$$

$$\varepsilon_r = A(\frac{q_r}{S-C+(1-\alpha)\sigma_3})^B v \qquad (8.7)$$

where:-   A, B, C, β and γ are the same constants as those in Equations 8.2 to 8.4.

α is the soil compressibility factor determined by the suction test.

Figure 8.23 shows the predicted and the measured resilient responses for the axial strain and the radial strain. Most of the predicted values of both the axial and radial
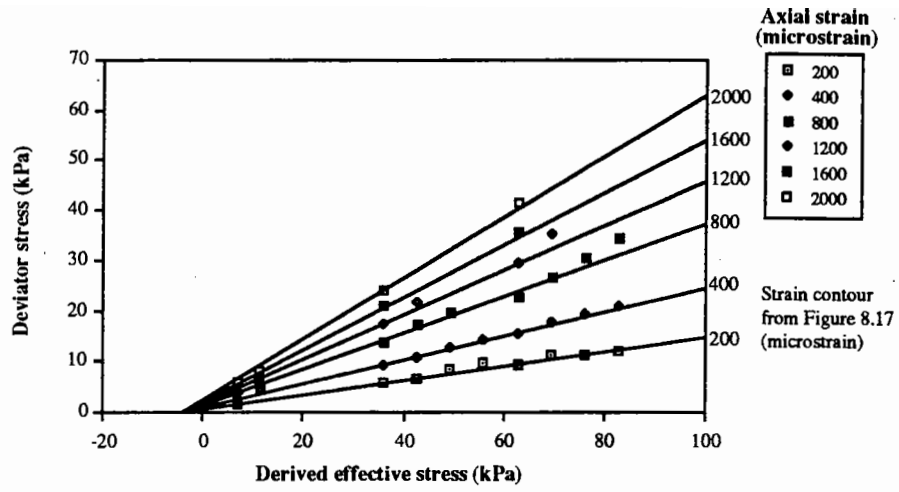
Figure 8.22a Comparison between strain contours and results obtained from confining tests for the Keuper Marl samples
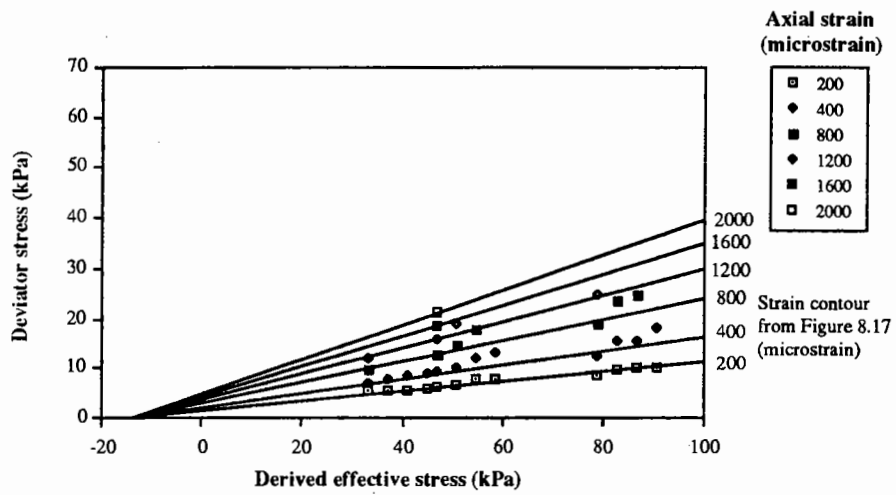
Figure 8.22b Comparison between strain contours and results obtained from confining tests for the Bothkennar clay samples
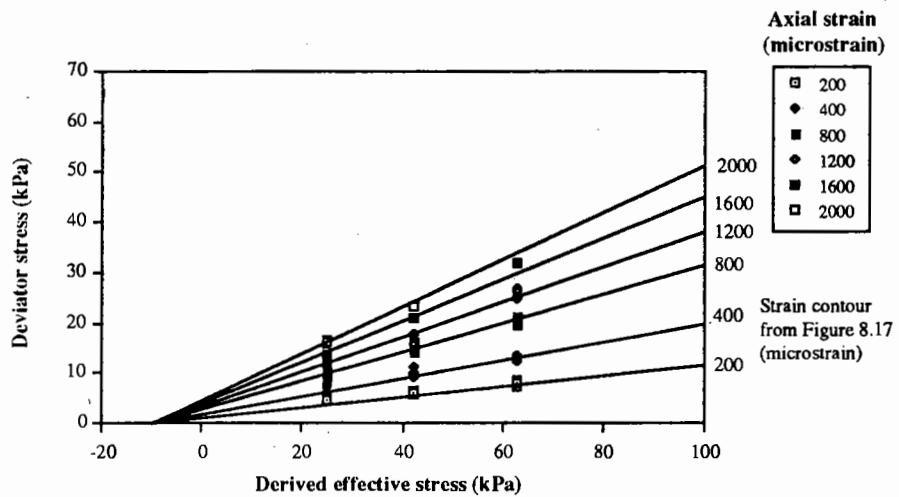
Figure 8.22c Comparison between strain contours and results obtained from confining tests for the London clay samples
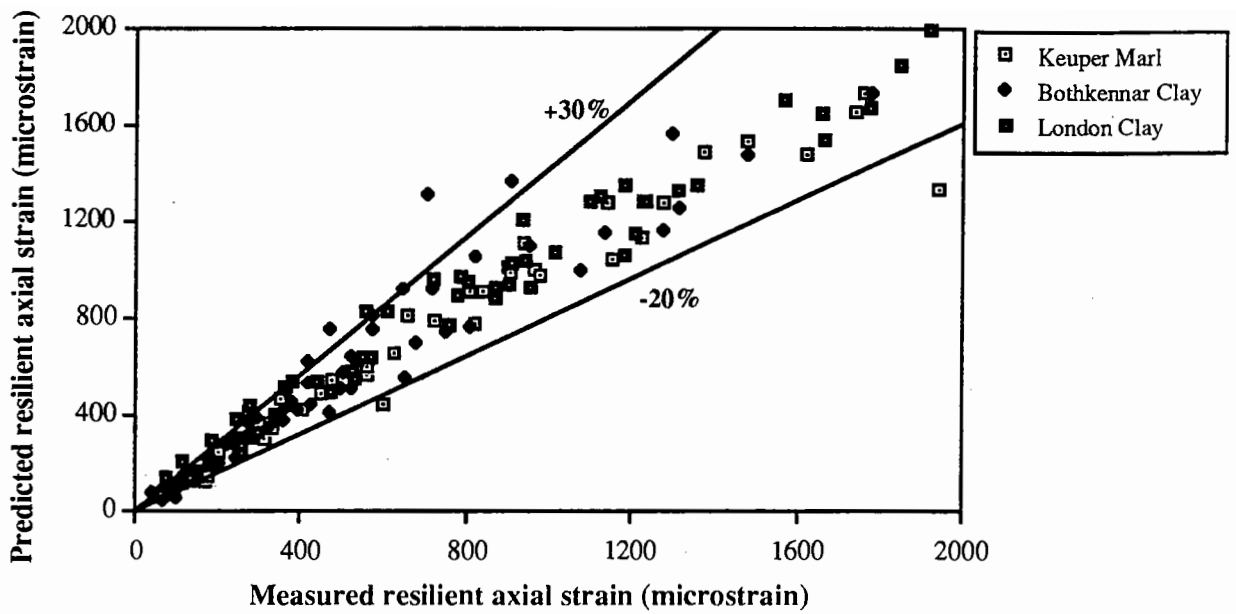
Figure 8.23a Comparison between the predicted (by Equation 8.5) and the measured

resilient axial strains
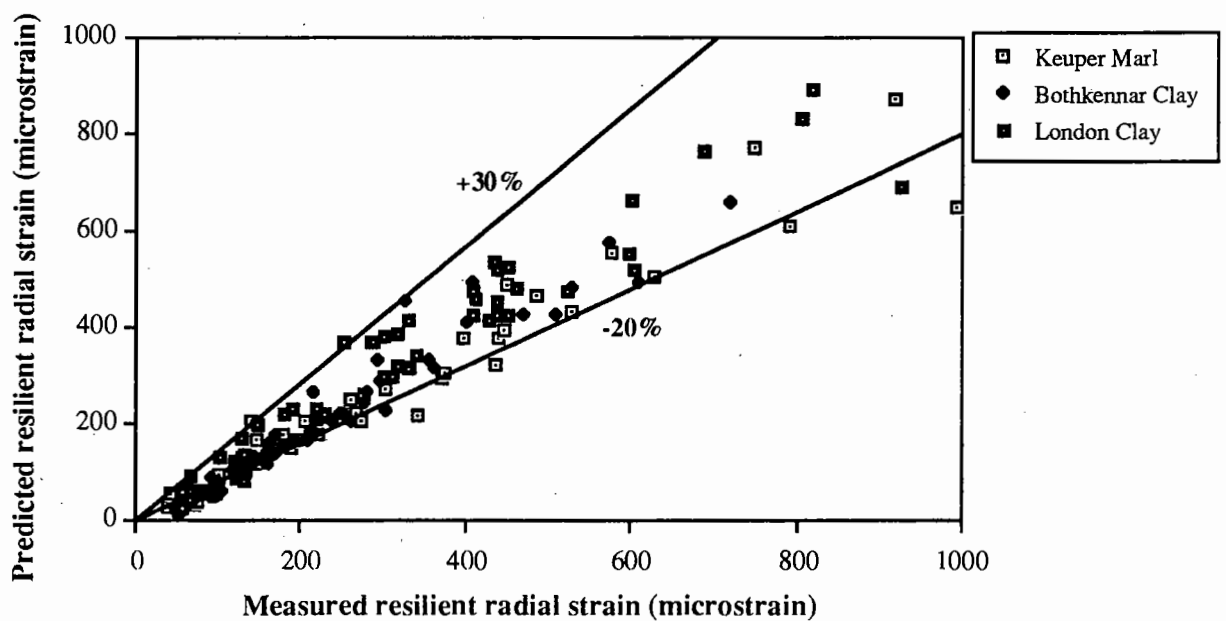
Figure 8.23b Comparison between the predicted (by Equation 8.7) and the measured

resilient radial strains

strains fall into the + 30% and -20% zone of the measured results. Therefore, the average predicted values was about 5% higher than the measured one. This is in agreement with the observations made in Figure 8.22 that some of the results were found lying above the contour strain lines. It follows that the predicted values slightly over-estimate the measured results.

Effect of material conditions

Figures 8.24 and 8.25 show the effects of the dry density and the moisture content on the resilient behaviour of soils. Within a soil type, samples of a higher density or a lower moisture content were stiffer. These observations agree with Kirwan et al's (1982) findings.

8.5.1.3   Strength

The strength of samples was determined by three types of strength test: uniaxial compression in the triaxial cell, shearing with a shear vane and probing with a hand penetrometer. The results are given in Table 8.8.

Comparison between the different measures of strength is presented in Figure 8.26. Broadly, linear relationships between the results, with the data points scattered along the line of equality, can be observed. A similar observation on the relationship between results of the compressive test and of the shear vane test was made by Wilson (1963) on cohesive soils. Thus any measure may be used to predict the other with reasonable accuracy.

For the uniaxial compression test, the upper limit of the axial strain was set at 20% as recommended by B.S. 1377 (1990). It was observed that for specimens which had failed before this limit, discrete failure planes or signs of distressed shear surfaces were formed. Otherwise, specimens were in a barrel shape at an axial strain of 20% and were undergoing progressive failure. Typical loading curves representing the different failure modes are given in Figures 8.27, 8.28 and 8.29. In all cases, little deformation was initially observed. The rate of straining increased after the initial period. For samples which failed with a discrete failure plane, as shown in 8.29, there was a sudden drop of axial stress recorded by the load cell when the failure took place. The stress-strain curve in Figure 8.28 is for a sample which failed only with some signs of
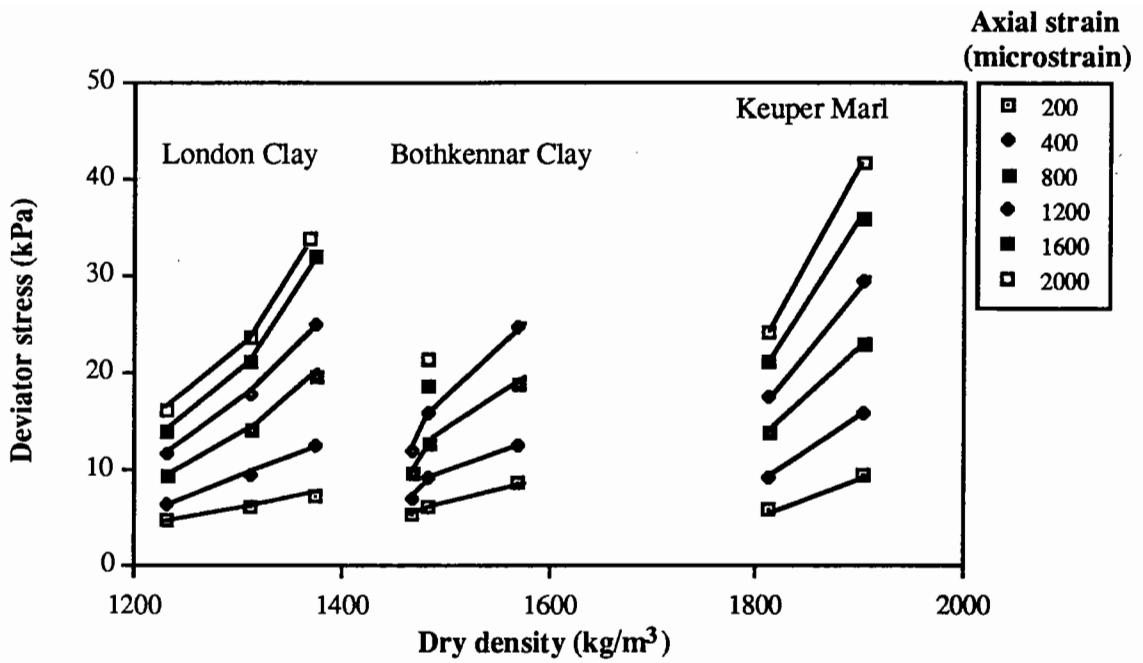
Figure 8.24 Effect of dry density on the resilient properties of the cohesive soils
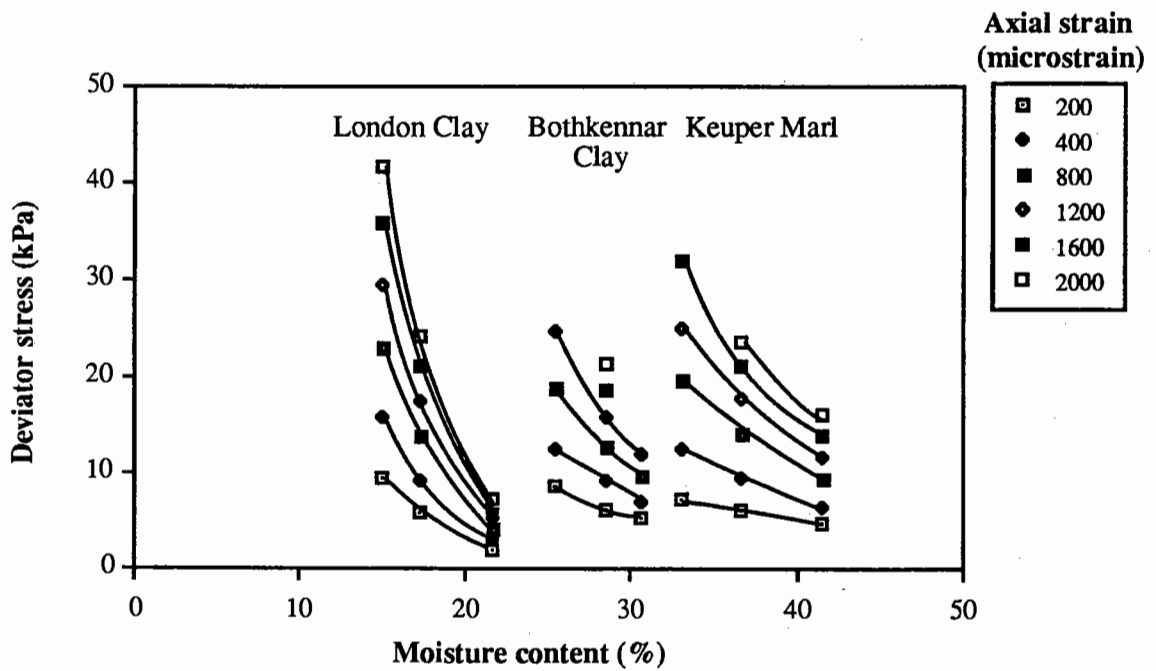
Figure 8.25 Effect of moisture content on the resilient properties of the cohesive soils
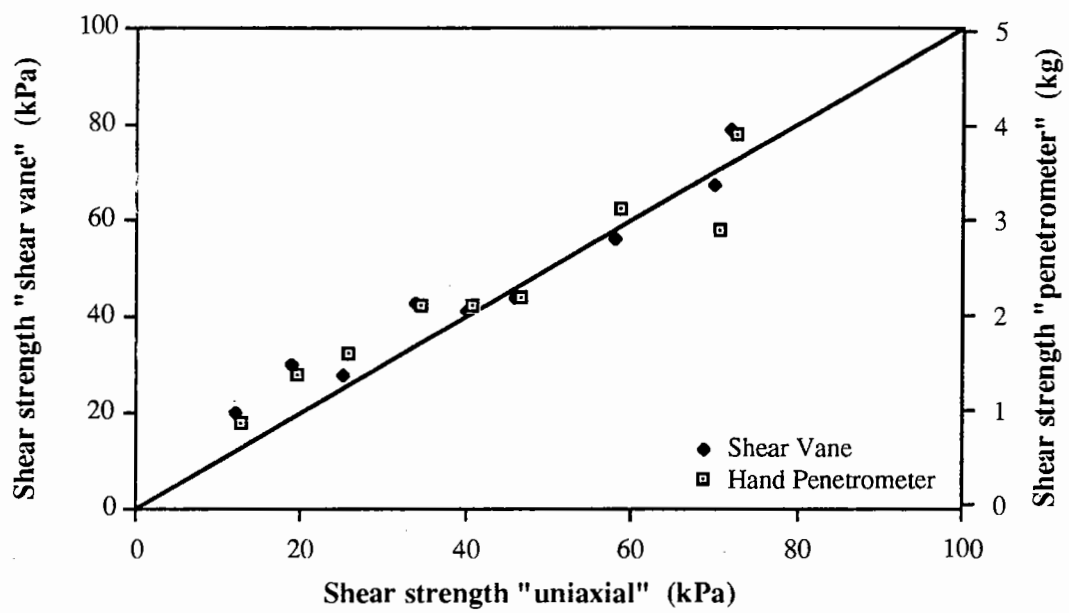
Figure 8.26 Comparison of shear strength between results obtained from uniaxial compressive test and from other methods
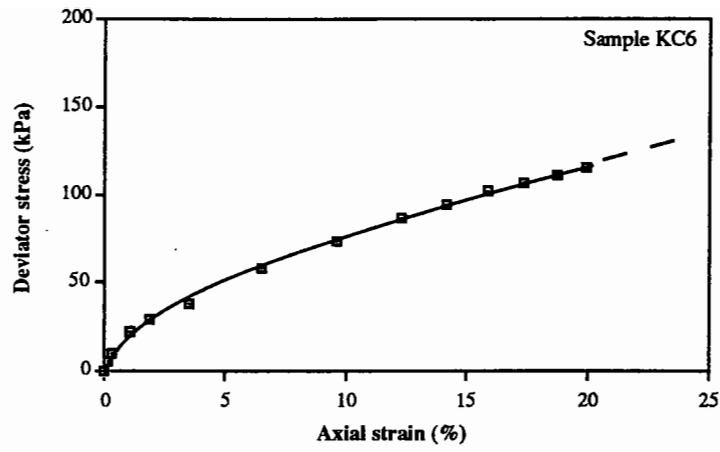
Figure 8.27 Typical plot of continuous failure without a maximum deviator stress value
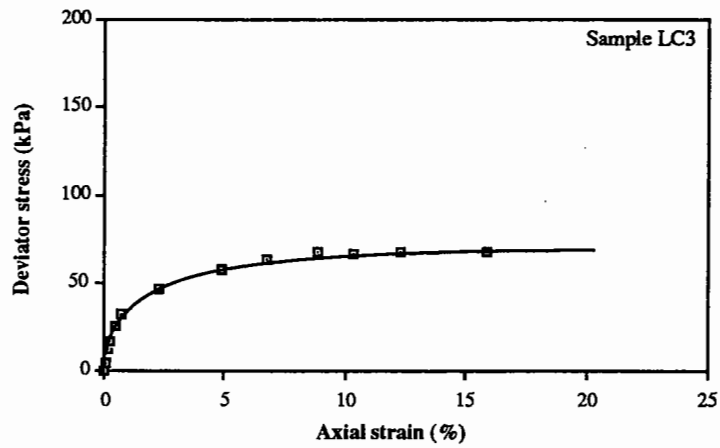
Figure 8.28 Typical plot of continuous failure with a maximum deviator stress value
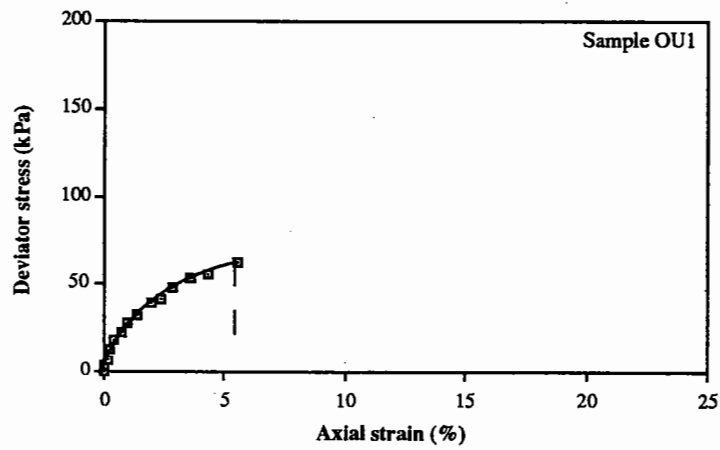
Figure 8.29 Typical plot of sudden failure

distressed shear surfaces. In this case, a peak stress is shown. For samples showing progressive failure and no sign of forming shear planes, the axial stress continued to grow even when 20% axial strain was reached (Figure 8.27).

Table 8.8   Strength test results (with soil suction value)

Sample	Soil suction	Uniaxial compression		Shear vane	Hand penetrometer
	(kPa)	Axial strain (%)	Shear strength (kPa)	(kPa)	(kg)
KC1	20	20	40	41	2.1
KC2	27	20	46	44	2.2
KC3	44	20	70	67	2.9
KC4	59	-	-	120	6.6
KC5	7	-	-	17	1
KC6	36	20	58	56	3.1
KC7	63	-	-	122	6.3
BC1	33	20	25	28	1.6
BC2	47	-	-	68	3
BC3	79	20	72	79	3.9
LC1	25	19	12	20	0.9
LC2	42	15	19	30	1.4
LC3	63	16	34	43	2.1
OU1	39	5.5	31	-	-
BU1	21	4	80	82	3.9
BU2	3	18	32	32	1.6

It was also observed that for each material type, the shear strength value increased with the soil suction. These soil data are reproduced in graphic form and presented in Figure 8.30. Although only limited data are available, straight lines radiating from the origin may be inserted onto the graph to represent the results from the compacted samples. Hence, for a compacted soil the relationship between the soil suction and the shear strength can be expressed as:-
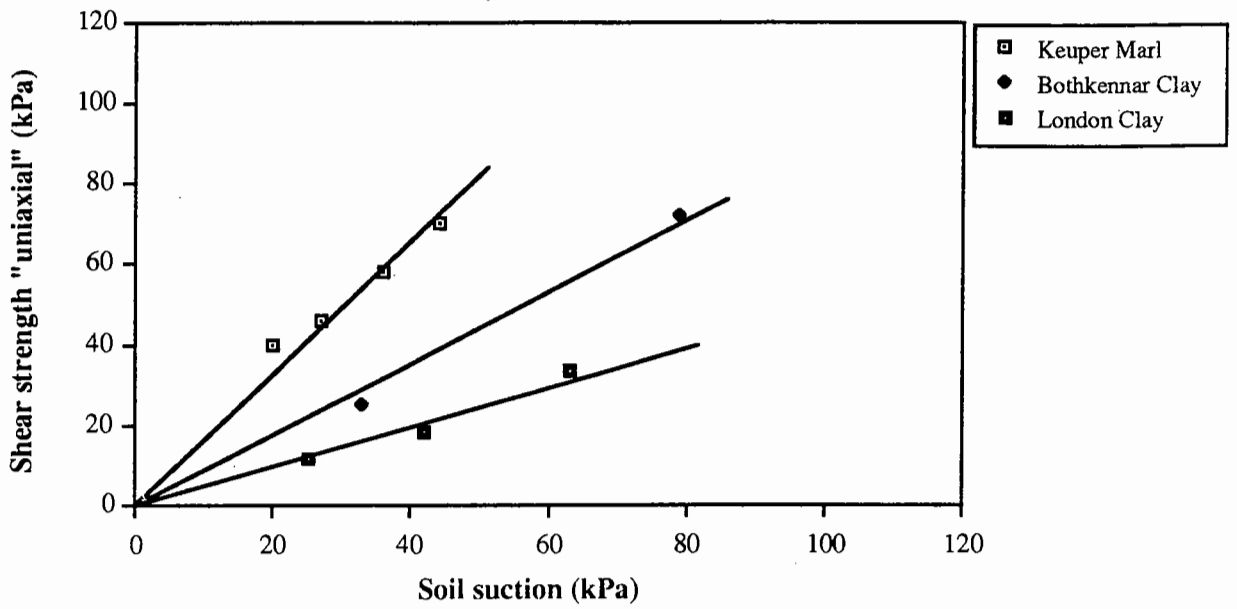
Figure 8.30 Relationship between shear strength and soil suction of the compacted soils
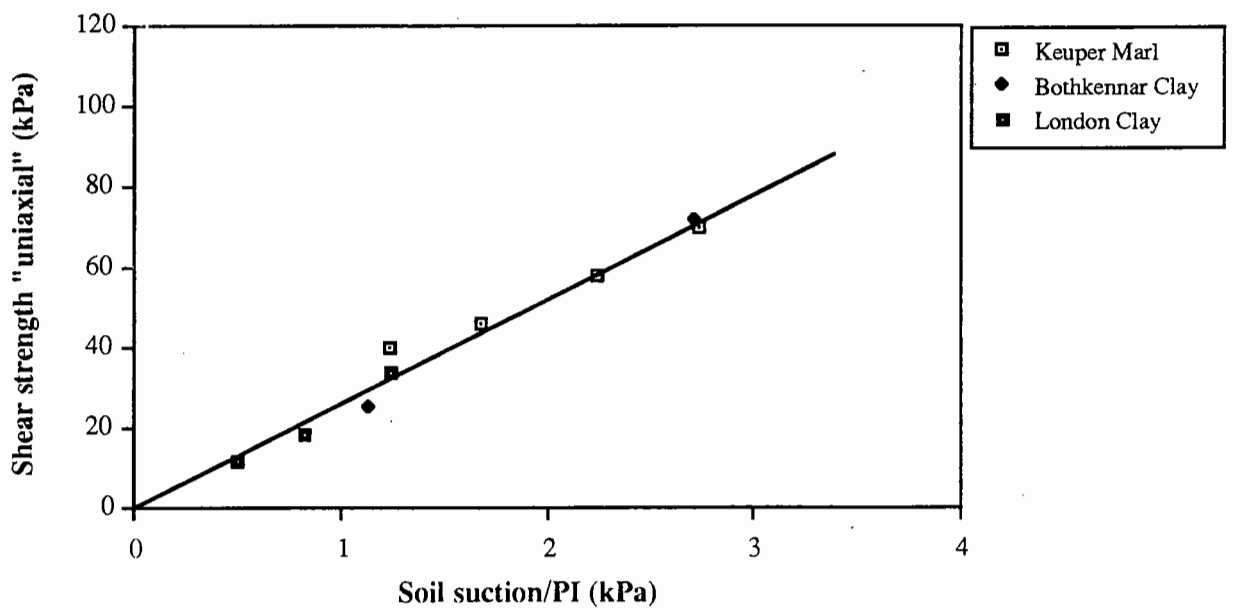
Figure 8.31 Relationship between shear strength and normalized soil suction

of the compacted soils

$$Cu = t \ S \qquad\qquad (8.8)$$

where:-   t is a constant.

Cu is the unconfined undrained shear strength from uniaxial compression test in kPa.

Table 8.9 lists the calculated "t" values for the compacted samples and indicates that the value decreases with the plasticity of the material. The plasticity of the London clay was very high, it possessed the lowest value. Keuper Marl had the lowest plasticity among the three materials, its t value was the highest. Similar results showing that the shear strength of soils of high plasticity was less sensitive to the change of soil suction were also reported by Croney (1977). Attempts were made to normalise the soil suction values by the plasticity index of the materials. The resulting graph is plotted as Figure 8.31. It can be noticed that all data points from the compacted samples fall onto a line. Hence, if the plasticity index can be used as the normalisation factor, then Equation 8.8 can be re-written as:-

$$Cu = T \ \frac{S}{PI} \qquad\qquad (8.9)$$

where:-   T is found to be 26.4.

PI is the plasticity index of the soil.

Since insufficient data are available for the undisturbed materials from site, no recommendations are made for these soils.

Table 8.9   Ratio between shear strength and suction

Material	t
Keuper Marl	1.7
Bothkennar Clay	0.9
London Clay	0.5

Effect of material strength on stiffness

To understand the effect of shear strength on the resilient behaviour of soils, the independent parameter of soil suction in Equation 8.3 was substituted by the suction

term from Equation 8.9. Hence, the unconfined material stiffness, M_r, can be expressed as:-

$$M_r = \frac{1}{A} q_r^{1-B} \left(\frac{Cu \, PI}{T} - C\right)^B \qquad (8.10)$$

Since the value of B is always larger than 1 (Table 8.6), this implies that stiffnesses decrease non-linearly with increasing q_r. The same observation, indeed, had been made by Brown (1967) and Hyde (1974) (refer to Chapter 2). The fact of B value greater than unity also indicates that soil stiffnesses increase with material strength. Based on Equation 8.10, Figure 8.32 presents the relationship between stiffness and strength for the three types of soil. It shows that the stiffnesses of soils increase non-linearily with the shear strengths of the materials. When the magnitude of the repeated loading is low (i.e. $q_r = 20$ kPa), the rate of increase of soil stiffness with respect to strength is much more significant than that at high deviator stress (i.e. $q_r = 100$ kPa). Effect of material type can also been seen when the curves in these three graphs are compared. In general, when the strength of soil is similar, the one with a higher plasticity possess higher stiffness and vice versa.

8.5.2 "Quick" test

Development of vertical permanent deformation during the "quick" test is presented in Figure 8.33. As expected, strain development is broadly linear when considered against a logarithmic base indicating that most of the strains were generated in the early part of the tests. Also, the higher the deviator stress to soil suction ratio of the sample, the more strain was produced. There was, however, a limit to the number of cycles which may be applied at high load level. A sample of London clay was found to collapse after ten cycles of repeated loading at a deviator stress of 65 kPa (about 1.6 times the suction value of the sample). Hence, a maximum ratio of 2 between deviator stresses and soil suctions, suggested by Brown and Dawson (1992) for the design of the subgrade of pavement foundation during construction, may be optimistic.

It is worth noting that the slopes, K, of the lines in Figure 8.33 increase with the amount of plastic strain, i, generated at the first cycle. The larger the plastic strain generated at the first cycle by a particular load pulse, the higher is the rate of the subsequent permanent deformation development. Table 8.10 shows the K and i values, together with their ratio, M, for the two soils.
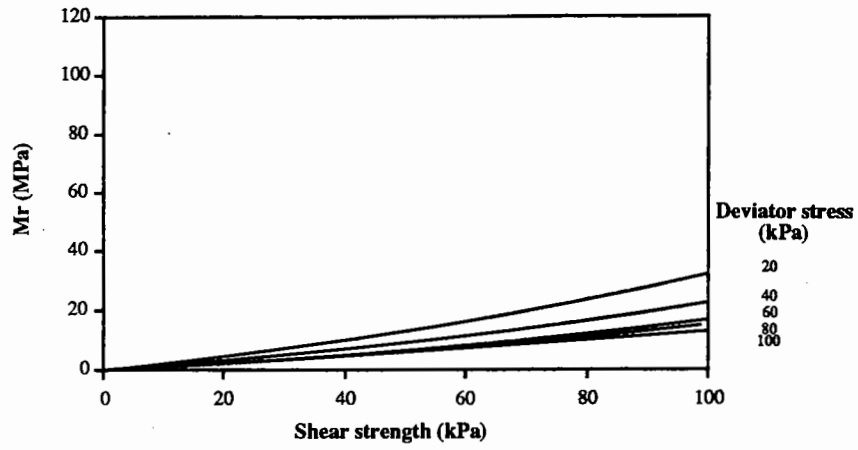
Figure 8.32a Predicted relationship between the resilient stiffness and the shear strength of Keuper Marl
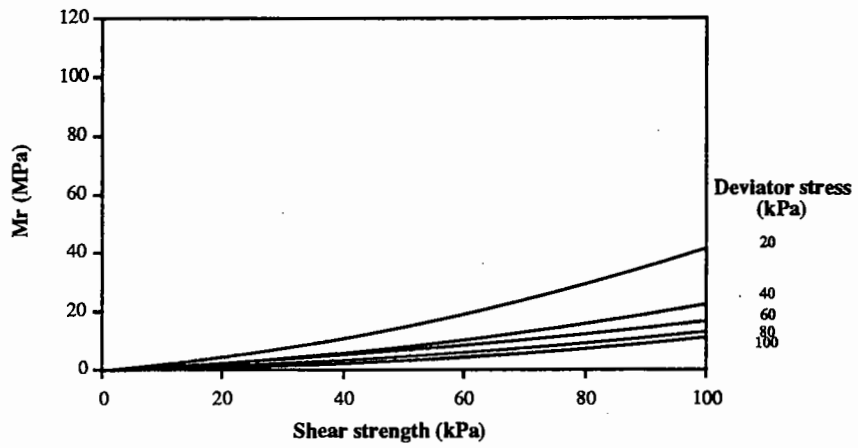
Figure 8.32b Predicted relationship between the resilient stiffness and the shear strength of the Bothkennar clay
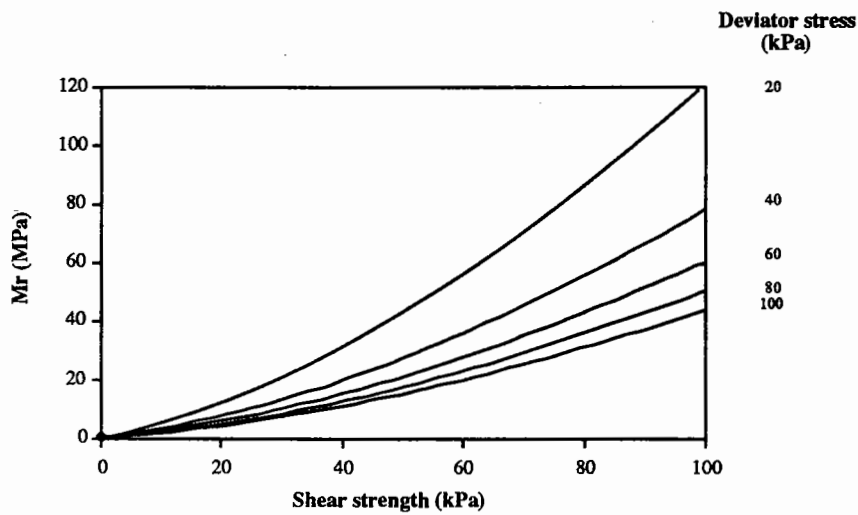
Figure 8.32c Predicted relationship between the resilient stiffness and the shear strength of the London clay
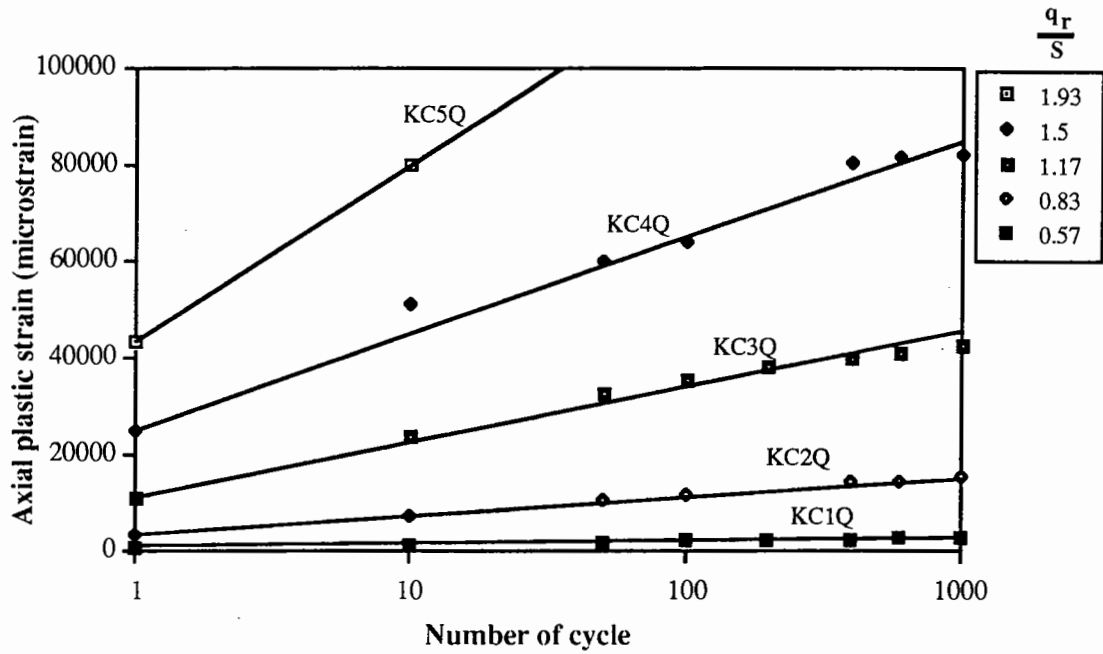
Figure 8.33a Development of axial plastic strain of Keuper Marl
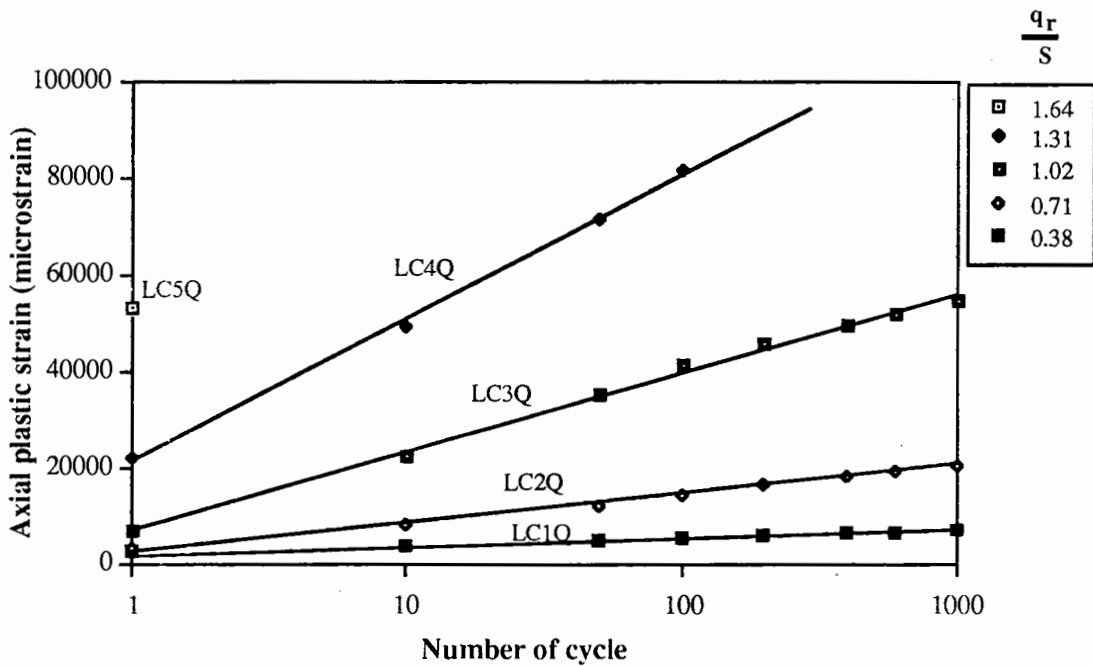
Figure 8.33b Development of axial plastic strain of the London clay

It has been observed in Section 8.5.1.1 that the development of permanent deformation is a function of deviator stress to soil suction ratio. Figure 8.34 indicates that the rate of the axial permanent deformation accelerates with this ratio.

Comparison between results of "quick" test and multi-stress path test

Figure 8.35 presents the "quick" test results together with the permanent deformation data from the most similar multi-stress path samples, KC3 for Keuper Marl and LC2 for the London clay. It is noticed that the two sources of data seem to fit in well with each other. This suggests that the repeated loads applied at smaller deviator stress magnitudes in the early part of the multi-stress path tests did not have a significant effect on the overall amount of permanent deformation formed. Hence, the total accumulated plastic strain, due to 1000 load repetitions, obtained at the end of a test with or without preceding repeated loading at lower stress levels will be similar.

Table 8.10
Permanent deformation parameters obtained from the "quick" test

Sample number	K	i	M = K/i
KC1Q	697	625	1.1
KC2Q	4153	3172	1.3
KC3Q	10534	12995	0.8
KC4Q	19492	27049	0.7
KC5Q	56771	53349	1.1
			average = 1.0
LC1Q	1462	2781	0.5
LC2Q	5805	3014	1.9
LC3Q	16298	7487	2.2
LC4Q	28925	21833	1.3
LC5Q	-	-	-
			average = 1.5
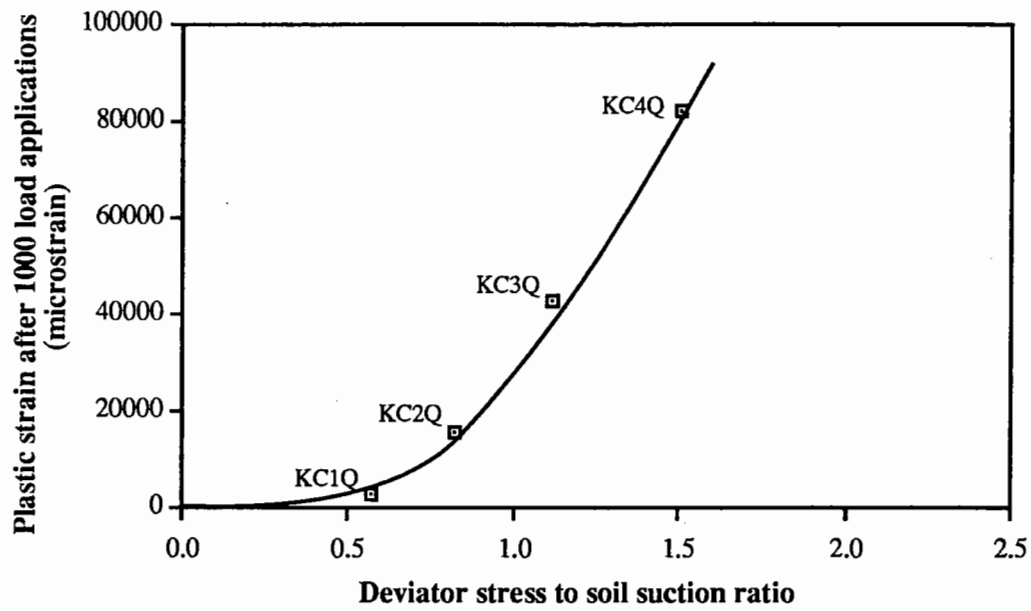
Figure 8.34a Relationship between plastic strain after 1000 load applications and deviator stress to soil suction ratio of Keuper Marl (linear scale)
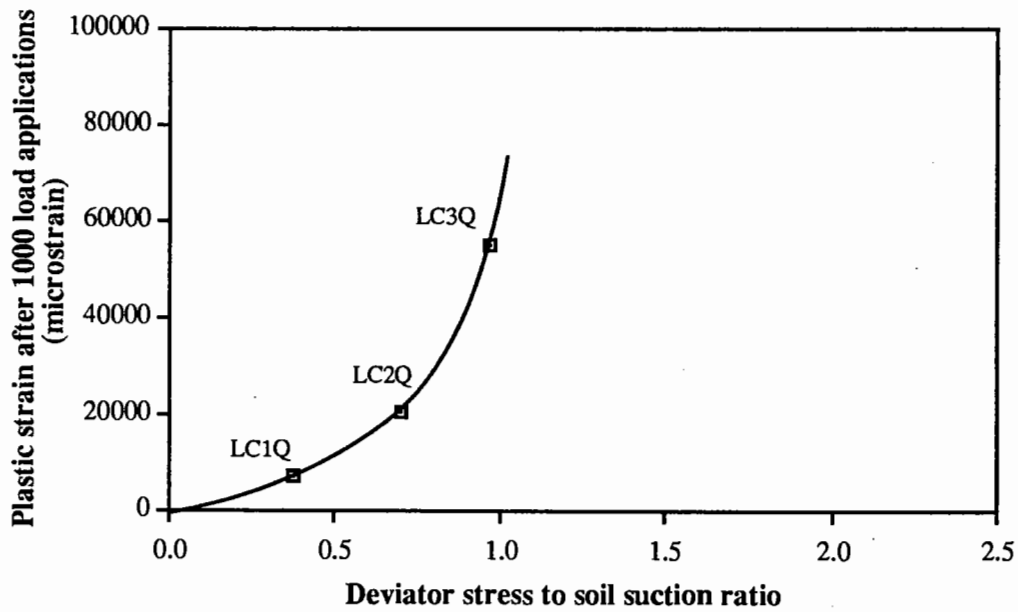
Figure 8.34b Relationship between plastic strain after 1000 applications and deviator stress to soil suction ratio of the London clay (linear scale)
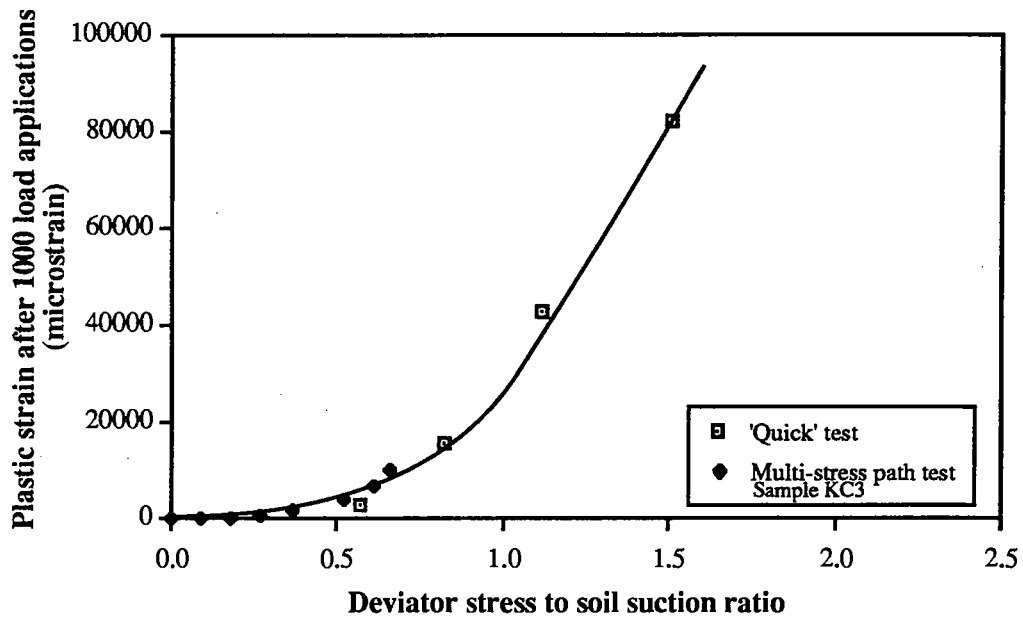
Figure 8.35a Comparison of plastic strain obtained from the 'quick' test and the multi-stress path test of Keuper Marl
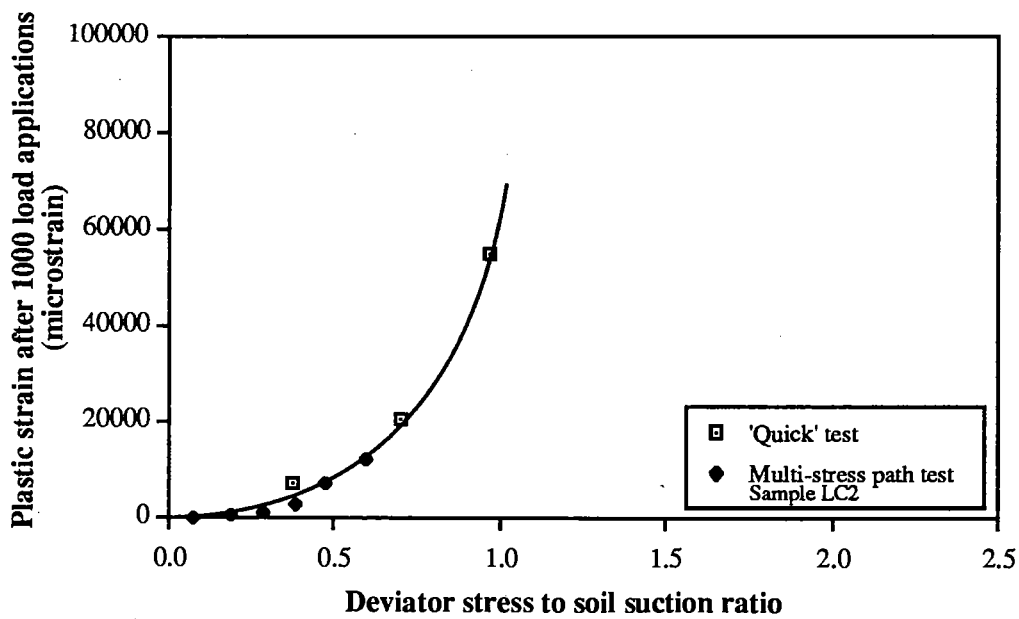
Figure 8.35b Comparison of plastic strain obtained from the 'quick' test and the multi-stress path test of the London clay

Relationship between permanent deformation, stresses and numbers of cycles

When the data is replotted as in Figure 8.36, it is seen that the relationship between the permanent deformation and the deviator stress to soil suction ratio can be expressed by:-

$$\varepsilon_p = d(\frac{q_r}{S})^e \qquad (8.11)$$

where:- d and e are material constants.

Attempts have been made to find a general formula to show the interrelationship between the permanent deformation generated under repeated loads, the deviator stress-suction ratio and the number of repetitions. Using the observations made in Figure 8.33, it is suggested that:-

$$\varepsilon_p(N) = D(\frac{q_r}{S})^E (\log(N) + F) \qquad (8.12)$$

The constants, D, E and F for the Keuper Marl and the London clay are presented in Table 8.11. Details of the derivation of the formula are included in Appendix R.

Table 8.11   Material constants for permanent deformation

Material	D	E	F
Keuper Marl	6323	2.78	1.00
London Clay	16889	2.98	0.75

Figure 8.37 compares the predicted and the actual permanent deformation measured by the "quick" test. Predictions based on Equation 8.12 are reasonable, suggesting that the "quick" test may provide a useful predictive tool for permanent deformation. Since the number of cycles used in the tests was only 1000, it is recommended that further tests are required to confirm the applicability of the equation for predicting permanent deformation for higher numbers of cycles.
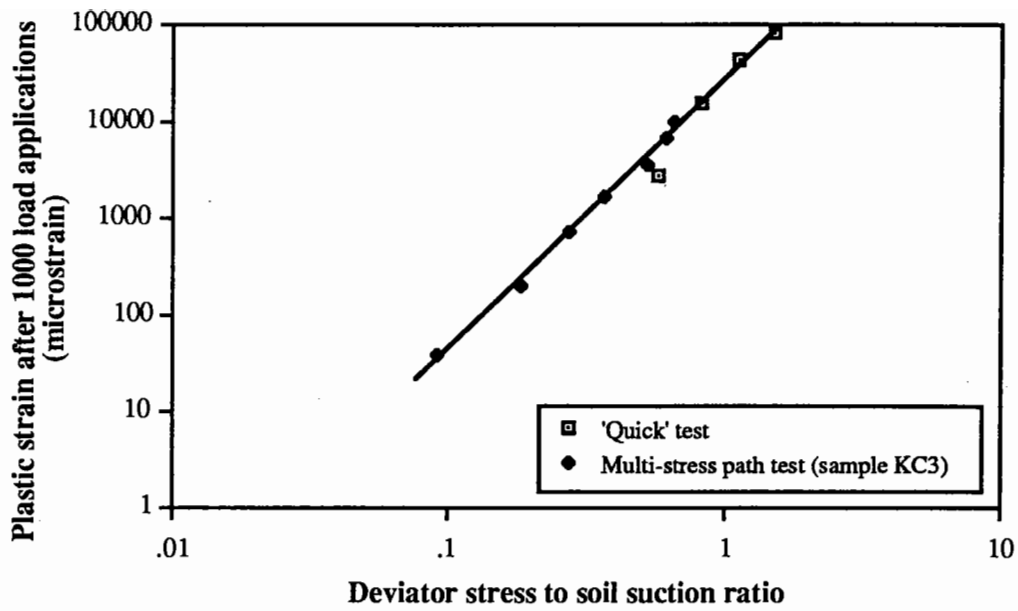
Figure 8.36a Plot of plastic strain after 1000 load applications against deviator stress to soil suction ratio for Keuper Marl (logarithmic scale)
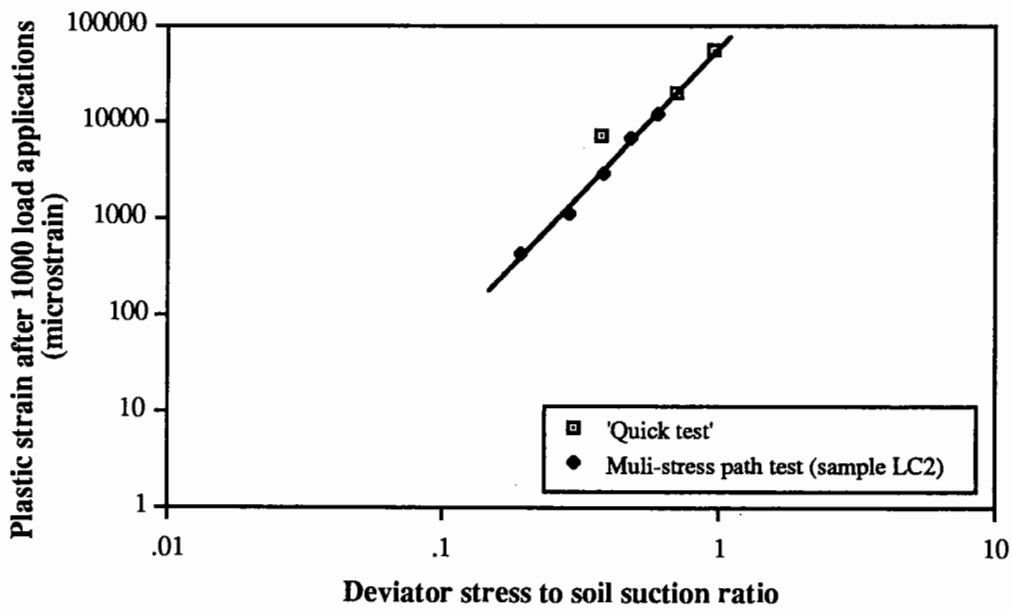
Figure 8.36b Plot of plastic strain after 1000 load applications against deviator stress to soil suction ratio for the London clay (logarithmic scale)
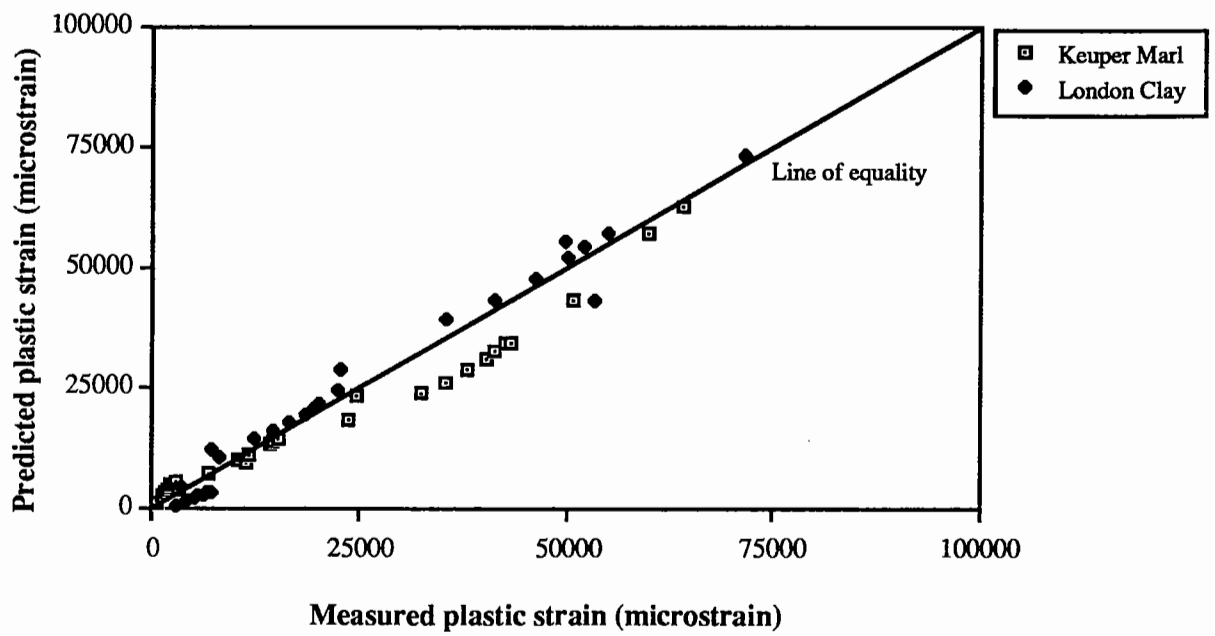
Figure 8.37 Comparison between the predicted and the measured plastic strains

<u>Effect of material strength on permanent deformation</u>

To understand the effect of shear strength on the permanent deformation behaviour of soils, the soil suction term in Equation 8.12 was replaced by the corresponding parameter in Equation 8.9 to give:-

$$\varepsilon_p(N) = D(\frac{Tq_r}{Cu\ PI})^E(\log(N) + F) \qquad (8.13)$$

Figure 8.38 shows the plastic strains expected after applying 1000 repetitions of different deviator stress levels for Keuper Marl and the London clay. It can be seen that the London clay, which is stiffer than Keuper Marl (refer to Section 8.5.1.3), is found to be more resistant to permanent deformation for soils of the same strength. This observation is consistent with that from the soil rutting tests (Section 7.54), where acceleration of rutting under repeated trafficking was observed for the Keuper Marl samples with shear strengths lower than 30 kPa, but the increase of rutting rate did not happen in samples of the Bothkennar clay and London clay with low shear strength. This may be explained by Equation 8.13, as an increase in plasticity will lower the D value and hence reduce the permanent deformation generated under repeated loading.

Furthermore, it is worth noting that, for parameters E and F in Table 8.11, the differences in parameter values between the two soils are not large. However, the D value of the London clay was about three times that of Keuper Marl. This is similar to the ratio of the plasticity index between the two materials. In the author's opinion, the plasticity index may be a normalizing factor for the permanent deformation characteristic of different types of soil. More tests are required to confirm this. Therefore, for cohesive soils of the same shear strength, the one possessing the higher plasticity should be likely to give a higher stiffness and a higher resistance to permanent deformation.

8.6 Comparison with results from the wheel tracking test

The test program in the soil rutting test (Chapter 7) was designed to investigate the development of permanent strain, comparison of results between the soil rutting test and the repeated load triaxial test might be possible. Since the stress regímes used in the two tests were different and the behaviour of the materials tested was stress dependent, comparison should be carried out carefully and focused mainly on general aspects.
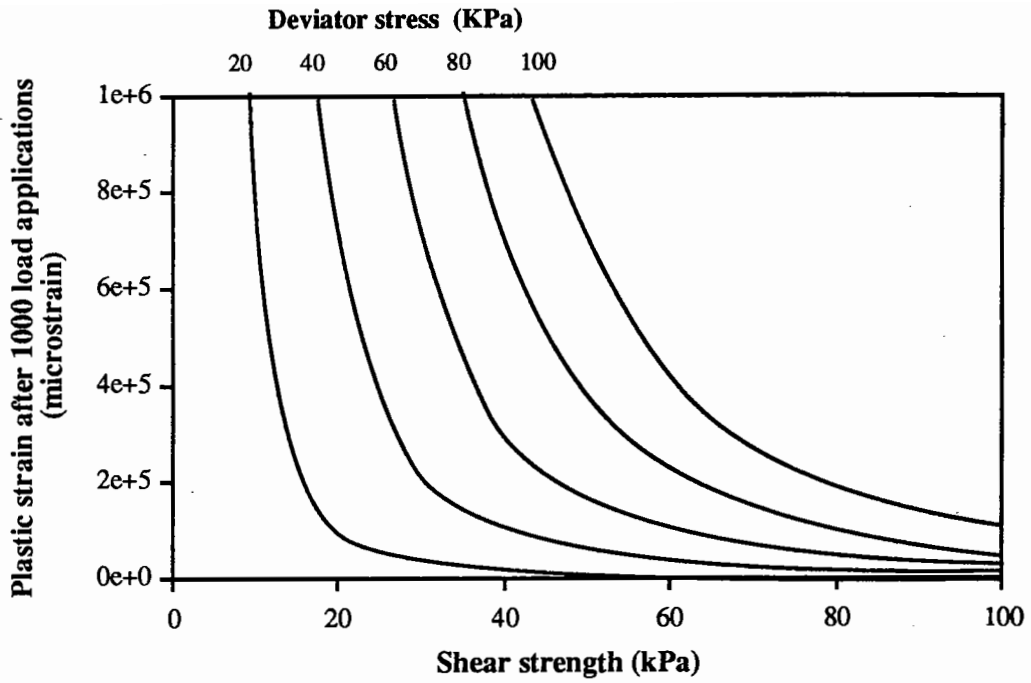
Figure 8.38a Predicted relationship between the plastic strain obtained after 1000 numbers of load applications and the shear strength for Keuper Marl
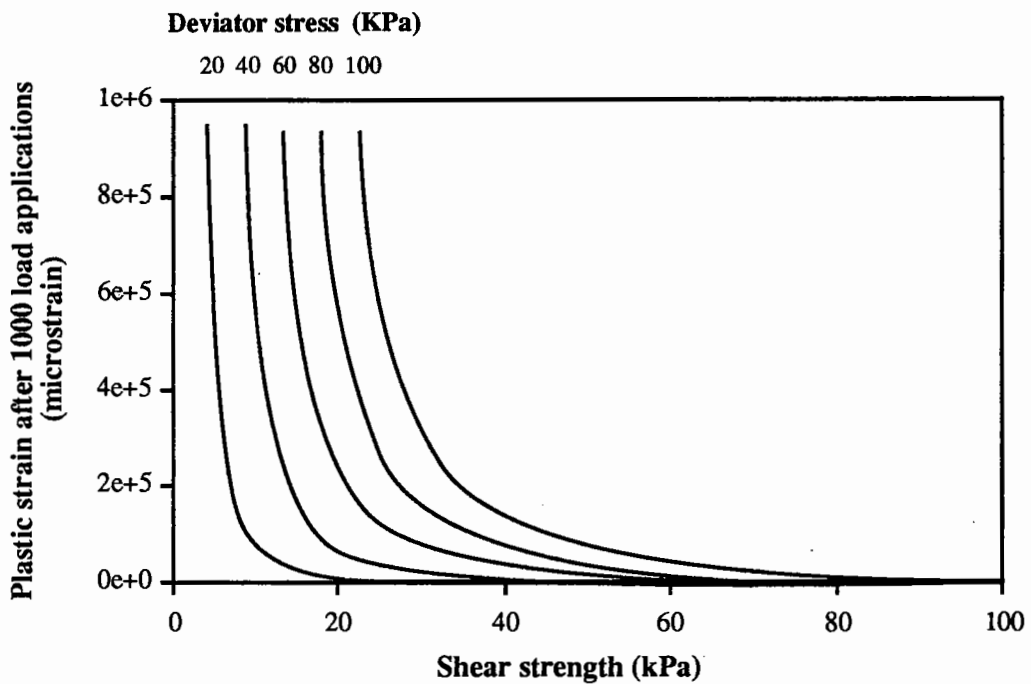
Figure 8.38b Predicted relationship between the plastic strain obtained after 1000 numbers of load applications and the shear strength for the London clay

Results from the repeated load triaxial test have indicated that there are relationships between permanent deformation and shear strength of soils. These results are reproduced in Figure 8.39. Corresponding data from the soil rutting test is also incorporated. Although the units used in the y-axes of the two graphs are not the same, in general the trend in one figure is mirrored in the other. Hence, the results obtained from both tests are generally consistent with each other. Soils of higher strength are more resistant to permanent deformation under repeated loading, and the relation between the development of plastic strain and shear strain is non-linear.

The agreement between the results from the two tests provide further confidence in using the newly developed repeated load triaxial apparatus as a tool to evaluate the permanent deformation characteristics of soils.

8.7 SUMMARY

Apparatus

(1)   The pneumatic loading system of the 100TA was able to provide good control of the axial repeated loads with a sinusoidal waveform up to a loading frequency of 3 Hz. Good quality data could be obtained from the newly designed on-sample instrumentation.

(2)   The reliability of the 100TA has been checked against the existing triaxial repeated load apparatus. Comparative results from the new repeated load triaxial apparatus were obtained.

(3)   A routine multi-purpose test procedure to provide a standard specimen pre-conditioning before resilient testing, to study permanent deformation characteristics and resilient deformation behaviour, and to determine the shear strength of cohesive soils, has been developed.

Material behaviour

(1)   It was demonstrated that preceding repeated loads at smaller stress magnitudes in the multi-test series had little effect on the amount of plastic strain accumulated by subsequent higher magnitude stress repetitions.
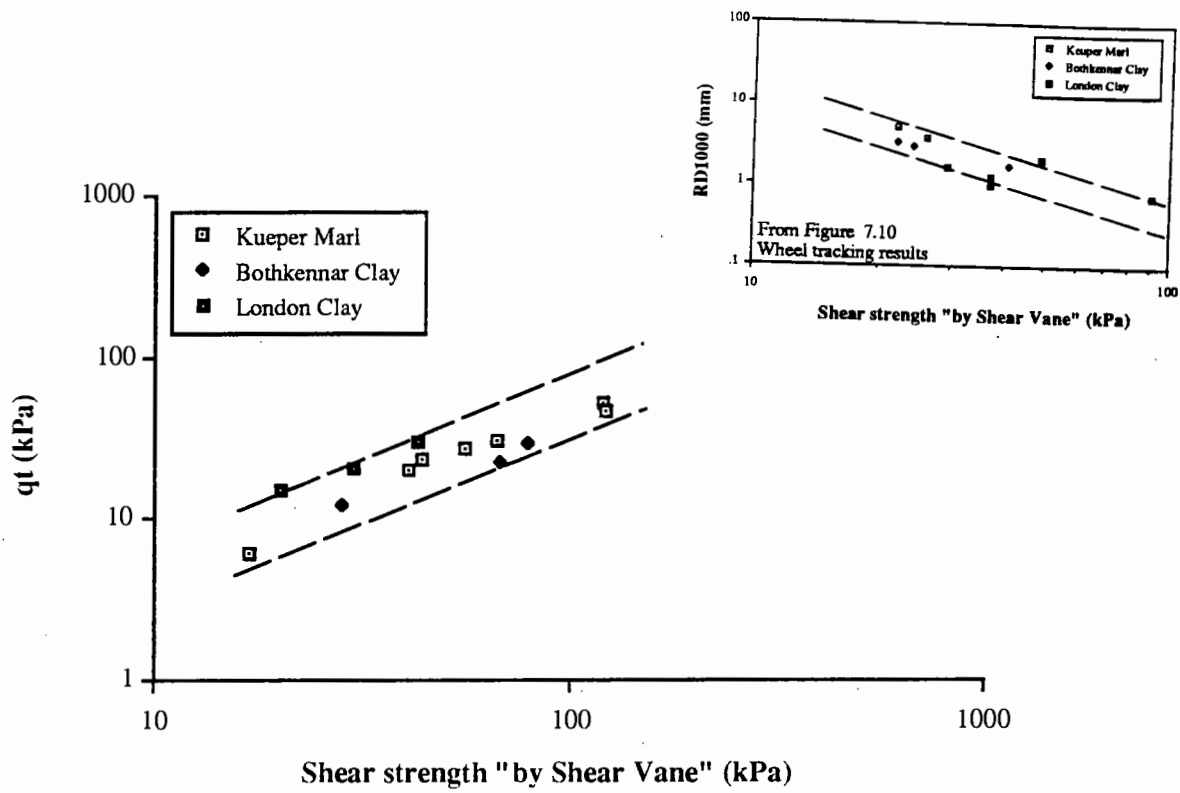
Figure 8.39 Relationships between permanent deformation performance of soils from different tests and shear strength

(2) For compacted materials, the resilient Poisson's ratio is unaffected by the deviator stress levels but decreases slightly with increasing soil suction.

(3) It was evident from the results that the resilient response of soils is a function of effective stress. Soil compressibility factors determined by the rapid suction test could be used to estimate the effective stresses in unsaturated cohesive soils when confining pressures were applied.

(4) The mathematical models recommended for the resilient axial and radial strains of soils under repeated loading are:-

$$\varepsilon_a = A(\frac{q_r}{S-C+(1-\alpha)\sigma_3})^B$$

$$\varepsilon_r = \varepsilon_a \upsilon$$

where:- $\upsilon = \beta(S+(1-\alpha)\sigma_3)+\gamma$

(5) It has been shown that plastic strain development of cohesive soils was primarily dependent upon the ratio of deviator stress to soil suction and on the logarithm of number of load repetitions applied. The mathematical model developed for the axial plastic strain development is:-

$$\varepsilon_p(N) = D(\frac{q_r}{S})^E(\log(N) + F)$$

(6) For remoulded cohesive soils, results from the undrained unconfined compressive tests may be estimated from the shear vane or from the hand penetrometer.

(7) There was a direct relationship between the soil suction and the shear strength of materials. Hence, both the resilient strain characteristics and the permanent deformation development can be related to the shear strength of the materials. However, the relationship varied with material types. It was found that the Plasticity Index of soils could be used to normalize the variation due to material types.

(8) An expression to describe the relationship between material stiffness and shear strength of cohesive soils was suggested:-

$$M_r = \frac{1}{A} q_r^{1-B} (\frac{Cu\ PI}{T} - C)^B$$

(9) An expression to describe the relationship between plastic strain development under repeated loading and shear strength of materials was suggested:-

$$\varepsilon_p(N) = D(\frac{Tq_r}{Cu\ PI})^E (\log(N) + F)$$

PART D

CONCLUSIONS, PRACTICAL IMPLICATIONS
AND
RECOMMENDATIONS FOR FUTURE WORK

CHAPTER 9

SUMMARIES AND CONCLUSIONS

Research work aimed at developing appropriate laboratory test methods - those able to describe the mechanical properties of granular materials and soils for the rational design of pavement foundations and to be used routinely in practice - has been carried out. Two pieces of laboratory equipment able to provide the loads envisaged have been designed, manufactured and commissioned. They are:-

(1)   A simplified repeated load triaxial apparatus with a specimen size of diameter 280 mm and height 560 mm suitable for performing tests on full sized unbound granular materials to the DoT Type 1 gradings.

(2)   A simplified repeated load triaxial apparatus with a specimen size of diameter 103 mm and height 206 mm suitable for testing recompacted or undisturbed samples of cohesive soils.

Compaction methods for granular materials and soils have been developed. A series of tests using the two devices on a range of aggregates and soils has been followed. The chief objective has been to look into the performance and the abilities of the apparatuses in describing the related pavement foundation materials. Ancillary tests to assess the performance of the new apparatuses, including using a large shear box and the Soil Rut Testing Facility, have also been performed on the same materials.

A prerequisite of a successful test method is the provision of the appropriate equipment and procedures. The main features and means of use of the two simplified apparatuses to fulfil this essential requirement are given below (Section 9.1). These are followed by a presentation of the conclusions of the principal results included in this thesis (Section 9.2).

9.1 LABORATORY EQUIPMENT

9.1.1 Apparatus for unbound granular materials

A repeated load triaxial apparatus has been developed. It has been demonstrated that the apparatus is capable of subjecting typical pavement foundation aggregate materials to loading broadly simulative of in-situ conditions.

The aim in developing the equipment (Chapter 1) had been to describe the behaviour of unbound granular pavement materials at an appropriate test condition with a test method which should not be too complicated and expensive to hinder the test from being used routinely in practice. This has been achieved by the following key features:

(a)   The use of a specimen size of 280 mm in diameter to cope with full grading of typical DoT sub-base aggregates (i.e. 40 mm nominal maximum particle size).

(b)   The use of an effective compaction method to produce high density specimens.

(c)   Omission of a big triaxial cell.

(d)   The provision of confining pressure by a constant internal partial vacuum.

(e)   The use of an inexpensive fabricated PVC membrane.

(f)   The provision of a simple loading system involving only manual tools for axial loads and a vacuum device for confining pressures.

(g)   The provision of high resolution "on-sample" instrumentation to monitor small displacements during repeated loading.

(h)   The use of a computerized data acquisition system.

(i)   The provision of a procedure for both setting up and testing which requires only one operator.

The test results have demonstrated that the routine testing procedure used with the apparatus is capable of:-

(a)   Determining the non-linear resilient modulus of unbound granular materials.

(b)   Ranking aggregate susceptibility to permanent deformation.

(c)   Evaluating the shear strength of materials.

Result comparisons between the new apparatus and the existing sophisticated repeated load triaxial equipment for aggregates have indicated that the new apparatus is capable of producing high quality results. Furthermore, it has been shown that the ability of the

new apparatus to characterize unbound granular materials for road foundations is much higher than that of a large shear box.

9.1.2 Apparatus for cohesive soils

A simplified repeated load triaxial apparatus for testing cohesive soils from the pavement foundation has been developed.

The apparatus and the testing procedure are capable of describing soil behaviour in pavement foundation conditions. This is achieved by a practical method which should encourage its use in practice. The key features are:-

(a)   Provision of sample preparation methods to simulate in-situ soil conditions.

(b)   The use of a simple and semi-portable loading frame.

(c)   The use of conventional triaxial specimens of diameter 103 mm to cater for remoulded or undisturbed samples with minimum preparation effort.

(d)   The ability to use an existing triaxial cell and base without major modification.

(e)   Provision of accurate "on-sample" displacement measurements to monitor minute movement of specimens under repeated loading.

(f)   The use of a pneumatic loading system to provide stress conditions simulative of those induced under traffic.

(g)   The use of an automatic control and data acquisition system to make the testing simple to carry out.

A routine testing method involving only one soil specimen has been proposed. The test results obtained by using the apparatus and by following the recommended testing procedures have shown that the test method is able to:-

(a)   Determine the non-linear resilient behaviour of cohesive soils.

(b)   Determine the permanent deformation characteristic of subgrade soils.

(c)   Evaluate the shear strength of soils.

Comparative testing by more sophisticated equipment has indicated that the simplified repeated load triaxial apparatus developed in this study is able to produce reliable results. Agreement with results obtained from the wheel tracking test has provided

further evidence of the capability of the new apparatus to characterize soils in road foundations.

9.2   MATERIAL TESTING

9.2.1   Aggregate Tests

A total of thirteen specimens, involving six types of aggregate, were tested by the 280TA in order to study the performance of the apparatus as well as (to a lesser extent) to increase the understanding of granular material behaviour. Some of the aggregates were also examined by a series of preliminary tests including particle examination and shear box testing. The conclusions of the results are given as follows:-

9.2.1.1   Preliminary tests

(1)   Low particle strength is usually associated with high water absorbency.

(2)   In general, high surface friction is related to the surface roughness of particles.

(3)   The compacted density of an aggregate appears to be affected by the shape of particles rather than the angularity and roundness.

(4)   The shear box may provide a means of ranking aggregates, which consist of finer gradings, with regard to their permanent deformation susceptibilities. However, because of the apparatus size effect, it may not be sufficient for testing materials of gradings near the coarse end of the DoT Type 1 sub-base envelope. Furthermore, it is not able to provide sufficient data for analytical pavement analysis procedures.

(5)   The shear strength and the resistance to permanent deformation of an aggregate are associated with the degree of compaction in the shear box.

(6)   Low stiffness, high permanent deformation susceptibility and low shear strength of an aggregate appear to be associated with materials containing more finer particles.

9.2.1.2 Repeated load triaxial tests

(1)   The significance of particle shape on material density is confirmed.

(2)   It appears that negligible particle size effect can be expected when a minimum specimen to particle size ratio of 7 is observed.

(3)   There is only a slight discrepancy between the resilient strains obtained by using a Manually-Controlled Actuator and by a servo-controlled hydraulic actuator.

(4)   There are some effects of waveform and load pulse frequency on the resilient behaviour of sub-base aggregates, but the effect can be considered as small.

(5)   Load pulse frequency and waveform shape have a significant effect on the development of permanent deformation.

(6)   The application of confining stresses either by an internal partial vacuum or by the external pressure method have a similar effect.

(7)   High resilient shear strain appears to be associated with weak particles (i.e. porous aggregates), low surface friction of particles and aggregates with high fines content.

(8)   No general rule, which links material density and the resilient response of aggregates, can be made.

(9)   High resilient volumetric strain appears to be associated with high fines content and aggregates of rounded particles.

(10)   Materials of high solids content and with particles of high angularity have high resistance to permanent deformation and compressive strength.

(11)   It appears that the strength of aggregates, in terms of c and ϕ, can be used to indicate the permanent deformation resistance of materials under repeated loading.

9.2.2 Cohesive soil tests

Three types of soils, Keuper Marl, a clay from Bothkennar and a London clay were tested in a preliminary study, which included careful soil classification, suction determination and wheel tracking tests using the Soil Rut Testing Facility, before repeated load triaxial tests were carried out in the newly developed simplified apparatus (100TA). Classification results indicate that the soils used in this research are typical of many British soils. A total of twenty-six specimens were prepared and tested by the 100TA. The main conclusions of the soil testing described in this thesis are listed as follows:-

9.2.2.1 Preliminary tests

(1)   For the soils tested it appears that there is a unique relationship between soil suction and moisture content of different soil types when liquid limit is used as a normalizing factor.

(2)   Soil compressibility is associated with soil plasticity and appears to be independent of water content.

(3)   Rut development in soils under rotating principal stress fields induced by direct wheel tracking appears to follow a semi-log function.

(4)   Permanent deformation resistance increases with dry density of soils, but decreases with increasing moisture content or void ratio.

(5)   It appears that permanent deformation can be related non-linearly to the strength related parameters of soils.

9.2.2.2 Repeated load triaxial tests

(1)   The resilient Poisson's ratio of compacted soils appears to decrease with increasing soil suction, but to be unaffected by the magnitude of deviator stresses.

(2)   The resilient behaviour of compacted soils is primarily associated with the deviator stress to soil suction ratio.

(3)   The resilient strain behaviour of compacted soils under repeated loading at constant cell pressure has been modelled.

(4)   The permanent deformation behaviour of soils is affected by the ratio of deviator stress to soil suction and relates to the logarithm of load pulse number.

(5)   A model for axial plastic strain development for compacted soils has been developed.

(6)   A general relationship appears to exist between soil suction and strength for different soils when plasticity index is used as a normalizing factor.

(7)   For compacted soils with the same shear strength, materials of a higher plasticity appear to possess higher abilities to resist the resilient and plastic deformations.

(8)   New models for expressing resilient and plastic stress-strain relationships for compacted soils have been suggested.

CHAPTER 10

THE USE OF THE SIMPLIFIED REPEATED LOAD TRIAXIAL TESTS

Two of the chief reasons why many research studies do not make an impact on existing practice are the highly sophisticated methods employed and the huge cost associated with these. It is, thus, not surprising to see that engineers in the pavement foundation construction industry keep to the existing empirical practice. Nevertheless, with increasing pressures brought about by scarce resources, limited finance and increasingly severe loading conditions (beyond which empiricism can handle) it is now necessary that a progressive, yet acceptable, alternative strategy be adopted. This project has therefore attempted to provide a solution to these pressing issues.

The main advance has been with the testing method, by employing two pieces of simplified repeated load triaxial apparatus. The chief advantage of the new equipment over the existing standard tests is the ability to describe the pavement foundation materials in terms of their basic mechanical properties so that structural design can be performed and prediction of pavement performance can be made analytically. Reasonable steps have been taken to bridge the gap between the existing empirical practice and the highly sophisticated methods which are often described by the industry as "untouchables".

10.1 RESILIENT AND PERMANENT DEFORMATION DATA

The importance of the ability of the current testing methods in providing the resilient and the permanent strain results is evident. Soil test results have indicated that different material types have their own unique elastic and plastic behaviour even though they possess the same shear strength (refer to Figures 8.32 and 8.38). The London clay was found to be stiffer than Keuper Marl and generated less permanent strain. On the other hand, it has been shown that stiffer granular materials do not guarantee better resistance to permanent deformation (Section 5.6.3.2).

10.2 REPEATED LOAD TESTING

The capacity of the two pieces of apparatus to practically apply repeated axial loads has provided a sensible advancement in the testing of pavement foundation materials for use in the construction industry because it has introduced realistic simulation of the traffic loading. From the results of the soil testing, it is clear that the 100TA is able to generate load pulses of well-defined waveform, precise period of loading and accurate stress magnitude. On the other hand, it is understood that only good control of deviator stresses and nominal control of the waveform and loading period are provided by the 280TA. However, test results demonstrate that the shape of loading normally has little significance for the resilient behaviour of granular materials (Section 5.6.2.1). The only exception is with a special waveform like a square wave, with sudden jumps at the beginning and at the end of the load pulse. Besides, in the tests carried out, the frequency of a load pulse has little effect on the resilient behaviour of aggregates even when the particle grading is at the fine end of the DoT Type 1 envelopes. In fact, it was demonstrated that the use of a hand-operated actuator to provide the repeated loading gave slightly higher resilient strains than those from a well-defined sinusoidal wave, hence, producing slightly conservative stiffnesses for design purposes (Section 5.6.2.4).

It is certain from the test results that development of permanent deformation of pavement foundation materials was dominated by the number of repetitions. Repeated load test results either from soil testing with well-controlled sinusoidal pulses or from aggregate testing with load pulses of constant energy (generated from the drop hammer) show that, in general, the rate of plastic strain accumulation decreases with the number of load repetitions. The ability to provide repeated loading is definitely a gateway towards successful permanent deformation characterization.

However, the usefulness of permanent deformation characterization without simulation of principal stress rotation, even if perfect control of repeated load pulses were to be given, is limited. The results may only be used as a means to check the permanent deformation susceptibility. This is particularly true for granular materials. The effect of principal stress rotation on the plastic strain behaviour of cohesive soils is less certain.

166

10.3 CONFINING PRESSURE

Provision of confining pressure is another important simulation of the stress conditions of materials in pavement foundations by the two apparatuses. Results from both aggregate and soil testing have confirmed that road foundation materials generally behave as stiffer materials when confining pressures are applied. This is due to the fact that effective stresses in the tested materials increase with increasing confining pressure. This phenomenon has been further demonstrated by the test on compacted clays of various soil compressibilities. The stiffnesses of soils with higher compressibility values are less sensitive to the change of confining pressure.

Since there was no intention in the repeated loading test to vary the confining pressure when the deviator stress is applied, total simulation of horizontal stresses in the pavement foundation under trafficking is not a provision of the tests. Nevertheless, careful consideration in selecting stress paths for material testing has been given so that most stress conditions under simultaneous axial and radial stress cycling which are likely to occur during the life of the pavement were covered within the selected stress zones (Sections 5.5.1.1 and 8.4.2). Though great attention was given to the use of proper stress paths in testing, it was found that simulation of the huge stresses generated in the sub-base layer due to direct loading during construction could not be applied in the routine laboratory tests. However, a reasonable prediction of strain response might be obtained for stress paths not included in the test, when proper material models are used with data obtained from the other stress paths. Nevertheless, examination of the applicability of material models for aggregate is outside the scope of this study. An appraisal of this subject has been given by Karasahin et al (1993).

10.4 REALISTIC SAMPLE

Test results from unbound granular materials show that the size of aggregate particles and the density of the tested specimens affect material behaviour under repeated loading. Smaller permanent deformations were observed when testing specimens at high densities. Higher stiffnesses were generally found on materials with bigger proportions of larger particles. Thus it is important to carry out tests on materials at their full gradings and at their desired in-situ densities. Investigations in this study indicate that the current specimen size is suitable for testing materials with the coarsest grading specified by the DoT for the sub-base layer. Compaction test results also reveal that the compaction method employed to make the specimen is capable of

producing materials of density similar to those produced by the B.S. 5835 compactibility test (refer to Table 5.2).

Sometimes granular materials for the capping layer consist of very large particles (DoT allows materials of aggregate size up to 125 mm). To make a specimen which is large enough to eliminate the particle to specimen size effect is considered unrealistic for routine testing. On the basis of the work by Marachi et al (1969), it is estimated that the size-related effect would be small if less than 30 percent of particles are greater than 40 mm in size. Hence, removal of the largest particles from the aggregates may be carried out. The effect of such an adjustment would likely be reduction of resilient stiffness. The effect on permanent deformation is less predictable.

Observations made on the soil testing programme clearly indicated that for each type of material the capability of resisting permanent deformation under repeated loading increases with increasing dry density. The combined ability of the 100TA and its sample preparation procedure has allowed compacted cohesive soils at different dry densities, as well as 100 mm diameter undisturbed samples from sites, to be tested. Some difficulties were encountered when installing the on-sample instrumentation onto the specimen of the boulder clay, which contained occasional particles of gravel size. It was either impossible to fix the studs, which held the strain loops, onto the specimen when a particle of gravel was encountered, or localized damage resulted when the studs were forced in. Nevertheless, this problem was overcome by carefully selecting the fixing locations using a fine needle as a probe to detect the possibility of meeting stones before the studs were installed.

10.5 ENVIRONMENTAL FACTORS

The moisture content of the compacted cohesive soils, which is the primary influential factor contributing to the effective stresses between soil particles, is important in determining the permanent deformation and the resilient strain properties. In general, the higher the moisture content, the lower the effective stress and, hence, the poorer the stiffness and the more susceptible to plastic deformation under repeated loading (Section 8.5). Clearly, results from the test programme indicate that the testing procedures used with the 100TA and the associated sample preparation methods are reasonably satisfactory for cohesive soils of a wide range of moisture contents.

However, indications from the aggregate testing with the 280TA show that it is more difficult to have an absolute control of the moisture content distribution in the granular material specimens. A moisture content gradient across the specimen with a lower moisture at the top and a higher value at the bottom due to gravitational forces was generally observed (Appendix F). Nonetheless, the possible effect arising from moisture content inhomogeneity was reduced to a minimum in the tests since measurements of the resilient strains and the permanent deformations were made in the middle portion of specimens. Moisture content extremities in the specimens were thus removed except when testing for material strength was performed. Nevertheless, the test results, although limited, show that the crucial factor affecting material strength is density and the effect of moisture content is not apparent provided the material is not near saturation. In fact, the slight moisture content variation at the middle third height of the specimen may be a benefit rather than a drawback because this is also likely to happen on site.

Tests carried out on granular materials further demonstrated that the moisture content of the tested materials was lower after testing. This was due to the application of partial vacuum as a means of providing the confining pressure. Although the reduction in moisture content in most of the aggregate samples was generally small, the test is not suitable for saturated or near saturated materials. Nonetheless, it is unwise to allow a sub-base layer to take up water and to become saturated. Certainly, a better solution is to prevent free water from entering the sub-base layer (or to ensure drainage) rather than to carry out assessment tests on saturated materials.

10.6 PRACTICALITY

It was recognized that measurements made at the top of the specimens show significant deviation from the results obtained from the on-sample instrument. The difference is due to errors involved in the measuring techniques of the former. The errors, most likely, come from two sources - end effects and system effects. It is obvious that the errors cannot be properly accounted for, even by careful calibration, because the end effect is material dependent. Thus, the use of the on-sample instrumentation employed in this study is indispensable for the proper monitoring of small displacements. It was noticed that the time needed for setting up on-sample instrumentation was reasonable - about 15 minutes for the 100TA and approximately one hour, which included the time for allowing the glue to set, for the 280TA.

From the experience gained in this study, it was found that sample preparation procedures for soil specimens either by compaction or by extrusion from a U100 tube was straightforward. For the unbound granular material testing with the 280TA, the average compaction time required for preparing the specimen was about six hours. Semi-automation of the compaction procedure needs to be considered further. Nevertheless, such a time scale is considered not unacceptable for laboratory testing. Furthermore, only one man was found necessary throughout the whole period of sample preparation.

The success of using a hand jack and a drop hammer for applying loads to characterize sub-base materials in this project means that the method may be the simplest form ever used to determine the resilient and plastic strain characteristics of aggregates in the laboratory. In addition, comparisons between results from tests carried out with provision of confining pressures by external pressure and by partial vacuum have justified the use of the latter method. Thus, it is likely that the current axial and radial loading mechanism is probably the cheapest and the simplest system for determining the fundamental mechanical properties of sub-base materials.

On the other hand, the use of pressurized air to provide the repeated axial loads and the constant confining pressures was found satisfactory for subgrade soil testing. It is considered that the loading system is cost effective when reasonably well-defined load pulses on a small specimen are required. In addition, although the air supply was from a single source, no interference between the applied confining pressure and the axial repeated load was apparent during testing.

Though the results show that reasonable control of loading rate for strength testing on soil is possible, it was found difficult to maintain a steady rate of loading in the strength testing on granular materials by the manually operated load actuator. Pike (1973), working on graded aggregates with a large shear box, reported that variations of the shear strength parameter, ϕ, between different shearing rates were slight even though the rate of displacement was one hundred times bigger than the other. Hence, it is likely that the effect of an uneven loading rate due to the manually controlled actuator would not be critical for aggregate strength testing.

Using computer technology to provide the necessary control and data acquisition has been found to be indispensable. The benefits were obvious in that the required

electronic and mechanical equipment was simplified. Moreover, efficiencies in data management and result analysis were tremendously increased.

CHAPTER 11

RECOMMENDATIONS FOR FUTURE WORK

11.1 LABORATORY TESTING

11.1.1 Materials

Using the testing methods and the two simplified repeated load triaxial apparatuses developed in this research, tests to describe the resilient properties and the permanent deformation characteristics of sub-base aggregate and subgrade soils should be able to be carried out routinely for the purpose of practical pavement foundation design. However, further tests and improvement work which are considered important (but not urgent) are still needed.

(1)   Due to the possible particle to apparatus size effect, no tests were performed on aggregates with particle distribution curves coarser than the DoT Type 1 sub-base unbound granular grading envelope. Coarse capping materials, which are occasionally introduced into the pavement foundations, have not been tested. Alternative or additional sample preparation techniques might be required if the proportion of large particles is high. One method worthy of consideration would be the removal of all, or many, of the large particles which exceed a certain maximum particle size. Another method would be to test scaled down samples with the same shape of particle distribution curve but with the maximum nominal particle size reduced to 40 mm. The effect of using such modified methods needs to be carefully assessed as it could be material dependent.

(2)   In view of the variability of unbound granular materials, testing has been carried out on aggregates of different gradings and origins. Nevertheless, the number of materials tested is still considered to be limited. More tests on different aggregate types are required to confirm the applicability of the testing to all materials. In particular, there was only one test on industrial wastes. The applicability of the testing method for a wide range of industrial wastes needs to be explored.

(3)   For soil testing, most of the effort has been directed to the testing of recompacted materials. Little attention has been given to undisturbed soils and no test was conducted on equilibrated samples of either recompacted or undisturbed soils which simulate other in-situ conditions. With the availability of the simplified repeated load apparatus and the sample preparation mould, a test programme on such soils to confirm the ability of the testing method at other soil conditions is warranted. It is believed that these further tests will provide a fuller picture of the performance of subgrade soils at different stages of a pavement's life.

(4)   The reliability of the apparatuses has been checked against the more sophisticated repeated load triaxial apparatuses. It is now worth testing some of the tested materials again to check the repeatability and to use identical apparatuses in other laboratories to investigate the reproducibility of the tests.

11.1.2   Simplified repeated load triaxial apparatus

The 280TA

(1)   The present actuator has a 10 tonne loading device which allows vertical pressure up to about 1600 kPa to be applied to a 280 mm diameter specimen. This capacity was found sufficient for most materials tested. However, it has been experienced that strong materials, such as QDB and QGB, possessing a high compressive strength, exceeded the capacity of the actuator. This loading device needs to be upgraded so that the strength of strong materials can be determined.

(2)   The use of a drop hammer to characterize the permanent deformation susceptibility of aggregates was found satisfactory. However, it was noticed that the frequency of load pulses generated was about thirty-five times that expected from trafficking. A useful modification would be to insert a rubber buffer somewhere between the load platen and the hammer to reduce the load pulse frequency. Such a technique is being studied by Brown (1992) in developing a drop hammer device for in-situ pavement foundation testing.

(3)   The use of the current automatic data acquisition and computing system was found very useful in data collection and preliminary analysis. A further

development is to upgrade the system to include the ability to produce full analysed results in a standard report for each set of routine tests.

(4)   High material density can be reproduced by the current compaction method but the device is in a primitive form. It was rather labour intensive to produce a compacted sample. Upgrading the compaction device will certainly reduce the man-power required.

The 100TA

(1)   The ability of the electro-pneumatic regulator to produce stable sinusoidal load pulses was found to be reasonable. It was able to follow the command signal up to a loading frequency of 3 Hz. Reduction of load response occurred at greater loading frequencies. To test soil specimens at a higher frequency, the present regulator should be upgraded.

(2)   The actuator used was able to provide a vertical stress of 200 kPa to a 103 mm diameter specimen. The load magnitude was sufficient for resilient strain and permanent deformation tests but was not adequate for strength tests when soils were stiff or very stiff. Hence, there is a need for an actuator which can generate higher vertical loads.

(3)   The performance of the transducers was considered satisfactory, although electronic noise was occasionally picked up by the proximity transducers. Since the disruption was about once in a month and for each occurrence it only lasted for a short while, it was found difficult to trace the source of interference. Nevertheless, upgrading the electronic facility so as to eliminate interference during testing is considered worthwhile - especially when permanent deformation tests, which cannot be repeated on the same specimen, are being carried out.

(4)   Provision of pore pressure measurement would enhance the capacity of the apparatus because more information can be obtained during testing which should lead to more accurate interpretation of the test results. However, incorporation of pore water measurement might complicate the apparatus and the test procedure.

(5)   As mentioned for the 280TA, a further refinement of the result analysis and management program so as to provide a full report in a standard form for each set of routine tests would be advantageous.

11.2 DESIGN METHOD

Having described the mechanical behaviour of pavement foundation materials by the simplified repeated load triaxial apparatuses, it is necessary to suitably interpret the laboratory test results and to put forward a better design method for pavement foundations based on an analytical analogue. Work in this area is underway in a study by Dawson et al (1993) at the University of Nottingham. Early suggestions have been made by them to design pavement foundations in two stages - during construction and in-service. The ability of a pavement foundation to resist excessive deformation would be the design criterion during construction and the ability of the foundation to properly spread wheel loads, without causing undue resilient deformation in the upper bound layers, the criterion in-service. The work of Dawson et al should provide a good means of assessing the adequacy of the test methods used in this study to provide data for analytical design.

11.3 LARGE SCALE TRIAL

Before full confidence in the use of the test methods which employ the simplified repeated load triaxial apparatuses developed in this study can be gained, large scale trials are required. They would provide validation of test results and provide checking of the correctness of result interpretation. Two levels of large scale trials are worth performing. The first of them involves the use of laboratory test pavements such as the Nottingham Pavement Test Facility (refer to Section 2.5.5 in Chapter 2). The benefit of using the laboratory test pavements is that stresses and deformations induced by wheel loads anywhere in the pavement can be measured under well-controlled conditions. Pressure cells and strain gauges placed beneath the line of the travelling wheel at different depths of the pavement foundation, especially near the subgrade surface, are advisable. The second level of trialling would be at pilot or full-scale on site. Such tests take varying environmental factors into account. The site trial should be fully instrumented and preferably materials tested in this research would be used.

Analyzing the data obtained from sites together with those from the test methods used in this study should result in better interpretation of the laboratory test results.

11.4 SIMPLE SITE TESTING DEVICE

Only half of the work is finished when an appropriate laboratory design test and the associated analytical design method are provided. The compliance of a design needs to be checked on site during and after construction. Assessment of the mechanical responses of pavement foundations necessitates the provision of a site testing device capable of evaluating the foundation layers in terms of stiffness and resistance to permanent deformation. Site equipment such as the Falling Weight Deflectometer (Tam 1987), Clegg Hammer (Clegg 1978), Plate Loading Test (Day 1976), Dynamic Cone Penetrometer (Scala 1956), Loadman (Al-Engineering Oy 1991) and Odin (Boyce et al 1989) may have their values in pavement foundation evaluation. An assessment of appropriate site devices is being undertaken at Loughborough University of Technology and a simple apparatus aiming at evaluating foundations in-situ is being developed (Brown 1992). Provision of such apparatus is an important factor in the implementation of a pavement design based on an analytical approach.
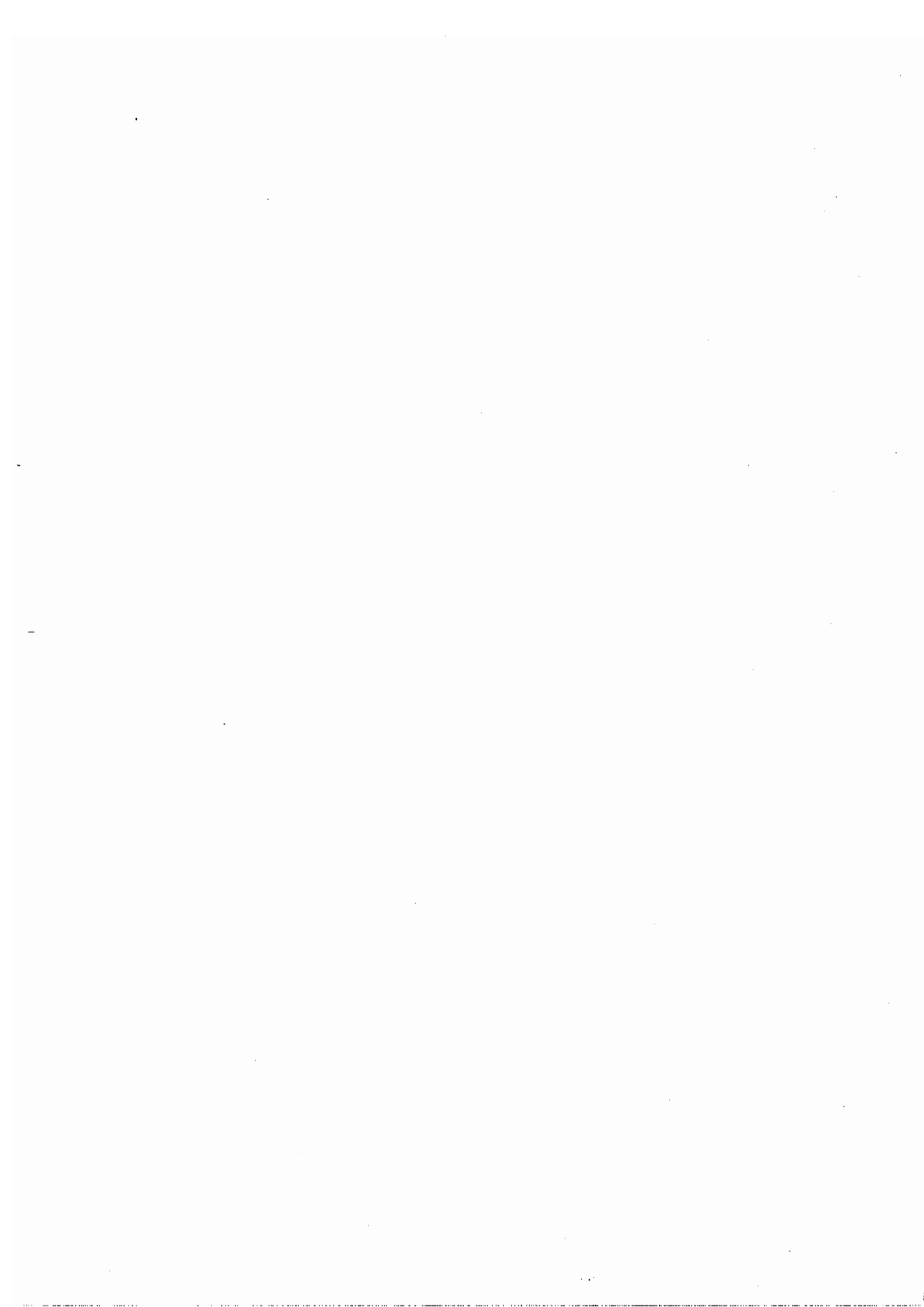
REFERENCES

Ahmed S F & Larew H G (1962), "A study of the repeated load strength modulus of soils", Proceedings of International Conference on the Structural Design of Asphalt Pavements, Ann Arbor, Michigan, USA.

Al-Engineering Oy (1991), "Loadman, portable falling weight deflectometer", Leppälinnunpolku, Espoo, Finland.

Almeida J R (1991) "Program FENLAP User's Guide" Report No: PR91010, Department of Civil Engineering, University of Nottingham.

Almeida J R (1993), "Analytical techniques for the structural evaluation of pavements", Thesis submitted to the Department of Civil Engineering, University of Nottingham for the degree of Doctor of Philosophy.

Allen J J & Thompson M R (1974), "Resilient response of granular materials subjected to time dependent lateral stresses", Transportation Research Record 510, pp 1-13.

American Association of State Highway and Transportation Officials (1986), "Standard method of test for resilient modulus of subgrade soils", AASHTO Designation : T272-82.

Ansell P (1977), "Cyclic simple shear testing of granular material", Thesis submitted to the Department of Civil Engineering, University of Nottingham for the degree of Doctor of Philosophy.

Aschenbrenner B C (1956), "A new method of expressing particle sphericity", Journal of Sedimentary Petrology, Vol. 26, No. 1, pp 15-31.

Austin G (1979), "The behaviour of Keuper Marl under undrained creep and repeated loading", Thesis submitted to the Department of Civil Engineering, University of Nottingham for the degree of Doctor of Philosophy.

Barksdale R D (1971), "Compressive stress pulse times in flexible pavements for use in dynamic testing, Highway Research Record No. 345, National Research Council, Washington DC.

Barksdale R D (1972), "Repeated load test evaluation of base course materials", Georgia Highway Department Research Project No. 7002, Georgia Institution of Technology, Atlanta, Georgia.

Barksdale R D & Itani S Y (1989), "Influence of aggregate shape on base behaviour", Transportation Research Board 1227, Rigid and Flexible Pavement Design and Analysis, Transportation Research Board, National Research Council, Washington DC, pp 173-182.

Bentsen R A (1990), "Drainage: all important, often overlooked", Asphalt, The Magazine of the Asphalt Institute, Vol. 4, No. 8, pp 12-13.

Bishop A W & Henkel D J (1962), "The measurement of soil properties in the triaxial test", The English Language Book Society.

Black W P M & Lister N W (1979), "The strength of clay fill subgrades: Its prediction in relation to road performance", Department of Transport: Transport Research Laboratory, TRL Report LR889, Crowthorne.

Boyce J R (1976), "The behaviour of a granular material under repeated loading", Thesis submitted to the Department of Civil Engineering, University of Nottingham for the degree of Doctor of Philosophy.

Boyce J R (1980), "A non-linear model for the elastic behaviour of granular materials under repeated loading", International Symposium on Soils under Cyclic and Transient Loading, Swansea, January 7-11.

Boyce J R, Cobbe J R & Fleming P R (1989), Technical Note: "Development of a prototype variable impact testing apparatus", Proceedings of the International Symposium on Unbound Aggregates in Road (UNBAR3), University of Nottingham.

British Standards Institution (1990), B.S. 812 : Testing Aggregates.

British Standards Institution (1990), B.S. 1377 : Method of test for soils for Civil Engineering purposes.

British Standards Institution (1980), B.S. 5835 : "Recommendations for testing of aggregates, compactibility test for graded aggregates", Part 1.

Broms Bengt B & Forssbland Lars (1969), "Vibratory compaction of cohesionless soils", Soil Dynamics : Proceedings of Specialty Session 2, 7th International Conference on Soil Mechanics and Foundation Engineering, Mexico City, Mexico.

Brown A J (1992), "Field Assessment of Road Foundations", 1st Year Report, Department of Civil Engineering, Loughborough University of Technology.

Brown S F (1967), "Stresses and deformations in flexible layered pavement systems subjected to dynamic loads", Thesis submitted to the Department of Civil Engineering, University of Nottingham for the degree of Doctor of Philosophy.

Brown S F (1974), "Repeated load testing of a granular material", Journal of the Geotechnical Engineering Division, Proceedings of ASCE, 110 (GT7), pp 131-138.

Brown S F, Austin G & Overy R F (1980), "An instrumented triaxial cell for cyclic loading of clays", Geotechnical Testing Journal, Dec. 1980, reprint American Society for Testing and Materials.

Brown S F & Brodrick B V (1981), "Nottingham Pavement Test Facility", Transportation Research Record 810, pp 67-72.

Brown S F & Dawson A R (1992), "Two-stage mechanistic approach to asphalt pavement design", Proceedings of 7th International Conference of Structural Design of Asphalt Pavements, Nottingham, Vol. 1, pp 16-34.

Brown S F & Hyde A F L (1975), "Significance of cyclic confining stress in repeated load triaxial testing of granular material", Transportation Research Record No. 537, pp 49-58.

Brown S F, Laskine A K F & Hyde A F L (1975), "Repeated load triaxial testing of a silty clay", Géotechnique, Vol. 25, No. 1.

Brown S F, Loach S C & O'Reilly M P (1987), "Repeated loading of fine grained soils", Contractor Report CR72, Transport Research Laboratory, Department of Transport.

Brown S F & Pappin J W (1982), "Use of a pavement test facility for the validation of analytical design methods", Proceedings of 5th International Conference on Structural Design of Asphalt Pavements, Vol. 1, Delft.

Brown S F, O'Reilly M P & Pappin J W (1989), "A repeated load triaxial apparatus for granular materials", Unbound Aggregates for Roads edited by Jones R H & Dawson A R, pp 143-158.

Chan F W K (1989), "Granular Bases for Heavily Loaded Pavements", Report submitted to the US Air Force, Department of Civil Engineering, University of Nottingham.

Chan F W K (1990), "Pavement deformation resistance of granular layers in pavements", Thesis submitted to the Department of Civil Engineering, University of Nottingham for the degree of Doctor of Philosophy.

Cheung L W (1991), "Research to improve road foundation design", 2nd Year Report, Department of Civil Engineering, University of Nottingham, PR91040.

Cheung L W & Dawson A R (1990), "Research to improve road foundation design", 3rd Quarterly Report, Department of Civil Engineering, University of Nottingham, PR90026.

Clare K E (1948), "Laboratory studies relating to the clay fraction of cohesive soils", Proceedings of 2nd International Conference of Soil Mechanics (Rotterdam), Vol. 1, pp 151-8.

Clegg B (1978), "An impact soil tester as an alternative to California Bearing Ratios", Proceedings of 2nd Conference on Road Engineering, Association of Asia and Australia, Manila, Philippines, October.

Collis L & Fox R A (1985), "Aggregates: sand, gravel and crushed rock aggregates for construction purposes", Geological society, Engineering Geology Special Publication No. 1.

Cooper K E & Brown S F (1986), "Surface dressing aggregates", Report submitted to Cumbria County Council.

Cooper K E & Brown S F (1989), "Development of simple apparatus for the measurement of the mechanical properties of asphalt mixes", 4th Eurobitume Symposium, Vol. 1, pp 495-499.

Cox L J (1987, "Review of past practice", Proceedings of National Workshop on Design and Construction of Pavement Foundations, Leamington Spa, Institution of Highways and Transportation, pp 1-20.

Crockford W W, Chau K M, Yang W S, Rhee S K & Senadheera (1988), "Response and performance of thick granular layers", Final Technical Report submitted to the US Air Force.

Croney D (1977), "The design and performance of road pavements", Transport Research Laboratory, Department of the Environment, Department of Transport.

Croney D & Croney P (1991), "The design and performance of road pavements", 2nd Edition, McGraw-Hill International Series in Civil Engineering.

Curtis C R & Loveday C A (1987), "Granular materials in pavement foundations, the practicalities of production and supply", Proceedings of National Workshop on Design and Construction of Pavement Foundation, Leamington Spa, Institution of Highways & Transportation pp 87-102.

Dawson A R, Brown S F & Barksdale R D (1989), "Pavement foundation developments", The Journal of the Institution of Highways and Transportation, pp 27-34, March 1989.

Dawson AR, Brown S F, Thom N H and Cheung L W (1993), "Improvements to road foundation design: Laboratory Tests and Design Method", Department of Civil Engineering", University of Nottingham, PGR93023.

Dawson A R, Cheung L W, Brown S F, Rogers C D F & Fleming P R (1990), "Requirements of laboratory design and field assessment tests for pavement foundations", Working Paper WP/PE/75, Transport Research Laboratory, Department of Transport.

Day J B A (1976), "Proof testing of unbound layers", Proceedings of 1st International Symposium of Unbound Aggregates in Roads, University of Nottingham.

Dehlen G L (1969), "The effect of non-linear material response on the behaviour of pavements subjected to traffic loads", Thesis submitted to the University of California for the degree of Doctor of Philosophy.

Department of Transport (1986), "New specification for highway works", Series 600-800.

Department of Transport (1987), "Structural design of new road pavements", Departmental Standard HD14/87, HMSO, London.

Department of Transport (1992), "Specification for highway works", Series 600-800, HMSO, London.

Department of Transport (1993), "Pavement design and maintenance", Part 2 HD 14/93, HNSO, London

Dupas J-M, Pecker A, Bozotto P & Fry J-J (1988), "A 300mm diameter triaxial cell with a double measuring device", pp 132-142, Advanced Triaxial Testing of Soil and Rock.

Dumbleton M J & West G (1968), "Soil suction by the rapid method : an apparatus with extended range", Journal of Soil Science, Vol. 19, No. 1.

Dyer M R (1986), "Observation of the stress distribution in crushed glass with applications to soil reinforcement", Thesis submitted to the University of Oxford for the degree of Doctor of Philosophy.

Dyer M R & Milligan G W E (1984), "A photoelastic investigation of the interaction of a cohesionless soil with reinforcement placed at different orientations", Proceedings of International Institution of Soil and Rock Reinforcement, Paris, pp 257-262.

Earland M G & Pike D C (1985), "Stability of gravel sub-bases", TRL Research Report 64, Transport Research Laboratory, Department of Transport.

Elliott R C (1990), "Advances in mix design for bituminous bases", Thesis submitted to the Department of Civil Engineering, University of Nottingham for the degree of Master of Philosophy.

Finn F N, Nair K & Monismith C L (1972), "Application of theory in the design of asphalt pavements", Proceedings of 3rd International Conference on the Structural Design of Asphalt Pavements, Vol. 1, London.

Fleming P R & Rogers C D F (1993), "Foundation testing in-situ for validation of design methods", Summary final report submitted to Transport Research Laboratory. Department of Civil Engineering, Loughborough University of Technology.

Fredlund D G, Bergan A T & Sauer E K (1975), "Deformation characterisation of subgrade soils for highways and runways in northern environments", Canadian Geotechnical Journal, Vol. 12, No. 2.

Fukushima S & Tatsuoka F (1984), "Strength and deformation characteristics of saturated sand at extremely low pressures", Soils and Foundations, Vol.

24, No. 4, pp 30-48, December 1984, Japanese Society of Soil Mechanics and Foundation Engineering.

Fuller W B & Thompson S E (1907), "The laws of proportioning concrete", Transaction of the American Society of Civil Engineering, Vol. 59, pp 67-172.

Gillett S D, Thom N H, Plaistow L, Ferreira V & Dastich I (1991), "A European Approach to Road Pavement Design", Progress Report No. 2, Contract No. SCI 0130 - C (SMA), The European Economic Community.

Grace H (1981), "Note on the drainage of roads", Proceedings of Symposium of Unbound Aggregates in roads, Edited by R H Jones, Department of Civil Engineering, University of Nottingham.

Grainger G D & Lister N W (1962), "A laboratory apparatus for studying the behaviour of soils under repeated loading", Géotechnique 121, pp 3-14.

Henkel D J & Gilbert G C (1952), "The effect of rubber on the measured triaxial compression strength of clay samples", Géotechnique, Vol. 3, pp 20-29.

Henkelow W & Klomp A J G (1962), "Dynamic testing as a means of controlling pavements during and after construction", Proceedings of the International Conference on the Structural Design of Asphalt Pavements, pp 667-679, University of Michigan, An Arbor.

Hicks R G (1970), "Factors influencing the resilient properties of granular materials", Thesis submitted to the University of California, Berkeley for the degree of Doctor of Philosophy.

Hicks R G & Monismith C L (1971), "Factors influencing the resilient response of granular materials", Highway Research Record 345, pp 15-31.

Hight D W & Stevens M G H (1982), "An analysis of the California Bearing Ratio test in saturated clays", Géotechnique , Vol. 32, No. 4, pp 315-322.

Humphries W K & Watts H E (1968), "Stress history effects on dynamic modulus of clay", Proceedings of ASCE, Journal of Soil Mechanics and Foundation Engineering Division, Vol. 94, No. SM2, pp 371-389.

183

Hyde A F L (1974), "Repeated load testing of soils", Thesis submitted to the Department of Civil Engineering, University of Nottingham for the degree of Doctor of Philosophy.

Jewell R A & Wroth C P (1987), "Direct shear tests on reinforced sand", Géotechnique 37, No. 1, pp 53-68.

Jouve P, Martinez J, Paute J L & Ragneau E (1987), "Rational model for the flexible pavements deformation", Proceedings of 6th International Conference on the Structural Design of Asphalt Pavements, pp 50-84.

Karasahin M (1993), "Resilient behaviour of granular material for highway pavement analysis", Thesis submitted to the Department of Civil Engineering, University of Nottingham for the degree of Doctor of Philosophy.

Kawakami F & Ogawa M S (1965), "Strength and deformation of compacted soil subjected to repeated stress application", Proceedings of the 6th International Conference on Soil Mechanics and Foundation Engineering, pp 264-268.

Kirwan R W, Farrel E R, Hartford D N D & ORR, TLL (1982), "The interpretation of repeated load parameters for a glacial subgrade from soil properties", Proceedings of 5th International Conference on Structural Design of Asphalt Pavement, Vol. 1, Delft.

Kirwan R W & Snaith M S (1976), "A simple chart for the prediction of resilient modulus", Géotechnique, Vol. 26, No. 1.

Krumbein W C (1941), "Measurement and geological significance of shape and roundness of sedimentary particles", Journal of Sediment, Petrol, 11 (2), pp 64-72.

Lashine A K F (1971), "Some aspects of the behaviour of Keuper Marl under repeated loading", Thesis submitted to the Department of Civil Engineering, University of Nottingham for the degree of Doctor of Philosophy.

Lees G (1964), "The measurement of particle shape and its influence in engineering materials", Journal of the British Granite and Whinston Federation, pp 1-22.

Lentz R W (1979), "Permanent deformation of cohesionless subgrade material under cyclic loading", Thesis submitted to the Michigan State University, East Lansing for the degree of Doctor of Philosophy.

Little P H (1993), "The design of unsurfaced roads using geosynthetics", Thesis submitted to the Department of Civil Engineering, University of Nottingham for the degree of Doctor of Philosophy.

Little P H & Dawson A R (1990), "Laboratory work on samples from haul roads at Bothkennar", Report submitted to the project consultative committee of SERC, June 1990.

Loach S C (1987), "Repeated loading of fine grained soils for pavement design", Thesis submitted to the Department of Civil Engineering, University of Nottingham for the degree of Doctor of Philosophy.

Loos W (1936), "Comparative studies of the effectiveness of different methods for compacting cohesionless soils", Proceedings of the International Conference on Soil Mechanics and Foundation Engineering, Vol. 3, pp 174-179.

Manuel Bronstein and Jorge Sousa (1990), "A new generation of laboratory testing software, ATS", DCS (Digital Control Systems).

Marachi N D, Chan C K, Seed H C & Duncan J M (1969), "Strength and deformation characteristics of rockfill materials", Report No. TE69-5, Department of Civil Engineering, Institute of Transportation and Traffic Engineering, University of California, Berkeley.

Mayhew H C (1983), "Resilient properties of unbound roadbase under repeated triaxial loading", Department of the Environment, Department of Transport, Transport Research Laboratory Report LR1088, Crowthorne.

Mayhew H C & Harding H M (1987), "Thickness design of concrete roads", Department of the Environment, Department of Transport, Transport Research Laboratory, Research Report 87.

Mitchell R J & King R D (1977), "Cyclic loading of an Ottowa area Champlain sea clay", Canadian Geotechnical Journal, Vol. 14, No. 2.

Moore W M, Britton S C & Scrivener F H (1970), "A laboratory study of the relation of stress to strain for a crushed limestone base material", Texas A and M University, Texas Transportation Institute, Research Report No. 99-JF, College Station, Texas.

Nataatmadja A (1989), "Variability of pavement material parameters under repeated loading", Thesis submitted to the Department of Civil Engineering, Monash University, Australia for the degree of Doctor of Philosophy.

Nievelt G (1989), "A new, more suitable approach to a mix design for heavy duty hot-mixes", Proceedings of 4th Eurobitume Symposium, Madrid 1989, Vol. 1, pp 335-340.

O'Reilly M P (1985), "Mechanical properties of granular materials for use in thermal energy stores", Thesis submitted to the Department of Civil Engineering, University of Nottingham for the degree of Doctor of Philosophy.

Overy R F (1982), "The behaviour of anisotropically consolidated silty clay under cyclic loading", Thesis submitted to the Department of Civil Engineering, University of Nottingham for the degree of Doctor of Philosophy.

Pappin J W (1979), "Characteristics of a granular material for pavement analysis", Thesis submitted to the Department of Civil Engineering, University of Nottingham for the degree of Doctor of Philosophy.

Parr G B (1972), "Some aspects of the behaviour of London clay under repeated loading", Thesis submitted to the Department of Civil Engineering, University of Nottingham for the degree of Doctor of Philosophy.

Pettibone H C & Hardin J (1964), "Research on vibratory maximum density test for cohesionless soils", American Society Testing Materials, Special Technical Publication No 377, pp 3-19.

Peutz M G F, Van Kempen H P M & Jones A (1968), "Layered system under normal surface loads - Computer Program BISTRO", Koninklijke/Shell - Laboratorium, Amsterdam, May 1968.

Pike D C (1973), "Shear-box tests on graded aggregates", TRL Report LR584, Transport Research Laboratory, Department of the Environment.

Powell W D, Potter J F, Mayhew H C & Nunn M E (1984), "The structural design of bituminous roads", Department of the Environment, Department of Transport, TRL Report LR1132, Transport Research Laboratory, Crowthorne.

Rada G & Witczak M W (1981), "Comprehensive evaluation of laboratory resilient moduli results for granular materials", Transport Research Record 810, pp 23-33.

Raybould M (1991), "University of Nottingham Triaxial Test Facility", Proceedings of Earthquake, Blast and Impact Measurement and Effects of Vibration, Edited by the Society for Earthquake and Civil Engineering Dynamics, (Elsevier Applied Science) pp 295-306.

Richards & Gordon (1972), "Prediction and observation of the performance of a flexible pavement on an expansive clay subgrade", 3rd International Conference on the Structural Design of Asphalt Pavements, The University of Michigan, pp 133-143.

Rochelle P la, Leroueil S, Trak B, Blais-Leroux & Tavenas F (1988), "Observational approach to membrane and area corrections in triaxial tests", Advanced Triaxial Testing of Soil and Rock, ASTM STP 977, Robert T Donaghe, Ronald C Chaney and Marshall L, Silver Eds, American Society for Testing and Materials, Philadelphia, 1988, pp 715-731.

Rösslein D (1941), "Steinbrecherunter suchungen unter besonderer", Berucksichtigung der Kornform, Forsch a.d. Strassenwesen Band 32, Berlin. (See also abridged translation by F A Shergold, Quarry Managers Journal, 30 (4) : 220-222.)

Russell E R & Mickle J L (1970), "Liquid limit by soil moisture tension", Proceedings of ASCE, Vol. 96, SM3.

Sangrey D A, Pollard W S & Egan J A (1977), "Errors associated with rate of undrained cyclic testing of clay soils", ASTM special technical publication No. 654.

Sauer E K & Monismith C L (1968), "Influence of soil suction on the behaviour of a glacial till subjected to repeated loading", Highway Research Board Record No. 215.

Scala A J (1956), "Simple methods of flexible pavement design using cone penetrometer", NZ Engineering 11 (2), pp 34-44.

Schultze E (1975), "Large scale shear tests", 4th International Conference on Soil Mechanics and Foundation Engineering, London 1957.

Seed H B & Chan C K (1958), "Effect of stress history and frequency of stress application on the deformation of clay subgrades under repeated loading", Proceedings of Highway Research Board, Vol. 37, pp 555-575.

Seed H B, Chan C K & Lee C E (1962), "Resilience characteristics of subgrade soils and their relation to fatigue failures in asphalt pavements", Proceedings of the 1st International Conference on Structural Design of Asphalt Pavements, Ann Arbor, Michigan, USA.

Seed H B, Chan C K & Monismith C L (1955), "Effect of repeated loading on the strength and deformation of compacted clay", Proceedings of Highway Research Board, Vol. 34.

Seed H B & McNeill R L (1958), "Soil deformations under repeated stress applications", Conference on Soils for Engineering Purposes, Mexico City, ASTM Special Technical Publication 232, American Society for Testing Materials.

Selig E (1987), "Tensile zone effects on performance of layered systems", Géotechnique, 37 (3), pp 247 - 254.

Shaw P (1980), "Stress-strain relationships for granular materials under repeated loading", Thesis submitted to the Department of Civil Engineering, University of Nottingham for the degree of Doctor of Philosophy.

Shenton M J (1987), "Deformation of railway ballast under repeated loading conditions", Railroad Track Mechanics and Technology, Pergamon Press, pp 205-255.

Sweere G T H (1990), "Unbound granular bases for roads", Thesis submitted to Faculty of Civil Engineering, Delft University of Technology, Road and Railroad Research Laboratory for the degree of Doctor of Philosophy.

Symes M J & Burland J B (1984), "Determination of load and displacements on soil samples", Geotechnical Testing Journal, ASTM 7.

Symons I F, Clayton C R I & Darley P (1989), "Earth pressures against an experimental retaining wall backfilled with heavy clay", Department of Transport, Transport Research Laboratory, Research Report RR192, Crowthorne.

Tam W S (1987), "Pavement evaluation and overlay design", Thesis submitted to the Department of Civil Engineering, University of Nottingham for the degree of Doctor of Philosophy.

Taylor K L (1971), "Finite element analysis of layered road pavements", Thesis submitted to the Department of Civil Engineering, University of Nottingham for the degree of Doctor of Philosophy.

Thom N H (1988), "Design of road foundation", Thesis submitted to the Department of Civil Engineering, University of Nottingham for the degree of Doctor of Philosophy.

Thom N H & Brown S F (1990), "The mechanical properties of unbound aggregates from various sources", Proceedings in Unbound Aggregates in Roads, pp 130-142.

Thom N G & Dawson A R (1993), "The permanent deformation of a granular material modelled using hollow cylinder testing", Proceedings of European Symposium on Flexible Pavements, Section 1, pp 97-128.

Transportation Research Board (1975), "Test procedures for characterizing dynamic stress-strain properties of pavement materials", Special Report 162, Washington.

Vaid Y P, Negussey D & Zergaun M (1988), "A stress and strain controlled monotonic and cyclic loading system", Advanced Triaxial Testing of Soil & Rock, ASTM STP 977, Robert T Donaghe, Ronald C Chaney and Marshall L, Silver Eds, American Society for Testing and Materials, Philadelphia, 1988.

Vallerga B A, Seed H B, Monismith C L & Cooper R S (1975), "Effect of shape, size and surface roughness of aggregate particles on the strength of granular materials", Road and Paving Material, ASTM, Special Technical Publication No. 212, pp 63-76.

Wadell H (1932), "Volume, shape and roundness of rock particles", Journal of Geology, Vol. 40, pp 443-451.

Williams G T (1963), "Stress/strain relationships of granular soils", Thornton Report R1297, "Shell" Research Limited.

Wilson N E (1963), "Laboratory vane shear tests and the influence of pore-water stresses", Laboratory shear testing of soils, ASTM Special Technical Publication No. 361, pp 377-389.

Wilson N E & Greenwood J R (1974), "Pore pressures and strains after repeated loading of saturated clay", Canadian Geotechnical Journal, Vol. 11, No. 2.

Wong R K S & Arthur J R F (1985), "Induced and inherent anisotropy in sand", Géotechnique 35, No. 4, pp 471-481.

Wood C E J & Boud J P (1987), "Foundation design principles", Proceedings of National Workshop on Design and Construction of Pavement Foundations, Leamington Spa, Institution of Highways and Transportation, pp 33-46.

Wood D M (1980), "Laboratory investigations of the behaviour of soils under cyclic loading: a review", Soil Mechanics-Transient and Cyclic Loads, edited by G N Pande and O Z Zienkiewicz, J Wiley & Sons.

Wright P (1955), "A method of measuring the surface texture of aggregate", Road Research Laboratory, Department of Scientific and Industrial Research, Magazine of Concrete Research, November.

Zingg T (1935), "Beitray zut schotteranalyse", Schueiz Mineral Petrog Mitt, 15, pp 39-140.

Zytynski M, Randolph M F, Nova R & Wroth C P (1978), "On modelling the unloading - reloading behaviour of soils", International Journal for Numerical and Analytical Methods in Geomechanics, Vol. 2.

APPENDICES

APPENDIX A

CALIBRATION DETAILS OF TRANSDUCERS, METERS AND DEVICES FOR THE LARGE REPEATED LOAD TRIAXIAL APPARATUS (280TA)

Equipment	Manufacturer	Sensitivity	Coefficient of correlation	Precision	Full range
vertical LVDT1	Lucas Schaevitz	0.624mm/volt	1.000	16με	12mm
vertical LVDT2		0.636mm/volt	1.000	17με	12mm
vertical LVDT3		0.644mm/volt	1.000	17με	12mm
large LVDT	RDP Electronics	9.874mm/volt	1.000	86με	100mm
horizontal LVDT1	RDP Electronics	0.763mm/volt	1.000	27με	6mm
horizontal LVDT2		0.779mm/volt	1.000	27με	6mm
horizontal LVDT3		0.664mm/volt	1.000	23με	6mm
load cell	University of Nottingham	12.112kN/volt	1.000	1kpa	100kN
vacuum meter 1	Automatic Valve System Ltd	0.132kPa/mmHg	1.000	0.7kPa	0 to -100kPa
vacuum meter 2		0.134kPa/mmHg	1.000	0.7kPa	0 to -100kPa
electro-vacuum regulator	SMC	13.034kPa/volt	1.000	0.5kPa	0 to -100kPa

APPENDIX B

TEST ON A 0.25 MM THICK PVC MEMBRANE

Consider the stresses along the welded joints of a cylinder, with an internal pressure (P) as shown in Figure B.1. The force (F) per linear length on the joint can be expressed as follows:

$$2 F = P (2 r) \tag{B.1}$$

where:-   r is the radius.

To find the stress-strain relationship of the membrane and hence calculate the membrane effect to the sample by the above mentioned formula, a special test has been carried out. Plate B.1 shows the device for the test. A PVC membrane of 20 mm in width is clamped at both ends. Load is applied by dead weights hung on the lower clamp. Two LVDT's, which are mounted at each side of the membrane, are used to measure the resilient strain of the membrane. The results of nine individual tests are shown in Figure B.2. A smooth curve is observed. This curve may be used to check the confining effect on the specimen due to the PVC membrane. It can be seen that the confining effect for a normal resilient test will be small since the radial strain, which is equivalent to the circumferential strain in the triaxial test, is normally less than 1000 microstrain. Thus use of the 0.25 mm thick PVC membrane should not cause undue specimen confinement. The corresponding confining stress of a radial strain of 1000 microstrain is about 0.1 kPa.
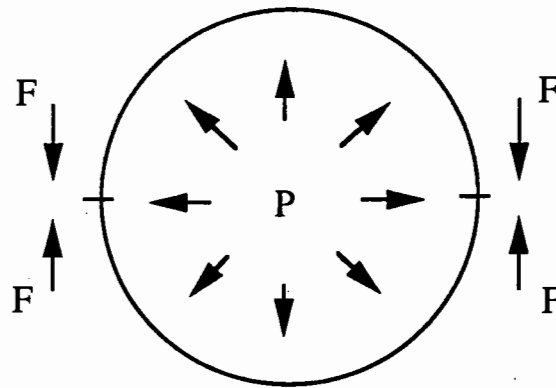
Figure B.1 Forces and pressures on a cylinder
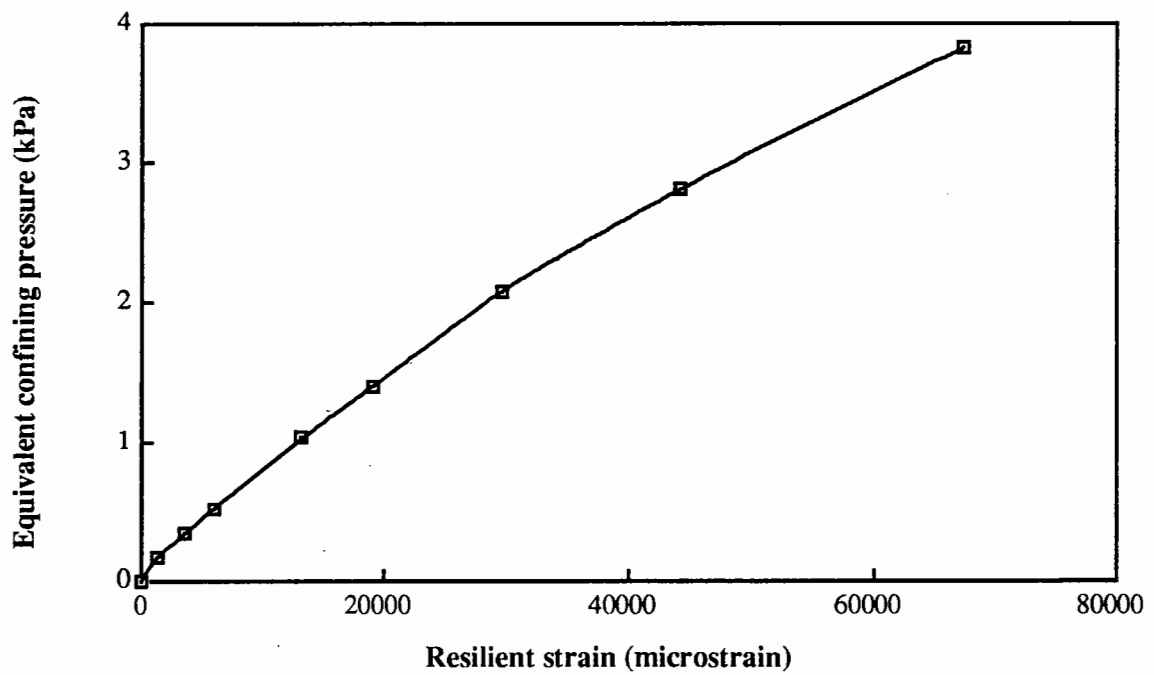
Figure B.2   Relationship between confining pressure and strain of PVC membrane
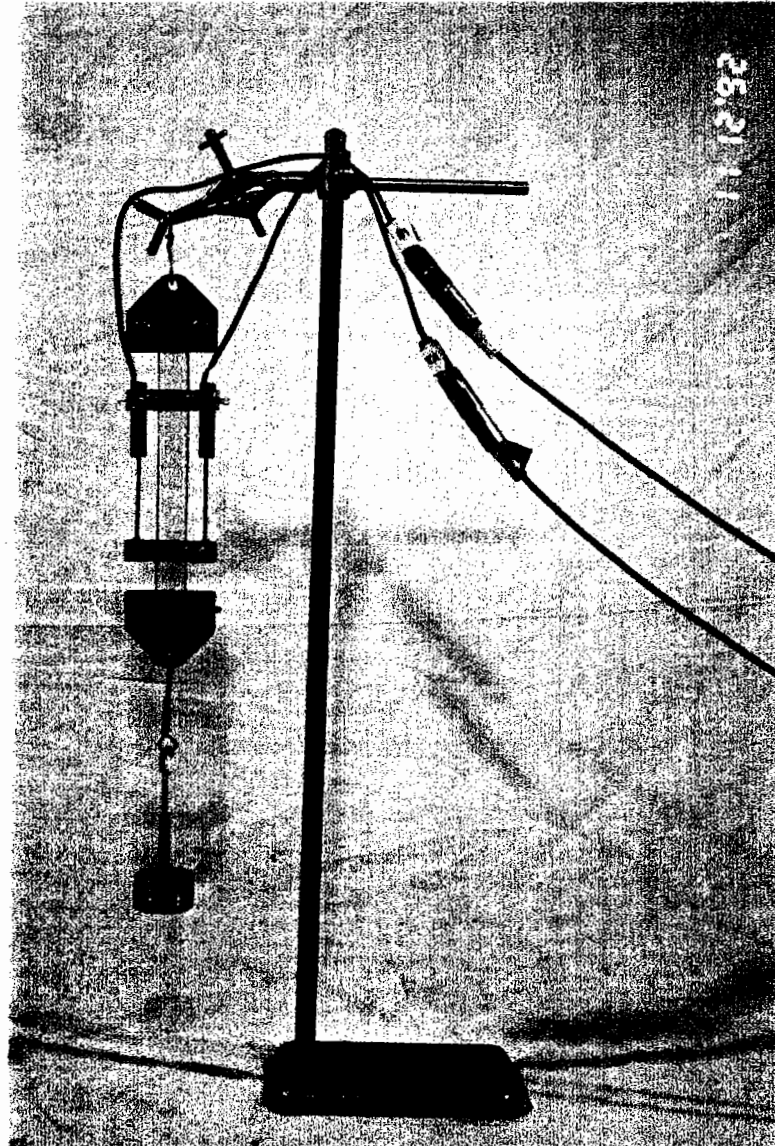
Plate B.1   Testing of PVC membrane

APPENDIX C

ELECTRONIC EQUIPMENT FOR THE 280TA

EQUIPMENT	QUANTITY	FUNCTION
Stabilized power supply TSV 30T/2/EL from Farnell Instruments Limited*	2	Power supplies to LVDTs and remote control box
Transducer amplifier type S7AC from RDP Electronics *	6	Signal conditioning for LVDTs which include AC excitation, synchronous demodulation and DC amplified output voltage
Miniature linear displacement transducer D5/100AG from RDP Electronics*	3	Radial displacement measuring
Miniature linear displacement transducer 250MHR from Lucas Schaevitz*	3	Vertical displacement measuring
Long stroke linear displacement transducer DCT/2000 from RDP Electronics*	1	Large vertical displacement measuring
Servo control unit MK5 No.1 from Nottingham University	1	Control for servo-hydraulic system
Oscilloscope 140A from Hewlett-Packard	1	Visual display of any electronic signals
Oscillator ULF Type 445A from DAWE Instruments Limited	1	High frequency waveform generation for releasing friction on the hydraulic ram
Switch box from Nottingham University*	1	Simplifying connection between individual device
Electro-vacuum regulator series IT209* from SMC	1	Providing automatic vacuum control
Waveform generator model A100 from PSI	1	Waveform generating for vertical load
Thurlby digital multimeter 1503-HA from RS	1	Digital visual display of signal from transducers
Digital multimeter pm 2421 from Philips*	2	Digital visual display of signal from transducers
Personal computer PC50-II from Commodore*	1	Data acquisition and data analysis
Tape back-up system 97TC 20MB from Xebec	1	Data back-up and storage
Load cell A1 from Nottingham University*	1	Vertical load measurement and providing feedback signals to the servo-hydraulic valve
IEEE 488 card from Roalan*	1	Interface between the personal computer and the A/D convertor
PCI 6380 multi-function instrument from CIL Microsystems Limited*	1	Converting the analogue signals from transducers to digital signals
Remote control box from the University of Nottingham	1	Providing emergency stop
Pen Recorder model 28000 from Bryans Southern Instruments*	1	Visual display and immediate record of any electronic signals

Note: * These units were used when the vertical axial loading was applied by the manually-
controlled actuator.

APPENDIX D

STRESS CONDITIONS IN THE SHEAR BOX

In 1987, Jewell and Wroth observed the movement of sands mixed with lead shot markers by using radiography. They noted that a deforming band at the mid-height of the sample was formed. The uniformity of the particle movement in the band was surprisingly high and the majority of sample strain was within this zone. Based on their observations, the stress and strain conditions of an element in the specimen at the mid-height of a shear box under shearing can be approximated as in Figure D1. (The current sign conventions can be found in the figure as well.) A uniform shear region of depth D may be assumed. It follows that

$$\delta\gamma_{xy} = -\frac{\delta x}{D} \tag{D.1}$$

$$\delta\varepsilon_y = \frac{\delta y}{D} \tag{D.2}$$

$$\tan \upsilon = \frac{\delta y}{\delta x} = \frac{\delta\varepsilon_y}{\delta\gamma_{xy}} \tag{D.3}$$

where:- υ is the dilatancy angle.

Figure D.2a includes the Mohr's circle of incremental strain to represent the strain conditions of the element in the shear band. Zero change in the direct strain along the x axis has been assumed in the construction of the Mohr's circle because the rigid boundary of the box should not allow direct strain of the sample in the horizontal direction. The angle of dilatancy can be determined directly by measuring the vertical and horizontal displacements of the box.

Dyer and Milligan (1984) observed the stress concentrations in, and the particle movement of, crushed glass in a shear box under polarized light. Their arrangement allowed the directions of principal stress and strain to be studied. Dyer (1986) suggested that the principal axes of stresses and strains on the shear plane in the shear box were coincident. The coincidence of principal axes of stresses and strains of granular materials was also reported by Chan (1990) when he applied shear stresses

onto granular materials in the hollow cylinder apparatus. The evidence of the coincidence of principal axes of stresses and strains inside the shear zone allows information, such as the dilatancy angle, in the Mohr's circle of incremental strain to be used in the construction of the Mohr's circle for stresses (Figure D.2b). With the direct measurement of the vertical loading and the horizontal shear loading, the vertical stress (σ_{yy}), and the shear stresses, (τ_{xy}) and (τ_{yx}), can be calculated. Hence, sufficient information to construct a Mohr's circle of stresses is provided. Other values, such as the horizontal stress (σ_{xx}), major principal stress (σ_1), minor principal stress (σ_3) and the angle of principal stresses (χ) measured from the horizontal axis in anti-clockwise, can be represented from Equations D.4 to D.9.

$$\sigma_{yy} = \frac{W}{L^2} \tag{D.4}$$

$$\tau_{xy} = -\tau_{yx} = \frac{F}{L^2} \tag{D.5}$$

$$\sigma_{xx} = \sigma_{yy} + 2\,\tau_{xy}\,\tan \upsilon \tag{D.6}$$

$$\sigma_1 = \frac{\sigma_{xx} + \sigma_{yy} + \sqrt{(\sigma_{xx} - \sigma_{yy})^2 + (2\,\tau_{xy})^2}}{2} \tag{D.7}$$

$$\sigma_3 = \frac{\sigma_{xx} + \sigma_{yy} - \sqrt{(\sigma_{xx} - \sigma_{yy})^2 + (2\,\tau_{xy})^2}}{2} \tag{D.8}$$

$$\chi = \tan^{-1}\left(\frac{\tau_{xy}}{\sigma_1 - \sigma_{xx}}\right) \tag{D.9}$$

where:-   L is the length of the box.

Note:- D is the thickness of uniform deformation zone.

+ve sign is for compressive normal stress, anticlockwise stress
rotation and shear stress which induces anticlockwise rotation.
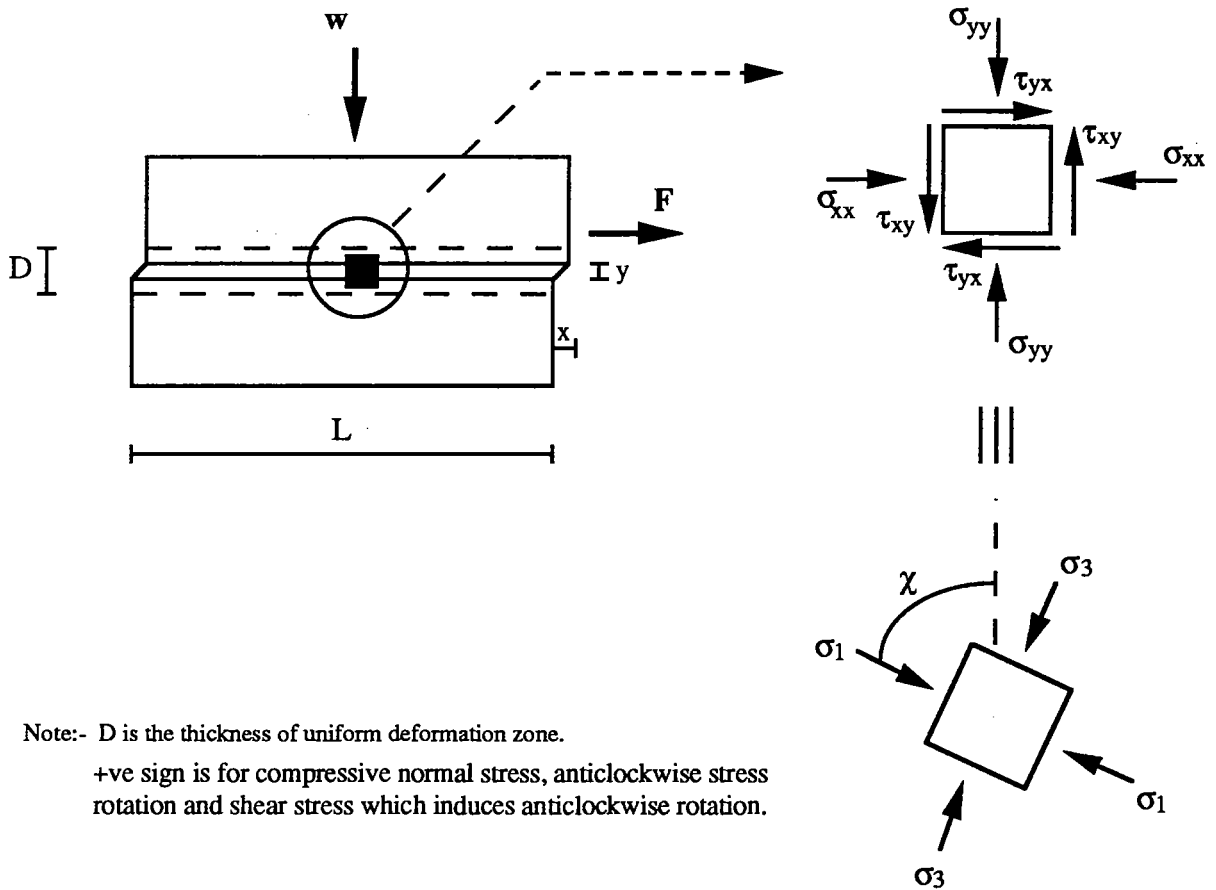
Figure D.1 Stress condition of an element in the shear box
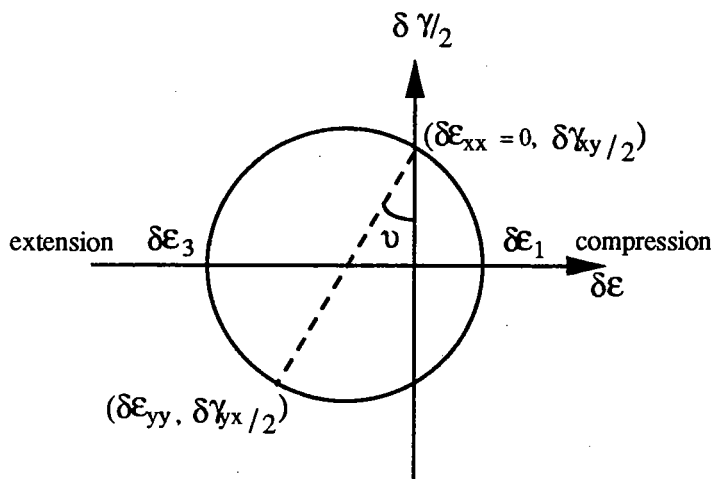
Figure D.2a Incremental plane strain   **Figure D.2b Stress**
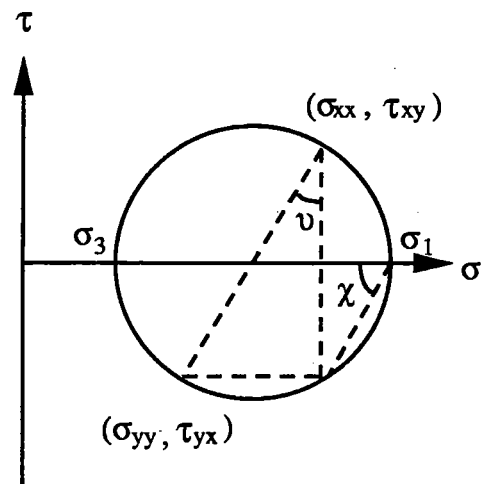
Figure D.2 Mohr's circle for strain and stress in the shear box
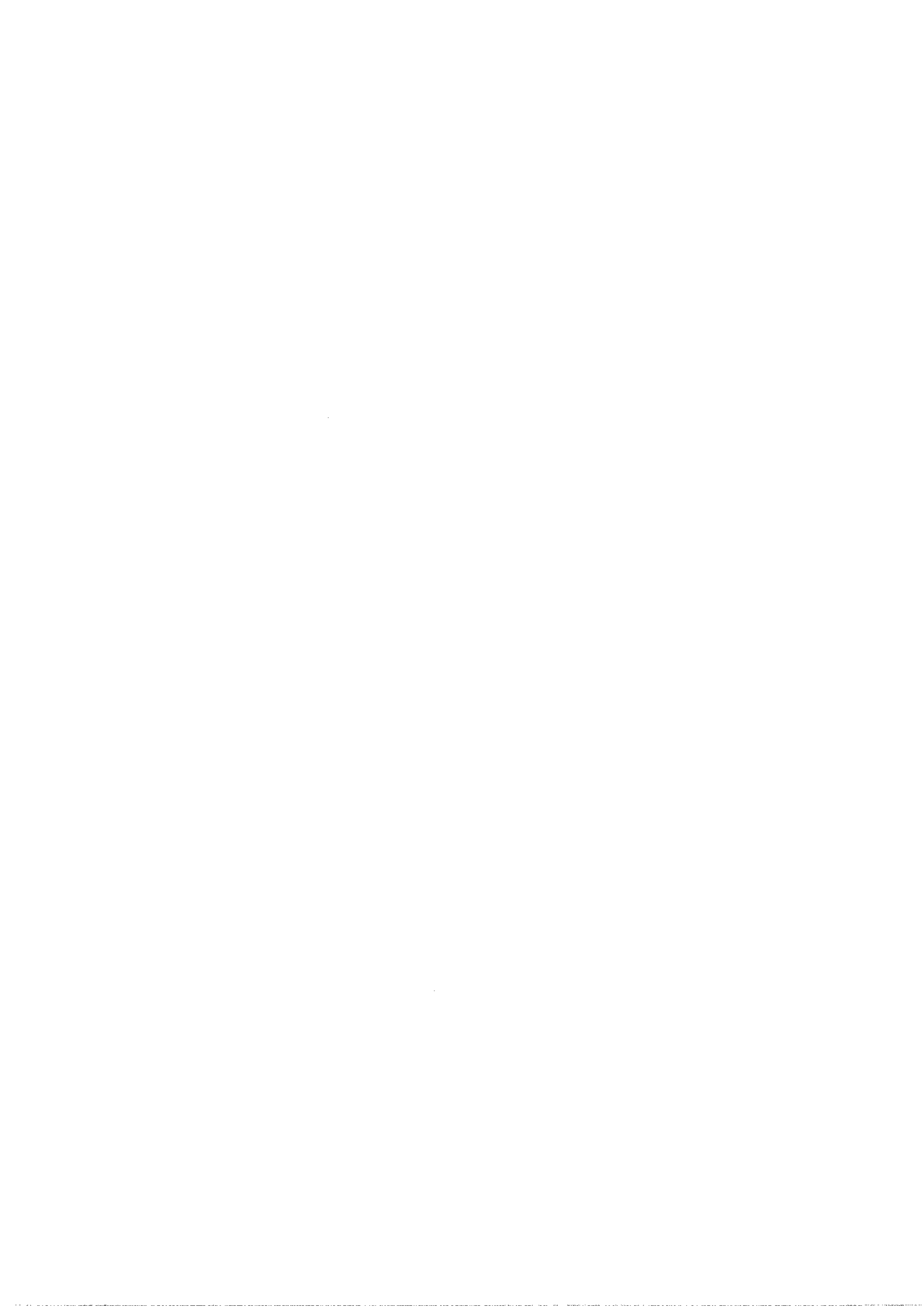
APPENDIX E

PARTICLE CHARACTERISTICS OF THE FURNACE BOTTOM ASH

Table E.1 Summary of physical property of particle

Relative Density :- surface dry oven-dried apparent	1.70 1.61 1.77
Water Absorption value	5.4%
Roundness	0.3
Sphericity	0.9
Shape Factor	0.96

Table E.2 Summary of mechanical property of particle

10% Fines Value (kN)	35
Aggregate Impact Value	51%
Aggregate Abrasion Value	9.4
Surface Friction Angle	40°

Note:- The particle characteristics of furnace bottom ash were different from the aggregates obtain from quarries. It had a low density and high water absorption which led to low particle strength in compression and under impact. However, the ability to resist abrasion was higher than the dolomitic limestones and it possessed a very high surface friction.

SAMPLE CONDITIONS OF THE UNBOUND GRANULAR MATERIALS

Series	Sample	ρ_d (kg/m³)	m.c. (before) (%)	m.c.[1] (after) (%)	m.c.[2] (after) (%)	Solid Content (%)	Void Ratio	Sr (%)
1	QDA	2030	3.2	3.0	3.3	72	39	24
	QDB	2343	6.3	5.2	5.3	83	20	72
	QDC	2197	7.4	6.3	6.3	78	28	63
	QGB	2317	5.5	4.0	4.0	87	15	70
	QSB	2328	5.0	4.2	4.3	88	14	81
2	LDN1	2172	4.5	4.5	4.5	77	30	43
	LDN2	2262	4.5	3.9	4.9	80	25	50
	LGN	2103	2.6	2.5	2.5	79	27	25
	LSN	2055	4.2	3.7	5.2	78	28	41
	LAN	976	22.9	16.5	26.8	55	82	47
3	BGN1	1931	3.6	-	-	68	47	-
	BGN2	2132	3.6	-	-	75	33	-
	BSN	2069	3.9	-	-	76	32	-

Note:-

ρ_d is the average oven dry density after compaction.

m.c. (before) is the moisture content of the sample before compaction.

m.c.[1](after) is the moisture content at the top of the specimen after testing.

m.c.[2](after) is the moisture content at the bottom of the specimen after testing.

Sr is the average degree of saturation of the specimen after testing.

APPENDIX G

PARTICLE SIZE DISTRIBUTION CURVES FOR MATERIALS FROM SITES
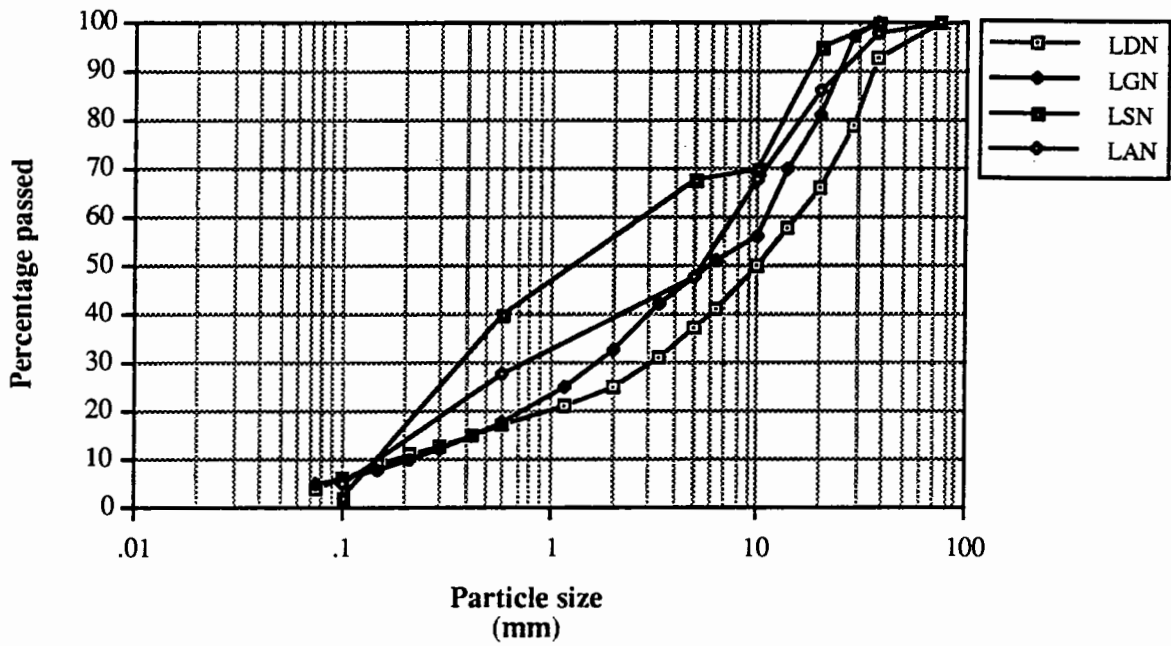
Figure G.1 Particle size distribution of materials from the Loughborough trial
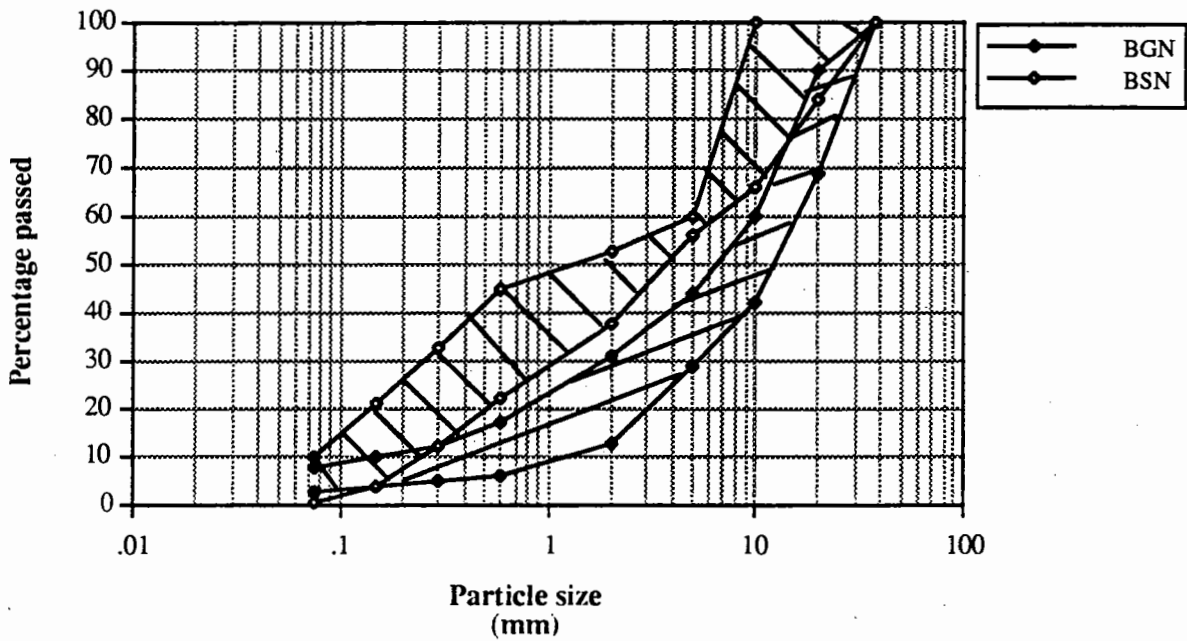
**Figure G.2 Particle size distribution of materials from the Bothkennar trial
(Little 1990)**

APPENDIX H

COMPACTIBILITY TEST

Three sets of compactibility tests to B.S. 5835 (Part 1) 1980 were completed. The material tested was dolomitic limestone from Whitwell Quarry. To represent coarse, medium and fine grading aggregate samples which might be encountered in the pavement foundation, the three particle distribution curves as shown in Figure 4.5 were selected for testing. Two of the tests, involving the gradings at the fine end of the DoT Type 1 sub-base grading envelope and at the Fuller's curve with n = 1.5 of maximum particle size 40 mm, were tested at the Engineering Services Laboratory in Northamptonshire. The third test was carried out on a sample with a curve at the fine end of the DoT capping 6F1 grading envelope. This testing was done in Nottingham.

Test results are presented in Figures H.1, H.2 and H.3 and summarized in Table H.1. It is interesting to notice that peak densities can be found at two locations in these compaction curves:- one at optimum moisture content and another one at dry condition. Between the peaks, a trough density was observed. This phenomenon was also recorded by Pike (1973) and Thom (1988). The range of optimum moisture content for the three gradings was between 3.2% and 7.4%. As expected, the finer the sample, the higher is the optimum moisture content obtained. This is due to the fact that the fine sample has a higher amount of surface area per unit volume. Hence, the fine sample requires more water to achieve the same lubrication effect as the coarse one.

Table H.1

Optimum moisture content and maximum dry density of dolomitic limestone

Grading	Optimum moisture content (%)	Dry density at optimum moisture content (%)
A	3.2	1835
B	6.3	2370
C	7.4	2300

Legend: A Fuller's curve with n = 1.5, maximum particle size = 40 mm

               B Fine side of DoT Type 1 sub-base grading envelope

               C Fine side of DoT 6F1 capping grading envelope
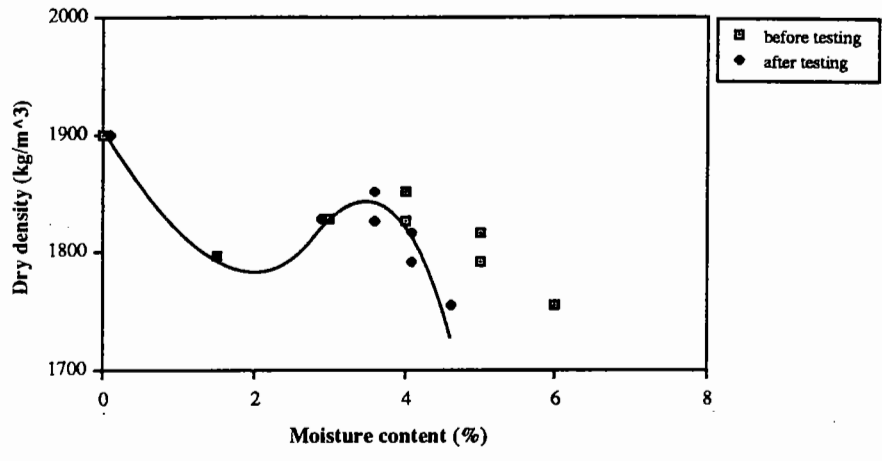
Figure H.1 Moisture-density curve of dolomitic limestone (grading is Fuller's curve of n=1.5, maximum particle size=40mm)
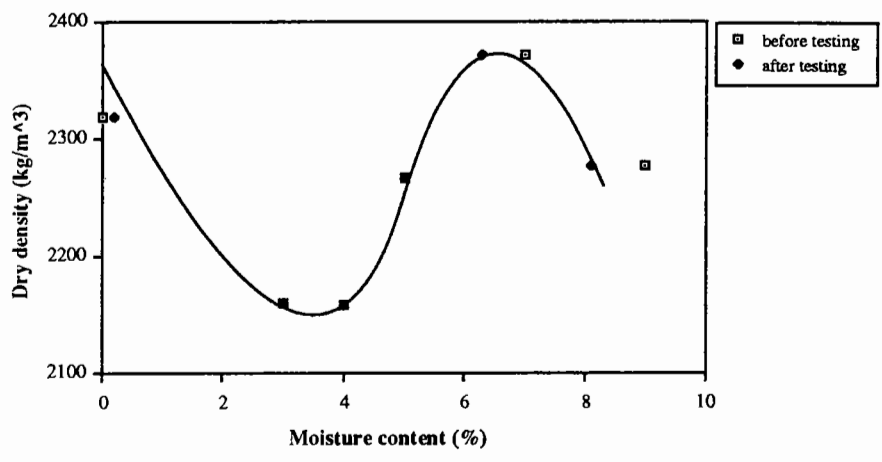
Figure H.2 Moisture-density curve of dolomitic limestone (grading is fine end of the DoT Type 1 sub-base envelop)
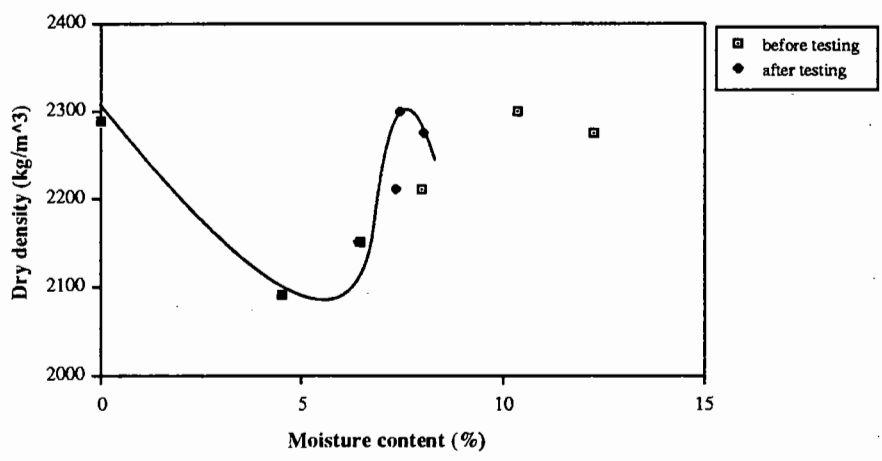
Figure H.3 Moisture-density curve of dolomitic limestone (grading is fine end of the DoT Type 6F1 Capping envelop)

APPENDIX I

TESTING PROCEDURES FOR UNBOUND GRANULAR MATERIALS

(1)   Prepare aggregates to the optimum moisture content as defined in the B.S. 5835 (1980). In case of in-situ materials, the existing moisture content is to be used.

(2)   Compact materials by the vibratory compaction method to above 95% of the maximum density as defined in the B.S. 5835.

(3)   Apply vacuum equivalent to a confining pressure of 10 kPa to the specimen.

(4)   Install "on-sample" instrumentation.

(5)   Leave the specimen for at least 12 hours.

(6)   Apply axial stresses by a hand-jack according to Table 5.4 at the current confining stress. For each stress path, 10 cycles are applied before stresses and strains are recorded. The time period allowed for each cycle is limited to 1 minute.

(7)   Increase the confining stress by 10 kPa.

(8)   Ensure the partial vacuum having achieved homogeneity inside the specimen by comparing readings of the vacuum gauges attached to the top and bottom platens before test is carried on. Usually the equilibrium period for aggregates is less than 40 minutes.

(9)   Repeat steps (6), (7) and (8) for confining stresses of 20 and 30 kPa.

(10)   Repeat step (6) for the confining stress of 40 kPa.

(11)   Reduce the confining stress to 10 kPa

(12)   Repeat step (8).

(13)   Drop a 10 kg hammer from a height of 300 mm for 25 times and recorded permanent strains generated by each drops.

(14)   Apply axial stresses by the hand-jack to the specimen until it approaches its ultimate strength. Record the stresses and strains.

(15) Increase the confining stress by 20 kPa.

(16) Repeat steps (8), (14) and (15).

(17) Apply axial stresses by the hand-jack to the specimen until the specimen fails. Record the stresses and strains.

(18) Determine the moisture content of the tested specimen.

APPENDIX J

RESULTS OF THE RESILIENT DEFORMATION TEST
ON GRANULAR MATERIALS

Sample	Confining pressure (kPa)	Minimum deviator stress (kPa)	Maximum deviator stress (kPa)	Axial strain (microstrain)	Radial strain (microstrain)
QDA	10	7	30.6	51	28
	10	7.6	40.5	69	37
	10	7.2	50.5	93	60
	10	7	60.6	107	78
	20	6.9	45.2	73	32
	20	6.8	70.2	118	57
	20	8.2	97.6	160	108
	20	6.9	120	183	149
	30	6.9	60.6	96	29
	30	7.2	100.5	147	83
	30	7.3	140.3	192	126
	30	7.2	180.6	229	185
	40	7.1	75.2	100	29
	40	6.7	131.3	178	97
	40	6.8	185.1	231	160
	40	7	240.3	282	246
QDB	10	7.9	30.6	60	17
	10	8	40.4	84	34
	10	7.9	50.4	111	45
	10	7.8	60.3	130	61
	20	7.8	45.3	73	21
	20	8	70.3	123	40
	20	8	95.3	168	69
	20	8	119.8	206	92
	30	8.1	60.6	84	16
	30	7.9	101	145	44
	30	8.3	139.9	195	80
	30	7.9	180.3	257	121
	40	7.9	75.2	94	27
	40	8.2	130	167	63
	40	8.2	185.2	232	90
	40	8.2	240	296	132

Sample	Confining pressure (kPa)	Minimum deviator stress (kPa)	Maximum deviator stress (kPa)	Axial strain (microstrain)	Radial strain (microstrain)
QDC	10	6.8	30.1	73	20
	10	6.5	40	109	31
	10	6.8	49.9	145	56
	10	7.3	60	181	81
	20	7.7	40.8	95	22
	20	7.8	61	152	60
	20	7.8	81	223	112
	20	7.7	101.1	314	179
	20	8	121.4	391	260
	30	8.7	61	145	50
	30	8.6	91	240	83
	30	8.7	120.8	341	185
	30	8.8	150.8	450	305
	30	8.7	180.9	567	452
	40	8.2	79.4	179	58
	40	8	119.3	284	124
	40	8	159	398	221
	40	8.1	198.9	525	349
	40	8.2	238.3	641	497
QGB	10	8	25.3	97	24
	10	7.8	35.6	144	41
	10	7.9	45.7	187	61
	10	7.9	56.5	245	81
	10	8	67.5	294	106
	20	7.9	25.4	95	22
	20	8.3	51.2	204	60
	20	8.3	77.6	312	94
	20	8.1	104	407	156
	20	8.4	130.3	513	211
	30	9.5	25.2	67	20
	30	9.5	67.9	238	59
	30	9.6	109.6	381	128
	30	9.5	151.6	514	193
	30	9.5	193.1	640	282
	40	9.3	81.5	262	66
	40	9.7	139.1	428	136
	40	8.2	196.9	597	227
	40	8.1	255.2	747	345

Sample	Confining pressure (kPa)	Minimum deviator stress (kPa)	Maximum deviator stress (kPa)	Axial strain (microstrain)	Radial strain (microstrain)
QSB	10	7.8	30.8	100	31
	10	8.1	40.4	147	47
	10	8.1	50.5	184	62
	10	7.9	60.5	221	64
	20	7.9	40.1	129	34
	20	8	60.3	201	72
	20	7.8	80	270	107
	20	7.7	100.4	316	153
	20	8.1	120.4	362	185
	30	7.9	68.8	194	57
	30	7.8	116.4	320	138
	30	8	162.5	418	209
	30	7.4	209.5	506	303
	40	6.7	75.4	203	61
	40	7.9	130.1	358	156
	40	7.8	185.5	465	247
	40	7.5	240	570	356
LDN1	10	7.2	20.1	47	20
	10	6.9	30.3	88	41
	10	6.9	40.2	111	54
	10	6.9	50.1	154	81
	10	6.8	60.1	185	106
	20	6.2	45.3	113	41
	20	6.2	70.3	181	85
	20	6.2	95.5	236	139
	20	6.6	120.3	296	188
	30	6.5	24.2	73	29
	30	6.1	68.8	169	75
	30	6.2	116.6	271	160
	30	6.3	162.9	354	222
	30	6.5	209.7	439	328
	40	7.3	86.6	197	96
	40	7.5	150.8	322	187
	40	7.5	215.6	413	296
	40	7.5	279.1	518	405

Sample	Confining pressure (kPa)	Minimum deviator stress (kPa)	Maximum deviator stress (kPa)	Axial strain (microstrain)	Radial strain (microstrain)
LDN2	10	7.7	21.1	44	17
	10	7.6	31.5	68	35
	10	7.6	42.3	98	48
	10	7.8	52.9	124	67
	10	7.9	63	148	89
	20	7.9	47.2	80	36
	20	8	73.2	140	75
	20	8.1	99.5	186	108
	20	8	126	240	160
	30	8.1	73.1	118	52
	30	8.3	121.4	209	122
	30	8.3	170.4	278	180
	30	8.3	219.9	351	262
	40	9.1	75.4	104	36
	40	9	130.3	198	107
	40	9.3	185.6	277	170
	40	9.5	240.7	336	229
LGN	10	6.9	31.2	123	28
	10	7.1	41.7	164	44
	10	6.9	52.1	204	54
	10	7.2	62.7	256	78
	20	7.2	47.2	146	36
	20	6.9	72.8	234	61
	20	6.9	99.5	310	82
	20	7.1	125.8	398	133
	30	6.8	72.3	201	43
	30	6.8	121.6	336	86
	30	6.8	170.4	453	143
	30	6.9	219.6	593	243
	40	6.7	90.7	233	56
	40	7.1	158.1	401	113
	40	7.2	226.5	555	179
	40	6.8	293.7	709	301

Sample	Confining pressure (kPa)	Minimum deviator stress (kPa)	Maximum deviator stress (kPa)	Axial strain (microstrain)	Radial strain (microstrain)
LSN	10	6.8	22.7	72	22
	10	6.8	32.9	119	46
	10	6.9	42.6	162	80
	10	6.9	53.2	205	110
	10	6.6	62.8	256	172
	20	7	22.5	57	20
	20	7	47.7	132	42
	20	7	73.8	213	99
	20	7	98	293	156
	20	7	122.8	383	271
	30	7.3	62.9	149	52
	30	7.3	103.1	262	96
	30	7.4	142.9	365	209
	30	7.3	182.8	541	466
	40	7.3	77.9	183	63
	40	7.3	133.7	316	151
	40	7.3	187.6	459	291
	40	7.6	241.9	725	737
LAN	10	3.6	20.1	140	32
	10	3.4	29.9	207	61
	10	3.4	40.2	274	95
	10	3.6	50.4	320	124
	10	3.6	59.9	362	150
	20	3.4	20	119	28
	20	3.2	44.7	225	58
	20	3.7	69.7	326	113
	20	3.5	94.7	410	153
	20	3.6	120	487	213
	30	3.4	69.3	275	77
	30	3.6	116.4	414	152
	30	3.6	163.1	542	237
	30	3.7	209.8	670	354
	40	4.2	86.7	292	81
	40	4.2	151.4	467	178
	40	4.2	215.2	625	300
	40	4.2	279.7	786	437

Sample	Confining pressure (kPa)	Minimum deviator stress (kPa)	Maximum deviator stress (kPa)	Axial strain (microstrain)	Radial strain (microstrain)
BGN1	10	6.6	18.9	130	42
	10	6.3	29	219	92
	10	6.7	39	287	120
	10	6.8	48.7	347	160
	10	6.8	59	402	190
	20	6.3	44.1	242	90
	20	6.2	68.7	368	155
	20	6.4	93.8	466	220
	20	6.4	118.7	558	289
	30	6.3	58.8	268	89
	30	6.2	99.2	409	173
	30	6.2	138.9	539	251
	30	6.2	179	653	337
	40	6.2	74	278	96
	40	6.3	129.3	454	191
	40	6.3	167.9	560	262
	40	6.3	239.2	759	393
BGN2	10	7.2	20.3	50	22
	10	7.5	30.4	101	28
	10	7.4	40.1	140	50
	10	7.5	49.5	177	76
	10	7.5	60.2	220	89
	20	7.2	40.2	108	29
	20	7.2	60	171	61
	20	7.4	80	233	87
	20	7.5	100	298	118
	20	7.5	120	353	144
	30	7.3	59.8	149	44
	30	7.3	90.5	233	74
	30	7.9	120.5	303	99
	30	7.8	149.9	384	142
	30	7.6	181	467	188
	40	7.5	80.6	182	46
	40	7.7	120	281	89
	40	7.7	160.2	370	119
	40	7.7	200.1	459	164
	40	7.9	240	541	211

Sample	Confining pressure (kPa)	Minimum deviator stress (kPa)	Maximum deviator stress (kPa)	Axial strain (microstrain)	Radial strain (microstrain)
BSN	10	6.9	19.4	54	17
	10	7	29.3	99	27
	10	7	39.3	134	53
	10	7	49.3	166	68
	10	7.1	59.3	199	79
	10	7.1	29.9	100	30
	20	7.1	44.3	125	42
	20	7	69.3	191	81
	20	7.1	94.2	245	126
	20	7.2	119.4	304	167
	20	7	44.2	124	49
	30	7.4	59.7	141	52
	30	7.4	99.3	225	97
	30	7.4	139.6	296	145
	30	7.4	180	370	211
	40	7.5	74.4	151	49
	40	7.5	130	244	110
	40	7.4	185	338	175
	40	7.5	240	431	264

APPENDIX K

ELECTRONIC EQUIPMENT FOR THE REPEATED LOAD TRIAXIAL APPARATUS FOR SOIL TESTING (100TA)

EQUIPMENT	QUANTITY	FUNCTION
Strain Loop made at the University of Nottingham	2	Vertical displacement measurement
Linear variable displacement transducer ACT/1000 from RDP	1	Large vertical displacement measurement
Proximity transducer 2UB from Kaman	2	Radial displacement measurement
Pressure transducer from Druck Limited	1	Cell pressure measurement
Load cell made at the University of Nottingham	1	Axial load measurement
Pressure switch from RS	1	Safety device to the electronic pressure regulator
Proportional pressure regulator 61000002 from Joucomatic	1	Regulating air pressures
Personal computer PC50-II from Commodore	1	Control, data acquisition and analysis
Controllers PG8800-2/2 from ATS	1	Axial load control
AC signal conditioner SC-5B from ATS	1	Signal conditioning for the load cell, LVDT, strain loops and the pressure transducer
KDM 8200 from Kaman	1	Signal conditioning for the proximity transducers
Amplifier made at the University of Nottingham	1	Conditioning signals from the proximity transducers and for the pressure regulator

APPENDIX L

CALCULATION FOR THE STRAIN GAUGE
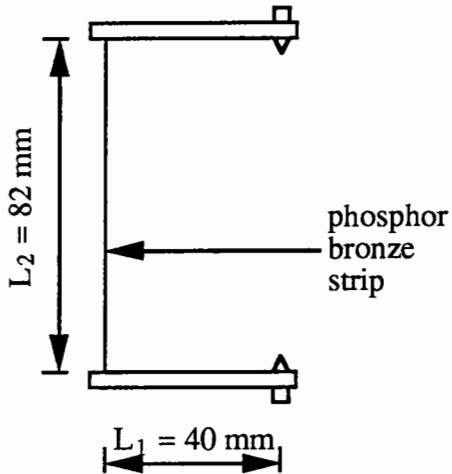
Detials of the phosphor bronze strip:-
Youngs Modulus (E) = 11488820 (gf/mm^2)
width = 5 mm
thickness = 0.56 mm

$I = 5 \times 0.56^3/12$
  $= 0.0732 \ (mm^4)$

The force required to generate a relative movement of 2 mm between the two fixing point is (F)

$$F = \frac{2 \times E \times I}{L_1^2 \times L_2}$$

= 25.6 (gf)

= 0.256 (N)
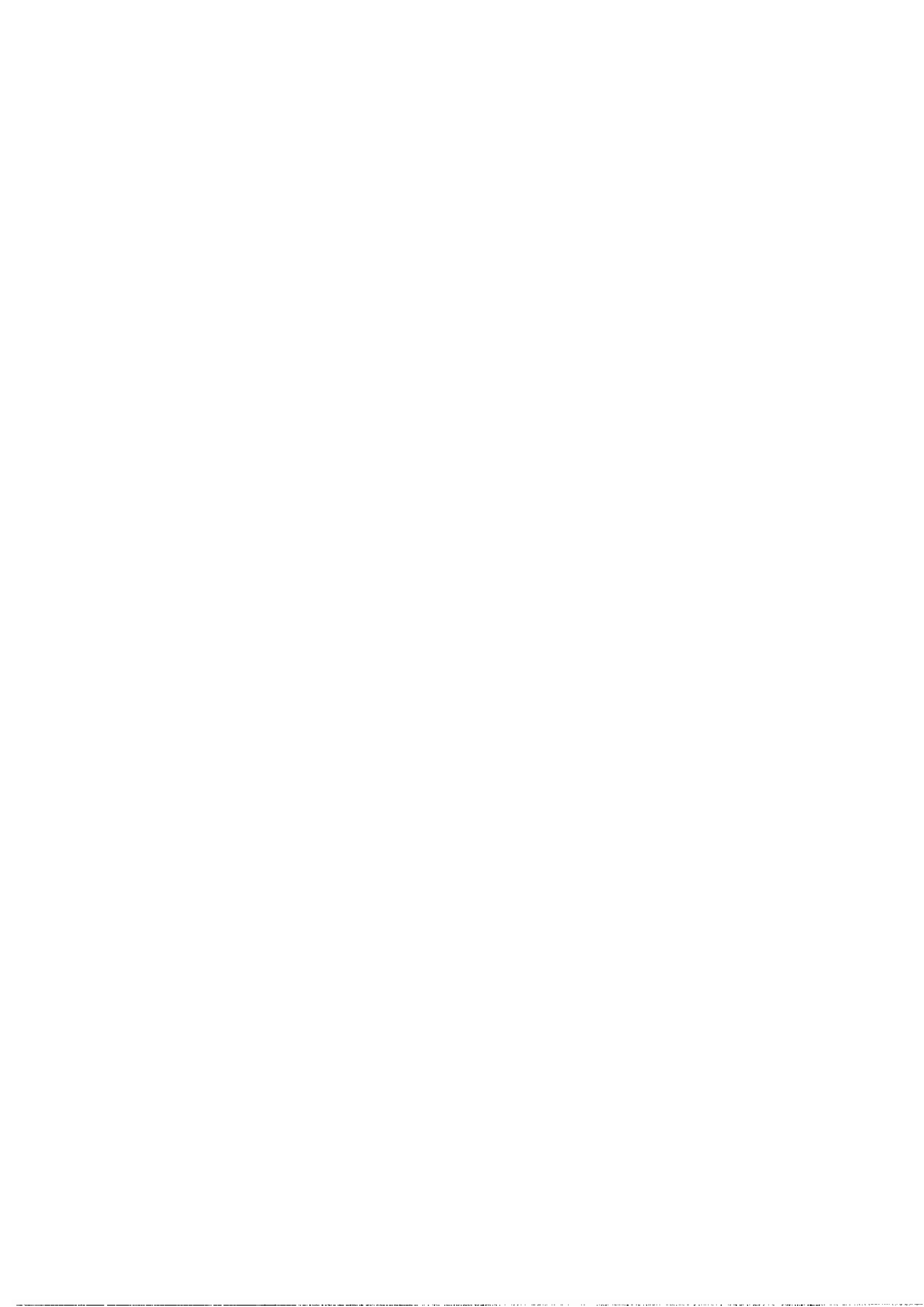
APPENDIX M

CALIBRATION RESULTS OF TRANSDUCERS FOR THE 100TA

ITEM	SENSITIVITY	PRECISION	COEFFICIENT OF CORRELATION	RANGE
strain loop 1	0.001842 mm/byte	28με	0.997	2mm
strain loop 2	0.001829 mm/byte	27με	0.997	2mm
proximity transducer 1	0.000500 mm/byte	10με	1.000	2mm
proximity transducer 2	0.000508 mm/byte	10με	1.000	2mm
LVDT	0.011003 mm/byte	53με	1.000	50mm
cell pressure transducer	0.073754 kPa/byte	0.4 kPa	0.999	700 kPa
load cell	3.27241 N/byte	0.4 kPa	1.000	8 kN

APPENDIX N

TESTING PROCEDURES FOR SUBGRADE SOILS

Multi-stress path test

(1)   Prepare soil sample to a target moisture content or to the optimum moisture content as defined in the B.S. 1377 (1990). In case of undisturbed samples, the existing moisture content is to be used.

(2)   Compact soils with a compactive effort equivalent to B.S. 1377 (1990) method 3.3.

(3)   Install "on-sample" instrumentation.

(4)   Leave the specimen for at least 24 hours before testing.

(5)   Open drainage valve before applying any stresses to the specimen.

(6)   Apply axial repeated loads of a deviator stress of 5 kPa at a loading frequency of 2 Hz. 1000 cycles are to be used. Record stresses and strains for the first five and the last five cycles.

(7)   Increase the deviator stress by 5 kPa.

(8)   Repeat steps (6) and (7) until the accumulated strain equals to (or just above) 1%.

(9)   Record the maximum deviator stress (q_t) applied.

(10)   Increase the confining pressure to 90 kPa.

(11)   Apply axial repeated loads according to Table 8.2 at the current confining pressure and at a loading frequency of 2 Hz for 50 cycles and record the stresses and strains for the last five cycles.

(12) Decrease the confining pressure by 30 kPa.

(13) Repeat steps (11) and (12) for confining pressures of 60 and 30 kPa.

(14) Repeat step (11) at a confining pressure of 0 kPa.

(15) Remove "on-sample" instrumentation.

(16) Apply monotonic axial stress at a rate of 10 kPa per minute to the specimen until it fails. Record the stresses and strains.

(17) Determine the moisture content.

APPENDIX O

DETAILS OF THE LOUGHBOROUGH SOIL

Table O.1 Grading of the Loughborough soil

Size	percentage smaller	
(mm)	sample 1	sample 2
2.000	84.9	94.0
0.600	82.2	93.3
0.212	61.7	69.3
0.063	45.1	50.2
0.020	22.9	27.1
0.006	12.6	16.6
0.002	9.2	12.9

Table O.2 Soil plasticity and specific gravity

Specific gravity (Gs)	2.71
Liquid limit (%)	26
Plastic limit (%)	16
Plasticity index	10
Plasticity	Low

Table O.3 Soil compressibility

Compressibility (α)	0.93

APPENDIX P

SAMPLE CONDITIONS OF THE COHESIVE SOILS

Sample	Dry density kg/m^3	% air voids	Degree of saturation	Moisture content (%)
KC1	1774	1.43	0.96	18.8
KC2	1769	2.41	0.96	18.4
KC3	1839	1.86	0.94	16.6
KC4	1898	1.18	0.96	15.3
KC5	-	-	-	21.7
KC6	1813	1.98	0.94	17.3
KC7	1903	1.49	0.95	15.0
BC1	1469	1.02	0.98	30.6
BC2	1485	3.09	0.93	28.5
BC3	1571	2.34	0.95	25.4
LC1	1232	4.78	0.92	41.6
LC2	1312	5.02	0.91	36.7
LC3	1374	5.44	0.89	33.1
OU1	1665	4.08	0.89	35.9
BU1	1428	1.68	0.97	32.1
BU2	1213	1.41	0.97	44.5
KC1Q	1809	2.91	0.91	16.9
KC2Q	1813	2.91	0.91	16.8
KC3Q	1836	1.48	0.95	16.9
KC4Q	1814	2.82	0.92	16.8
KC5Q	1838	1.54	0.95	16.8
LC1Q	1326	4.76	0.91	36.1
LC2Q	1323	4.62	0.91	36.4
LC3Q	1317	3.97	0.93	37.2
LC4Q	1337	3.85	0.93	36.2
LC5Q	1321	3.82	0.93	37.1

APPENDIX Q

RESULTS OF THE RESILIENT DEFORMATION TEST
ON COHESIVE SOILS

Sample	Confining pressure (kPa)	Repeated axial stress (kPa)	Axial strain (microstrain)	Radial strain (microstrain)
KC5	80	8.1	1504	729
	60	6.5	1431	713
	40	2.7	451	225
	40	3.9	599	342
	40	7.4	1634	811
	0	2.7	272	140
	0	4.7	980	448
	0	6.3	1476	749
	0	6.8	1757	918
KC6	90	5.0	69	38
	90	7.7	115	86
	90	11.9	201	134
	90	17.3	425	220
	90	23.2	656	338
	60	6.4	92	62
	60	9.0	175	110
	60	13.5	280	160
	60	18.8	614	306
	60	22.1	887	432
	30	5.5	109	62
	30	11.0	267	128
	30	12.4	459	220
	30	19.2	904	446
	30	22.6	1279	628
	0	4.9	135	82
	0	7.7	310	148
	0	11.9	561	262
	0	17.1	1150	528
	0	21.3	1625	790
	0	25.2	2139	1054

Sample	Confining pressure (kPa)	Repeated axial stress (kPa)	Axial strain (microstrain)	Radial strain (microstrain)
KC7	90	9.3	169	72
	90	17.8	330	134
	90	24.1	475	188
	90	31.2	657	262
	90	38.1	941	376
	60	8.9	119	76
	60	17.2	325	134
	60	23.9	549	220
	60	31.2	811	304
	60	38.7	1141	440
	30	9.6	153	74
	30	16.7	341	120
	30	23.1	626	206
	30	30.4	961	332
	30	39.1	1373	484
	0	7.4	135	74
	0	17.5	452	146
	0	23.4	819	278
	0	29.9	1223	396
	0	38.2	1738	578
	0	45.2	2242	776
BC1	90	4.1	102	64
	90	4.5	145	90
	90	6.5	220	130
	90	7.6	294	162
	90	9.3	415	212
	60	3.3	39	52
	60	4.5	142	84
	60	6.9	266	142
	60	8.2	358	192
	60	9.1	521	260
	30	3.2	66	60
	30	5.3	179	92
	30	6.8	321	170
	30	7.9	421	214
	30	8.9	649	302
	0	3.3	89	66
	0	5.6	213	122
	0	6.7	360	188
	0	7.9	494	248
	0	9.7	749	360
	0	11.4	1073	508
	0	12.4	1280	608

Sample	Confining pressure (kPa)	Repeated axial stress (kPa)	Axial strain (microstrain)	Radial strain (microstrain)
BC2	90	3.7	97	48
	90	7.4	187	98
	90	10.2	274	142
	90	15.0	472	214
	90	20.3	706	326
	60	5.2	142	72
	60	8.4	219	116
	60	11.3	364	168
	60	15.8	646	292
	60	19.7	906	406
	30	5.6	153	78
	30	9.3	337	160
	30	11.6	503	230
	30	16.5	948	402
	30	20.0	1299	574
	0	6.1	200	100
	0	9.1	392	164
	0	12.1	680	280
	0	16.7	1314	528
	0	19.9	1781	720
	0	23.9	2381	978
BC3	90	5.5	79	52
	90	10.0	193	94
	90	14.3	275	126
	90	19.2	419	180
	90	22.3	575	238
	60	4.5	65	52
	60	9.5	173	92
	60	14.0	340	130
	60	18.9	518	208
	60	23.1	716	176
	30	4.7	63	54
	30	9.2	183	98
	30	15.1	379	148
	30	19.9	575	220
	30	23.9	819	296
	0	4.4	68	46
	0	9.6	238	104
	0	13.7	471	160
	0	19.2	811	254
	0	24.2	1135	356
	0	27.7	1482	470

Sample	Confining pressure (kPa)	Repeated axial stress (kPa)	Axial strain (microstrain)	Radial strain (microstrain)
LC1	90	6.0	243	128
	90	9.6	554	252
	90	11.0	907	412
	90	15.0	1565	688
	90	16.2	1952	868
	60	6.5	272	148
	60	9.6	606	288
	60	11.3	1011	458
	60	15.8	1846	806
	60	17.2	2486	1076
	30	7.2	361	190
	30	9.2	755	338
	30	11.2	1181	520
	30	16.5	1916	816
	30	18.4	2930	1256
	0	7.0	470	228
	0	10.3	951	426
	0	11.8	1398	602
	0	14.1	2219	924
	0	18.2	3416	1464
	0	20.3	4595	1990
LC2	90	4.9	118	66
	90	7.4	231	126
	90	10.9	377	224
	90	15.4	715	300
	90	17.7	930	408
	60	5.1	126	56
	60	7.5	252	122
	60	10.9	439	218
	60	15.6	783	216
	60	18.6	1121	438
	30	4.8	131	56
	30	8.0	280	128
	30	11.4	524	218
	30	16.2	938	330
	30	18.8	1310	448
	0	5.8	188	54
	0	8.0	376	130
	0	11.0	639	220
	0	15.2	1111	350
	0	19.0	1569	504
	0	21.7	2034	688

Sample	Confining pressure (kPa)	Repeated axial stress (kPa)	Axial strain (microstrain)	Radial strain (microstrain)
LC3	90	10.8	281	126
	90	16.7	547	224
	90	20.6	777	300
	90	25.6	1092	408
	60	9.6	249	122
	60	16.5	535	218
	60	21.4	801	316
	60	26.5	1177	438
	30	9.9	257	128
	30	16.8	567	218
	30	21.1	864	330
	30	25.6	1225	448
	0	9.3	265	130
	0	20.4	850	311
	0	25.6	1234	435
	0	29.9	1653	597
OU1	90	4.8	150	66
	90	8.2	320	156
	90	10.3	487	248
	90	13.7	805	406
	90	17.6	1206	632
	60	5.1	150	90
	60	9.0	391	200
	60	10.9	624	336
	60	13.8	942	504
	60	18.6	1352	726
	30	5.9	207	110
	30	8.7	444	242
	30	10.5	701	374
	30	14.6	1060	578
	30	17.6	1480	832
	0	5.4	217	124
	0	7.5	451	248
	0	10.8	775	452
	0	13.5	1122	642
	0	16.5	1546	892
	0	21.0	1873	1098

Sample	Confining pressure (kPa)	Repeated axial stress (kPa)	Axial strain (microstrain)	Radial strain (microstrain)
BU1	90	7.1	465	220
	90	12.7	1038	478
	90	17.9	2021	948
	90	24.0	3116	1476
	90	28.8	4029	1896
	60	7.7	509	254
	60	12.5	1127	538
	60	18.4	2265	1076
	60	23.3	3226	1518
	60	28.4	4161	1962
	30	8.4	551	280
	30	12.8	1362	666
	30	19.1	2636	1240
	30	24.1	3540	1670
	30	29.4	4380	2068
	0	7.8	653	342
	0	12.9	1572	764
	0	19.9	2894	1398
	0	24.6	3779	1806
	0	29.8	4522	2158
	0	35.4	5277	2506
BU2	90	6.1	531	282
	90	8.7	890	434
	90	10.9	1447	698
	90	13.9	2138	1016
	90	17.2	2760	1300
	60	5.3	465	240
	60	8.0	1045	506
	60	10.4	1618	762
	60	14.7	2461	1154
	60	18.6	3217	1512
	30	5.8	607	310
	30	8.3	1156	554
	30	11.2	1810	868
	30	15.4	2715	1288
	30	17.6	3233	1530
	0	5.4	617	326
	0	7.6	1116	542
	0	11.0	1930	932
	0	15.8	2710	1292
	0	18.6	3278	1560
	0	22.5	3828	1804

APPENDIX R

DERIVATION OF A FORMULA TO DESCRIBE PERMANENT DEFORMATION BEHAVIOUR OF COHESIVE SOILS

From the observations made in Section 8.5.2, it is evident that the accumulation of permanent deformation is functions of the number of load cycles and the deviator stress to soil suction ratio:

$$\varepsilon_p = fn \ (N, \frac{q_r}{S}) \qquad (R.1)$$

It has been seen in Figure 8.33 that the plastic strain accumulation is proportional to the logarithm of the number of load pulses. Equation R.2 may be used to represent this relationship.

$$\varepsilon_p \ (N) = K \ (\log \ (N)) + i \qquad (R.2)$$

where:-   K is the rate of plastic strain accumulation in a semi-log plot. (Figure 8.33).

i is the amount of plastic strain generated at the first cycle.

Equation R.2 can be re-written as:-

$$\varepsilon_p \ (N) = K \ (\log \ (N) + \frac{1}{M}) \qquad (R.3)$$

where:-   M is the ratio between K and i.

To derive the link between the deviator stress and the number of cycling, the permanent deformation measured after applying 1000 cycles of repeated loads was used. Equation 8.11 can be expressed as:-

$$\varepsilon_p \ (1000) = d \left(\frac{q_r}{S}\right)^e \qquad (R.4)$$

And Equation R.3 becomes:-

Hence,

$$d \left(\frac{q_r}{S}\right)^e = K \left(\log (1000) + \frac{1}{M}\right) \qquad (R.6)$$

By combining Equations R.3 and R.6, the general expression for permanent deformation development under repeated loading is formed:

$$\varepsilon_p (N) = D \left(\frac{q_r}{S}\right)^E (\log (N) + F)$$

where:- $D = \dfrac{Md}{3M + 1}$

$E = e$

$F = \dfrac{1}{M}$